2007

Energy Flow in a Floodplain Aquifer Ecosystem

Brian Reid
The University of Montana

ENERGY FLOW IN A FLOODPLAIN AQUIFER ECOSYSTEM

By

Brian LeGare Reid
BS, Cornell University, 1990

Dissertation
presented in partial fulfillment of the requirements
for the degree of
Doctor of Philosophy in Biology

The University of Montana
Missoula, MT
May 2007

Approved by:

Dr. David A. Strobel, Dean
Graduate School

Dr. F. Richard Hauer, Chair
Flathead Lake Biological Station
Division of Biological Sciences

Dr. Ray Callaway
Division of Biological Sciences

Dr. James Gannon
Division of Biological Sciences

Dr. Mark Lorang
Flathead Lake Biological Station
Division of Biological Sciences

Dr. Jack Stanford
Flathead Lake Biological Station
Division of Biological Sciences

Dr. William Woessner
Geology Department

Reid, Brian, PhD, May 2007 Biology

Energy Flow in a Floodplain Groundwater Ecosystem

Chairperson: Dr. F. Richard Hauer

ABSTRACT

We developed an energy budget to identify energy sources for the invertebrate community of a large 20 km^2 floodplain aquifer, based on biomass distributions, organismal respirometry, *in situ* community respiration, mesocosm and microcosm experiments, stable isotopes and invertebrate gut contents. The invertebrate respiration scaling exponent was 0.474 (+/- 0.068, 95% CI) across six orders in body mass, which is significantly lower than the ¾ power scaling predicted by metabolic theory. Invertebrate production was dominated by copepods (*Diacyclops, Acanthocyclops, Bryocamptus*), *Stygobromus* amphipods, and amphibiont stoneflies, and ranged from 26.9 to 4200 mg C/m^3 sediment/year. Production and density showed a U-shaped response to dissolved oxygen (high production at both low and high oxygen concentrations). Production declined exponentially with depth for most sites, but at sites with orthograde oxygen profiles there was an exponential increase at the oxycline. Aerobic microbial community production ranged from 1210 to 2020 mg C/m^3 sediment/year, also showing a U-shaped response to oxygen. System respiratory quotient (RQ) ranged from ≈ 0 to 9.5, indicating a significant contribution of anaerobic production to system energy flow. We documented multiple lines of evidence for DOC (soil, river) and buried POM carbon sources, however POM was by far the largest carbon reservoir in the aquifer at ≈ 10^8 (to 10^{10}) mg C/ m^3 sediment. Energy from POM breakdown was the only source sufficient to explain microbial and invertebrate production. Carbon stable isotope signatures showed strong levels of depletion for invertebrates ($\delta^{13}C$ -25‰ to -70‰). These results suggest a significant anaerobic subsidy of aerobic food webs in the subsurface, and a potential methane subsidy of 10% to 99% of invertebrate energy flow. Oxygen showed high, non-random, spatial and temporal variation across the aquifer, with a large scale decline in oxygen along the axis of the floodplain, and distinct hotspots of low oxygen. Low oxygen hotspots corresponded with migration of stonefly nymphs 100's of meters into the aquifer. The U-shaped responses and biogeochemical trends suggest a major threshold at bulk oxygen concentrations of 3-5 mg/l. Collectively, these findings indicate the role of dissolved oxygen as a key variable in groundwater ecosystems.

ACKNOWLEDGEMENTS

I would like to thank Dr. Jack Stanford for providing the opportunity to work on one of the most interesting and least explored ecosystems in the world. I thank my advisor Dr. F. Richard Hauer, and my committee, Drs. Ray Callaway, Mark Lorang, Matthias Rillig, Jack Stanford and William Woessner. Dr. James Gannon offered abundant advice, and thanks also to Dr. William Holben and Dr. Emily Bernhardt. Dr. Charlie Hall provided a simple insight that set everything in motion. I would particularly like to thank the Dalimata family, especially John, Ruth, Chris and Steve, for pulling my truck out of the mud, ideas, friendship, the most amazing field site in the world, the new amphipod *Stygobromus presleyii*, the smartest dog I've ever had, and pulling my truck out of the mud again. Every graduate student would benefit from having a farmer on their committee. Access to field sites was also provided by the Wheeler and Pouliat families. Vincent and Neil Dalimata (who coined the term "hyperactive weaselcosm"), helped with some of the most abusive field work I could come up with, all for a few lousy sandwiches. Curtis and Dave from Rocky Boys (supported by project TRAIN) made possible the well oxygen sampling that ended up tying the whole story together. Jason and Mark from Salish Kootenai College helped drive wells and dig several enormous holes that kept filling back in, which is a great metaphor too. Big thanks to fellow field slave, lab mate, statistics coach and best friend Michelle Anderson. Scott Relyea: we should have died in that canoe. Kristin Olsen: beware the sound of breaking glassware. Mark Potter and Eric Anderson for all the help in the shop. All the staff at FLBS. Sherrie at DBS for supporting the "sleeping bags for science" campaign. And the list of people who helped in the field: Sandra Adams, Jake Chaffin, Cain Diehl, Nathan Gordon, Adam Johnson, Mike Machura, Bonnie McGill, Phil Mattson, Mike Morris, Chris Platt, Phillip Ramsey, Jessica Schultz, Audrey Thompson. Thanks, List! Thanks in advance to taxonomic gurus Euyalem Abebe (nematodes), Bob Newell (insects), Janet Reid (copepods), Rhithron Associates (chironomids) and Howard Taylor (rotifers). And finally to my friend Jessica Schultz and my grandmother Sunny, who encouraged me to hang in there. And my dad Walter Reid, the engineering brains.

This project was supported in part by a two-year fellowship from the Inland Northwest Research Alliance (INRA) Subsurface Science Research Initiative (SSRI). Additional research support was from NSF Biocomplexity in the Environment grant # 0120523, and material support by an NSF Dissertation Improvement Grant and INRA.

TABLE OF CONTENTS

LIST OF FIGURES

Chapter 1: Oxygen Dynamics and Community Respiration in a Montane Floodplain Aquifer

Chapter 2: Distribution and Isotopic Composition of Buried Organic Matter in Sediments of a Floodplain Aquifer

Chapter 3: Large Scale Invertebrate Dynamics in Response to Oxygen Gradients in a Floodplain Aquifer

Chapter 4: An in situ Solar Powered Mesocosm for Monitoring and Experimentation in the Hyporheic Zone

Chapter 5: Effects of Substrate, Organic Matter, and Oxygen on Invertebrate Density and Biomass: A Mesocosm Experiment in the Hyporheic Zone.

Chapter 6: Carbon Energy Flow in a Floodplain Aquifer Ecosystem

LIST OF TABLES

INTRODUCTION

Raymond Lindeman, building upon the earlier concept of community economics (Thienemann 1926), was the first to systematically treat entire ecosystems from an energetics approach. Lindeman's "Trophic–Dynamic" energy budget for a small late-succesional pond (Lindeman 1942a) inspired a generation of ecologists, a handful of whom conducted system energy flow budgets for other ecosystems: a coral atoll (Odum and Odum 1955), a large subtropical springbrook (Odum 1957), a small temperate cold spring (Teal 1957), a salt marsh (Teal 1962), a small stream (Fisher and Likens 1973), fish migration in a larger stream continuum (Hall 1972), a small forest-stream catchment (Gosz et al. 1978) and a millpond (Strayer and Likens 1986). There are several things that we note from this rather complete list. First, this approach has not been applied very often. Second, it has not been attempted in quite some time. Lastly, these are some of the most frequently cited works in the field of ecology. While the reasons behind the apparent lapse in the systems energetics approach would make for interesting discussion, our purpose here is merely to apply an old but effective method in examining one of the worlds least understood ecosystems. Our system is a floodplain aquifer, the large lateral extent of the hyporheic zone within a mountain valley.

The hyporheic zone, defined as river water penetrating the subsurface and interacting with ground water, was first described by Orghidan (1959). Hyporheic zone dynamics have been increasingly recognized as a strong driver of ecosystem processes in rivers, regulating riverine thermal regimes, biogeochemistry, productivity and community metabolism (Jones and Mulholland 2000, Stanford et al. 2005). The hyporheic zone is considered by definition a transition zone or ecotone (Brunke and Gonser 1997). Consequently, the assessment of hyporheic zone function has almost always focused unidirectionally on the significance to surface waters (Grimm and Fisher 1984, Valett et al. 1994, Baxter and Hauer 2000, Jones and Mulholland 2000, Pepin and Hauer 2002), or more rarely upon the terrestrial zone (Harner and Stanford 2003, Mouw et al. 2003). We believe that in larger systems, this limited perspective may vastly underestimate the extent and complexity of groundwater-surface water interaction.

Large hyporheic systems such as fluvial aquifers could sometimes be considered ecosystems, rather than transitional zones. The discovery of subsurface stonefly nymphs

in highly permeable floodplain sediments kilometers from the river channel dramatically demonstrated the potentially large spatial extent of the hyporheic zone (Stanford and Gaufin 1974, Stanford and Ward 1988). Large populations of obligate groundwater invertebrates (stygobionts) occur throughout bounded floodplain groundwater systems, along with the specially adapted amphibiont stoneflies. Together they contribute to a unique and highly specialized community of organisms, and this fluvial aquifer community is probably a repeatable feature of mountain and piedmont valley groundwater systems throughout the world (Stanford and Ward 1993). There have been very few ecological studies of fluvial aquifer ecosystems, almost exclusively limited to three study systems: The Rhone River in France (Dole-Olivier et al. 1994), The Lobau wetland of the Danube aquifer in Austria (Pospisil 1994, Danielopol et al. 2000), and the Flathead River System in Montana, USA (Stanford et al. 1994).

Alluvial groundwaters are not only dynamic components of river ecosystems, but they are situated at the interface of human land use and drinking water resources. In mountain and piedmont valleys, urban and agricultural land use overlap with shallow alluvial groundwater resources. Abstraction of groundwater continues to grow steadily: societal demand for fresh water has increased almost 8-13% in the past 20 years (Gleick 2000), and over 30% of global freshwater resources are stored in groundwater. Land use impacts potentially extend to human health via shallow groundwater, and ultimately affect surface water resources through valley hyporheic flow and exchange with surface water.

Floodplain aquifers are the Atlantis of freshwater ecology and aquatic biodiversity. Fluvial aquifers are widely represented throughout western North America, yet they are very poorly understood. The science of groundwater ecology is challenged by sampling limitations (Palmer 1993). Much of what is known about groundwater comes from degraded systems (e.g. groundwater remediation), which is largely practiced in the private sector. There is high potential for innovative research and discovery, and also significant social relevance in the research and long term monitoring of groundwater ecosystems. Fluvial aquifers represent a unique opportunity to understand population biology and systems ecology near the extremes of low productivity. Alluvial aquifer substrate, although heterogenous and difficult to sample, is much more uniform over

large spatial and geochemical gradients compared to karstic and epikarstic groundwater systems. There is also the potential role of aquifers in the still largely unexplored concept of a hyporheic continuum (Ward and Palmer 1984, Stanford et al. 1993, Ward and Voelz 1994). Fluvial aquifers are probably an energetically important feature in this continuum, and a major biogeographical link for highly endemic groundwater organisms.

Although considered impractical for subsurface systems (Danielopol et al. 2000), we demonstrate herein that the traditional study of whole system energy flow (Lindeman 1942, Odum 1957, Teal 1957, Teal 1962, Hall 1972, Fisher and Likens 1973, Strayer 1986) can provide valuable insight into a largely unknown ecotype. In fact this basic approach, which is the foundation of much of the traditional subjects of ecology, is probably essential to the ontogeny of groundwater science. We developed an energy budget for the invertebrate community of a large 20 km^2 floodplain aquifer, based on biomass distributions, closed chamber respirometry, *in situ* community respiration, mesocosm and microcosm experiments, stable isotopes and invertebrate gut contents. Considered as a system, floodplain aquifers are isolated from solar energy, and are probably limited by carbon bioavailability. Our energy budget incorporates multiple lines of evidence for the relative contribution of carbon energy from river water, soils, and buried organic matter. The relative contribution of these three energy sources will in turn provide essential insight into the management and conservation of alluvial groundwaters.

In Chapter 1 we begin with an overview of dissolved oxygen systematics across the floodplain aquifer. The changes in oxygen concentration with depth and over the annual cycle, and the spatial patterns of community respiration, provide the foundation for understanding invertebrate populations and energy flow discussed in subsequent chapters. Chapter 2 accomplishes the same objective for organic matter distribution in aquifer sediments. Chapter 3 describes the invertebrate sampling, and response of invertebrate populations to 25 attributes of hyporheic habitat, including oxygen and organic matter data from Chapters 1 and 2. Chapter 4 is an overview of the design and performance of large, in situ experimental mesocosms, which were used to estimate respiration rates in chapter 1. We demonstrate the experimental use of these mesocosms in Chapter 5, with paired treatments of wood jam sediment, with and without organic matter.

Chapter 6 is a synthesis of preceding chapters in the form of a system energy budget for the floodplain aquifer. Our budget was composed of four representative hyporheic habitat types: (I) aquifer recharge zones; (II) midgradient zones (longer flowpaths); (III) low oxygen zones; (IV) the oxycline below type III sites. These habitat types are based on patterns of community respiration (Chapter 1) and invertebrate distribution and density (Chapter 3). This research is integrated with a larger floodplain ecosystem study of biogeochemical cycling, hence we report our energy budget in equivalent units of carbon, instead of more traditional energy units (kilocalories).

REFERENCES

Baxter, C. V. and F. R. Hauer. 2000. Geomorphology, hyporheic exchange, and selection of spawning habitat by bull trout (*Salvelinus confluentus*). *Can. J. Fish. Aquat. Sci*., 57: 1470-1481.

Brunke, M. and T. Gonser. 1997. The ecological significance of exchange processes between rivers and groundwater. *Freshwat. Biol.* 37: 1-33.

Danielopol, D.L., P.P. Pospisil, J. Dreher, F. Mosslacher, P. Torreiter, M Geiger-Kaiser, A. Gunatilaka. 2000. A groundwater ecosystem in the Danube wetlands at Wien (Austria). In: Wilkens, H., D.C. Culver and W.F. Humphreys, Eds. *Ecosystems of the World 30: Subterranean Ecosystems.* Elsevier.

Dole-Olivier, M.J., P. Marmonier, M. Creuzé des Chateliers, & D. Martin.1994. Interstitial Fauna Associated with the Alluvial Floodplains of the Rhône River (France). *IN*: Gibert, J., D. L. Danielopol and J. A. Stanford (eds.), *Groundwater Ecology*. Academic Press, San Diego, California, USA. 571 pp.

Fisher, S.G. and G.E. Likens. 1973. Energy flow in Bear Brook, New Hampshire: an integrated approach to stream ecosystem metabolism. *Ecol. Mon.* 43: 421-439.

Gleick, P.H. 2000. *The World's Water 200-2001*. Island Press, Washington D.C.

Grimm, N.B. & S.G. Fisher. 1984. Exchange between interstitial and surface water: Implications for stream metabolism and nutrient cycling. *Hydrobiol.* 111: 219-228.

Hall, C.A.S. 1972. Migration and metabolism in a temperate stream ecosystem. *Ecology* 53(4): 585-604.

Harner, M.J., & J.A. Stanford. 2003. Differences in cottonwood growth between a losing and a gaining reach of an alluvial flood plain. *Ecology* 84: 1453-1458.

Jones, J.B. and P.J. Mulholland. 2000. *Streams and Ground Waters.* Academic Press, San Diego.

Lindeman, R.L. 1942. The trophic-dynamic aspect of ecology. *Ecology* 23: 399-418.

Mouw, J.E.B.& P.B. Alaback. 2003. Putting floodplain hyperdiversity in a regional context: An assessment of terrestrial-floodplain connectivity in a montane environment. *J. Biogeogr.* 30: 87-103.

Odum, H.T. 1957. Trophic structure and productivity of Silver Springs, Florida. *Ecol. Mon.* 27(1): 55-112.

Orghidan, T. 1959. Ein neuer Lebensraum des unterirdischen Wassers, der hyporheische Biotop. *Arch. f. Hydrobiol.* 55: 392-414.

Palmer, M.A. 1993. Experimentation in the hyporheic zone: challenges and prospectus. *J. N. Am. Benthol. Soc.* 12: 84-93.

Pepin, D.M. & F.R. Hauer. 2002. Benthic responses to groundwater-surface water exchange in two alluvial rivers in northwestern Montana. *J. N. Am. Benthol. Soc.* 21: 370-383.

Pospisil, P. 1994. The Groundwater Fauna of a Danube Aquifer in the “Lobau” Wetland in Vienna, Austria. *IN*: Gibert, J., D. L. Danielopol and J. A. Stanford (eds.), *Groundwater Ecology*. Academic Press, San Diego, California, USA. 571 pp.

Stanford, J.A. and A.R. Gaufin. 1974. Hyporheic communities of two Montana rivers. *Science* 185: 700-702.

Stanford J.A., M.S. Lorang and F.R. Hauer. 2005. The shifting habitat mosaic of river ecosystems. *Verh. Internat. Verein. Limnol.* 29(1): 123-136.

Stanford, J.A. and J.V. Ward. 1988. The hyporheic habitat of river ecosystems. *Nature* 335: 64-66.

Stanford, J. A. and J. V. Ward. 1993. An ecosystem perspective of alluvial rivers: connectivity and the hyporheic corridor. *J. N. Am. Benthol. Soc.* 12(1):48-60.

Stanford, J. A., J. V. Ward and B. K. Ellis. 1994. Ecology of the alluvial aquifers of the Flathead River, Montana (USA), pp. 367-390. *IN*: Gibert, J., D. L. Danielopol and J. A. Stanford (eds.), *Groundwater Ecology*. Academic Press, San Diego, California, USA. 571 pp.

Strayer, D.A., G.E. Likens. 1986. An energy budget for the zoobenthos of Mirror Lake, New Hampshire. *Ecology* 67(2): 303-313.

Teal, J.M. 1957. Community metabolism in a temperate cold spring. *Ecol. Mon.* 27(3): 283-302.

Teal. J.M. 1962. Energy flow in the salt marsh ecosystem of Georgia. *Ecol. Mon.* 43(4): 614-624.

Valett, H.M., S.G. Fisher, N.B. Grimm, P. Camill. 1994. Vertical hydrologic exchange and ecological stability of a desert stream ecosystem. *Ecology* 75(2): 548-560.

Ward, J.V. and M.A. Palmer. 1994. Distribution patterns of interstitial freshwater meiofauna over a range of spatial scales, with emphasis on alluvial river-aquifer systems. *Hydrobiol.* 287: 147-156.

Ward, J.V. and N.J. Voelz. 1994. Groundwater fauna of the South Platte River system, Colorado. pp. 391-423. *IN*: Gibert, J., D. L. Danielopol and J. A. Stanford (eds.), *Groundwater Ecology*. Academic Press, San Diego, California, USA. 571 pp.

Chapter 1

OXYGEN DYNAMICS AND COMMUNITY RESPIRATION
IN A MONTANE FLOODPLAIN AQUIFER.

ABSTRACT

In mountain and piedmont valleys, gravel-bed river floodplains exhibit complex and dynamic interactions between terrestrial, aquatic, and groundwater systems. Of these three, groundwaters are among the most poorly understood components of river ecosystems. At our study site on a montane river floodplain in western Montana, we used oxygen concentrations from well and surface water, coupled with estimates of community respiration from *in situ* hyporheic mesocosms, to evaluate the spatial and temporal patterns of energy flow within the floodplain shallow groundwater aquifer. Dissolved oxygen (DO) showed non-random spatial and temporal variation across the aquifer. The large-scale aquifer pattern (1 to 10 kilometers) showed a decline in oxygen along the axis of the floodplain, corresponding with aquifer-scale flowpaths. At smaller scales (10 to 100+ meters) we observed distinct hotspots of low DO. Oxygen generally remained constant with increased depth, but 20% of our sampling wells showed strong clinograde oxygen profiles, with hypoxia in the top 2-3 meters below the water table, and higher oxygen concentrations with increased depth. Community respiration averaged 2.7 μgO_2/l sed/hr (bdl to 6.7), which is among the lowest rates ever reported for fluvial sediments. Aerobic respiration rates were similar among shallow (1 meter) and deeper (2 meter) depths. We observed two distinct seasonal respiration patterns. In the aquifer recharge zone, respiration was positively correlated with temperature, expressing low winter respiration, a rise in respiration rate during spring snowmelt and flood pulse, and a maximum respiration rate from July through September. On longer flowpaths, respiration showed depressed summer rates and two maxima: one in the spring, and a second larger peak in the fall and winter. Aerobic respiration was strongly influenced by temperature gain (an artifact) at all sites, arguing against ecosystem resilience against temperature changes. Modeled oxygen concentration using the seasonal pattern of mesocosm respiration rates (corrected for artifacts) corresponded well with observed seasonal oxygen cycles. The DO patterns provide evidence for three potential energy sources: (1) direct input of energy (DOC) from the river, the extent of influence depending on season, as mediated by temperature; (2) indirect influence of the river on soil based energy sources, through change in river stage and a rising water table; (3) concentrated patches of energy, probably associated with buried organic matter or debris jams. These latter focal areas appear as local biogeochemical hotspots at the scale of tens of meters, and may be important to the overall aquifer energy budget. The overall patterns in oxygen concentration and community respiration indicate the large (kilometer) scale and dynamic influence of the river on floodplain groundwater.

"A skillful limnologist can probably learn more about the nature of a lake from a series of oxygen determinations than from any other kind of chemical data"

– G. Evelyn Hutchinson

INTRODUCTION

Alluvial groundwaters are a dynamic component of river ecosystems, and play an important role at the interface of human land use and drinking water resources. Over 30% of global freshwater resources are stored in groundwater, and societal demand for fresh water has increased almost 8-13% in the past 20 years (Gleick 2000). In mountain and piedmont valleys, urban and agricultural land use overlap with alluvial groundwater resources, and urban encroachment and abstraction of groundwater continues to grow steadily. Through valley-scale subsurface flow and exchange with surface water, the risk posed by human activity and land use extends to both shallow groundwater and surface water resources.

The interface between surface water, groundwater and the terrestrial zone has long been recognized at smaller scales: hyporheic zone dynamics are a strong driver of ecosystem processes in rivers, and there is a rapidly increasing interest in groundwater-surface water interaction in rivers and streams (Valett et al 1993, Dahm 2006). Alluvial aquifers represent a large lateral extension of the hyporheic zone, demonstrated by the unique community of amphibiont stoneflies. These animals migrate hundreds of meters to kilometers into alluvial aquifers, and return to the main channel to complete their life cycle (Stanford and Gaufin 1974, Stanford and Ward 1988). Viewed as large-scale hyporheic systems, alluvial aquifers also exhibit complex physical and biogeochemical properties comparable to the more traditional limnological systems, with relatively high flux rates coupled with high spatial heterogeneity in the substrate (Jones at al 1995). Alluvial groundwater systems are widely represented throughout western North America, yet they are very poorly understood from an ecological perspective. There is high potential for innovative research and discovery, and also significant social relevance in the research and long term monitoring of groundwater ecosystems. Yet the science of groundwater ecology is challenged by sampling limitations (Palmer 1993) and partly for

this reason lags behind other sub-disciplines within the aquatic sciences. Truly, floodplain aquifers remain the Atlantis of freshwater ecology and aquatic biodiversity.

Hutchinson's advice on the utility of oxygen (Hutchinson 1975) is perhaps broadly applicable to any aquatic system, and it is particularly useful in the subsurface. Although oxygen was long assumed to be depleted in the subsurface, well oxygenated conditions occur widely and with spatial complexity (see Malard and Hervant 1999 for an excellent review), and sub-saturated conditions are common even in deep groundwater (Winograd and Robertson 1982). Given the availability of sampling wells, which corresponds strongly with human population and water supplies, oxygen can be readily measured using conventional electrodes. Oxygen is essential to the survival of aquatic animals, although some have adaptations for low oxygen. Oxygen is biochemically important; of all the pathways for oxidation of organic matter, oxygen is by far the most energetically favorable reactant (Stumm and Morgan 1996). Its absence is equally significant, since oxygen depletion enables a broader range of terminal electron acceptors and energetic pathways. In contaminated groundwater, oxygen concentration may influence bioremediation: oxygen is considered the rate limiting factor in hydrocarbon degradation (Borden et al 1986), but it may interfere with breakdown of chlorinated solvents (Morean et al 2007) via halorespiration. Groundwater contaminants such as arsenic may be immobilized or released depending on the system redox state (Moore 1994), largely driven by changes in oxygen. Techniques such as air sparging and oxygen releasing materials are frequently employed in attempts at *in situ* bioremediation (Wiedemeier et al 1999). Most importantly, oxygen consumption implies aerobic respiration, a functional variable that effectively quantifies system metabolism and production, as pioneered by Howard Odum (1956).

References to oxygen are abundant in the aquatic literature, however oxygen depletion is only infrequently used as an independent variable (Connolly et al 2004), taking a back seat to redox potential (Rose and Long 1988). Since natural systems are rarely in equilibrium, and because of an inherent bias in measuring redox potential with electrodes, Eh has limited usefulness as a field measurement (Lindberg and Runnels 1984, Scott and Morgan 1996), and may not even remotely correspond with oxygen tension (reviewed in Giere 1993). A more recent approach to measuring redox couplets

(Baker et al 1999) or oxidative capacity (Eary and Schramke 1990) is a workable alternative, however as several authors note, the availability of metal ions may be complicated by solid phase oxyhydroxides and metal sulfides (Rose and Long 1988, Moore 1994).

A fluvial aquifer could be considered somewhere between a river and a lake. A bounded alluvial valley is essentially a basin that has become filled with gravel. Yet it also shares properties with rivers, such as hydraulic gradients, which are expressed more or less as linear flow (i.e. flowpath, *sensu* Fisher et al 2004). Subsurface systems are heterotrophic, disconnected from solar energy and, as we argue below, are probably closed, but not isolated, systems. Dissolved oxygen is supplied through aquifer recharge, via surface water or infiltration through the soil and vadose zones. Once in the system, oxygen is consumed with organic matter degradation, and unlike nutrients, is essentially non-renewable with respect to internal spiraling (*sensu* Mulholland and DeAngelis 1979). In an aquifer where oxygen demonstrates spatial patterns of depletion, it may be one of the most useful field measurements.

Herein, respiration estimates are intended towards developing a system energy flow budget for an alluvial aquifer. Respiration may be used as a surrogate for microbial community production, thereby indicating food availability for hyporheic invertebrates that are abundant throughout the aquifer. Based on preliminary invertebrate sampling in the aquifer, we observed a strong but unusual U-shaped relationship between invertebrate density and estimated production and porewater oxygen concentration (Chapter 3). Our primary purpose was therefore to map the extent and temporal pattern of low oxygen zones in the aquifer, including vertical oxygen dynamics. Secondly, we measured aerobic respiration rates over a two year period, using eight in-situ flow-through mesocosms drawing water from the hyporheic zone of the floodplain.

We report on invertebrate community dynamics and system energy flow elsewhere (Chapter 3, Chapter 6). Collectively these patterns in oxygen and community respiration reported in this paper represent emergent properties. First, the seasonal pattern in oxygen concentration and respiration indicate the large spatial extent and complex dynamics of river-aquifer interaction. Secondly, as system variables, they offer indirect evidence for the sources of the energy for subsurface production, either from

river water or soil water (dissolved organic carbon), or buried organic matter (similar to the vertical profiles predicted by Kaplan and Newbold 2000). We hypothesized that temporal oxygen patterns (concentration and respiration rate) will reflect pulses of energy from either floods, snowmelt or rain events. The spatial pattern will further indicate the distribution of energy sources, from overlying soils, buried energy in the form of particulate organic matter (POM) associated with debris jams, and carbon sources from infiltrating river water (Figure 1). We predicted that with river water as the primary energy source, respiration will increase and oxygen will decrease following the flood pulse. During baseflow conditions, we expected steady gradients of oxygen decline, regardless of location or terrestrial cover type. Conversely, with the potential contribution of energy from the soils, we expected a patchy distribution and steep vertical gradients in oxygen concentration and respiration, depending on cover type, and the response would follow the annual cycle of aboveground production. Buried particulate carbon would show similar patterns, but would also show uneven horizontal gradients in oxygen distribution, and the timing of these patterns would not be as strongly coupled to above-ground production.

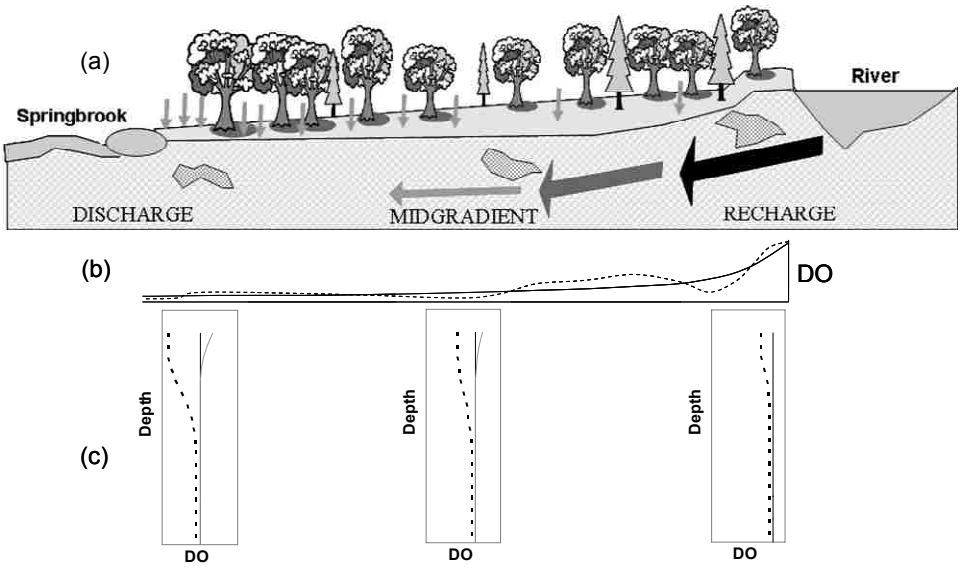

Figure 1: Conceptual model of a lateral flowpath. (a) potential sources of energy along a flowpath, from soil or river DOC, or buried organic matter; (b) predicted longitudinal pattern that may be either uniform (solid line) or non-uniform (dashed line) in response to spatial complexity in buried organic matter, river recharge, or aquifer-soil interactions; (c) predicted pattern of vertical gradients along flowpath in response to soil interaction (dashed), no interaction (dark line), and dispersive influx of oxygen (gray line).

This question of energy flow is conventionally approached from a range of field and experimental studies at smaller scales. We believe that at the scale of entire aquifers (1 to 10 km^2 or more), the oxygen distribution and the annual cycle of respiration rates are the most comprehensive starting point, indicating the relevant spatial and temporal scales of subsequent investigation.

METHODS

Study site

The study site was the Nyack Floodplain located on the Middle Fork of the Flathead River (48° 27' 30" N, 113° 50' W). This fifth order gravel-bed river has its headwaters in the Bob Marshall-Great Bear Wilderness Complex and is located along the southwest boundary of Glacier National Park in western Montana, USA (Figure 2a). The 20 km^2 floodplain is 10 km long and averages 2 km in width. The floodplain is bounded laterally by valley walls with bedrock knickpoints at both the upper and lower ends. The river along the length of the floodplain is anastomosed, with the active channel and parafluvial zone of the river tending toward the northeastern side of the valley. The more mature, orthofluvial floodplain forest and agricultural pasture is to the southwest. Over 30% of the main channel flow is lost to the aquifer at the upstream end of the floodplain (Stanford et al. 1994) and various gaining and loosing reaches have been documented and modeled throughout the floodplain (Stanford et al 2005, Poole 2006).

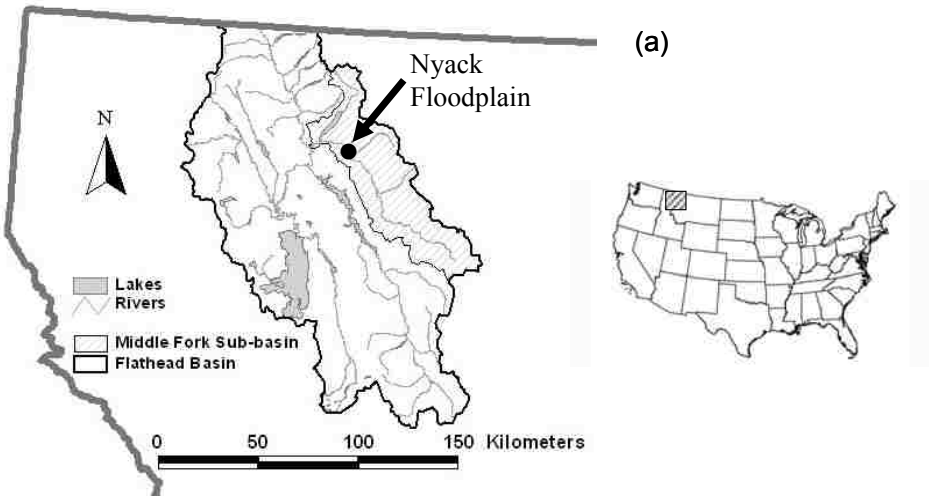

Figure 2 (a): Study site: Nyack Floodplain, Middle Fork Flathead River (MT USA).

The Middle Fork Flathead River has a spring snowmelt hydrograph, with an average baseflow of ≈ 12m^3/s (at the Nyack floodplain) and an average peak discharge ≈ 420 m^3/s, typically occurring in late May or early June. Annual precipitation is approximately 35 cm/year, and precipitation accounts for less than 1.1% of the aquifer water budget (Poole 2000). The site has been the focus of research by the Flathead Lake Biological Station for over 20 years, and additional site description is offered in Stanford et al (1994).

Well Grid Installation and Design

The floodplain sampling network consisted of 57 groundwater wells and eight surface water sampling locations (Figure 2b). We installed 20 three-inch nominal (inside diameter 7.6 cm) PVC wells using a hollow-stem auger drilling rig. Most of these wells were located on two longitudinal transects along the length of the flood plain, with the first transect (wells HA2 through 11) averaging 160 meters (range 60-300m) from the river channel, and the second transect (wells HA12-20) averaging 605 meters (range 120-960m) from the channel (Figure 2b). An additional well was located on an alluvial fan (HA1) and three well sites were sited to accommodate and serve the groundwater mesocosms (see community respiration below). Another 37 two-inch nominal (inside diameter 5.1cm) PVC wells were installed using a Geoprobe™. These wells were located to represent the range of lateral hyporheic positions (Figure 1): aquifer recharge zones, aquifer discharge zones, and midgradient zones (infiltration, advection and exfiltration zones, *sensu* Brunke and Gonser 1999, and commonly referred to as areas of downwelling and upwelling). To the extent possible, well locations were further stratified to represent the upstream, middle and downstream sections of the aquifer, and the major surface cover types (gravel bar, cottonwood and mature conifer forests). Two-inch and three-inch wells were finished with continuous 100 slot (2.55 mm) and 80 slot (2.04 mm) screens, respectively. The open area extends from just below the soil horizon to total depth, which ranged from 6 to 15 meters for 3" wells and 3 to 5m for 2" wells (see Diehl 2004 for additional details on well design). Since there are some limitations on drill rig portability, especially in more vegetated areas, the floodplain scale well grid is neither random nor entirely systematic. This is balanced by the fact that, to our knowledge at

least below the soil horizons and surficial channel features, the physical habitat of the subsurface cannot be readily predicted by passive surface cues. Furthermore, hyporheic position can vary within a site over time, depending on river stage and channel activation.

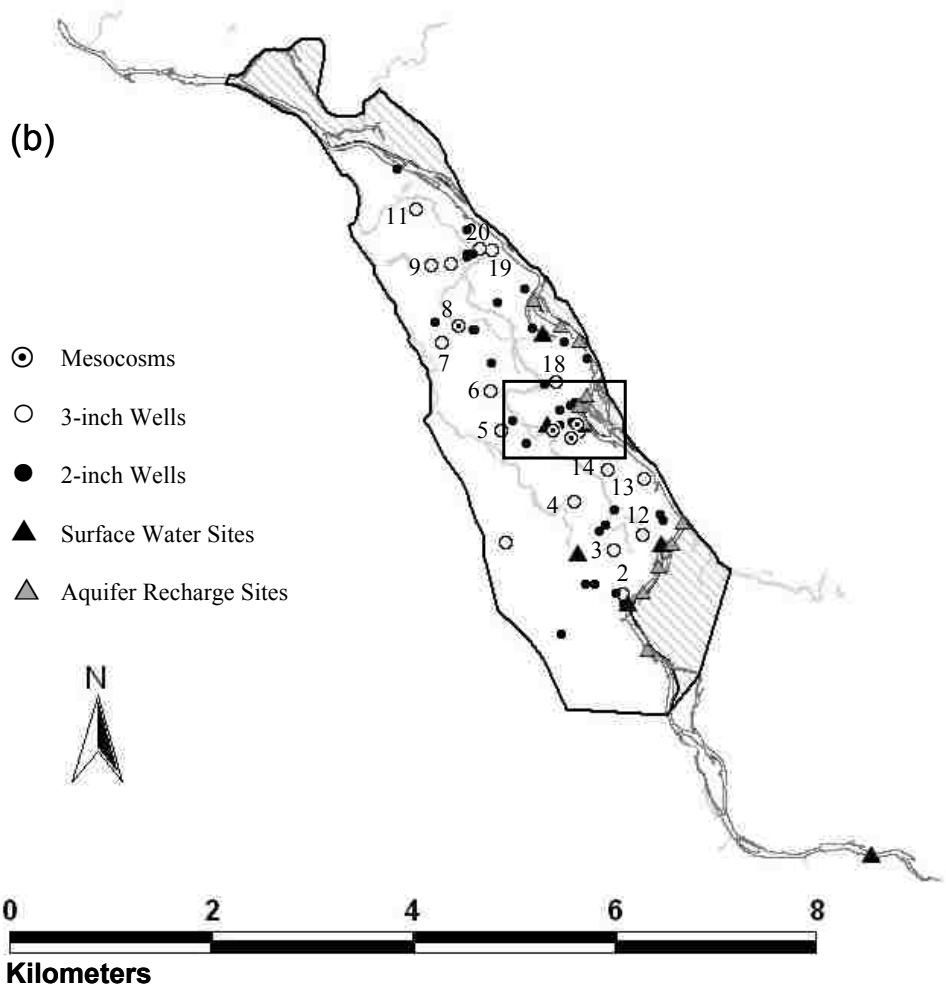

Figure 2 (b). Nyack floodplain: The main channel is furthest to the right (dark gray), and flows from south to north. Smaller channel features are spring brooks and other off-channel habitats (light gray). Dissolved oxygen sampling locations include 2-inch and 3-inch diameter wells (circles), and surface water sampling points (Black triangles). Three inch well network used for vertical profiles is labeled in two longitudinal transects, from south to north (wells 2 through 11 and 12 through 20 respectively). Remaining wells (unlabeled), and aquifer recharge sites (explained in text) were used for contouring. Solid black line shows floodplain boundary used for contouring, while excluded areas (blanking) are cross hatched. Mesocosm pair M4 is located at well #8.

Well and surface water sampling

Wells and surface water sites were sampled during the snowmelt-floodpulse-receding limb cycle (Feb, Apr, May and Jul of 2004), and less frequently during baseflow (Nov 2003 and Oct 2004). Wells were initially purged using a gas-powered diaphragm pump to sample (and remove) invertebrates (Stanford et al 1994). Wells were then sampled for DO, Temperature, pH, Specific conductance, alkalinity and water chemistry. Hence 5-7 days were required to sample the entire network. Surface water sites included four main channel locations and three springbrooks. Surface water DO was measured using a YSI 55 dissolved oxygen probe (Yellow Springs Instruments). Continuous temperature loggers (VEMCO and iButton loggers) recorded temperature at 1 to 2 hour intervals, and at specific depth intervals at all sites (Chapter 3)

Three-inch wells were sampled at one meter depth intervals, from the water table to the bottom of the casing. Water was drawn from the wells using a 12V electric submersible pump (Whale Submersible 881, Whale Systems Specialists), discharging at a rate of 12 liters per minute into an overflowing 1 liter container containing the DO probe. Water was sampled from 50 to 100cm beneath the water table. Pump depth was adjusted to maintain pressure during water drawdown. We used a modified straddle packer design to isolate respective sampling intervals. The pump was first inserted into a flexible hose which was slightly smaller that the well diameter (Tiger Flex, 2.5 inch dia.). The hose in turn was sealed at the end, the lowest 50 cm interval with intake holes on the side of the hose (2cm diameter, approximately 25% open area), and a 4cm wide foam packer on either side of this sampling interval (see Figure 3c). By manipulating the depth of the intake hose, this design also allowed for DO sampling at multiple depths (see below) and is the same hose used for invertebrate sampling along vertical well profiles (Reid 2007, Chapter 3).

A similar design was used to sample the 2-inch wells, but instead of a flex hose we used a 1 meter long section of 1.5-inch nominal PVC pipe (3.8mm), slotted with a band saw, and mounted on a smaller diameter PVC pole. Instead of foam packers to isolate the top interval, we used PVC slip caps machined to less than 1mm clearance within the well. Water was purged for at least 3 minutes, however some wells required up to an hour of purging to remove fine sediments before water samples were taken. DO and

other meter readings generally stabilized within 1 minute of pumping, and remained stable regardless of pumping duration. We sampled vertical well profiles for DO in the 3-inch wells in June, August, and November 2004, and January and May 2005. The sampling hose was marked at one meter intervals, and starting with the lowest well interval (up to 12 meters below the top of the well casing), we sampled 50cm intervals in 1 meter increments until we reached the water table.

Oxygen profiles were compared to vertical hydraulic conductivity (K) profiles, obtained from pneumatic slug tests (data from Diehl 2004, corrected for height of casing). Profiles were also compared to sediment structure from drilling logs (data from Diehl 2004, and additional unpubl. data on soil depth). The sediment profiles were based on the resistance to drilling, (i.e. low resistance indicated sand horizons, while high resistance and vibrations indicated cobble substrate or larger), and they are only a qualitative estimate of average grain size. We collected split spoon samples to verify the substrate at the deepest point of drilling. These profiles cannot be used to estimate permeability, which is influenced more by grain size distribution than average size, however they do provide our best indication of sediment facies within the subsurface.

Oxygen Contouring

We used Surfer v7.0 (Golden Surfer Software) to contour oxygen isopleths across the floodplain. Interpolation between points was done using kriging. Linear features such as the main channel require special consideration when contouring: most surface waters were usually only slightly subsaturated, and DO was high DO relative to most of the aquifer, yet surface waters were sampled at only few points. We therefore established "false nodes" (Figure 2b) to represent a DO boundary (we used near saturation DO values based on the nearest surface water sampling point). False nodes were established only in areas of known recharge to the aquifer, corresponding with recharge sites identified by hydrologic modeling (Diehl 2004, Poole et al. 2006), and also concurring with water mass balance and radon measurements (Stanford et al 2005, T. Gonser pers. comm.). Most of the lateral habitats have consistently low hydraulic conductivity in the bed sediments (based on extensive sandpoint slug tests, F.R. Hauer, pers. obs.). We therefore assumed that tributaries and springbrooks offered only very limited groundwater recharge

(light gray channel features in Figure 2b). The leading edge of the contouring boundary was established approximately 2 km downstream of the upper knickpoint, where the first clusters of wells were located. We excluded additional areas within the floodplain from contouring where subsurface oxygen data was lacking, which generally included the eastern boundary of the river and mid channel gravel bars (Figure 2b).

Flowpath Oxygen and Cumulative Respiration

For each well, we developed a temperature vs. oxygen regression for the top 1 meter depth interval. The slope and intercept of these site-specific models, combined with the average temperature metric calculated from continuous temperature data (Chapter 3, Anderson et al in prep) were in turn used to estimate average DO (essentially an average value from continuous data). We estimated residence time based on the phase shift of the temperature peak between river water and respective well sites (Chapter 3). We modified the equation of Chapelle (1993), to calculate cumulative flowpath respiration (CFR) for each well site:

$$\text{CFR} = \frac{(\overline{DO}sw - \overline{DO}w) \times 1000}{\tau \times n \times 24} \quad (1)$$

where CRF is the cumulative flowpath respiration rate [µg O_2/l sed/hr], $\overline{DO}sw$ and $\overline{DO}w$ are the mean annual DO for surface water and well sites respectively (calculated from continuous data as above), τ [d] is the residence time (based on temperature phase shift), and n is the sediment porosity (assumed to be ≈ 0.4). We then regressed aquifer DO and CFR against flowpath residence time.

Community Respiration

We used *in situ* flow-through mesocosms to estimate community respiration of aquifer sediment. The mesocosms were constructed of 20 foot long (6.1m) segments of 12 inch (30.5 cm) nominal diameter PVC pipe. The mesocosms were solar powered, drawing water from wells using variable speed peristaltic pumps, and operating at flow rates similar to local groundwater flux (mean velocity of 12.8 m/d, compared to 13 m/d estimated in the field by Diehl 2004). We installed four pairs of mesocosms at wells representing the range of aquifer hyporheic positions (Figure 2c). Pump intake water was

(c)

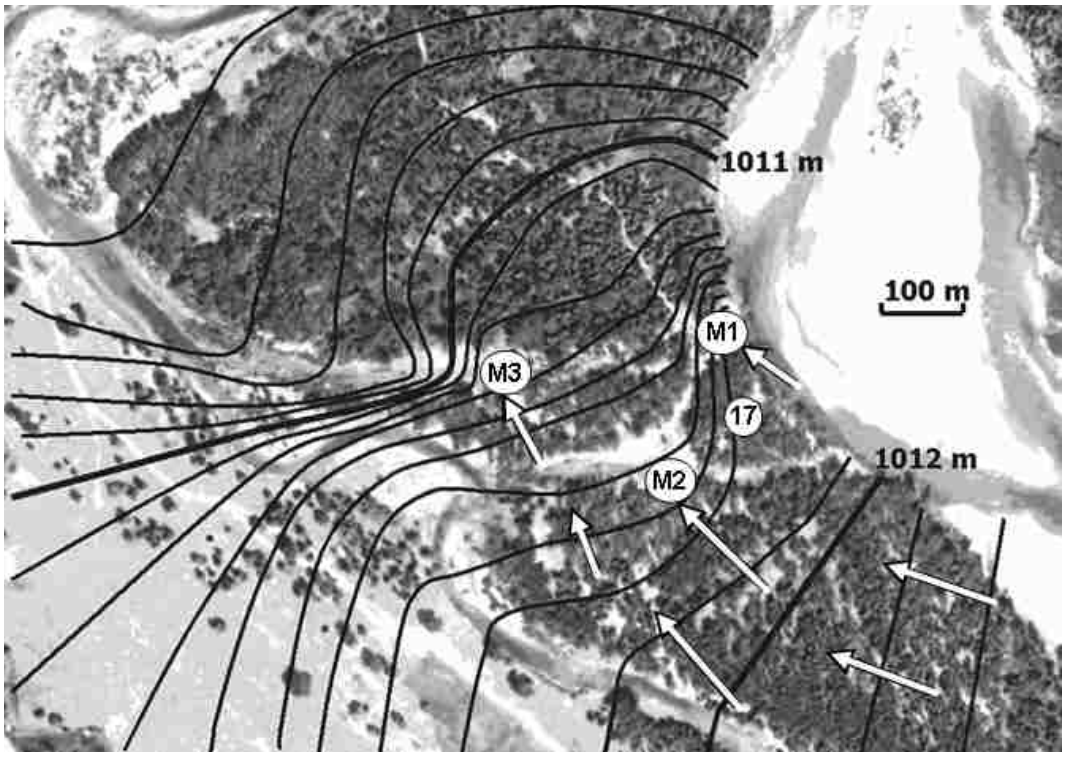

Figure 2 (c): Close-up of mesocosm locations for pairs M1 through M3, superimposed on a potentiometric map (contours show water table elevations, and arrows show direction of groundwater flow). Mesocosm sites M1 (Aquifer recharge), M2 (midgradient) and M3 (discharge zone – spring head) are shown, in addition to 3-inch well #17. Basemap courtesy of Cain Diehl, used by permission.

drawn from colonization canisters filled with gravel obtained from the Nyack floodplain, the canisters baffled to isolate a discrete 1 m interval within the respective well: either shallow (0-1m below estimated mean low water MLW), or deep (1-2 meters below MLW). Mesocosms 1a and 1b (both shallow, due to well limitations) were sited in an area of known aquifer recharge (residence time estimated as 1.6 days; Johnson 2002). Mesocosms 2a (shallow) and 2b (deep) were located in the middle of a cottonwood forest, upgradient of an old channel feature (residence time 7-19 days, estimated from temperature lag). Mesocosms 3a (deep) and 3b (shallow) were located at the head of a spring, draining into a larger orthofluvial springbrook (residence time 45-50 days, based on temperature lag). Mesocosms 4a (deep) and 4b (shallow) were located farther down the floodplain, at a presumed discharge zone into the same orthofluvial springbrook. This last mesocosm pair was developed from our original prototype mesocosm run in 2003, and was based on an older design (Chapter 4), hence we will refer to this last pair only

for qualitative comparisons. All mesocosms were in operation continuously from April 2004 through the end of the study.

Mesocosms were filled with local sediments simulating a bimodal gravel formation (Huggenberger et al 1998) typical of alluvial aquifer deposits: a 2cm layer of sand (average grain size 1mm) topped by 2cm of fine gravel (average 4-5 mm), with the remaining volume of the mesocosm filled with medium gravel (17.6mm +/- 7.0 mm). The mesocosms were intended for multiple purposes, including invertebrate density and production estimates and experimentation, in addition to community respiration. Hence the gravel distribution was chosen to imitate the general structure of bimodal gravel (Figure 3a), to better represent invertebrate habitat and also enable the sampling of multiple substrate types in future experimentation. All sediments were collected from the floodplain or nearby fluvial gravel deposits, and were washed of organic matter and fine particles and sieved to achieve uniform size classes: they were otherwise not pretreated. For additional details on mesocosm design, and more extensive commentary on the assumptions and limitations, refer to Chapter 4.

Water residence time was estimated using mass balance, and porosity was estimated as the specific yield of water recovered from substrate-filled sampling canisters. Both were confirmed using salt tracer tests in July and September 2004. We maintained flow rates at 250ml/min (residence time $\tau \approx 20.3$ hrs) for all mesocosms, except as follows: (1) during winter months (Nov-Feb) flow was maintained at maximum rates (350-400 ml/min, $\tau \approx 8.4$ and 7.4 hrs respectively) to prevent freezing and minimize temperature loss; (2) from Sept 2005-Nov 2005 flow was reduced to 150 ml/min ($\tau \approx$ 19.6 hrs) to increase residence time and attempt to better estimate uptake rates of naturally occurring solutes (DOC, NOx etc. – unpubl. data). Flow adjustment was made to all mesocosms on the same dates, maintained within 10% of target flow rates, and were all within the range of groundwater velocity estimated for the floodplain (Diehl 2004).

DO of each mesocosm was measured every one to two weeks using YSI probes. The probe was inserted into a machined PVC flow cell, which we first attached to the outlet risers. Air was purged from the cell, and the probe was backed out slightly to allow flow over the probe body. We found that temperature compensation performed poorly

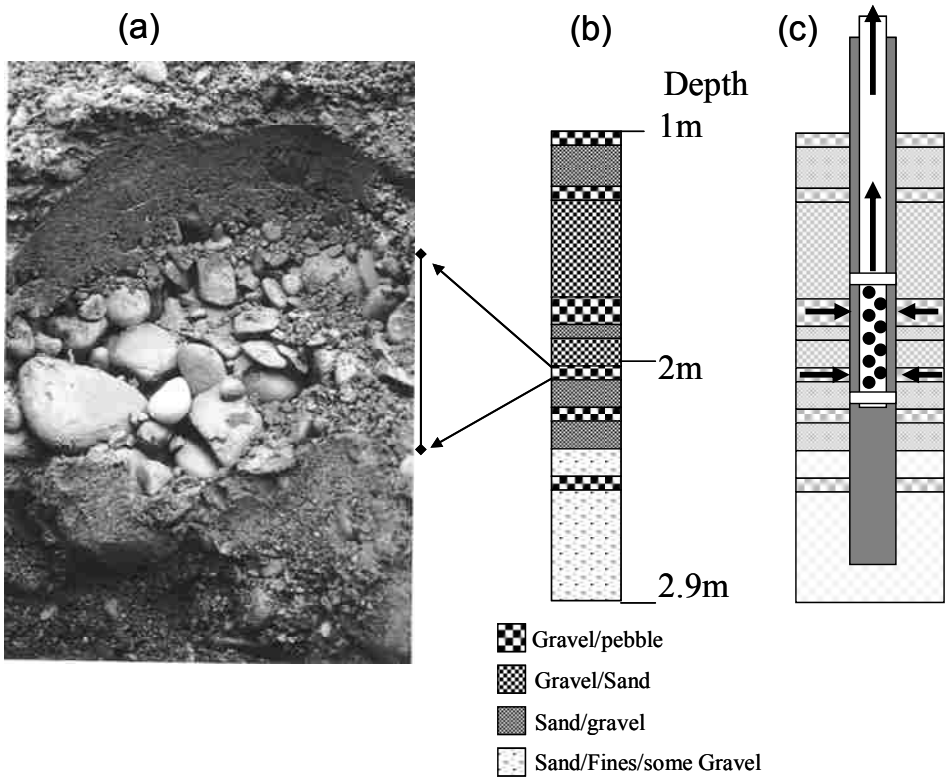

Figure 3: (a) Photograph of a vertical stratigraphic sequence, with upwardly fining material overlying a layer of coarse gravel (bimodal gravel - scale bar is 5 cm); (b) typical gravel profile (mapped using a clear plexiglass well and submersible video camera); (c) sampling hose design, showing foam packers for isolation of 1 meter well intervals, and side-oriented intake holes. Majority of discharge from well sampling is assumed to be drawn from high conductivity zones (preferential flow, shown by arrows).

unless flow was maintained over the probe body. We discarded respiration estimates from Nov 2004 through March 2005 due to a faulty YSI 200 probe, which was unable to compensate at low temperatures. DO was recorded after 3 minutes to allow for stabilization, and the procedure was repeated for the mesocosm inlets. Respiration was estimated as the change in oxygen concentration divided by the water residence time τ [hr], calculated from flow rate at the time of sampling, and multiplied by the porosity of the mesocosm to convert to respiration per unit volume of sediment.

(2) $$\text{Resp [mg/l sed/hr]} = \frac{\Delta DO}{\tau} n$$

Because the mesocosms were located above ground, we observed temperature changes, either gain or loss, depending on air temperature. Temperature gain was monitored using iButton data loggers (Dallas Semiconductor, Inc.) in the well intake, and

in two locations along the mesocosm gradient. An additional Vemco temperature logger was installed at the mesocosm outlets. Mesocosms were initially insulated with a layer of Reflectix insulation (7mm thick reflective material). In the summer of 2004 we observed warming in excess of 7 °C, and subsequently added layer of ½" bubble wrap (13mm) in August. A large 3m x 7m concrete curing blanket was added in December. Greenhouses were constructed over the mesocosms to maintain warm air temperature in the winter, and were shaded with tarps in the summer. With insulation, the average absolute value of temperature gain or loss was only 1.1 °C (± 1.0). The advantages of above ground location and general implication of temperature gain on mesocosm studies are discussed in detail in Chapter 4.

Respiration rates were initially transformed with the natural logarithm to approximate normality (transformed respiration still showed a positive kurtosis). We then used stepwise multiple regression with partial correlation to evaluate the effects of temperature, temperature gain, and oxygen on mesocosm respiration (SPSS ver. 12.0). Temperature gain is an artifact of the mesocosm design, so we corrected respiration rates by subtracting respiration attributed to gain. Outliers in dissolved oxygen and respiration rate were observed during changes in river hydrograph. The respiration estimate assumes that conditions within the mesocosms are at steady state; however, this assumption is violated during changes in river flow. We calculated change in discharge as the rate of increase or decrease in discharge over the preceding 24, 48 and 96 hour period (dQ24 etc.). We found that most outliers were associated with dQ24, and we systematically removed all respiration estimates from the dataset whenever dQ24 exceeded 1.0 cms/hr.

Respiration model

We developed a simple oxygen model with a weekly time step that predicts annual oxygen patterns observed in wells, using the respiration estimates measured with the mesocosms. We observed that DO in the river channel can be estimated using a linear regression with temperature: (DO = -0.2568 * (Temp) + 12.669; r^2=0.80). The annual pattern for surface water approximates a sine wave, so we modeled river DO as a sin function of time (b) with an amplitude (a) of 2 mg/l, an axis (c) centered on 11 mg/l, and a phase shift of +12 weeks:

(3) $$DO = a*Sin\left(\frac{(b+12)\pi}{52*180}\right) + c$$

We applied monthly respiration rates to the second week of each month, and interpolated for the weeks between. We then subtracted the annual respiration cycles derived from respective mesocosms, assuming a 10 to 20 day residence time, and compared the resulting wave form with the patterns actually observed in wells in the floodplain. The model assumes that the system is closed to diffusion from the atmosphere, and ignores the effects of mixing.

RESULTS

Seasonal and spatial patterns in dissolved oxygen

All surface water and groundwater sampling stations showed distinct seasonal trends in oxygen, typically with a summer minimum and winter maximum. Figure 4a shows a representative sample from the inlet of one of each pair of mesocosms 1 through 3 (June 2004 through June 2006). DO in the source water in the main river channel (inferred from continuous temperature data) varied around a sine wave pattern, averaging 11.1 mg/l, and ranged from 9 to 13 mg/l. The recharge zone well site showed a similar pattern, however the axis was lower (average 9.24 mg/l), the amplitude was 45% greater (5.9-11.7 mg.l), and the wave form divergence from the surface water was greater in the summer. This is what would be expected if respiration was highest in summer. The midgradient and discharge sites showed similar patterns, with a mean of 5.28 mg/l and a range of 3.7-6.2 mg/l. However, the oxygen waveform at these sites was flattened and skewed to the right. The midgradient site also showed a distinct downward deflection and recovery in late summer, which is another common signature in groundwater sites.

Departures from these waveforms, indicated by arrows, correspond with changes in the hydrograph (Figure 4b), or with changes in the rate of change of the hydrograph (Figure 4c). Hydrograph changes, both positive and negative, reflect departures from steady state conditions. There was a close correlation between river discharge and height of the water table in all wells, demonstrated by pressure transducers (Johnson 2003) and also water table-discharge regressions (Chapter 3). Every well in the aquifer showed a strong linear relationship, with r^2 typically exceeding 0.95 (range 0.66 to 0.99). Hence

river discharge may affect the steady state condition in the well environment, resulting in the outliers.

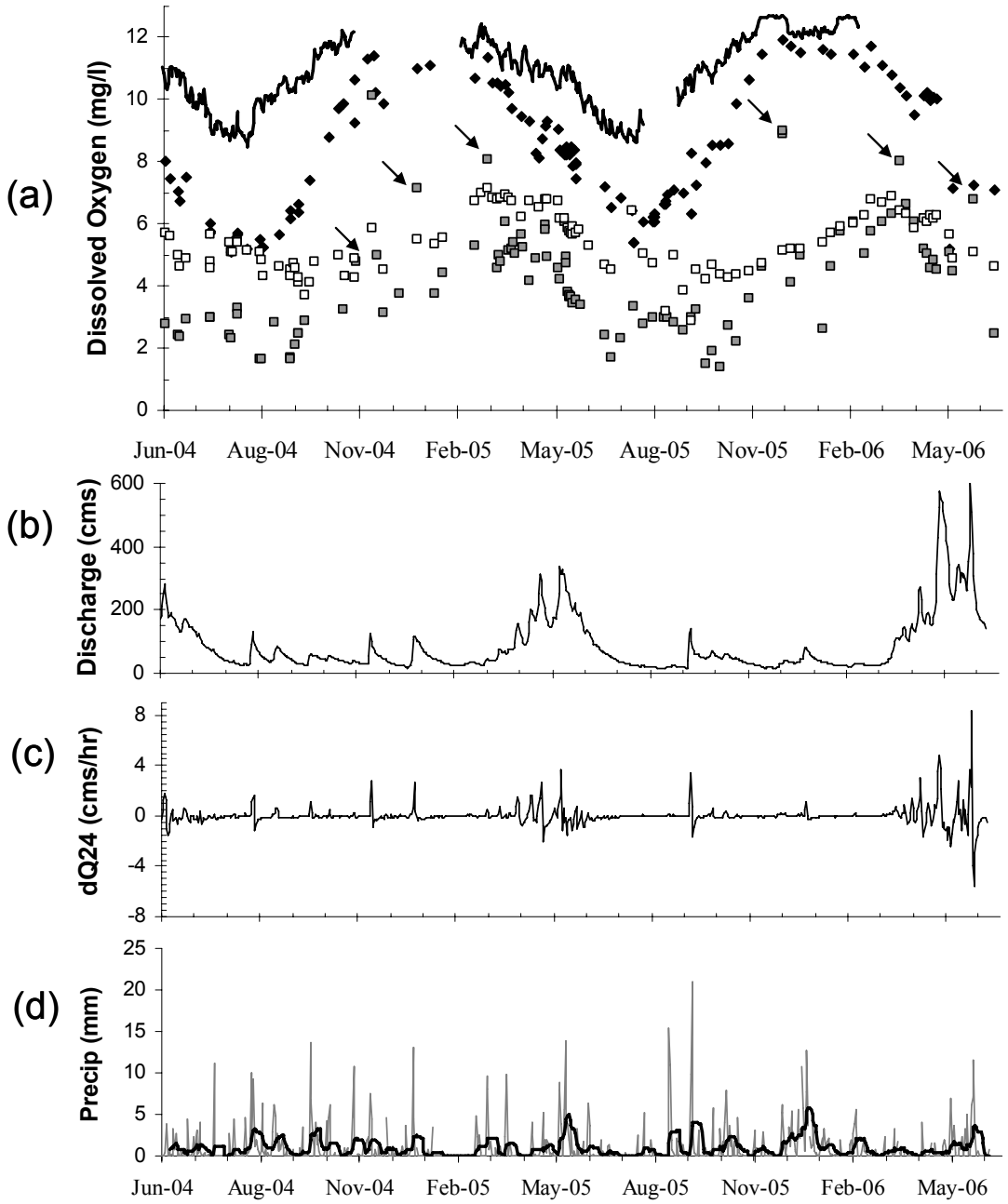

Figure 4: Annual cycle of dissolved oxygen, hydrograph, and hydrograph rate of change from June 2004 to June 2006; (a) DO from well water at three mesocosm sites (intake water). Solid line = river DO estimated from temperature, diamonds = recharge zone mesocosms (1a), closed squares = midgradient (2a), open squares = discharge zone (3a). Arrows show outliers due to non-steady state conditions (explained in text). (b) Discharge for the same time period, (c) Rate of hydrograph change over 24 hour period, and (d) precipitation (dark line is 10 day moving average).

The spatial pattern of oxygen systematics is shown in Figure 5. We note two basic patterns in oxygen distribution. There is a large scale pattern of oxygen recharge and depletion along the length of the floodplain, with higher oxygen in recharge zones in the winter and spring, and a large portion of the lower aquifer (upper left) becoming hypoxic in the fall. By late October, oxygen is at a minimum throughout most of the floodplain, and nearly 10% of the aquifer is hypoxic (<3 mg/l). More striking is the smaller scale pattern of local hypoxic zones, which retract in winter and expand in unison from the summer through fall. There is no direct explanation for these local hypoxic zones, although they must be related to localized patches of organic matter, or energy hotspots. While some of these hotspots are clearly located within or downgradient from buried debris jams, other locations includes areas of sandy channel fill, an alluvial fan, and an agricultural field. If low oxygen hotspots were the result of patches of fine sediments, we would expect to see corresponding steep gradients in potentiometric contours at such sites. Examination of Figure 2c provides no such evidence for reduced K at low DO zones (mesocosm site M2 and well 17), nor are such features evident elsewhere in the floodplain (Diehl 2004).

Vertical trends in oxygen distribution (Figure 6a through n) show two distinct patterns in vertical profiles: eight wells have relatively straight profiles, while four wells have distinct orthograde profiles (*sensu* Åberg and Rodhe 1942), with low oxygen in the top 2-3 meters. Two wells have only slight orthograde patterns. Although in two cases (HA17 and HA4), the oxygen inflection appeared to coincide with hydraulic conductivity, it is obvious from the range of profiles that neither K nor stratigraphy are good predictors of vertical oxygen gradients at the 1m scale. Wells closer to areas of river recharge (HA2, 3 and the entire inner transect) also showed strong seasonal separation between each vertical profile. Only in one well (HA13) did we see any evidence of a clinograde oxygen profile, with an increase of 1-1.5 mg/l in oxygen at the top of the well profile.

Flowpath Oxygen and Cumulative Respiration Patterns

The temperature DO relationship was generally linear and significant for all sites. (mean $r^2 = 0.68$, ranging from 0.28 to 0.95, $p<0.03$). The slope of this relationship

Figure 5: Oxygen isopleths.for shallow groundwater (0-1 meter below water table) for six sampling dates: Novemeber 2003 (base flow), February 2004 (pre-snowmelt), April 2004 (post snowmelt), May 2004 (flood pulse), July 2004 (receding limb), October 2004 (base flow). Circles show well locations.

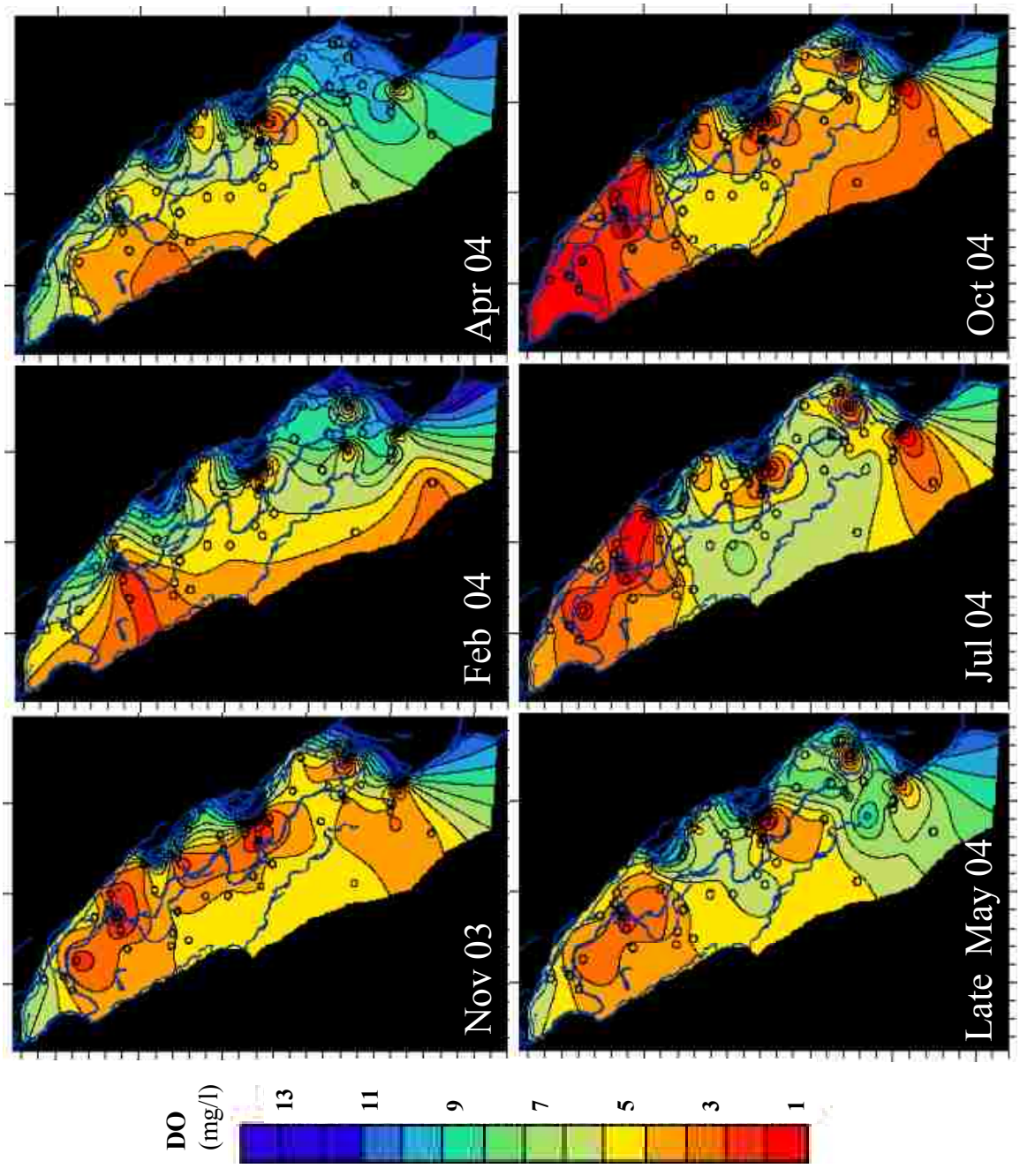

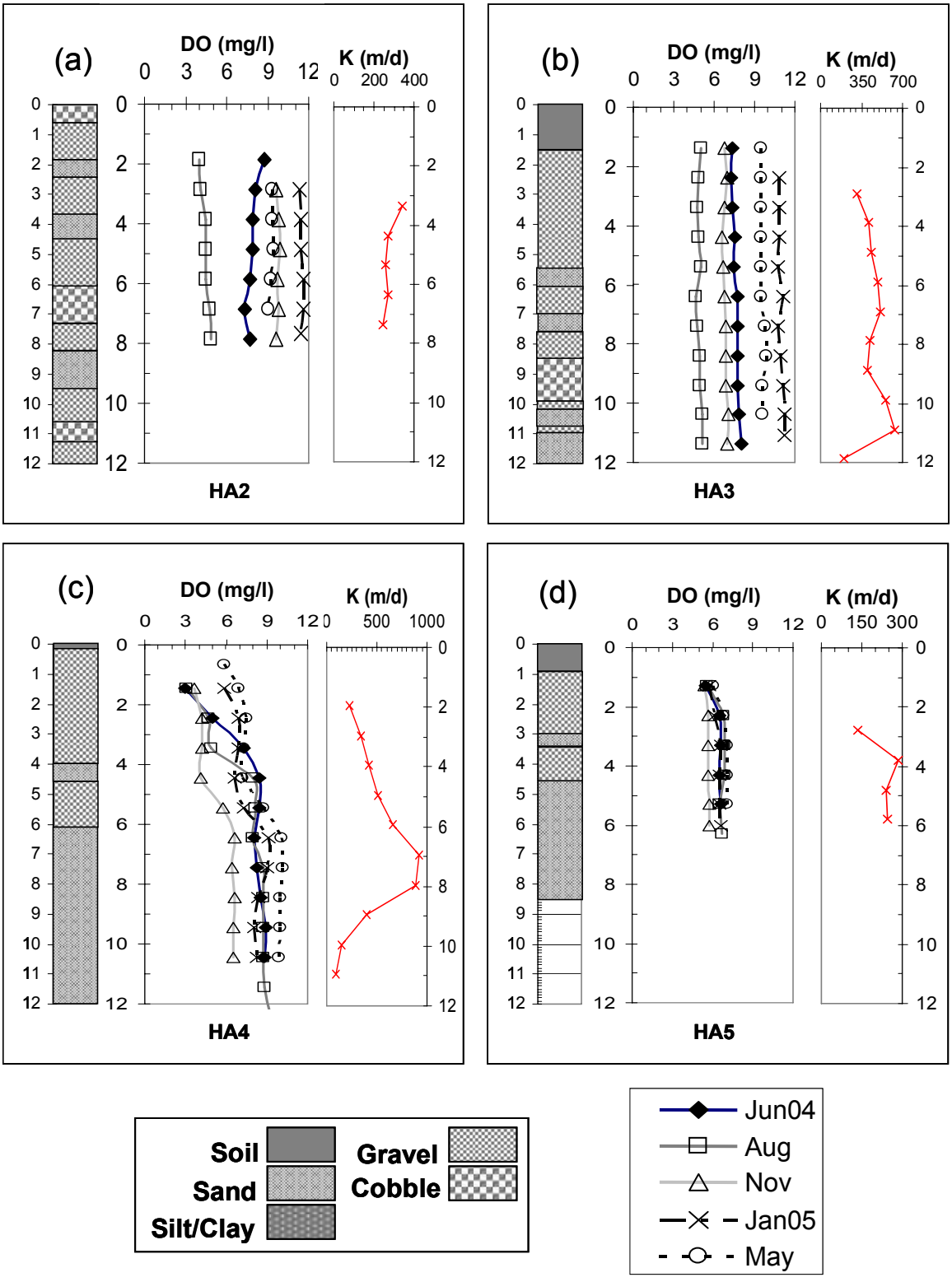

Figure 6: Vertical profiles for oxygen, hydraulic conductivity and general sediment grain size (interpreted from drilling logs).

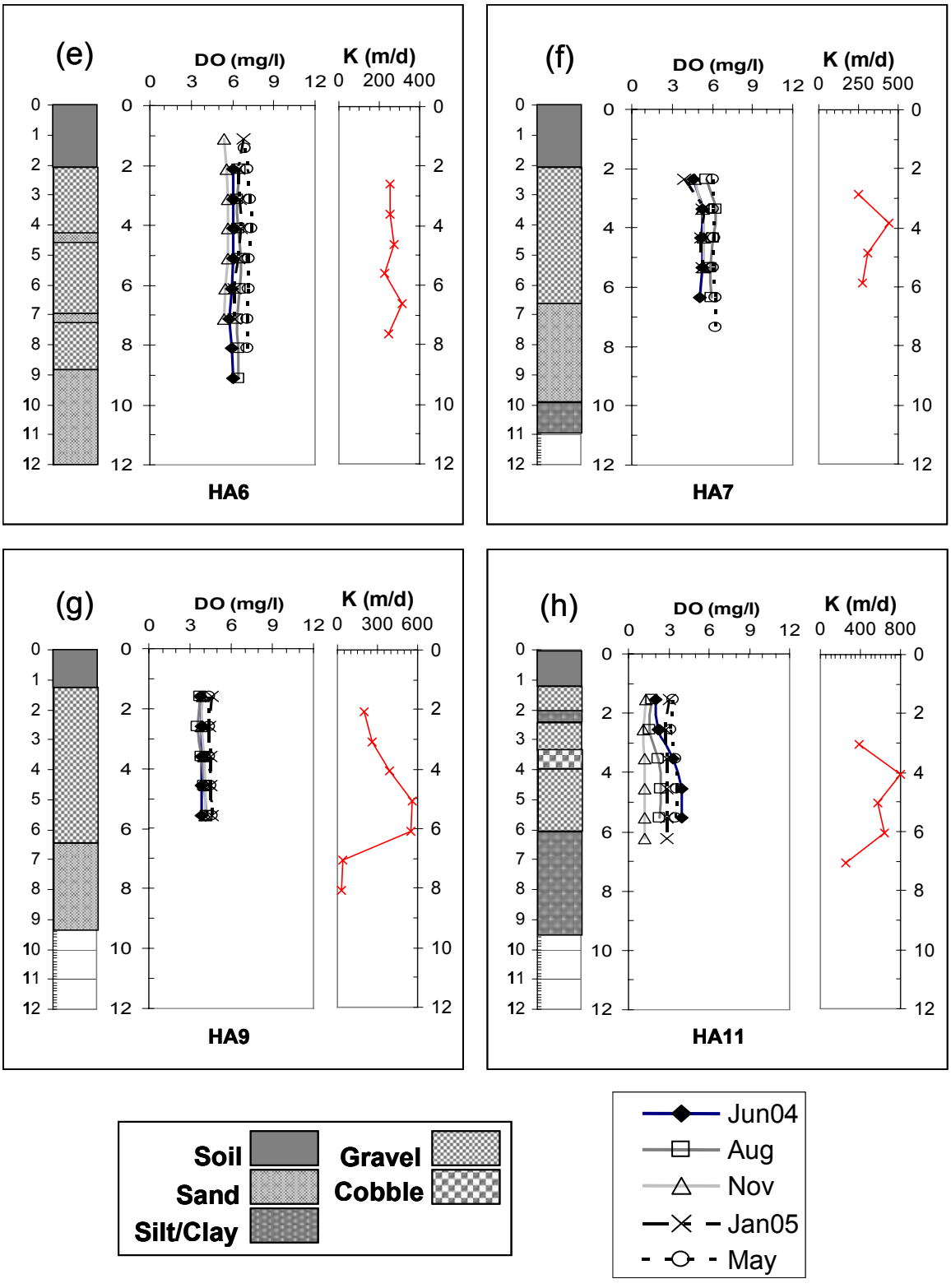
(e)
DO (mg/l)
K (m/d)
HA6
(f)
HA7
(g)
HA9
(h)
HA11
Soil
Sand
Silt/Clay
Gravel
Cobble
Jun04
Aug
Nov
Jan05
May

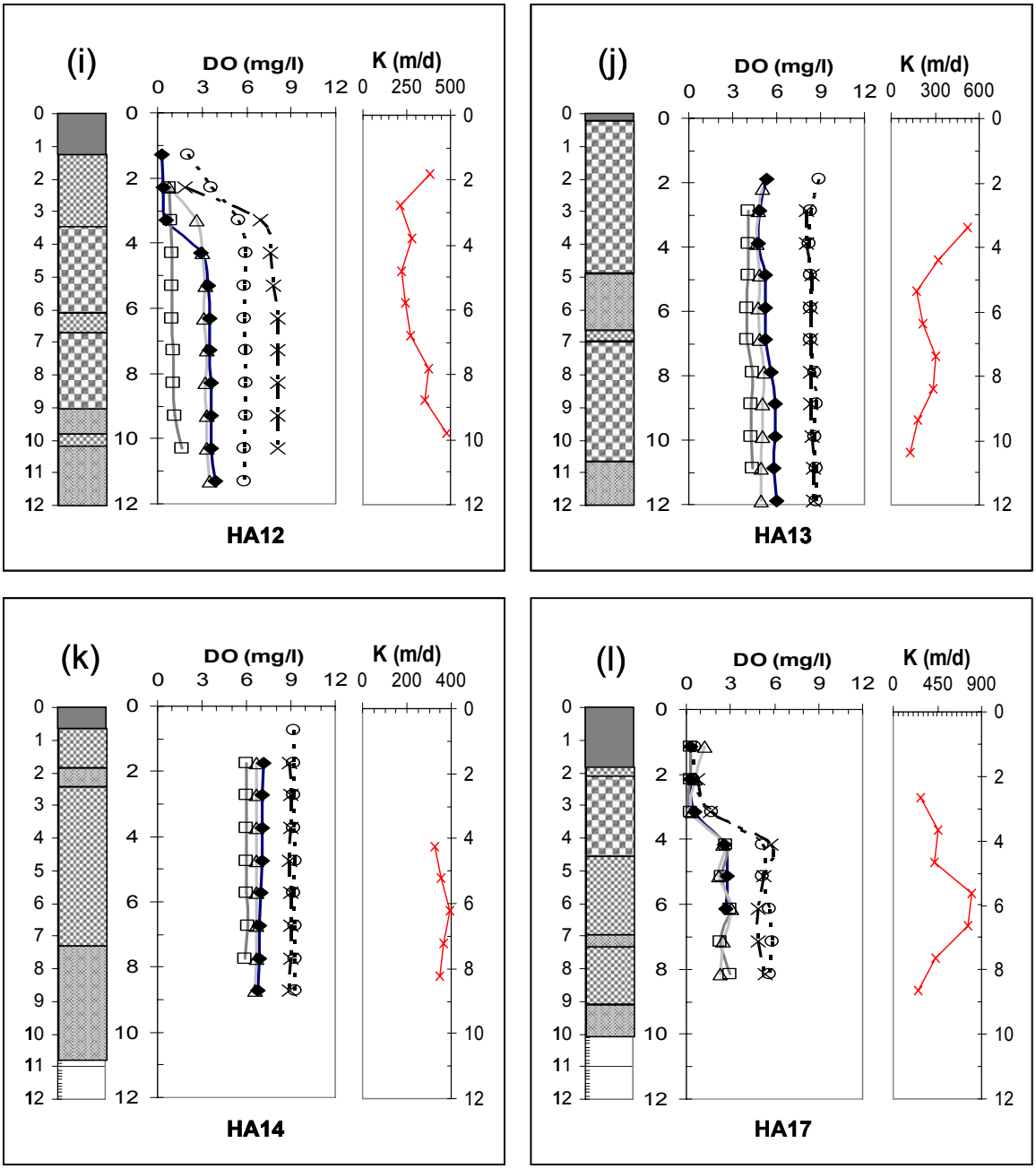
(i)
DO (mg/l)
K (m/d)
HA12
(j)
HA13
(k)
HA14
(l)
HA17
Soil
Sand
Silt/Clay
Gravel
Cobble
Jun04
Aug
Nov
Jan05
May

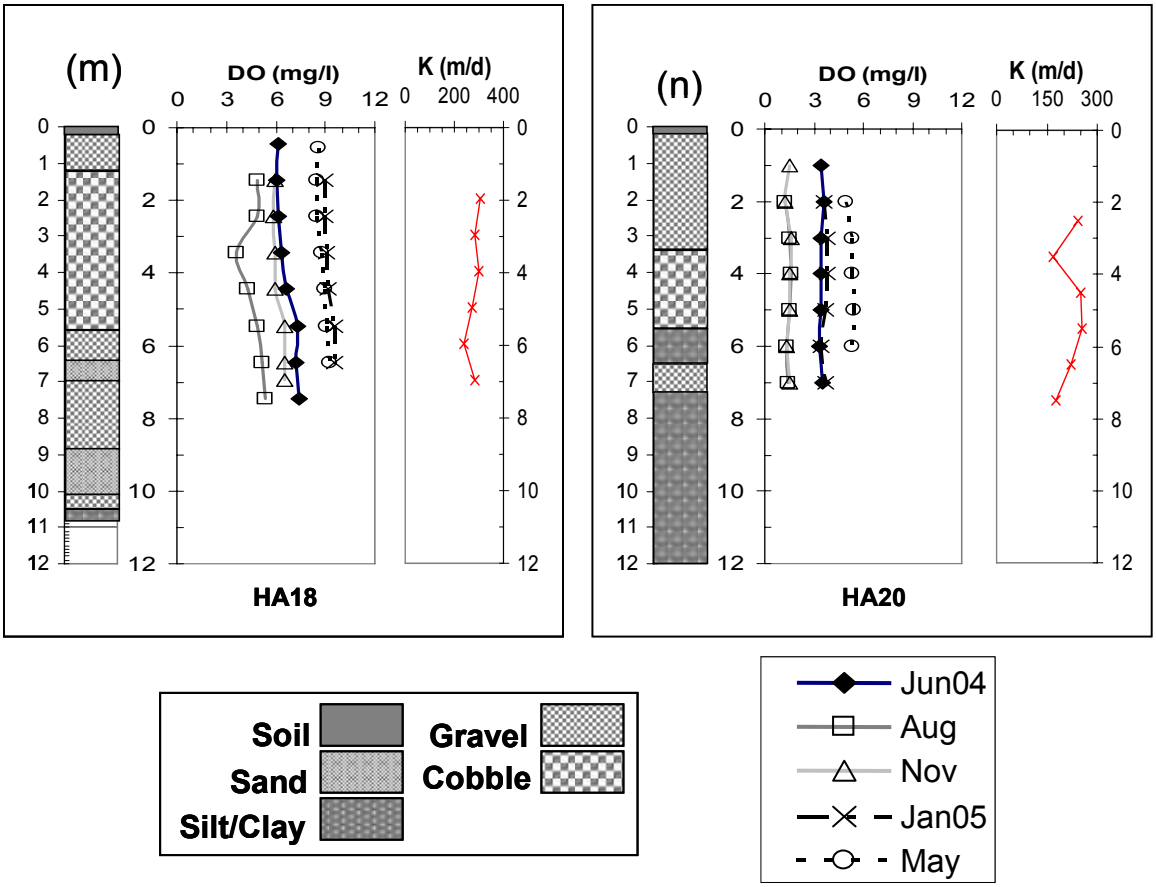

(Temp/DO sl) was not globally uniform and differed among sites. We believe this to be an indication of differences in cumulative respiration over respective river-to-well flowpaths. In Figure 7a we see that groundwater DO shows a parabolic or U-shaped response to flowpath residence time: DO generally decreases as flowpath length increases with high variability for the short flowpath lengths. This considerable variation in DO for the short flowpaths implies a high range of respirations rates near aquifer recharge zones, and corresponds with the DO distribution in Figure 5. This pattern corresponds with the observations reported by Findlay (1995) and Baker et al (2000a). The subsequent rise in DO for very long flowpath residence times is more dramatic than the slight rise evident in (but not noted by) Baker et al (2000a). [Their maximum reported residence time was < 10 days].

Cumulative flowpath respiration (CFR) was highly skewed, with a median of 7.5 µg O_2/l sed/hr (range 0.81 to 122.2). In Figure 7b we see that CFR declined exponentially with flowpath residence time – suggesting that very high respiration rates occur only on

very short flowpaths in river recharge zones. We caution that both axes in this figure are a function of our estimate of residence time. An alternative approach using a surrogate for residence time (the site-specific slope of the regression of depth to water (DTW) table vs river discharge, DTW slope, essentially a stage-discharge function, see Chapter 3) also produces a similar but slightly weaker exponential response ($r^2 = 0.285$, $p<.05$).

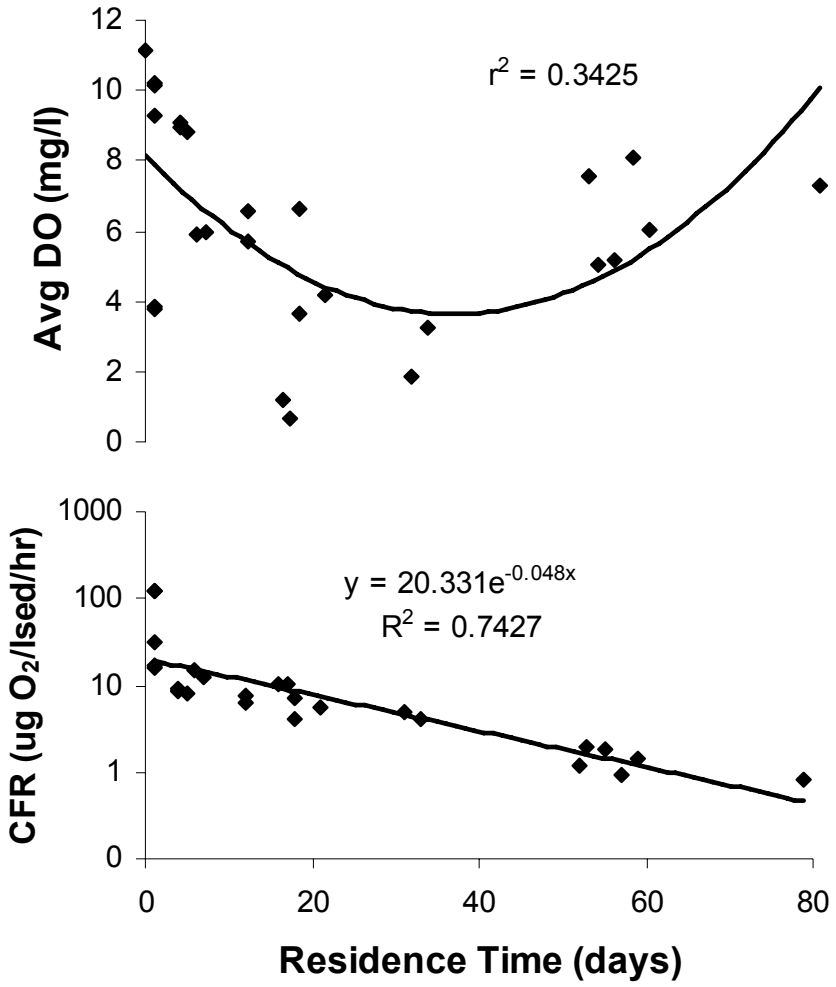

Figure 7: Effect of flowpath residence time on: (a) mean annual average DO; (b) cumulative flowpath respiration rate (CFR).

Mesocosm Community Respiration

Community respiration measurements from the mesocosms showed a great deal of variation. Respiration showed the strongest correlation with temperature gain for all sites (Table 1), and a weaker correlation with temperature. Temperature gain is an artifact of the mesocosm environment. Normal groundwater flowpaths would not likely be

Table 1: Summary of regression models. Columns two and three show multiple regression models for effects of temperature gain and inlet temperature on respiration for each mesocosm.. Beta values are partial correlation coefficients, and r^2 in column three is for the combined model. Corrected respiration rates are shown in column 4. Oxygen vs. temperature regressions are shown in column five.

			Tgain		Tgain and Temp		Corrected Resp (mg/lsed/hr)	Dissolved Oxygen vs Temp	
SITE	Depth	Zone	β	r^2	β	r^2	Mean (± sd)	*b*	r^2
M1a	sh	Recharge	0.540	0.28 *	0.390	0.39 *	3.17 (± 1.35)	-0.365 (± 0.012)	0.81 *
M1b	sh	Recharge	0.576	0.33 *	0.315	0.39 *	2.99 (± 1.46)	-0.375 (± 0.018)	0.81 *
M2a	sh	Midgradient	0.555	0.30 *		ns	2.38 (± 2.05)	-0.494 (± 0.054)	0.45 *
M2b	de	Midgradient	0.717	0.51 *		ns	3.29 (± 3.21)	-0.588 (± 0.090)	0.30 *
M3b	sh	Discharge	0.768	0.59 *		ns	2.54 (± 2.96)	-0.744 (± 0.064)	0.57 *
M3a	de	Discharge	0.650	0.42 *		ns	1.83 (± 0.99)	-0.592 (± 0.057)	0.52 *
M4b	sh	Discharge	0.724	0.52 *		ns	1.85 (± 1.94)	-0.269 (± 0.060)	0.20 *
M4a	de	Discharge	0.657	0.37 *	-0.286	0.41 *	2.04 (± 2.14)	0.022 (± 0.059)	0.00 ns

*$p \leq 0.001$

exposed to diel cycling and increased warmth with distance, except in wells very close to river recharge zones, or possibly in cases of very shallow groundwater. We did not observe diel temperature cycling in any of the mesocosm inlets (Chapter 4), and cycling was not observed in any of the well loggers (Chapter 3) except where there was direct recharge from river water. We therefore factored out the effects of temperature gain, using the slope of the relationship for each respective mesocosm. Once this correction was made, temperature showed a positive correlation with respiration rate at only the two recharge zone mesocosms (1a and 1b) and a weaker correlation with one of the discharge zone mesocosms (4a – shallow).

Another source of variation was the result of non-steady state conditions, when concentrations of inlet solutes changed at rates that were different from outlet concentrations. We identified two causes of this. Diel cycling has a major effect on river temperature, oxygen and other solutes, and the effects propagate into the aquifer in areas with short residence times. Diel cycling in the hyporheic zone also occurs at the recharge zone mesocosms. On two occasions we confirmed diel cycling of oxygen and respiration, with respiration estimates varying by 100% and including negative values. We were unable to correct for this effect, and must assume that this source of variation is minimized with repeated measurements over the course of the year. A second cause of non-steady state conditions was apparent from changes in the hydrograph. Rapid changes in hydrograph correspond with rapid changes in water table. During these periods we observed strongly negative and strongly positive respiration outliers when respiration was regressed against temperature (Figure 8). Recent changes in hydrograph ($d24Q > 1$ cms/hr) appeared to best predict respiration outliers, although the effect was clearly more visible in the recharge and midgradient zones of the four mesocosms sites (Figure 8a and b). We conservatively and systematically removed all respiration estimates when discharge exceeded this value, regardless of whether the estimate appeared to be an outlier. Once these corrections were made, a few (<5%) of the respiration estimates were slightly negative. Despite this obvious error, instead of assuming that they were below detection (≈0), we retained the negative values, so that our calculations of monthly and annual respiration were not biased.

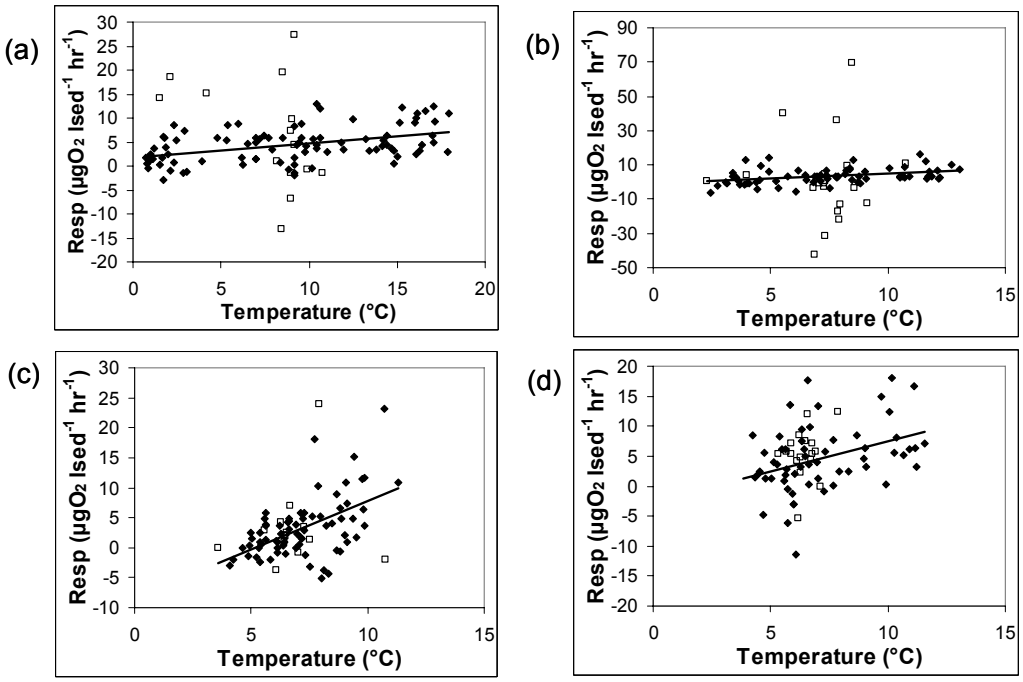

Figure 8: Uncorrected mesocosm respiration rate as a function of temperature. Respiration outliers indicated by open squares are associated with non-steady state conditions (hydrograph change: dQ24 > 1 cms/hr). (a) mesocosm M1a - recharge; (b) mesocosm M2a - midgradient; (c) mesocosm M3a – discharge; (d) mesocosm M4a – discharge II.

Monthly average respiration rates for mesocosm pairs one through three (Figure 9 a-d) show a strong seasonal pattern of respiration. The first six months of measurements produced rates that had much higher variance. This was likely the result of insufficient insulation and temperature change, as discussed above. Even when corrected for temperature gain, respiration was almost twice as high as in the same time period in the following year of operation. We suspect that this may be a result of biofilm formation and response to disturbance, or a container effect (silicone sealants and epoxy used in mesocosm construction). Within mesocosms pairs, there were occasional differences in rate, primarily in November and December. These differences do not consistently relate to depth of mesocosm source water. There were differences in seasonal pattern, more clearly shown when data from mesocosm pairs are combined (Figure 9e). The recharge zone mesocosm showed a seasonal pattern with rates rising in May and falling in October. All other pairs of mesocosms had an annual cycle with two modes. Rates rise in April/May, then fall in June, and remain depressed until October/November. In the fall they rise again to their highest levels, returning to lower levels in February.

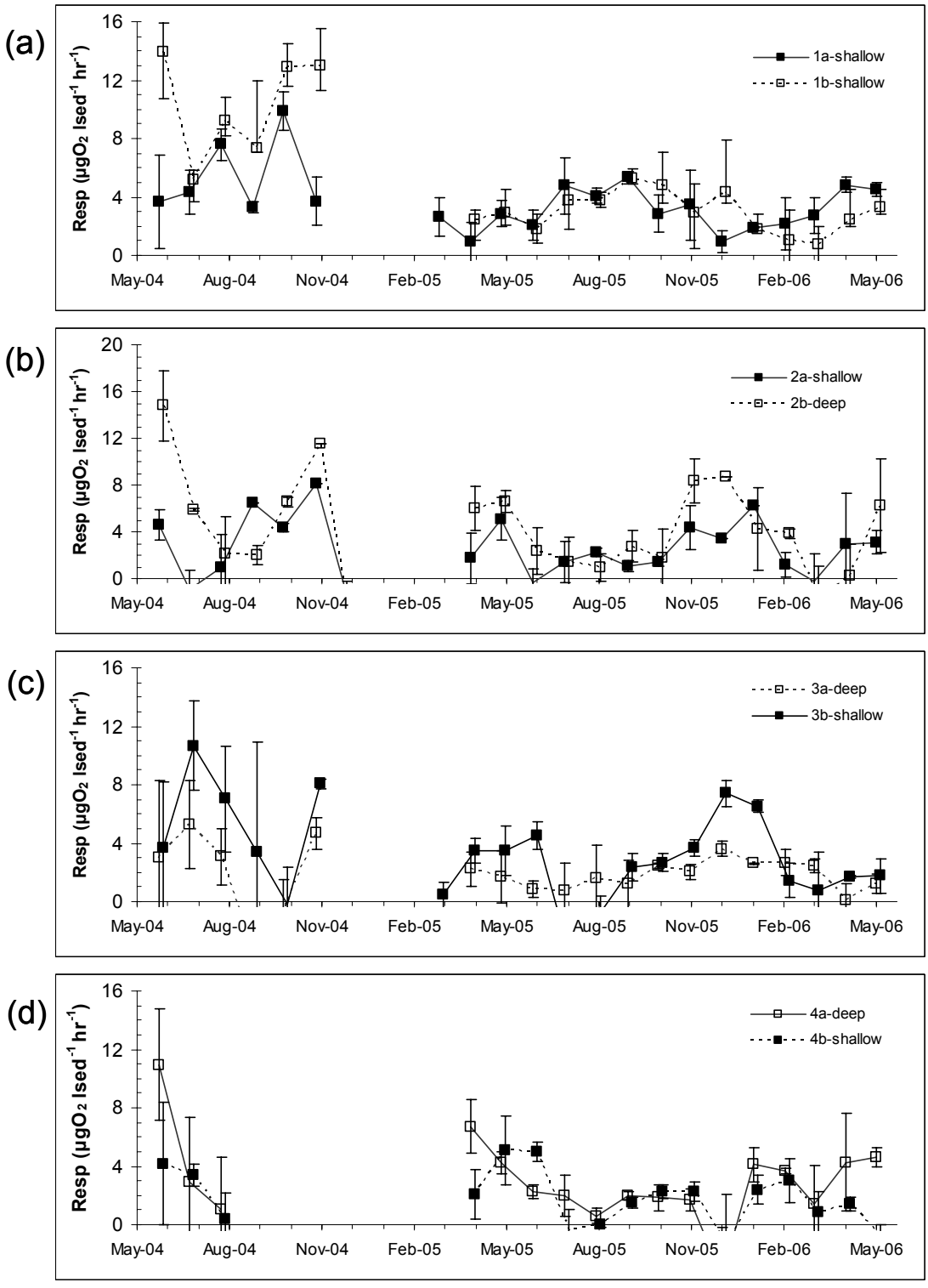

Figure 9: Two year cycle of mesocosm community respiration, showing seasonal trends in community respiration, and high respiration rates during the initial incubation period. Shallow mesocosms (0-1m) are closed symbols, while deep mesocosms (1-2m) are open symbols. (a) recharge zone (same depth); (b) midgradient (shallow and deep); (c) discharge – spring head (shallow and deep); (d) discharge II – spring brook.

(e)

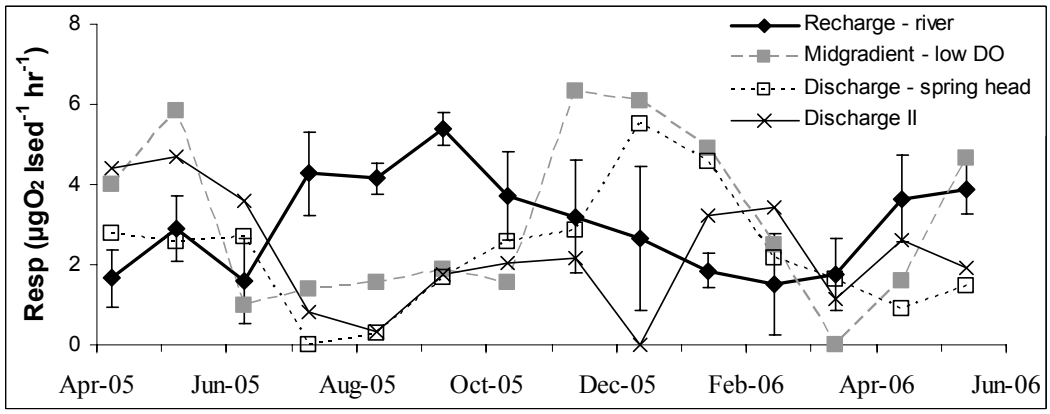

Figure 9: (e) combined respiration for each hyporheic position, averaged for both depths. (Error bars indicate +/-1 SE, shown only for recharge site for clarity).

Respiration model

We used the respiration rates for mesocosm 1 (recharge) and mesocosm 2 (midgradient) as the two representative seasonal patterns of respiration. We refer to these two patterns as summer respiration and winter respiration respectively. We simulated a short flowpath by using the summer respiration pattern and a 10 day residence time, and a longer flowpath using the summer pattern and then winter pattern, with a 10 day residence time for each. The results of the model show that summer respiration resulted in a lowering of the axis of the annual cycle, and an increase in amplitude (Figure 10).

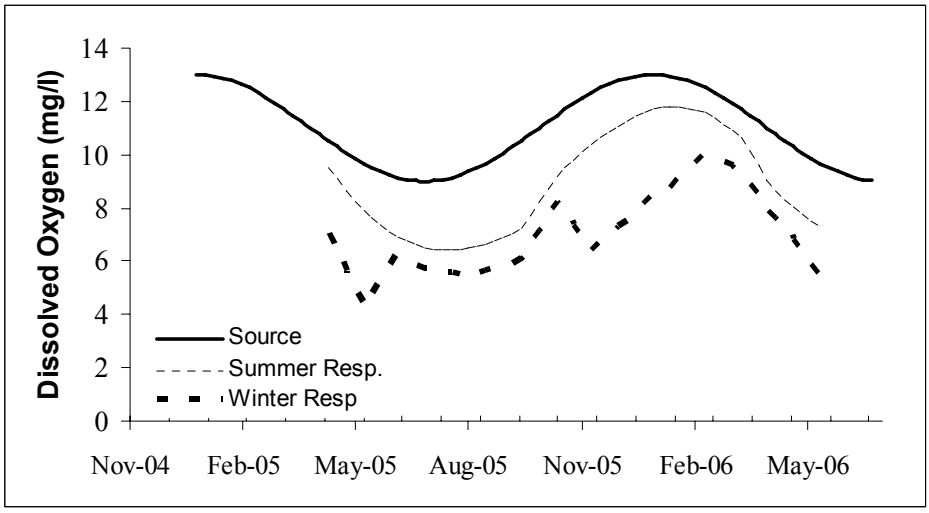

Figure 10: Modeled seasonal oxygen patterns, using a sine wave as the source concentration, and applying the summer and winter respiration cycle using data from figure 8. Summer respiration results in a downward shift of the annual oxygen cycle, while winter respiration results in a flattened and skewed annual DO cycle, very similar to seasonal pattern shown in Figure 4.

The summer respiration waveform also shows the same pattern of summer divergence and winter convergence with the source water, as we saw in Figure 4a. The winter respiration model produced an irregular and skewed profile, with the wave tending more to the right, and a downward deflection in September/October, also similar to the midgradient waveform in Figure 4a.

DISCUSSION

Sources of energy: rivers, soils or buried organic matter?

The seasonal pattern of oxygen distribution across the floodplain clearly shows areas of high biogeochemical activity, indicating high spatial heterogeneity of energy resources. These features are shallow, limited to the first few meters below the water table. Contouring of the oxygen isopleths may not provide a reliable estimate of the size of these features. However, based on their depth of 1-4 meters, and assuming that vertical hydraulic conductivities are typically one tenth that of horizontal conductivity (Fetter 2001), they are at least 10-40 meters in the horizontal plane. If these patterns are the result of interaction with the soil horizons, then the influence of surface energy sources is clearly patchy. However, these low oxygen hotspots persist over time, the orthograde profiles shifting uniformly towards higher oxygen levels, but retaining their shape. We suspect these hotspots are caused by buried organic matter, probably associated with buried wood debris jams. However, such deposits may also interact with rhizosphere biogeochemistry. We believe that these may be common features in fluvial groundwaters. Similar low DO hotspots were evident on the Boyne River, Ontario, CA (Carlyle and Hill 2001) and Queets River, WA (Clinton 2001). We propose that nested well grids and analysis of core samples at finer scales would be a reasonable next step towards understanding the anatomy of these biogeochemical hotspots.

We observed two basic patterns of seasonal respiration in the Nyack floodplain aquifer: summer respiration peak and bimodal pattern, the latter with spring and winter respiration peaks. The summer respiration pattern is what we would expect if energy sources are derived directly from the river. This seasonal cycle for recharge zone wells is similar to observations on stream bed respiration made by Pusch and Schwoerbel (1994), with low rates through March and elevated rates in May through September. Jones et al

(1995) also observed an annual respiration cycle in the shallow hyporheic zone, with a respiration peak in June and July. The second pattern, shown by all other mesocosms, showed a bimodal annual cycle, with respiration peaks in May, and a later and higher peak in the fall and winter. To our knowledge, this is the first evidence for a winter respiration peak in aquatic systems, although the seasonal rates reported on the Rio Calaveras floodplain (Baker et al 2000b), also showed similar trends (although n=1 for the winter measurements). The phase shift resulting in the winter respiration pattern may represent a resource pulse, originating from the river, and propagating through the aquifer. However, this does not concur with our estimates of flowpath residence time for the respective mesocosms. If a pulse was truly propagating through the aquifer, we would expect a phase shift for peak respiration of 10-20 days for the midgradient mesocosm (M2), instead of the observed shift of 90 to 120 days or more. Secondly, all mesocosms showed an initial, but often smaller, respiration increase in May, apparently synchronized among sites and occurring during the flood pulse (i.e., with no apparent phase shift). We propose that suppressed summer respiration and a fall-winter respiration maximum may in fact be related to temperature. Respiration responds directly to temperature (once temperature gain is factored out) in only three of the eight mesocosms (Table 1). However the fall rise and winter peak in respiration on longer flowpaths, at aquifer temperatures of roughly 5-6 °C, also coincides with lower temperatures and lower respiration rates near the river (typically 0 to 4 °C). In other words, metabolism on longer flowpaths may be affected by energy sources originating from the river, but only when temperatures are low enough to inhibit rapid metabolism of these resources in the channel and in aquifer recharge zones. Hence energy from the river (such as DOC) may have a much longer uptake length in the winter, as a function of the spatial distribution of temperature in the aquifer. When we compare respiration rate in the aquifer to temperature in the river source water, the regressions in Table 1 improve significantly for one of the three sites ($r^2 = 0.42$ for mesocosms 3, $p<.01$).

There are several implications of this winter respiration pattern. This phase shift in respiration can be used as an indication of microbial production, which in turn would affect the production of invertebrates. Where longer residence time groundwater erupts to the surface, this winter peak may ultimately influence production and energy flow in

floodplain springs and river benthos in upwelling zones. There may therefore be an energetic advantage for groundwater upwelling, beyond the well recognized effects of temperature and nutrients (Stanford et al 2005), potentially offering an explanation for the life history of winter stoneflies.

The spring respiration maxima, common to all mesocosm sites, may be explained by either energy from the river during the flood pulse, or rising water tables increasing the exchange of energy between groundwater and the vadose zone. As we have previously mentioned, water depth in wells is strongly correlated with river hydrograph. Again, considering relative residence time of the sites, and the fact that the midgradient and discharge zone sites showed higher respiration rates than the recharge zone, we suspect that spring respiration is the result of the water table rising into the vadose zone. Alternatively, this may be the result of a rapid increase in flow rate caused by the change in gradient, and also the change in flow lines (i.e., changing flowpaths). Evidence for the latter can be found in the sudden drop observed in oxygen along entire vertical profiles observed at many sites during the rising and falling limb of the hydrograph (Figure 6 a-b and j-n).

When we compare the modeled oxygen cycle to the observed annual oxygen cycle, clearly the general pattern is reproduced, validating our observation of a winter peak in mesocosm respiration rates. Looking more closely, the deflections in the modeled waveform, both in May and November, roughly correspond with the oxygen deflections observed in June and October filed data. These deflections are probably caused by rapid changes in respiration rate at certain points in time along the seasonal cycle. This is in fact what we observed in the mesocosm respiration rates, and any divergence between the timing of modeled and observed deflections in DO is probably due to our calculating monthly average rates. There are two implications of these rapid respiration rate changes. An energy pulse occurs during flood pulse and/or rapid rise in water table elevation (energy contribution of the vadose/soil horizons). Secondly, energy is suddenly available in the fall to longer flowpaths, corresponding with a decline in river temperature and aquifer recharge zone respiration. The energy source in the latter case could be riverine DOC, which would propagate further into the aquifer under these conditions. Alternatively, the timing of this fall rate increase corresponds with the oxygen minima,

after which reduced species, including methane, might be oxidized with the rise in bulk oxygen concentration (see Chapter 6 for additional evidence of a methane subsidy).

In comparison to other microcosm studies, the respiration rates reported here are some of the lowest ever observed in hyporheic sediments (Table 2), and are almost two orders of magnitude lower than previous lab-based measurements from the same study area (Craft et al 2002). We admit to uncertainty in our respiration estimates, a consequence of the high temporal variability, effects of non-steady state conditions, and the substantial effect of correcting respiration for temperature gain. One obvious explanation for our lower rates is that long lateral hyporheic flowpaths such as ours are decidedly energy poor compared the many studies from the shallow hyporheic zone (stream bed sediments). Our mesocosms were also essentially free from particulate organic matter, which is probably one of the most important factors in sediment community respiration (Hedin 1990). Several of the comparative estimates cited in Table 2 are also from the Flathead basin; however, the observed differences may be a function of the choice of methods. In one case, the production estimates based on thymidine uptake (Ellis et al. 1998) predict an oxygen demand that is reasonably close to our measurements. The two remaining sources (Craft et al 2002 and M. Pusch unpubl data) were both based on lab incubations, and were not *in-situ*. Given the high variance and relatively high magnitude that we observed in the first six months of mesocosm operation (Figure 8), this difference could in part be due to the effects of disturbance in transporting sediment to the lab. Another important factor is that the latter two studies used a much smaller grain size, and larger grain sizes may have lower respiration rates per unit volume (Jones 1995).

We can use an alternative method to compare literature values of aquifer respiration, calculated from well transects using the equation of Chapelle (1993). This is equivalent to the CFR calculation described previously, and is based on the change in oxygen concentration, the average linear velocity, and the length of the flowpath. We express some caution in employing this method, for reasons discussed in more detail below. Malard and Hervant (1999) reviewed the relevant literature, to which we add a more recent estimate from the Queets River (Clinton et al 2001). These estimates were originally reported in terms of rate per unit of water, so we multiplied by as assumed

Table 2: Summary of aerobic respiration studies in hyporheic sediments.

Location	Type †	Rate ($ugO_2/hr^{-1}lsed^{-1}$)	Season	Organic Matter: Grain Size	Organic Matter: % AFDM	Reference
Steina (GE)	SB	326 (64-960)	annual average	1-2 mm/ 2-4 mm	0.58%	Pusch and Schwoerbel 1994
Sycamore Creek (AZ)	SB	50-4410	annual range	sand/fine gravel	0.0031-0.010%	Jones et al 1995
*Kalispell Aquifer (MT)	FP	5.44 (2.06-10.44) ‡	summer	48 mm	bdl	Ellis et al 1998
		1.77 (0.79-3.16) ‡	winter			
Rio Calaveras (NM)	FP	275 (± 106)	spring	1-2 mm	1%	Baker et al 2000
		148(± 85)	summer			
		233 (± 106)	fall			
		455 (n=1)	winter			
	SB	370 (± 106)	spring			
		0.00 (± 0.00)	summer			
		465 (± 60)	fall			
		212 (n=1)	winter			
Kalispell Aquifer (MT)	FP	133.8 (± 97.5)	spring-fall	8-12 mm	bdl	Craft et al 2002
Hugh White Creek (NC)	SB	32(± 16.0)	fall	11.3 mm	1.5(± 1)	Crenshaw et al 2002
Two Ocean Lake Creek (WY)	SB	250 (160-550)	summer?	gravel/sand	0.0026-0.020%	Marshall and Hall 2004
Nyack Aquifer (MT)	FP	180 (60-360)	summer	8-12 mm	bdl	Pusch (unpubl. data)
Nyack Aquifer (MT)	FP	2.7 (bdl-6.3)	annual average	17.6 mm	bdl	Reid et al 2007

† SB = stream bed (vertical hyporheic sediments), FP = floodplain (lateral hyporheic sediments)

‡ Estimated from aerial production (Thymidine uptake); Assuming BGE = 0.3, RQ = 0.85, C:O = 0.375, grain size 24mm, and 0.1512 m^2 per liter of sed

porosity (*n*) of 0.25 to 0.4 (coarse gravel, Fetter 2001) to convert to a rate per unit sediment (which is more typical of microcosm studies, and more useful in terms of scaling up the results). We arrive at an average CFR from literature values of 44.9 to 71.8 μg O_2/lsed/hr (depending on *n*) and a range of 0.7 to 195.5 μg O_2/lsed/hr among the ten studies and eight systems. These literature CFR rates are within the range of both our mesocosm respiration rates and floodplain CFR rates, but our values (via both methods) are on average an order of magnitude lower. Estimates from the Stillaguamish River, WA (Vervier and Naiman 1992) and Mirabel Canal, France (Marmonier and Dole 1986, summarized in Malard and Hervant 1999) are closest to our estimated rates.

Limitations, Assumptions, and Future Directions

The vertical profiles help illustrate one of our major assumptions and a significant challenge in sampling at the floodplain scale. Typically, vertical profiles of solutes in the subsurface are developed from sampling sediment pore water from boreholes, or from nested wells with short open intervals. The former is expensive and not amenable to repeated sampling to capture variation over time. The latter requires a prohibitive number of wells at the floodplain scale. Continuously slotted wells are a reasonable compromise. However, we stress that the conclusions about subsurface biogeochemistry are limited to the most permeable layers in the sediment profile (preferential flow zones) from where most of the water is drawn (Figure 3c).

We can estimate the percentage of aquifer material that our observations apply to. We have observed that these preferential flow zones consist of well sorted medium and fine gravel, typically 4-5cm wide, sandwiched by layers of much less permeable sands and sand/gravel. The well sorted material has an intrinsic permeability that is orders of magnitude larger than the mixed material. We estimate a K of 12,000 m/d using Hazen's equation, assuming a median grain size of 15 mm (Fetter 2001). Using the same equation, well sorted sand (1 mm grain size) would have a K of 44 m/d, while poorly sorted material would be much lower (<<1 m/d). We know that average bulk hydraulic conductivity, based on pneumatic tests and a floodplain scale hydrogeologic model (Diehl 2004) is approximately 400 m/d. Using a binary mixing model, with K values of 12,000 and 1 as the two end members, and the output K as 400 m/d, we estimate that

preferential flow zones are only about 3%, or 3cm out of every meter in depth. Our observations on oxygen distribution, although they describe the most hydrologically dynamic part of the aquifer, and may be relevant with respect to groundwater – surface water exchange and invertebrate population in the aquifer, are nevertheless representative of only a small part of the aquifer. With higher resolution sampling, we might in fact conclude that 90% or more of the aquifer may be anaerobic.

Another major assumption pertains to interpreting the spatial patterns of oxygen distribution through interpolation. Because the aquifer is a flow environment, and is anisotropic, contouring can provide only an approximate distribution of oxygen or other solutes. With interpolation, a given point upgradient may well predict a point downgradient, but the reverse is not necessarily true. We would also expect that the low oxygen zones would more likely resemble the redox plumes commonly described in the subsurface contamination literature (Wiedemeier et al 1999), which are typically elliptic and oriented along the axis of groundwater flow. Finally, we assumed that aquifer recharge primarily occurred at certain points along only the main channel. However, this ignores smaller scale exchange near springbrooks, and the change in patterns of groundwater exchange with changes in river discharge (Poole et al submitted). A more realistic distribution would require coupled flow and solute transport models. As of yet, we know of no such 3 dimensional models for dissolved oxygen.

Despite our uncertainty in the absolute range of aerobic respiration rates, we feel that our model provides strong supporting evidence not only for the seasonal patterns observed, but also the magnitude of respiration rates, at least for the mesocosms and in longer flowpaths. The accuracy of the modeled oxygen concentrations rests on the assumption of residence time. The modeled 10 to 20 day residence time is realistic for the midgradient site, compared to our estimate of 7 to 19 days based on temperature lag (Chapter 3). While the oxygen waveform for this site is adequately represented by our model, the modeled oxygen values are somewhat high. Also, the residence time for the recharge mesocosm probably is no more than 1-2 days, based on radon and temperature data (Johnson 2003), compared to our 10 day modeled residence time. Hence the modeled oxygen values, which approximate the observed values, are probably based on a respiration rate that is too low, by a factor of somewhere between 2 to 5. There are

several explanations for these discrepancies. First, the mesocosms are filled primarily with coarse sediment, with only a small area of contact with fine sediment at the bottom of the mesocosms. Actual flowpaths will have extensive contact with fine sediments at both the top and bottom of the coarse sediment layer, and this interaction would be enhanced by any changes in orientation of preferential flow zones (i.e. interbedded sediments). Secondly, the mesocosm respiration rates are valid only for the immediate spatial vicinity of the respective well sites, whereas the actual respiration along a flowpath is a cumulative function of respiration along the entire flowpath length. In fact, cumulative average respiration for the mesocosm sites is probably higher than that measured within the respective mesocosms. With respect to the reacharge zone sites (M1), respiration rate probably increases substantially as one approaches energy sources from the river; a reasonable assumption considering the rates reported for shallow hyporheic metabolism (Table 2). Secondly, there may be more uncertainty in the estimates from the recharge zone mesocosm, due to the effects of diel cycling. Inlet concentrations of DO showed a summer diel cycle at this site, and since the mesocosm residence time was typically less than 24 hours, our respiration estimates would vary significantly when repeated measurements were taken over the course of the day. At any given time, DO might be increasing in the inlet and decreasing the outlet, or vice versa, resulting in a respective overestimate or underestimate (and occasional negative respiration values). On average, over multiple samples this probably does not influence our estimation of the annual cycle of respiration, but it may result in an underestimate of summer respiration. Removal of outliers during flood pulse events remains another concern. Clearly, such events may in fact produce high respiration rates, and reflect real energy pulses. However, the absolute concentrations of oxygen also changed considerably at these times as well (Figure 4a) and without continuous measurements there is no reliable way to estimate respiration during these periods. This problem could potentially be bypassed by using a head tank as a steady source of uniform water (Sobczak and Findlay 2002), provided the system is very heavily insulated against temperature changes.

The initially high respiration rates and high variance observed for all mesocosm respiration reflect a general concern with respect to any mesocosm experiments in the

field or lab. On one hand, they may reflect real successional changes in biofilm activity, rising to a maximum and declining to a lower steady state. This would follow closely with biofilm successional patterns observed in bacteria density and species richness (Jackson et al 2001). Respiration rates estimated from short term manipulations or lab based studies, while useful with respect to experimental treatments, may be less than realistic when scaled up to infer system metabolic rates. We think that there may be a strong positive bias in respiration resulting in the disturbance and manipulation of sediment, that may take months to return to normal conditions.

A major assumption concerns the contribution of oxygen from the overlying vadose zone, which assumed that shallow groundwater is an open system. This influx could negatively bias any floodplain scale interpretations of oxygen consumption. We observed little evidence from the vertical DO profiles of dispersive influx of oxygen from the overlying vadose zone. Malard and Hervant (1999), citing Rose and Long (1988), insist that this is a significant factor. We disagree with Rose and Delong's basic assumption that vadose oxygen concentration is near saturation, when there is considerable evidence that vadose oxygen is typically depleted (Glinski and Stepniewski 1985, Brady and Weil 1996). Even under ideal conditions such as lake re-aeration, the contribution of diffusion across the air-water boundary layer is very small. Hutchinson (1975) offers an extensive review of the physical basis for oxygen supply in lakes, concluding that the contribution of diffusion is infinitesimal. We know of no similar mathematical treatments for gas influx to aquifers through the water table, but suspect that the relative vertical contribution of gases below the water table would be very low in high flow systems, especially in light of the diffusion boundary layer and highly stratified sediment layers. We also know of no direct empirical estimates of vertical oxygen recharge of aquifers via diffusion, and the steep vertical oxygen gradients summarized from the literature by Malard and Hervant (1999) argue against their case. However, we can suggest three alternative explanations for Rose and Long's presumption: (1) oxygen may be either replenished by direct infiltration (e.g. artificially from stormwater in the overlying City of Tuscon, or naturally as a consequence of channel activation at the Nyack floodplain); (2) by mixing and dispersion from deeper groundwater; or (3) entrainment of air bubbles and phase transfer of oxygen during times of rapid water table

rise, demonstrated under laboratory conditions (Williams and Oostrom 2000). Lacking any data on depth distribution of oxygen for the Tuscon site, we cannot eliminate any of these alternatives. At the Nyack site the second alternative, dispersive influx of O2 from deeper sediments, is supported by several lines of evidence. First, DO is low for medium residence times (≈ 40 days) but rebounds for longer residence times (Figure 7a). Secondly, during the winter and spring replenishment of oxygen, the vertical oxycline tends to shift upward (particularly evident in Figures 6h and 6i). Finally, positive vertical hydraulic gradients generally predominate in the downstream half of the aquifer (Diehl 2004), which corresponds with longer flowpaths. There is weaker evidence for the alternative one and three. Outliers of high oxygen occurred at only one of eight mesocosm sites (arrows in Figure 4a), and corresponded with both a change in hydrograph and precipitation event. As previously noted, river hydrograph corresponds closely with change in water table elevation for all sites. However these high oxygen outliers occurred at only one of four mesocosm sites (M2), and were more pronounced in the shallow mesocosm at that site. This site is also bordered by a flood flow channel, which connects to the main channel during flood pulse, but also accumulated precipitation during significant rain events. Entrapment of air bubbles with water table rise is thus the least likely mechanism for oxygen recharge at this site, or at best has a small or prolonged effect that is overwhelmed by the increase in respiration rate that occurs during the flood pulse.

We wonder whether shallow unconfined aquifers should really be considered open systems with respect to dissolved gases, as is commonly assumed (Stumm and Morgan 1996). Shallow aquifers are certainly open with respect to the direct exchange of water, from surface water recharge near channels, or soil leaching in regions where precipitation contributes significantly to water mass balance. Based only on gas diffusion, we suspect that the contribution of vapor phase oxygen to shallow aquifers may be negligible, and shallow groundwater systems may be effectively be considered closed to surficial gas exchange.

Ecosystem resistance?

Beyers (1962) provided experimental evidence that aquatic microcosms showed minimal respiration response to changes in system temperature. To date this is only study of its kind, and is compelling evidence for emergent properties of ecosystems. It is well established that individual organismal metabolic rate responds positively to increased temperature, however Beyers' microcosm experiment showed that ecosystems may be resistant to such changes, possibly due to compensation among the myriad species within the system. Our mesocosm community respiration rates contradict the idea of system resistance, both on the basis of absolute temperature (two sites) and diel temperature fluctuations (the strong effect of temperature gain artifacts upon respiration for all mesocosms). The first effect of absolute temperature is relatively easy to explain, since this effect occurred only in aquifer recharge zones. At these sites, energy inputs (riverine DOC) may covary with seasonal temperature cycles. Although this would require more thorough studies of carbon bioavailability, the obvious factor here is that flow-through systems are subject to external loading, while Beyers microcosms were self-contained batch systems. The second observation, the strong effect of temperature gain, is more problematic. We do not know why temperature cycling would outweigh the effects of average temperature on metabolism. Degassing artifacts are unlikely since the inlet water was well below oxygen saturation for all sites. The metabolic effects of temperature cycling has received little attention in the ecology literature (Kelly 1971), and perhaps this warrants more investigation. As to why Beyers did not observe such an effect, we have two potential explanations. Beyers' experiments measured a response to a single cycle of temperature decrease, increase, and return to initial conditions, with each step change lasting 24 hours. Natural diel cycling occurs with greater frequency (see Chapter 4), and hence may be provide a greater intensity of "disturbance" or stress. Secondly, Beyers measured dissolved CO_2 as a response variable. There are obvious problems here in that, depending upon pH, bicarbonate will eventually evolve from the respired CO_2. The same carbonate system that buffers pH would also buffer the effects of respired CO_2, rendering Beyers' results questionable. The lack of any observable short-term effects of oxygen concentration on community respiration (primarily microbial) concurs with other

empirical studies that show resilience of lake microbes to low oxygen (Zobell and Stadler 1940).

Flowpaths to Progress?

The results of this work have somewhat contradictory implications for flowpaths as the central organizing concept for stream and hyporheic biogeochemistry (Fisher et al. 2004). On the one hand, defining a flowpath in the field is difficult, because natural systems are often not in steady state: flowpaths are in fact quite transient. This is evident even when a flowpath is artificially constrained (i.e. in our mesocosms). We urge caution in that in practice it is not a simple matter of establishing a transect or well grid and interpreting changes in chemistry or other properties along a perceived gradient. Investigators must first account for diel cycling and relative rates of change in the source water, an approach that requires a very accurate estimate of residence time and a comprehensive time series of source water chemistry in order to back calculate initial concentrations. In practice, this is more in the realm of modeling, and is empirically challenging, except where continuous data loggers are available. However, at the annual time scale, as is shown in this work, flowpaths may indeed integrate larger scale biogeochemistry as proposed by Fisher et al. (2004), at least for semi-conservative species such as oxygen. Moreover, if the relationship between temperature and oxygen exists beyond the Nyack alluvial aquifer, one could make reasonable predictions on patterns of respiration in other systems using continuously logged temperature, and analyzing the resulting waveform. While we are not certain this simplified approach could be transferable to other chemical species, the general approach of comparing source and end members over an annual cycle, and supporting with mesocosm or microcosm studies of, for example, nutrient uptake rates or enzyme activities, is certainly worth further attention.

CONCLUSIONS

Oxygen distribution in the aquifer is clearly heterogeneous and dynamic, but with distinctly non-random spatial patterns. The spatial and temporal patterns of oxygen distribution provide evidence for three potential energy sources to the Nyack floodplain

aquifer. The river may influence aquifer metabolism directly, but the extent of influence may depend on season, as mediated by temperature in the river. Summer respiration corresponds with warm temperatures in aquifer recharge zones. In winter, colder temperatures in the river and aquifer recharge zones may result in a more spatially extensive delivery of resources into the aquifer, resulting in a winter respiration peak in the aquifer interior. We also saw a peak in aquifer respiration on the rising limb of the hydrograph in April. The river may indirectly contribute to soil based energy sources to the aquifer, through change in river stage and a rising water table. We saw no consistent vertical pattern in oxygen that would indicate leaching of soil horizons as an energy source. Where we did observe surficial areas of low DO (orthograde oxygen profiles), they extended up to 4 meters below the water table. These hypoxic zones or hotspots were persistent throughout the year, providing evidence for large concentrations of persistent energy inputs, most likely in the form of buried particulate organic matter. The effects of temperature and temperature gain artifacts on aerobic respiration calls into question the previous observation that ecosystem metabolism shows resilience with respect to temperature. Finally our analysis of the seasonal oxygen waveform, combined with time series community respiration estimates, is a potentially productive approach for evaluation of complex non-steady-state flowpath dynamics. These patterns in oxygen concentration and respiration are decidedly general, and bear confirmation using smaller scale studies on the pools, loading rates and bioavailability of energy resources, coupled with experimental manipulations. However at the aquifer scale they do inform us as to the relative importance, spatial extent, and timing of energy sources, as they affect subsurface energy flow. The overall patterns in oxygen concentration and community respiration indicate the large (kilometer) scale and dynamic influence of the river on floodplain groundwater.

REFERENCES

Åberg, B & W. Rodhe. 1942. über die Milieufaktoren in einigen südschwedischen Seen. *Symbol. Bot. Upsalien.* 5(3), 256p.

Anderson, M.L. and others. In prep. Temperature dynamics in a floodplain ecosystem.

Baker, M. A., H.M. Valett, and C.N. Dahm. 1999. Acetate retention and metabolism in the hyporheic zone of a mountain stream. *Limn. Ocean.* 44(6): 1530-1539.

Baker, M.A., H.M. Valett, C.N. Dahm. 2000a. Anoxia, Anaerobic Metabolism, and Biogeochemistry of the Stream-water-Ground-water Interface. In: Jones, J.B. and P.J. Mulholland, eds. *Streams and Ground Waters*. Academic Press, San Diego USA.

Baker, M. A., H.M. Valett, and C.N. Dahm. 2000b. Organic carbon supply and metabolism in a shallow groundwater ecosystem. *Ecology* 81(11): 3133-3148.

Beyers, R.J. 1962. Relationship between temperature and metobilism of experimental ecosystems. *Science* 136 (3520): 980-982.

Borden, R.C., P.B. Bedient, M.D. Lee, C.H. Ward, J.T. Wilson. 1986. Transport of dissolved hydrocarbons influenced by oxygen-limited biodegradation: 2. field applications. *Wat. Res. Research* 22(13): 1983-1990.

Brady, N.C. and R.R. Weil. 1996. *The Nature and Properties of Soils.* 11th ed. Prentice.

Brunke, M. and T. Gonser. 1997. The ecological significance of exchange processes between rivers and groundwater. *Freshwat. Biol.* 37: 1-33.

Brunke, M. and T. Gonser 1999. Hyporheic invertebrates: the clinal nature of interstitial communities structured by hydrological exchange and environmental gradients. *J. N. Am Benthol. Soc.* 18 (3): 344-362.

Carlyle, G.C. and A.R. Hill. 2001. Groundwater phosphate dynamics in a river riparian zone: effects of hydrologic flowpaths, lithology and redox chemistry. *J. Hydrol.* 247: 151-168.

Chapelle, F.H. 1993. *Ground-Water Microbiology and Geochemistry*. Wiley.

Clinton, S.M. 2001. Microbial metabolism, enzyme activity and production in the hyporheic zone of a floodplain river. Unpublished PhD dissertation. University of Washington.

Connolly, N.M., M.R. Crossland and R.G. Pearson. 2004. Effect of low dissolved oxygen on survival, emergence, and drift of tropical stream macroinvertebrates. *J. N. Am. Benthol. Soc.* 23(2): 251-270.

Craft, J.A., J.A. Stanford and M. Pusch. 2002. Microbial respiration within a floodplain aquifer of a large gravel-bed river. *Fresh. Biol.* 47: 251-261.

Crenshaw, C.L., H.M. Valett and J.R. Webster. 2002. Effects of augmentation of coarse particulate organic matter on metabolism and nutrient retention in hyporheic sediments. *Fresh. Biol.* 47: 1820-1831.

Dahm, C. 2006. President's address. North American Benthological Society. Anchorage Alaska.

Diehl, C.J. 2004. Controls on the magnitude and location of groundwater/surface water exchange in a gravel dominated alluvial floodplain system, northwestern Montana. Unpublished MS Thesis. University of Montana.

Eary, L.E. and J.A. Schramke. 1990. Rates of inorganic oxidation reactions involving dissolved oxygen. In: Melchior, D.C. and R.L. Bassett, Eds. *Chemical Modeling of Aqueous Systems II*. American Chemical Society.

Ellis, B.K., J. A. Stanford and J. A. Ward. 1998. Microbial assemblages and production in alluvial aquifers of the Flathead River, Montana, USA. *J. N. Am. Benthol. Soc.* 17(4): 382-402.

Fetter, C.W. 2001. *Applied Hydrogeology 4th ed.* Prentice.

Findlay, S. 1995. Importance of surface-subsurface exchange in stream ecosystems: The hyporheic zone. *Limnol. Oceanogr.* 40(1): 159-164.

Fisher, S.G., R.A. Sponseller and J.B. Heffernan. 2004. Horizons in stream biogeochemistry: flowpaths to progress. *Ecology* 85(9): 2369-2379.

Giere, O. 1993. *Meiobenthology*. Springer. Berlin, Germany.

Gleick, P.H. 2000. *The World's Water 200-2001.* Island Press, Washington D.C.

Glinski, J. and W. Stepniewski 1985. *Soil Aeration and its Role for Plants*. CRC Press, Boca Raton FL.

Hedin, L.O. 1990. Factors controlling sediment community respiration in woodland stream ecosystems. *Oikos* 57: 94-105.

Huggenberger, P., E. Hoehn, B Beschta, and W. Woessner. 1998. Abiotic aspects of channels and floodplains in riparian ecology. *Fresh. Biol.* 40: 407-425.

Hutchinson, G.E. 1975. *A Treatise on Limnology, Vol 1, Part 2: Chemistry of Lakes.* John Wiley and Sons. New York.

Jackson, C.R., P.F. Churchill, and E.R. Roden. 2001. Successional changes in bacterial assemblage structure during epilithic biofilm development. *Ecology* 82(2): 555-566.

Johnson, A.N. 2003. Preliminary hydrogeological and ground penetrating radar investigation of preferential flow zones in a gravel dominated floodplain, northwest Montana. Unpublished MS Thesis. University of Montana.

Jones, J.B. 1995. Factors controlling hyporheic respiration in a desert stream. *Fresh. Biol.* 34: 91-99.

Jones, J.B., S. B. Fisher and N.B. Grimm. 1995. Vertical hydrologic exchange and ecosystem metabolism in a Sonoran Desert stream. *Ecology* 76(3): 942-952.

Kaplan, L.A. and J.D. Newbold. 2000. Surface and Subsurface Dissolved Organic Carbon. In: Jones, J.B. and P.J. Mulholland, eds. *Streams and Ground Waters*. Academic Press, San Diego USA.

Kelly, R.A. 1971. The effects of fluctuating temperature on the metabolism of freshwater microcosms. PhD dissertation, University of North Carolina, Chapel Hill.

Lindberg, S.E. and D.D. Runnels. 1984. Ground Water Redox Reactions. *Science* 225: 925-927.

Malard, F. and F. Hervant. 1999. Oxygen supply and the adaptations of animals in groundwater. *Fresh. Biol.* 41: 1-30.

Marmonier, P. and Dole M.J. 1986. Les amphipods des sediments d'un bras court-circuité du Rhône-logique de répartition et réaction aus cruex. *Sciences de l'Eau* 5: 461-486.

Marshall, M.C. and R.O. Hall. 2004. Hyporheic invertebrates affect N cycling and respiration in stream sediment microcosms. *J. N. Am. Benthol. Soc.* 23(3): 416-428.

Moore, J.M. 1994. Contaminant mobilization resulting from redox pumping in a metal-contaminated river – reservoir system. In: Baker, L.A. ed. *Environmental Chemistry of Lakes and Reservoirs.* Advances in Chemsitry Series 237. American Chemical Society, Washington DC.

Moran, M.J., J.S. Zogorski, P.J. Squillace. 2007. Chlorinated solvents in groundwater of the United States. *Environ. Sci. Technol.* 41:74-81.

Mulholland, P.J. and D.L. DeAngelis. 2000. Surface-Subsurface Exchange and Nutrient Spiralling. In: Jones, J.B. and P.J. Mulholland, eds. *Streams and Ground Waters*. Academic Press, San Diego USA.

Odum, H.T. 1956. Primary production in flowing waters. *Limnol. & Oceanogr.* 1(2): 102-117.

Palmer, M.A. 1993. Experimentation in the hyporheic zone: challenges and prospectus. *J. N. Am. Benthol. Soc.* 12: 84-93.

Poole, G.C. 2000. Analysis and dynamic simulation of morphologic controls on surface and groundwater flux in a large alluvial floodplain. PhD Dissertation, University of Montana.

Poole, G.C., J.A. Stanford, S.W. Running, C.A. Frissell. 2006. Multiscale geomorphic drivers of groundwater flow paths: subsurface hydrologic dynamics and hyporheic habitat diversity. *J. N. Am. Benthol. Soc.* 25(2): 288-303.

Pusch, M. and J. Schwoerbel. 1994. Community respiration in hyporheic sediments of a mountain stream (Steina, Black Forest). *Arch. Hydrobiol.* 130(1): 35-52.

Rose, S. and A. Long. 1988. Dissolved oxygen systematics in the Tuscon basin aquifer. *Wat. Res. Res.* 24(1): 127-136.

Scott, M.J. and J.J. Morgan. 1990. Energetics and Conservative Properties of Redox Systems. In: Melchior, D.C. and R.L. Bassett, Eds. *Chemical Modeling of Aqueous Systems II*. American Chemical Society.

Sobczak, W.V and S. Findlay. 2002. Variability in bioavailability of dissolved organic carbon among stream hyporheic flowpaths. *Ecology* 83(11):3194-3209.

Stanford, J.A. and A.R. Gaufin. 1974. Hyporheic communities of two Montana rivers. *Science* 185: 700-702.

Stanford J.A., M.S. Lorang and F.R. Hauer. 2005. The shifting habitat mosaic of river ecosystems. *Verh. Internat. Verein. Limnol.* 29(1): 123-136.

Stanford, J.A. and J.V. Ward. 1988. The hyporheic habitat of river ecosystems. *Nature* 335: 64-66.

Stanford, J. A., J. V. Ward and B. K. Ellis. 1994. Ecology of the alluvial aquifers of the Flathead River, Montana (USA), pp. 367-390. *IN*: Gibert, J., D. L. Danielopol and J. A. Stanford (eds.), *Groundwater Ecology*. Academic Press, San Diego, California, USA. 571 pp.

Stumm, W. and J.J. Morgan. 1996. *Aquatic Chemistry* 3rd ed. John Wiley and Sons, Inc. New York.

Valett, H.M., C.C. Hakenkamp, A.J. Boulton. 1993. Perspectives on the hyporheic zone: integrating hydrology and biology. *J. N. Am. Benthol. Soc.* 12(1): 40-43.

Vervier, P. and R.J. Naiman. 1992. Spatial and temporal fluctuations of dissolved organic carbon in subsurface flow of the Stillaguamish River (Washington, USA). *Arch. Fur. Hydrobiol.* 123: 401-412.

Wiedemeier, T.H., H.S. Rifai, C.J. Newell, and J.T. Wilson. 1999. *Natural attenuation of fuels and chlorinated solvents in the subsurface*. Wiley.

Williams, M.D. and M. Oostrom. 2000. Oxygenation of anoxic water in a fluctuating water table system. *J. Hydrol.* 230: 70-85.

Winograd, I.J. and F.N. Robertson. 1982. Deep oxygenated groundwater: anomaly or common occurrence. *Science* 216: 1227-1229.

Zobell, C.F. and J. Stadler. 1940. The effect of oxygen tension on the oxygen uptake of lake bacteria. *J. Bacter.* 39: 307-322.

Chapter 2

DISTRIBUTION AND ISOTOPIC COMPOSITION
OF BURIED ORGANIC MATTER
IN SEDIMENTS OF A FLOODPLAIN AQUIFER.

ABSTRACT

We investigated the organic matter content and carbon and nitrogen isotopic signature of aquifer sediment, to characterize the food base and carbon sources for groundwater/hyporheic invertebrates at the Nyack Floodplain aquifer (West Glacier, MT USA). We recovered fine sediments pumped from wells, and separated POM (derived from buried plant detritus) from more strongly associated particulate organic matter (SAPOM: biofilm, coatings, sorbed material). We estimated the total pools of these two fractions, and evaluated the carbon isotopic signatures as potentially distict end members. Total organic carbon content of aquifer fine sediments had a median of 0.10% by weight, and was strongly skewed (range 0.05-15.5%). Particulate organic matter (POM) was composed mostly of wood fragments, followed by charcoal and roots, and accounted for 84 ± 8% of the total carbon (but up to 99.9% for outliers). SAPOM was on average 16 ± 8% of the total carbon, and had a lognormal distribution. SAPOM was strongly correlated with POM content, but only in samples from older orthofluvial aquifer formations. SAPOM content varied with depth and season (June vs October), and was generally much higher in shallow sediments, particularly in June. $\delta^{13}C$ signatures of the two pools were generally very similar, clustering strongly around -25‰. SAPOM and POM carbon signatures from low DO sites were more strongly depleted, ranging as low as -29‰ (POM) and -42‰ (SAPOM). During October baseflow, a few sites had a shift in SAPOM $\delta^{13}C$ signature close to river DOC (≈ -22‰). We saw no differences in SAPOM $\delta^{13}C$ signatures and C:N ratio with depth (1 meter vs. 2 meters below the water table). $\delta^{15}N$ of SAPOM was slightly more depleted at deeper sites in October. Together these findings indicate that decomposition of buried POM may ultimately supply much of the SAPOM pool, and that turnover time of SAPOM may be on the order of < 6 months. Carbon isotopic signatures were generally not distinct among the two fractions. However we observed highly depleted SAPOM $\delta^{13}C$ from low DO sites, possibly the product of methanotrophy. We feel that a better classification of particulate organic matter is needed, analogous to carbon quality in dissolved species, and analyzed with respect to forms that are physically available to feeding invertebrates.

INTRODUCTION

Most of the world's organic matter is "finely-disseminated" within sediments (Stumm and Morgan 1996). In aquatic systems this organic matter may dominate energy fluxes (Wetzel 1995), and is an important energy source for heterotrophic microbes and invertebrate food webs. While the most obvious examples of detrital systems are from lake and river benthos, organic matter availability may persist indefinitely with burial in deep fluvial sediments: an extreme example would be lithophilic bacteria in sedimentary formations (MacMahon and Chapelle 1991). Between these extremes in time lies a range of diagenic conditions, well studied in soils and lake and marine sediments, but less well characterized in fluvial systems.

The hyporheic zone of rivers represents the early diagenesis of recently deposited (e.g. Holocene) fluvial sediment. In the more recent riverine deposits, shallowly buried organic matter in streams can exceed surface (benthic) material (Metzler and Smock 1990), potentially influencing stream bioenergetics, nutrient cycling and carbon spiraling (Pusch et al. 1998). The distribution of organic matter in larger scale hyporheic or fluvial aquifer systems is unknown. The occurrence of diverse populations of metazoans, persisting over long time periods across kilometer-scale floodplain aquifers (Stanford et al. 1994) alludes to a potential source of carbon energy throughout these aquifer formations. Buried organic matter is the most obvious energy source, as a stable energy subsidy for subsurface aquatic food webs. The primary purpose of this study was to evaluate the distribution, magnitude and quality of buried carbon, as a potential energy reservoir for subsurface invertebrates. The second purpose of this study, consequent to quantifying and separation of organic matter fractions, was to determine the isotopic signature of the organic matter fractions, as a natural tracer of organic matter supply to the invertebrate food web.

There are a wide range of analytical approaches to measuring organic matter in sediments, not all of which are consistent with our purposes. Ash content, or % LOI is still widely used to estimate organic matter in fluvial systems (Wallace et al. 2006). This method is effective when working with debris deposits in streams. However, the approach is often extended to mineral sediments (Claret et al. 1997), despite clear

limitations (Bretschko and Liechtfried 1987). The problem lies in the loss in weight from volatilization of dolomite, some loss of carbonate and other minerals, and loss of refractory water content. Each of these processes likely occurs at different rates. Therefore, the problem is greatly magnified when the mineral fraction dominates sediment volume and also when carbonates are present. This problem is magnified by the inconsistency in the length of time sediments are reportedly ashed (variously 1, 4, 6 or 24+ hours).

In sediments with low organic matter content, elemental analyzers offer much greater accuracy. Elemental analyzers are widely used in soil science, and are the recommended method for benthic sediments (Bretschko and Liechtfried 1987). As a time saving measure, it is also possible to use %LOI to predict %C (Goldin 1987), although the relationship may be site specific. However there are several drawbacks to using elemental analyzers for sediments with extremely low carbon content. Our preliminary trials indicated that a typical sample of aquifer sediment contained no more than 25-80 μg of carbon and 6-7 μg N. The additional step of acidification of carbonates results in considerable error from loss of organic carbon (Beyers et al. 1978). The time-consuming process of pulverizing mineral sediments has a high potential for contamination. Elemental analyzers will not distinguish particulate organic matter from sediment coatings and biofilms, and mechanical separation of animals and detritus is rarely complete. One alternative lies in a wide range of analytical techniques designed to chemically extract specific compounds such as proteins, humin, carbohydrates etc (see Greiser and Faubel 1992, Murphy et al. 1992, Carter 1993). However, existing procedures employing chemical extractions are not always efficient (Greiser and Faubel 1992), are insensitive to grain size (Bonde et al. 1992), and are incompatible with stable isotope analysis.

Based on preliminary analysis of invertebrate gut contents (Chapter 6), we developed a simplified approach that separated organic matter in fine sediments into two functional components. We separated particulate organic matter (POM), which is primarily plant detritus in origin, via mechanical separation using elutriation. The residual mineral sediment was processed for strongly associated particulate organic matter (SAPOM), defined as material that cannot be readily separated from mineral

particles through mechanical means such as agitation (*sensu* Pusch & Schwoerbel 1996). SAPOM should not be confused with soil organic matter, or sedimentary organic matter (e.g. Hartog et al. 2005) which are more inclusive definitions. We used low intensity sonication to remove SAPOM, including exo-polymeric saccharrides (EPS), biofilm, cells, organic matter coatings, sorbed compounds (organo-clay complexes), and possibly ultra fine particulate organic matter (UFPOM) bound to EPS. This procedure excludes lithified organic matter, although such compounds may be available as a microbial substrate (McMahon and Chapelle 1991, Murphy et al. 1992). We refer to both POM and SAPOM as organic matter, however we report all organic matter in units of carbon content.

The second purpose of this study focused on isotopic signature of the POM and SAPOM fractions. We were particularly interested in the SAPOM fraction as a potential indicator of the microbial biofilm signature. Current methods for estimating biofilm isotopic signature are limited. Scraping is typically done in surface systems where biofilm density is high, but this method is inadequate for low organic matter concentrations in the subsurface. Indirect measurement of respired CO_2 is occasionally used (Coffin and Cifuentes 1993), but in natural waters this method requires correction for calcite dissolution. In more dynamic hyporheic systems, corrections are confounded because the source water (river) has a variable end member: correction requires a precise estimate of residence time, degree of mixing, and a continuous record of surface water signature. We used low intensity sonication to remove biofilm and attached mineral particles (Craft et al. 2002).

We predicted that SAPOM dual isotope signatures would vary spatially, depending on distance to potential sources of organic matter. SAPOM in aquifer recharge zones near the river channel would be expected to have signatures similar to riverine DOC. Shallow groundwater underlying older orthofluvial formations with well developed vegetation, would have signatures similar to soil DOC. At sites with considerable POM content, SAPOM content and/or signature would reflect POC signatures. Our predictions for SAPOM $\delta^{15}N$ are more general, since we did not measure river or soil end members. Our goal here is to document the spatial variability of ^{15}N, as a natural tracer.

We predicted that aquifer SAPOM was likely to have moderate to long turnover times, as has been observed in soils (Bonde et al. 1992). SAPOM signatures should therefore be stable across sampling dates. If isotopic signatures of SAPOM are spatially predictable and temporally stable, isotopes could function as a natural tracer of organic matter flow through subsurface food webs. Alternatively, natural C and N isotopes may show spatial and temporal patterns in the food base, as has been observed in surface aquatic systems (Finlay et al. 1999, Finlay et al. 2002). In this case, isotopic signatures could be used to indicate timing and magnitude of carbon loadings, variously from terrestrial or aquatic sources.

METHODS

Sediment Collection

Our study site was the Nyack floodplain of the Middle Fork, Flathead River MT (48° 27' 30" N, 113° 50' W). We collected sediment and organic matter from wells using a hand-operated diaphragm pump. The intake hose was modified with baffles and side mounted holes to allow for collection of material from discrete depth intervals along continuously slotted wells (see Chapter 3 for additional details on well sampling). We maintained a roughly constant discharge of 60-80 l/m. All material, including groundwater invertebrates, was collected in a 64 μm Nitex mesh plankton net. We concentrated the sample in a 64 μm Nitex mesh bolus net, and froze the bulk sample in the field with dry ice, for later processing. Occasionally when large amounts of sand were collected, we separated the organic matter and invertebrates from most of the sand via elutriation in the field, estimating and recording the amount of sand remaining. We sampled wells monthly throughout 2004. Herein we report on sediment samples from June (post flood-pulse), August (mid summer), and October (baseflow), for 23 sites and (1-)2 depths (depending on the available depth of the well) from each well.

Particulate (Detrital) Organic Matter Processing

Samples were thawed with running cold water in the lab, and initially processed for invertebrates and particulate organic matter. Organic matter and invertebrates were removed using elutriation, using only chilled reagent grade DI water. Elutriation was

repeated until there was no or minimal evidence of POM remaining in the sand fraction (<<1%). We set aside a 10ml of sand from the August samples, which we stained with Rose Bengal and carefully scanned at 25x to estimate efficiency of removal of invertebrates. Typically there were no invertebrates remaining (>99.9% of invertebrates were removed), although a few samples had remnants of archiannelids adhered to sand grains, and sites with very high densities of invertebrates had a few copepods or rotifers remaining in the sand fraction. The washed sand was then refrozen for later processing for sediment associated organic matter (SAPOM). A small subset of samples from October was processed for SAPOM immediately, to compare the effects of multiple freezing on carbon isotope signature.

We rinsed the elutriated fraction through a 500 μm sieve to separate coarse and fine fractions. Although FPOM technically is below 1mm in size, the sieve size was chosen to reflect the standard for separation of meiofauna, and hereafter we refer to the 64-500 μm fraction as FPOM. The CPOM fraction is therefore >500 μm, however the upper limit of this fraction is determined by the slot width of the wells (2.04 mm). The CPOM fraction was picked at 12x for invertebrates until complete removal. The FPOM fraction was washed into a 100 ml beaker, diluted to 80-100 ml, and subsampled twice with a 5ml Henson-Stimple pipette. Occasionally we diluted to 200-800 ml, which was required when there was a large volume of organic matter, or estimated invertebrate density was very high. The subsamples were pooled and the resulting sample was stained with Rose Bengal for 24hrs, washed of residual stain, scanned at 25x, and all invertebrates were removed. The remaining material from both CPOM and FPOM fractions was dried at 60 °C for 24 hrs, weighed, and ashed at 500 °C for 1 hour. Samples with a large volume of organic matter were ashed for 4 hours, which was sufficient complete combustion, leaving only an ash and inorganic residue. We converted Ash Free Dry Mass to carbon using a conversion of 0.45 (based on carbon content of CPOM from stable isotope samples).

We processed FPOM and CPOM for stable isotope analysis for a subset of sites. We used October samples for isotopic analysis, since invertebrate densities in these samples were generally low, thus ensuring more complete separation of organisms from the organic matter. Material for CPOM was processed as above, and we also conducted a

qualitative visual estimate of the composition of CPOM (root, leaf, wood, flocculate, charcoal, and pollen). FPOM material for isotope analysis was taken from the sample material remaining after subsampling, since the Rose Bengal stain would likely affect $\delta^{13}C$ signatures. We centrifuged FPOM at 2800 rpm for 10 minutes to separate mineral sediment. We removed FPOM from the top of the tube using a pipette, and material was transferred to a watch glass. We then removed all invertebrates (very small invertebrates such as copepod nauplii were impossible to remove completely). CPOM and FPOM were dried as above, milled to a fine powder, and stored in weighed tin capsules. Analysis was done by the UC Davis Stable Isotope Laboratory. Results are reported as per mil difference from PDB belemnite ($\delta^{13}C$) and atmospheric nitrogen ($\delta^{15}N$).

Using elutriated sand from a well with high organic matter content, we ashed coarse (>500um) and fine (64-500 um) sand fractions. Our purpose was to compare our estimates of POM using separation via flotation against the minimum resolution of the commonly used % LOI. Sand fractions were elutriated until visibly free of organic matter as above, placed in aluminum boats, and dried at 60 °C for 24hrs. The samples were subsequently ashed at 500 °C for 1-4 hour intervals over a total of 24 hours, rewetting, drying and desiccating and reweighing each time.

Strongly Associated Particulate Organic Matter Processing

We thawed sand samples under running water in an ice bath, and transferred approximately 10 ml of sand to an acid-washed flask. During sonication trials, we added 20 ml of reagent grade DI water, mixed the flask thoroughly, and decanted this water as an initial rinse. We then added another 75 ml of water and suspended the flask in an ice bath within a Bransonic 12 low intensity sonicator (47 kHz, 50W, Bransonic Inc). We sonicated the material in succession for a total of 15, 30 and 60 minutes, decanting and adding 75 ml of water to the sediment after each sonication. We decanted the rinse and sonicant (water and suspended sediment) through a 20 μm Nitex sieve, and transferred 20 ml from each into a 40 ml borosilicate vial. We added a stir bar and 0.5ml $HgCl_2$ as a preservative, and analyzed for TOC on a Tekmar-Dormann carbon analyzer. We collected POM from 15 ml of the sonicant on 0.7 μm Whatman pre-ashed and pre-

weighed glass fiber filters. Filters were dried overnight at 60 °C, weighed and ashed at 500 °C to estimate % loss on ignition.

Based on the trial runs, we sonicated sediment taken from October and June samples using 90 ml of water and a 30 minute sonication time, discarding the rinse but otherwise following the above procedure. We added 40 µl of concentrated phosphoric acid as a preservative. The residual sand was dried and weighed, and we normalized TOC data as ug C per g sediment. We estimated ^{15}N signatures of sonicant by collecting the POM fraction of 10-15 ml of TOC on 0.7 µm Whatman Glass fiber filters (HCL rinsed, pre-ashed and pre-weighed). Filters were dried overnight at 60 °C, dessicated, and reweighed on a microbalance to the nearest 1ug (Sartorius microbalance). All sonication and filtering was done in the dark to minimize autotrophic production during processing.

For October samples, we also estimated C:N ratio of SAPOM and calculated a mass balance between TOC, DOC and POC fractions. For C:N ratio, 10-15 ml of sonicant was collected on replicate filters. We acid fumigated one replicate for 6 hours (Harris et al. 2001) to remove carbonates, and re-dried the filters. We trimmed all filters to remove excess filter material, folded the filters and placed them in 7x9 mm tin capsules. Samples were analyzed using continuous flow IRMS (Europa 20/20, UC Davis Stable Isotope Facility) for TOC ($\delta^{13}C$), untreated filter borne sediment (dual isotope $\delta^{13}C$/ $\delta^{15}N$), and acid fumigated filter ($\delta^{13}C$).

We were unable to reliably calculate organic C:N from mass loss on acidification because acidified filter sediment (silts, clays, and hygroscopic $CaCl_2$) was very sensitive to humidity, and could not be weighed with precision. Instead, we corrected the dual isotope filter for inorganic carbon content, based on the change in delta value between acidified and non acidified samples, and assuming that inorganic carbon has $\delta^{13}C \approx 0‰$.

$$\% \text{ PIC} = \frac{(\delta_f - \delta)}{\delta_i}$$

where δ_i and δ_f are the initial and final (acidified) delta value for the filter-borne sediment organic matter. Organic carbon was then calculated as 1 - % PIC. Mass balance and molar C:N ratio was then calculated from the mass of organic carbon, once corrected for inorganic carbon content. We assumed that most or all of the PIC was from weathered rock such as tertiary sediments. It is also possible that some PIC may be formed via

secondary mineralization, which might have a much more depleted signature if the CO_2 was primarily biogenic. In this case, our estimate of %PIC would be biased low, however our estimate of the organic carbon isotope signature would not be affected.

For SAPOM mass balance, we converted TOC and POC (filter-borne carbon), measured during isotope analysis, to μg/g sediment as described above. We also analyzed the filtrate for DOC on a Tekmar-Dormann carbon analyzer, likewise converting to common units. We calculated mass balance error as the difference between TOC and the sum of POC and DOC, and reported the difference as a percentage of TOC.

Several of the sand fractions are from samples that, prior to processing, had high organic matter content or very high invertebrate densities. As noted above, it is impossible to completely remove all of this material through elutriation. Residual animal and plant matter might potentially be broken down by sonication, thereby affecting SAPOM content and isotopic signature. We examined the material collected in the 20 μm sieve, and noted at 25x that when animals were collected, there was no evidence that they had been damaged by low-intensity sonication. We also mounted several drops of sonicant to glass slides, and scanned at 100x. While fine sediment and amorphous material was abundant, we observed no intact cells, which we would expect if ultra fine plant-derived detritus had passed the sieve.

RESULTS and DISCUSSION

SAPOM: Sonication Trials and Mass Balance of Carbon Fractions

We observed from the sonication trials that cumulative dry mass of particles and material released via sonication increased as a linear function of time (Figure 1a). Meanwhile, the total cumulative mass of carbon, based on TOC content, also increased with time, but at a much slower rate. As we would expect from these differing slopes, the rate of increase of cumulative % LOI slows with time, following a natural logarithm pattern (Figure 1b). Because of this clear decrease in sonication efficiency, we settled on a sonication time of 30 minutes as the standard for subsequent sample processing. The TOC response fits a polynomial curve, and based on the first differential of this equation TOC is expected to reach a maximum at 108 minutes. In reality, the TOC curve should be

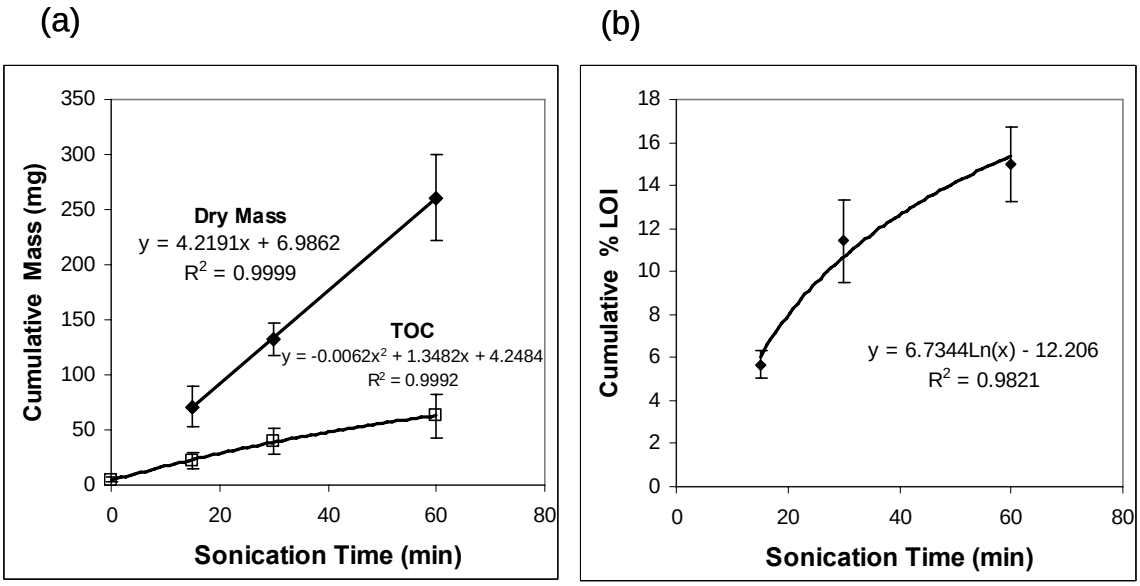

Figure 1: Sonication trials. (a) Effects of sonication time on dry mass of suspended sediment, and TOC content. (b) Effect of sonication time on percentage of organic matter, estimated as loss on ignition. n = 4 for all trials; error bars indicate ± 1 sd.

a Monod function, reaching an asymptote instead of curve. A 30 minute sonication time produces a TOC that is slightly less than half of the expected total SAPOM. The TOC at 30 minutes therefore provides only an index of total SAPOM and not an actual estimate.

The simultaneous production of both mineral particles and TOC with sonication has interesting implications. Leichtfried (1991) showed SEM images of biofilm with attached sediment particles. The cloudy suspension of silts and clays produced from sonicating what is otherwise clean, washed sand may represent particles released from the biofilm matrix, rather than fractured material from larger mineral particles. In soils, most organic matter is associated with silt and clay particles (Bonde et al. 1992). The DOC component of TOC was small, averaging 8.1% (± 4.8%). Therefore, most of the organic matter in the sonicant is still physically attached or sorbed to the silt and clay particles (<20μm). This is not surprising given the high sorption capacity and specific surface area of clay particles, and clay content can have a major effect on catchment DOC concentration (Kaplan and Newbold 2000).

Acid fumigation had a clear effect on the ^{13}C signature of the POC on filters (Figure 2). Untreated filters had consistently higher ^{13}C signature and much greater scatter than treated filters. Fumigated filters showed a very strong 1:1 correspondence

with the TOC signature, indicating that most of the SAPOM was still associated with fine mineral particles.

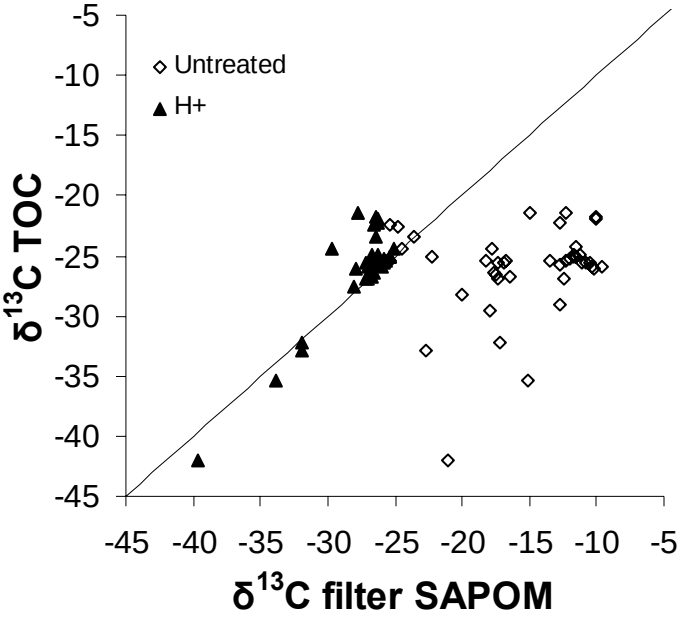

Figure 2: Comparison of 13C signatures between two methods of estimating strongly associated particulate organic matter (SAPOM) evolved from sonicated sand: TOC and filter-borne SAPOM. Line indicates 1:1 correspondence. Acid fumigation (H+ treatment) results in much stronger correlation.

Mass balance error had a median of -62.4%: the estimate from filter-borne organic matter was somewhat higher than the estimate from TOC. There are two potential explanations for this error. We considered the possibility that TOC value may be low due to analytical error, possibly due to settling of particles during the time between sample withdrawal and combustion (samples were stirred, but settling may occur within the instrument). If this was true, we would also see a consistent decrease in TOC between replicates, and possible carryover between consecutive samples. We did not observe either of these effects. The second explanation is that the SAPOM is overestimated due to settling of particles. Samples were agitated by hand before withdrawal by micropipette, which is not as consistent as continuous magnetic stirring. A lapse of more than a few seconds would result in some of the silt particles settling out before the sub-sample was taken. The sub-sample was not taken from a consistent depth, and withdrawal of solution

from the bottom of the container could result a high bias of sediment particles and associated organic matter. The error variance was generally higher at lower TOC (Figure 3), also suggesting analytical error. Filter blanks accounted for < 0.5% of organic carbon on filters.

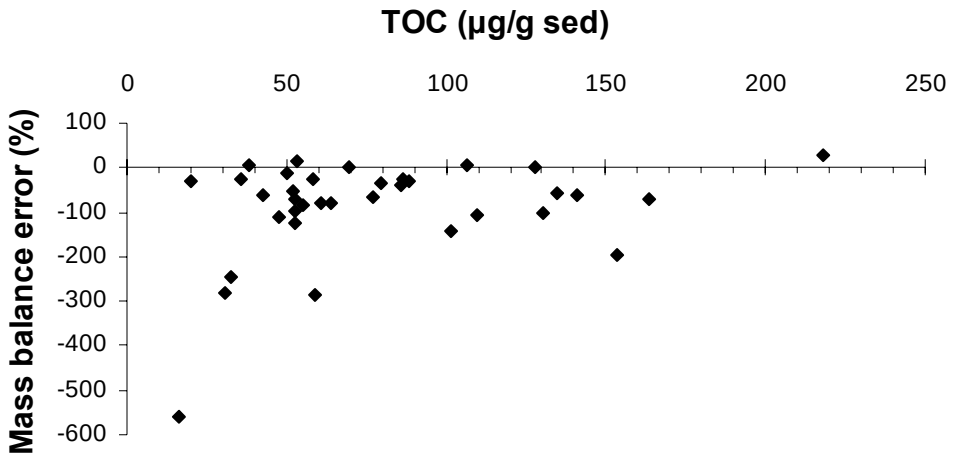

Figure 3: Mass balance of particulate + dissolved vs TOC material evolved from sonicated sediment. Mass balance error averages -62.4% and is negative (either TOC underestimated or filter-borne POC overestimated). Error magnitude increases with low TOC content, suggesting analytical error.

The contribution of the reagent water to the isotopic signature is unknown, since the DOC concentration is too low for isotopic analysis. We can make a conservative estimate of effects based on several assumptions. The most extreme isotopic signatures that we might expect from our samples would be ≈ -60‰ (for a system derived purely from heterotrophic methanogenesis) and ≈ 0‰ (for a system derived from autotrophic production, based in turn on calcite dissolution). Our raw TOC concentrations average 15.8 mg/l (±8.3), and are in the range of 2.56 to 37.49. DOC concentration of DI water blanks was never higher than 0.26 mg/l, therefore the contribution of reagent water to TOC was usually << 10 %. With these assumptions, and based on mixing calculations using the two isotopic extremes, the effect of reagent water on ^{13}C signature will be on average < 0.7 ‰ (based on the extreme mixing scenario). The DOC signature for natural waters for this area is actually in the range of -20 to -24 ‰, which is much closer to the signatures for TOC reported here: we expect that the effects are insignificant.

POM: distribution and relationship to SAPOM

Organic matter was dominated by wood fragments (64%), followed by charcoal (19%), roots (16%), and leaves (<2%), based on six sites with high organic matter content. A seventh site had almost no recognizable organic matter, but was dominated by an amorphous orange flocculate (we have observed similar material in the guts of amphibiont stoneflies in the aquifer – see Chapter 6). Another site in the parafluvial zone had a high content of pine pollen at 8m depth, observed consistently over 7 sampling dates. Overall POM content was highly skewed, with a median value of 0.088%, and ranged from 0.02% to 15.4% (Figure 4). The distribution between CPOM and FPOM was fairly even, except for the two outliers, which had 8 and 25 times more FPOM respectively. The three sites with unusually high POM content were located in an area of channel fill and a gravel bar, with no other surface indication of subsurface carbon buried. When we cored sediment from a debris jam (Chapter 5), we measured POM concentrations of ≈ 1%.

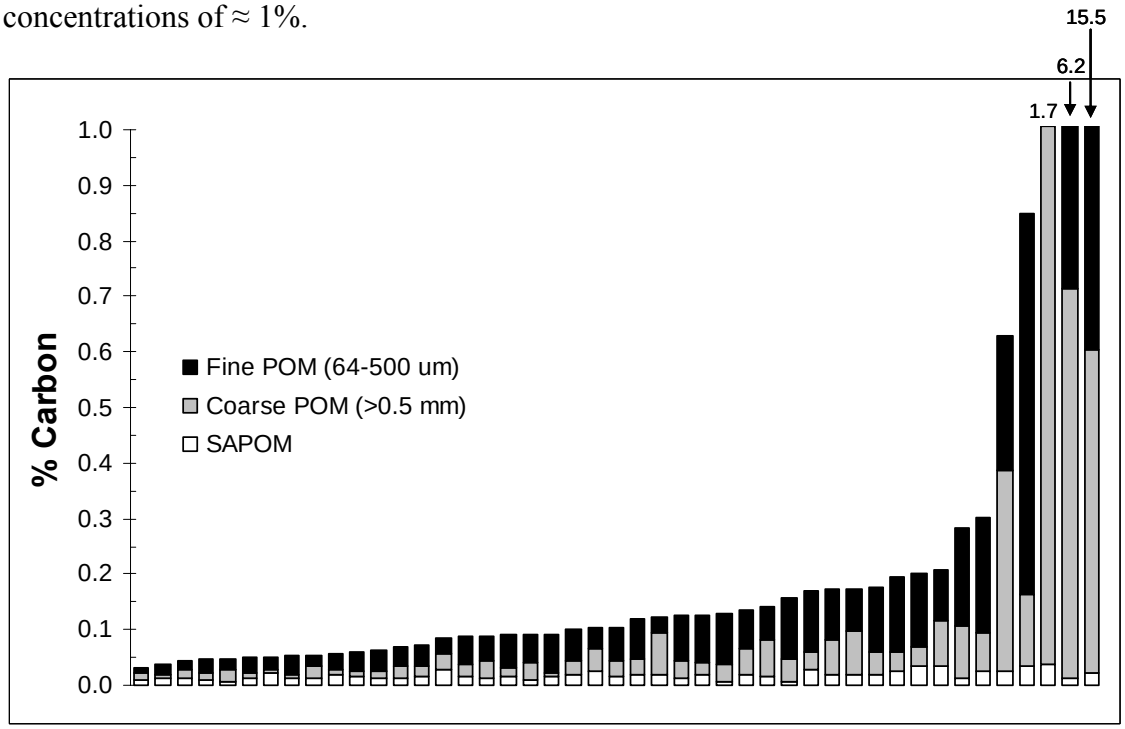

Figure 4: Distribution of particulate organic matter: POM (separated via elutriation) and strongly associated particulate organic matter SAPOM (evolved from sonication), across the well network. Each bar represents one well site at the 1 meter depth interval. Values are % carbon by weight for a unit volume of sand pumped from wells. Numbers at upper right correspond to total carbon content of three outliers.

Estimated total SAPOM content (approximated by multiplying by a factor of 2.1, as a correction for <50% efficiency for 30 minute sonication time) had a log normal distribution, averaging 0.018% (± 0.008). Total organic carbon content, combining POM and SAPOM, had a median of 0.10% (range 0.05-15.5). Of the total organic matter buried within or attached to fine sediments, POM averaged 84% (± 8) while SAPOM average 16% (± 8).

Ash Free Dry Mass (AFDM) of washed sand, after removing POC, shows values that are often much higher than SAPOM and POC combined. It is evident from Figure 5 that organic matter content based on AFDM is not sensitive to an actual POM below 0.2-0.3 % organic carbon content (approximately 0.4-0.6 % LOI). Moreover, AFDM is much less sensitive with increased ash time: a one-hour ash time is already above the average POC and SAPOM content observed in sediments of the Nyack aquifer. In other words, particulate organic matter that is visible to the eye and readily concentrated by elutriation may be well below the detection limit for %LOI. Ash free dry mass results clearly depend on the time span that material is in the furnace (Figure 5). Although this is somewhat obvious, shown graphically the differences between the commonly employed methods (1 hour, 4 hours, 6 hours, 24 hours, or until "constant weight") are evident. This confounds any comparison between studies where different ash times are used, and none of these times provide a definitive estimate. Even approaching 24 hours we still do not see an asymptote.

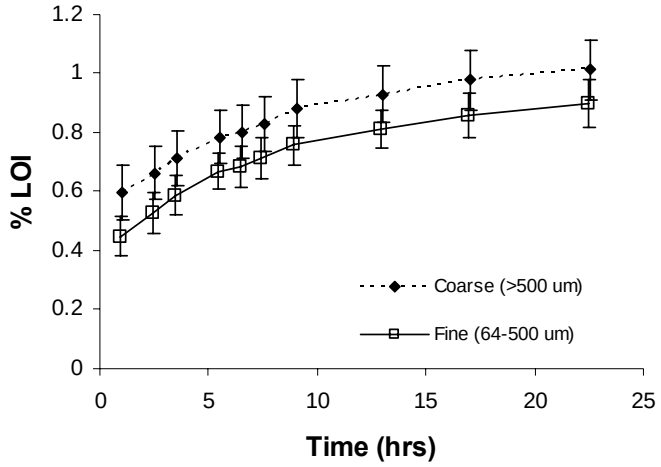

Figure 5: Cumulative % loss on ignition (at 500 °C) as a function of time and grain size. Error bars indicate ± 1 sd (n=4). Symbol locations were adjusted slightly for clarity.

SAPOM content showed a strong positive relationship to POC content (Figure 6a, $p<0.001$, ln transformed data). The relationship implies that POM may contribute to SAPOM content, either directly via capture of entrained UFPOM in biofilm, or indirectly via microbial uptake of POM and subsequent exopolymer production. The relationship holds for aquifer sites overlain by well vegetated floodplain (grassland, cottonwood and conifer forest). It does not appear to hold for sparsely vegetated gravel bar sites, implying that soil/sediment age may be a factor in defining the relationship between POC and SAPOM. Neither of these patterns hold when we compare POM to C:N ratio of SAPOM. If UFPOM was passively captured by biofilm, we would expect a stronger effect on CN ratio of SAPOM, since the CN ratio of FPOM and CPOM is between 22 and 101 (from the stable isotope samples, n = 19). In fact, sites with the highest abundance of POM had very low SAPOM content. Instead, these patterns suggest that metabolism of POM may strongly contribute to SAPOM, with the effects increasing with the age of the sediments.

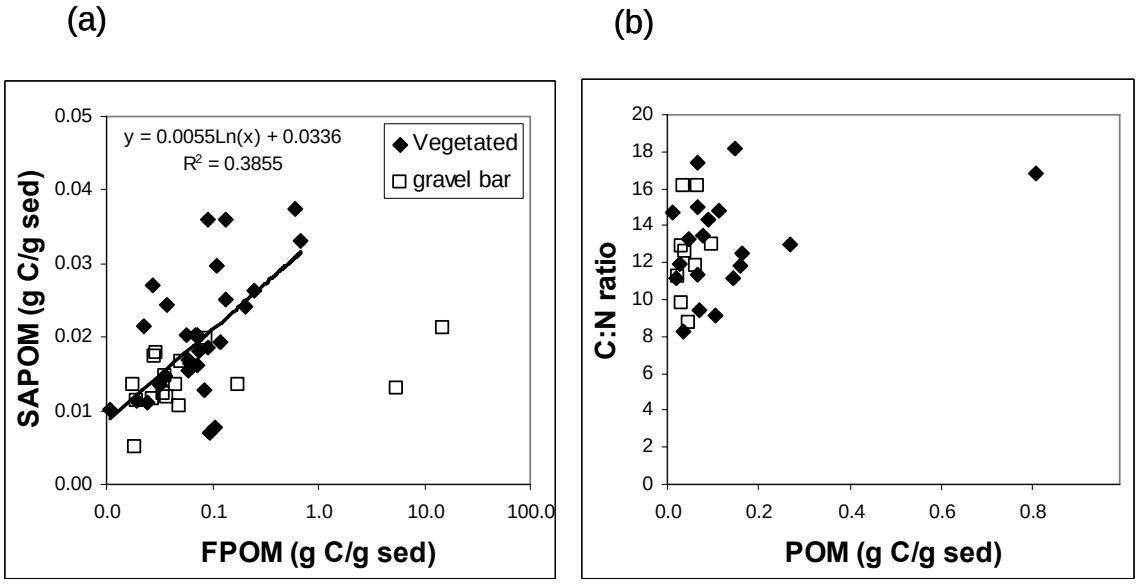

Figure 6: Relationship between POC content and (a) corresponding SAPOM content (log scale, two outliers excluded from regression); (b) molar C:N ratio of SAPOM.

C:N ratio of SAPOM averaged 12.9 (± 2.6). We note that this is at best an approximation, since we do not know the N content of dissolved species that may have evolved from sonication. It is worth noting that the values are somewhat higher than that expected for animal tissue and microbes (≈ 5), slightly lower than humic acid (≈ 14) and

is far lower than the value expected if SAPOM was dominated by biofilm polysaccharides. Others report polysaccharide content at about 7.3% for expixylic biofilms (Couch and Meyer 1992). Humin may dominate organic matter in stream sediments, up to 80% of the organic carbon content (Rice and MacCarthy 1989). If the bulk of SAPOM was polysaccharides, it would also have to be ≈ 40% bacterial cells, ≈ 20% protein, or ≈ 11% sorbed ammonium by weight. In marine systems, sorbed inorganic NH_4 may contribute significantly to the N content in sediments with clays (Muller 1977), and/or sediments with organic matter (Rosenfeld 1979). A combination of cells, protein, ammonia and humin coatings probably explain the N content of SAPOM, and could be important fractions in addition to biofilm polysaccharides.

Stable isotopes of POM and SAPOM

Isotopic signatures of samples that were refrozen were not consistently different from samples processed immediately. The average difference was 0.55 per mil, and ranged from 0.61‰ lighter 1.7‰ heavier (n = 4). The POM end members for $\delta^{13}C$ and $\delta^{15}N$ showed differences associated with porewater oxygen concentration (Figure 7). High DO sites (>3mg/l) had $\delta^{13}C$ of -25.7 ± 0.7‰ and $\delta^{15}N$ of -2.5 ± 2.7‰. Low DO sites were depleted in $\delta^{13}C$ (-29.9 ± 3.5‰) and enriched in $\delta^{15}N$ (0.3 ± 1.5‰). Carbon signatures did not differ between coarse and fine fractions for respective sites, but FPOM nitrogen was consistently more enriched, and had a lower C:N ratio than CPOM. The former may be due to selective uptake of lighter nitrogen during mineralization, while the latter observation may reflect microbial and fungal biomass associated with finer organic matter fractions.

Carbon signatures of SAPOM are strongly clustered around -25‰ (Figure 7), which is similar to the average signature for buried POM (terrestrial litter) and also soil DOC (Dawson et al. 2002, Reid Chapter 6). Another smaller cluster occurs in October at -21 to -22‰, close to river DOC. Many of these sites are located at known aquifer recharge zones near the river. Scattered sites have more depleted signatures ranging from -26 to -42‰, which is well beyond the range of our end members. Fractionation associated with methanogenesis can result in highly depleted $\delta^{13}C$ values, anywhere from -60‰ (heterotrophic methanogenesis) to -120‰ (autotrophy) (Whitticar 1999). Our

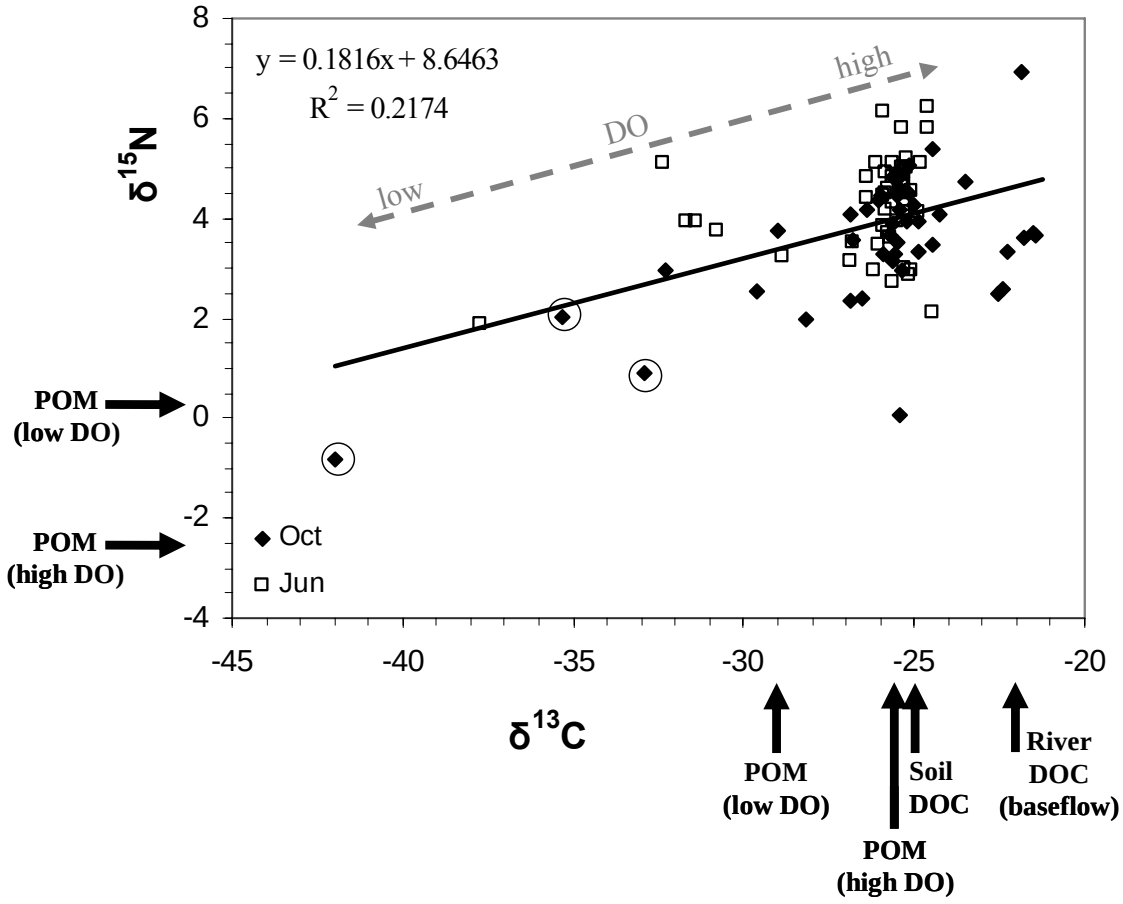

Figure 7: Carbon and Nitrogen stable isotope biplot for SAPOM. Arrows show end members for various carbon and organic nitrogen sources (DOC data from Chapter 6). Carbon and nitrogen signatures show a corresponding decrease (isotopically lighter) with a decline in oxygen. The lowest values are from oxyclines (low oxygen transition zones) at 2-4 meters depth below the water table (circled symbols).

lowest values (circles in Figure 7) occur at the vertical transition zones between low and high oxygen, specifically in October (which is the peak development of the clinograde oxygen profile, described in Chapter 1). $\delta^{13}C$ and $\delta^{15}N$ show a strong linear correlation, both becoming isotopically lighter with decreasing oxygen concentration. The $\delta^{13}C$ trend strongly suggests that methane may contribute to SAPOM signature. SAPOM $\delta^{15}N$ signatures are generally 2-3 trophic transfers from the $\delta^{15}N$ of POM. However at lower oxygen, SAPOM $\delta^{15}N$ converges with POM $\delta^{15}N$, indicating that POM may increasingly contribute to SAPOM composition as anaerobic conditions are approached. Alternatively, lower oxygen zones are expected to have higher ammonium concentrations, and ammonification and also subsequent microbial uptake is selective for lighter nitrogen

(Dawson et al. 2002). We also expect that $\delta^{15}N$ enrichment will increase with flowpath length, due to nutrient spiraling and the lack of exchange with atmospheric nitrogen, the alluvial aquifer as essentially a semi-closed system. The seasonal dynamics indicate that turnover times for SAPOM may be relatively short, at least near aquifer recharge zones and anaerobic sites.

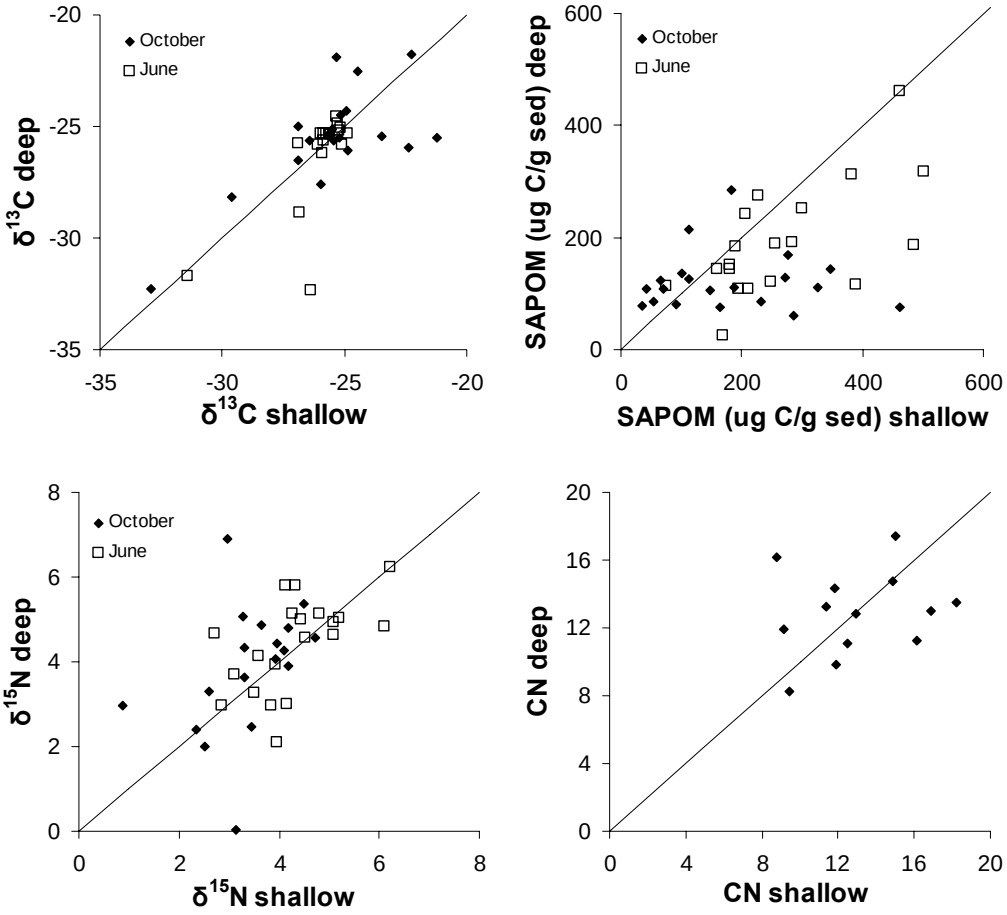

Figure 8: C and N isotopic composition and organic carbon content of SAPOM as a function of depth. Shallow depth (1st meter below MLW) is on the x-axis, and deep (2nd 1 meter below MLW) is on the y axis.

Variation in organic matter properties with depth

We compared shallow (1m below mean low water MLW) and deep (2 meters below MLW) sampling zones for each sampling site. We observed no differences in $\delta^{13}C$ signature with depth (Figure 8a). This is not unexpected, since we cannot distinguish soil DOC from buried POM natural isotopes, and cannot use natural carbon tracers to identify terrestrial carbon loading to the aquifer. We did observe differences in total SAPOM

content (Figure 8b). SAPOM was higher at shallower depths in June (Mann Whitney Test, p=0.05). These differences depended on season, with less difference between depths for the October samples (p=0.149). These samples were taken following flood pulse, where water levels rise and fall several meters over short time periods throughout the aquifer. These seasonal effects may represent the seasonal redistribution and mass transfer of organic matter to deeper depths following flood pulse.

^{15}N signatures also showed differences with depth in October, with more enriched nitrogen at the deeper depths (Figure 8c). The difference was not significant (paired t-test, p=0.18), however most of this observed difference was contributed by vegetated sites (p=0.125), as opposed to gravel bar sites (p=0.866). ^{15}N enrichment can occur due to mineralization and removal of lighter nitrogen, via decomposition or denitrification. Lighter nitrogen is expected as one approaches atmospheric sources and terrestrial vegetation, becoming heavier with progressive decomposition. The difference in ^{15}N signatures with depth may further support the effect of terrestrial organic matter loading to the subsurface. Loading of inorganic nitrogen from overlying soils is also probable, especially considering the low retention of nitrate in soils. However we saw no difference in C:N ratio of SAPOM with depth (Figure 8d). This argues against the possibility of nitrate loading from soils, as we would expect uptake of nitrate in the shallow aquifer, and lower C:N ratios.

Contribution to aquifer organic matter budget

Scaling these results to the aquifer requires a few assumptions. The POM sample is clearly an underestimate, since particles <64 μm would have escaped the sampling net, while particles greater than 2-3 mm would be blocked by the well screen. Large size fractions of buried wood are likely present in the aquifer, and are clearly visible in shallow soils on the floodplain. It is of course not possible to pump a tree out of a well. A more accurate estimation of organic matter content would require extensive coring, and the large size fractions would have to be assayed by excavation. Both approaches are impractical at the spatial scale of the aquifer. We assume here that sand and organic matter collected from well pumping provides an indication of the smallest and perhaps most biologically available organic matter. We assume that the larger fractions are only

available at much longer time scales, as large organic material is broken down into smaller fractions.

Our organic matter estimates are reported in terms of percentage carbon by weight of fine sediments. This also leads to an overestimate of volumetric organic matter density, since much of the aquifer consists of mixed sand and gravel, with occasional deposits of more sorted sand-sized material. Also, silt/clay layers, which are uncommon but may dominate below 10 meters at the downstream end of the floodplain (Diehl 2004) may harbor much more organic matter than reported here. Such formations are probably difficult to extract via well pumping, and their contribution to POM and SAPOM content are unknown. We estimate that fine sandy sediments may comprise roughly 10-40% of the aquifer on average, the high end being roughly the porosity of well sorted gravel, with sand potentially forming the matrix.

The organic carbon POM pool (1.69×10^5 gC/m^3, range 6.4×10^4-1.3×10^7) is clearly greater than the SAPOM pool (2.97×10^4 gC/m^3) by an average of 1 order of magnitude. We consider this is a low estimate, considering the assumption of 10% sand and not accounting for larger wood particles (but conversely, smaller material may be more available for decay). Based on a general estimate of exponential POM decay in the aquifer (-0.00024 d^{-1}; Chapter 5), the POM pool may supply 1.42×10^4 gC/m^3/year. Considering the patchiness of highly concentrated particulate organic matter, local contributions of POM to energy flow can be 3 orders of magnitude higher than this average loading rate (1.8×10^6). By comparison, the DOC concentration in the aquifer is on average 0.65 mg/l (+/- 0.32), which is slightly less than DOC of the source water (main channel). Assuming a mean velocity of 13 m/d (Diehl 2004) and a porosity of 0.3 (mixed sand and gravel, Fetter 2001), annual loading of DOC is approximately 926 gC/m^3/year (+/- 427), which is 5.8 times lower than the potential carbon loading from the POM pool. This POM as a potential energy source is not unlike a battery, storing energy for aquifer food webs for long periods of time, and contributing to the stability of groundwater ecosystems (Wetzel 1995).

Organic Matter in Aquifer Food Webs

We feel that a better classification of particulate organic matter is needed, analogous to carbon quality in dissolved species (e.g. Findlay and Sinsabaugh 2003), and fractionated with respect to forms that are physically available to feeding invertebrates. The two fractions that we studied (POM and SAPOM) may differ in availability to the respective microbial and invertebrate food webs. There is much evidence for microbial response to POM in the subsurface (Jones et al. 1995, Galas et al. 1996, Pusch 1996, Push and Schwoerbel 1996, Crenshaw et al. 2002b). Invertebrate response to buried particulate organic matter can be positive (Crenshaw et al. 2002a, Tillman et al. 2003), weakly positive (Strayer et al. 1997), or neutral (Boulton and Foster 1998, Storey and Williams 2004). Hyporheic invertebrate guts are often filled with sediment, but POM is only observed in guts as a potential component of amorphous material (Chapter 6). The importance of relative assimilative value is underscored by the distribution of the two fractions: POM content varied by orders of magnitude across the aquifer, while the organic matter content of SAPOM had a relatively even distribution. Although a larger pool, POM is essentially non-renewable, and is presumably metabolized in place and depleted over long time scales (there may be some movement of a small component of POM through sediments, as entrained UFPOM – Chapter 5). Meanwhile, SAPOM is renewable via DOC loading in flowing water systems. SAPOM sources may be external (through DOM loading from upgradient sources and immobilization), or local (POM metabolism by microbes, and subsequent uptake or or abiotic sorption) (Pusch et al. 1998, Findlay and Sobczak 2000).

REFERENCES

Beyers, S.C., E.L. Mills and P.L. Stewart. 1978. A comparison of methods of determining organic carbon in marine sediments, with suggestions for a standard method. *Hydrobiol.* 58(1):43-47.

Bonde, T.A., B.T. Christensen and C.C. Cerri. 1992. Dynamics of soil organic matter as reflected by natural 13C abundance in particle size fractions of forested and cultivated oxisols. *Soil Biol. Biochem.* 24(3): 275-277.

Boulton, A.J. and J.G. Foster. 1998. Effects of buried leaf litter and vertical hydrologic exchange on hyporheic water chemistry and fauna in northern New South Wales, Australia. *Freshwat. Biol.* 40: 229-243.

Bretschko, G. and M. Leichtfried. 1987. The determination of organic matter in river sediments. *Arch. Hydrobiol. Suppl.* 68(3): 403-417.

Carter, M.R. Ed. 1993. *Soil Sampling and Methods of Analysis*. Canadian Society of Soil Science, Lewis Publishers.

Claret, C., P. Marmonier, J. Boisssiere, D. Fontvieille, P. Blanc. 1997. Nutrient transfer between parafluvial interstitial water and river water: influence of gravel bar heterogeneity. *Freshwat. Biol.* 37: 657-670.

Coffin, R.B. and L.A. Cifuentes. 1993. Approaches for measuring stable carbon and nitrogen isotopes in bacteria. In: P.F. Kemp, B.F. Sherr, E.B. Sherr and J.J. Cole, eds. *Handbook of methods in aquatic microbial ecology*. Lewis, Boca Raton, FL.

Craft, J.A., J.A. Stanford and M. Pusch. 2002. Microbial respiration within a floodplain aquifer of a large gravel-bed river. *Fresh. Biol.* 47: 251-261.

Couch, C.A. and J.L. Meyer. 1992. Development and composition of the epixylic biofilm in a blackwater river. *Fresh. Biol.* 27:43-51.

Crenshaw, C.L., H.M. Valett, J. Tank. 2002a. Effects of coarse particulate organic matter on fungal biomass and invertebrate density in the subsurface of a headwater stream. *J. N. Am. Benthol. Soc.* 21(1): 28-42.

Crenshaw, C.L., H.M. Valett and J.R. Webster. 2002b. Effects of augmentation of coarse particulate organic matter on metabolism and nutrient retention in hyporheic sediments. *Fresh. Biol.* 47: 1820-1831.

Dawson, T.E., S. Mambelli, A.H. Plamboeck, P.H. Templer and K.P. Tu. 2002. Stable isotopes in plant ecology. *Ann. Rev. Ecol. Syst.* 33: 507-59.

Diehl, C.J. 2004. Controls on the magnitude and location of groundwater/surface water exchange in a gravel dominated alluvial floodplain system, northwestern Montana. Unpublished MS Thesis. University of Montana.

Fetter, C.W. 2001. *Applied Hydrogeology 4th ed.* Prentice.

Findlay, S.E., and R.L. Sinsabaugh, eds. 2003. *Aquatic Ecosystems, Interactivity of Dissolved Organic Matter.* Academic Press, San Diego CA.

Findlay, S. & W. Sobczak. 2000. Microbial communities in hyporheic sediments. In: Jones, J.B. & P.J. Mulholland, eds. *Streams and Ground Waters.* Academic Press, San Diego.

Finlay, J.C., M.E. Power, G. Cabana. 1999. Effects of water velocity on algal carbon isotope ratios: Implications for river food web studies. *Limnol. Oceanogr.* 44(5): 1198-1203.

Finlay, J.C., S. Khandwala, M.E. Power. 2002. Spatial scales of carbon flow in a river food web. *Ecology* 83(7): 1845-1859.

Galas, J., T. Bednarz, E. Dumnicka, A. Starzecka and K Wojtan. 1996. Litter decomposition in a mountain cave water. *Arch. Hydrobiol.* 138(2): 199-211.

Goldin, A. 1987. Reassessing the use of loss-on-ignition for estimating organic matter content ion noncalcareous soils. *Comm. Soil. Sci. Plant. Anal.* 18(9): 1111-1116.

Greiser, N. and A. Faubel. 1992. Biotic Factors. IN: Higgins, R.P. and H. Thiel, eds. *Introduction to the Study of Meiofauna*. Smithsonian. Washington DC.

Harris, D., W.R. Horwath and C. van Kessel. 2001. Acid fumigation of soils to remove carbonates prior to total organic carbon or carbon-13 isotopic analysis. *Soil Sci. Soc. Am. J.* 65: 1853-1856.

Hartog, N., J. Griffioen, P.F. van Bergen. 2005. Depositional and peleohydrologeological controls on the distribution of organic matter and other reactive reductants in aquifer sediments. *Chem. Geol.* 216: 113-131.

Jones, J.B., S. B. Fisher and N.B. Grimm. 1995. Vertical hydrologic exchange and ecosystem metabolism in a Sonoran Desert stream. *Ecology* 76(3): 942-952.

Kaplan, L.A. and J.D. Newbold. 2000. Surface and Subsurface Dissolved Organic Carbon. In: Jones, J.B. and P.J. Mulholland, eds. *Streams and Ground Waters*. Academic Press, San Diego USA.

Leichtfried, M. 1991. POM in bed sediments of a gravel stream (Ritrodat-Lunz study area, Austria). *Verh. Internat. Verein. Limnol.* 24: 1921-1925.

McMahon, P.B. and F.H. Chapelle. 1991. Microbial production of organic acids in aquitard sediments and its role in aquifer geochemistry. *Nature* 349: 233-5.

Metzler, G.M. and L.A. Smock. 1990. Storage and dynamics of subsurface detritus in a sand-bottomed stream. *Can. J. Fish. Aquat. Sci.* 47: 588-594.

Muller, P.J. 1977. C/N ratios of marine sediments: effect of inorganic ammonium and sorbed organic nitrogen of clays. *Geochim. Cosmochim. Acta.* 41:765-776.

Murphy, E.M., J.A. Schramke, J.K. Fredrickson, H.W. Bledsoe, A.J. Francis, D.S. Sklarew and J.C. Linehan. 1992. The influence of microbial activity and sedimentary organic carbon on the isotope geochemistry of the Middendorf Aquifer. *Wat. Res. Res.* 26(3): 723-740.

Pusch, M. 1996. The metabolism of organic matter in the hyporheic zone of a mountain stream. *Hydrobiol.* 323: 107-118.

Pusch, M., D. Fiebig, I. Brettar, H. Eisenmann, B.K. Ellis, L.A. Kaplan, M.A. Lock, M.W. Naegeli and W. Trauspurger. 1998. The role of micro-organisms in the ecological connectivity of running waters. *Fresh. Biol*. 40: 453-495.

Pusch, M. and J. Schwoerbel. 1994. Community respiration in hyporheic sediments of a mountain stream (Steina, Black Forest). *Arch. Hydrobiol.* 130(1): 35-52.

Reid, B.L. 1997. Chapter 1: Oxygen Dynamics and community respiration in a montane floodplain aquifer. For submission to Limnology and Oceanography.

Reid, B.L. 2007. Chapter 3: Large scale hyporheic invertebrate community dynamics in response to oxygen and temperature gradients in the lateral hyporheic zone of an alluvial aquifer. For submission to Freshwater Biology.

Reid, B.L. Chapter 5: Effects of substrate, organic matter, and oxygen on invertebrate density, biomass and production in the hyporheic zone: a mesocosm experiment. For submission to JNABS

Reid, B.L. 2007. Chapter 6: Energy flow in an alluvial aquifer. For submission to Ecology.

Rice, J.A. and P. MacCarthy. 1989. Characterization of a stream sediment humin. IN: I.H. Suffet And P.A. MacCarthy, eds. *Aquatic Humic Substances: Influence on Phase and Treatment of Pollutants*. Adv. Chem Ser, vol. 219, American Chemical Society, Washington DC.

Rosenfeld, J.K. 1979. Ammonium adsorption in nearshore anoxic sediments. *Limnol. Oceanogr.* 24(2): 356-364.

Stanford, J. A., J. V. Ward and B. K. Ellis. 1994. Ecology of the alluvial aquifers of the Flathead River, Montana (USA), pp. 367-390. *IN*: Gibert, J., D. L. Danielopol and J. A. Stanford (eds.), *Groundwater Ecology*. Academic Press, San Diego, California, USA. 571 pp.

Storey, R.C. and D.D. Williams. 2004. Spatial response of hyporheic invertebrates to seasonal changes in environmental patterns. *Fresh. Biol.* 49: 1468-1486.

Strayer, D., S. May, P. Nielsen, W. Wollheim and S Hausam. 1997. Oxygen, organic matter, and sediment granulometry as controls on hyporheic animal communities. *Arch. Hydrobiol.* 140(1): 131-144.

Stumm, W. and J.J. Morgan. 1996. *Aquatic Chemistry* 3rd ed. John Wiley and Sons, Inc. New York.

Tillman, D.C., A. Moerke, C. Ziehl and G. Lamberti. 2003. Subsurface hydrology and degree of burial affect mass loss and invertebrate colonization of leaves in a woodland stream. *Fresh. Biol.* 48: 98-107.

Wallace, J.B., J.J. Hutchens and J.W. Grubach. 2006. Transport and storage of FPOM. In: Hauer, F.R. and G.A. Lamberti, eds. *Methods in Stream Ecology*, 2nd ed. Academic Press.

Wetzel, R.G. 1995. Death, detritus, and energy flow in aquatic ecosystems. *Fresh. Biol.* 33: 83-89.

Whitticar, M.J. 1999. Carbon and hydrogen isotope systematics of bacterial formation and oxidation of methane. *Chem. Geol.* 161: 291-314.

Chapter 3

LARGE-SCALE INVERTEBRATE COMMUNITY DYNAMICS
IN RESPONSE TO OXYGEN GRADIENTS
IN A FLOODPLAIN AQUIFER.

ABSTRACT

In mountain and piedmont valleys, gravel-bed rivers exchange water with their floodplain aquifers at the scale of kilometers. Compared to small scale hyporheic systems, the invertebrate community dynamics, energy sources, and community drivers of large scale systems is virtually unexplored. We investigated the spatial and temporal patterns of hyporheic invertebrate populations throughout a 20 km^2 gravel-bed river alluvial aquifer in western Montana USA. We sampled 25 wells at discrete depth intervals of 1 to 6 meters below the water table. We developed 25 metrics for predicting invertebrate density and distribution, including a range of potential hyporheic "habitat" types (aquifer recharge, midgradient and discharge zones), and vegetation cover types (gravel bar, cottonwood and conifer forest). Invertebrate density varied spatially across the floodplain over 5 orders of magnitude in the top 1 meter interval (<1 to 6 $x10^5/m^3$ sediment). Invertebrate density showed a strong U-shaped response to dissolved oxygen, initially declining with decreasing dissolved oxygen (DO). The trend reversed at about 6mg/l, with highest invertebrate densities at DO < 2 mg/l (≈ 10% of well sites). Invertebrate density declined exponentially with depth at most sites; however, wells with orthograde oxygen profiles (low DO wells with increasing DO with depth) had an exponential increase in invertebrate density at the oxycline. The highest invertebrate densities in the floodplain therefore occurred at the ecotone between low and high oxygen, where small size classes of amphibiont stonefly nymphs were especially abundant. Invertebrate populations showed strong seasonal trends, with densities varying 2-3 orders of magnitude within sites over the annual cycle. Most sites peaked in density 1-2 months after flood pulse, and experienced a second peak in late fall. The oxycline showed a distinct seasonal peak at in September, which was not observed at shallower depths, and corresponded with the oxygen minima in the overlying shallow aquifer. The timing and distribution of invertebrate populations suggest a potential anaerobic subsidy of invertebrate food webs in the alluvial floodplain aquifer. DO also showed a strong positive linear relationship to Nitrate, while pH, specific conductance, strongly associated particulate organic matter (SAPOM) and DOC showed nonlinear responses to DO. Inflections in the water chemistry response to DO indicated that a major biogeochemical threshold occurred at DO < 3-4 mg/l. These results Place oxygen as the central driver in subsurface ecosystems, and contradict the commonly held assumption that declining oxygen tension has negative consequences for aerobic communities.

INTRODUCTION

Likens and Bormann (1974) pointedly state the case for the interaction between land and water as critical to management of both aquatic and terrestrial systems. Aquatic systems such as streams have ecosystem properties of their own, but streams can also be viewed as indicators of entire catchments. While the catchment may ultimately drive the system properties of streams, the interaction between water and sediment at small scales, operating cumulatively throughout the catchment, is the physical mechanism for this linkage. The degree of interaction between sediment and water depends on flux rate and sediment contact area, flux being driven by hydraulic gradient and sediment grain size distribution. Systems with high flux rates and high sediment heterogeneity may have high biogeochemical reactivity (Jones et al. 1995). With shallow depth to bedrock, these small-scale interactions may not be as apparent in the Hubbard Brook Ecosystem which inspired Bormann and Likens' paper. Only with the more recent discovery of the hyporheic zone of rivers has the extent, complexity and magnitude of water-sediment interactions in streams been appreciated.

Hyporheic zone dynamics are a strong driver of ecosystem processes in rivers, and there is a rapidly increasing interest in river ground water-surface water interaction. The hyporheic zone of rivers and streams, first described by Orghidan (1959), is generally considered a transition or ecotone between the channel surface water and phreatic groundwater (Brunke and Gonser 1997). Consequently, most ecological studies of the hyporheic zone have focused unidirectionally upon the significance to surface water (Grimm et al 1987, Valett et al 1993, Baxter and Hauer 2000, Jones and Mulholland 2000, Pepin and Hauer 2002). In general, biotic investigations of the hyporheic zone still proceed on a relatively simple and descriptive level, focusing on the hyporheic interface of smaller streams, mainly due to challenges of sampling deep interstitial environments (Palmer 1993). Smaller scale studies that include some component of site-specific geomorphology and hydrology have proven somewhat insightful (Dole-Olivier and Marmonier 1992a, 1992b, Brunke and Gonser 1999). The few large-scale studies of hyporheic biota have demonstrated only weak distribution patterns (Marmonier et al 1992, Ward and Palmer 1994, Ward and Voelz 1994, Ward et al 1994, Mosslacher and Ward 1999).

In mountain and piedmont valleys throughout western North America gravel-bed rivers exchange surface and ground waters with their floodplains at large spatial scales from hundreds to thousands of meters laterally and tens of meters vertically (Stanford at al 1994). These floodplain aquifers have complex physical and biogeochemical properties, with relatively high flux rates coupled with high spatial heterogeneity, the ingredients for biogeochemical reactivity (Jones at al 1995). Fluvial ground waters also support a suite of organisms from microbes to higher invertebrates, many of which are poorly known. Some of these organisms are found in karst ground water, while others are unique to these systems, such as the amphibiont stoneflies which migrate hundreds of meters into the hyporheic aquifers and return to the main channel to complete their life cycle (Stanford and Gaufin 1974, Stanford and Ward 1988).

We believe that large hyporheic systems of alluvial floodplain aquifers should be considered ecosystems rather than transitional zones. Hyporheic ecosystems have intrinsic properties such as respiration that may be only partly be driven from external (riverine) sources, and may vary significant from adjacent surface systems (Chapter 1). This concept is further supported by the presence of large populations of groundwater obligates such as the aforementioned suite of amphibiont stoneflies. As in any migratory behavior, there must be some energetic basis for the migration, some resource in the floodplain groundwater that is not available in the stream benthos. Considered as a system, floodplain aquifers are isolated from solar energy and probably limited by carbon bioavailability. We hypothesize that a study of whole system energy flow (Odum 1957, Teal 1957, Teal 1962, Strayer 1986) will have more success in explaining subsurface invertebrate communities.

Our primary research objective is to identify the sources of energy for the invertebrate community in a large hyporheic aquifer system. Our research identifies three potential sources of energy: river-derived organic carbon, infiltrating soil organic carbon, or buried and stored particulate organic carbon. We believe that these energy sources will be indicated by patterns of biomass and production in the invertebrate community (Chapter 6). Production is a response variable derived from density, biomass distribution and community composition. In this chapter we focus on the intermediate step: invertebrate distribution and abundance patterns can also indicate potential sources if

energy. Concurrently, environmental variables that most strongly predict invertebrate populations would also allow us to scale invertebrate production to the whole aquifer.

Our more specific predictions can be subdivided into both spatial and temporal patterns of subsurface invertebrate populations. The spatial predictions are formalized in Figure 1, which shows a conceptual lateral flowpath, major organic matter inputs, and predicted spatial patterns of invertebrate abundance. The major source of water to the aquifer is from the river channel, based on mass balance (Poole et al submitted). We therefore expected than invertebrate density would decline with distance from the river (Figure 1b – solid line), following a decline in DOC (shown as arrows with decreasing size from the river). We expected local increases in invertebrate abundance in areas or concentrated buried POM (Figure 1b – dashed line). Finally we predict that invertebrate density would decline strongly with depth, reflecting the influence of the soil & vadose zones, the effect increasing with flowpath length (Figure 1c).

The spatial predictions above are not mutually exclusive, hence we also rely on temporal patterns of invertebrate populations as an indication of energy inputs. Buried POM is generally a static input in older formations. Invertebrate populations will not likely show as much temporal variation in response to this energy source. This is not the case with soil or riverine inputs to the system. Soil infiltration events will occur generally during snowmelt (3rd week of March through 2nd week of April), rising water table (hydrograph rise in April through late May) and major precipitation events (potentially throughout the year). Riverine energy inputs will also be temporally complex, and will track with major pulses (late May through June) or minor pulses in the river hydrograph. Unlike low-order systems (e.g. Rio Calaveras, Baker et al 2000), the local snowmelt pulse is not synchronous with the flood pulse. The complexity of riverine drivers is apparent in the overlap between temperature (peak in mid August), productivity (main channel Chl *a* peak in September, springbrook peak in mid-October to mid-November, Anderson et al in prep), and dissolved organic matter (corresponding with discharge – G.C. Poole pers. com.). Since flowpath residence time can range from hours to months or more (Diehl 2004), each potential driver will likely produce a response in the invertebrate community that is shifted in time, depending on subsurface residence time. Each well site therefore will have a specific time lag in response to river-driven annual cycles.

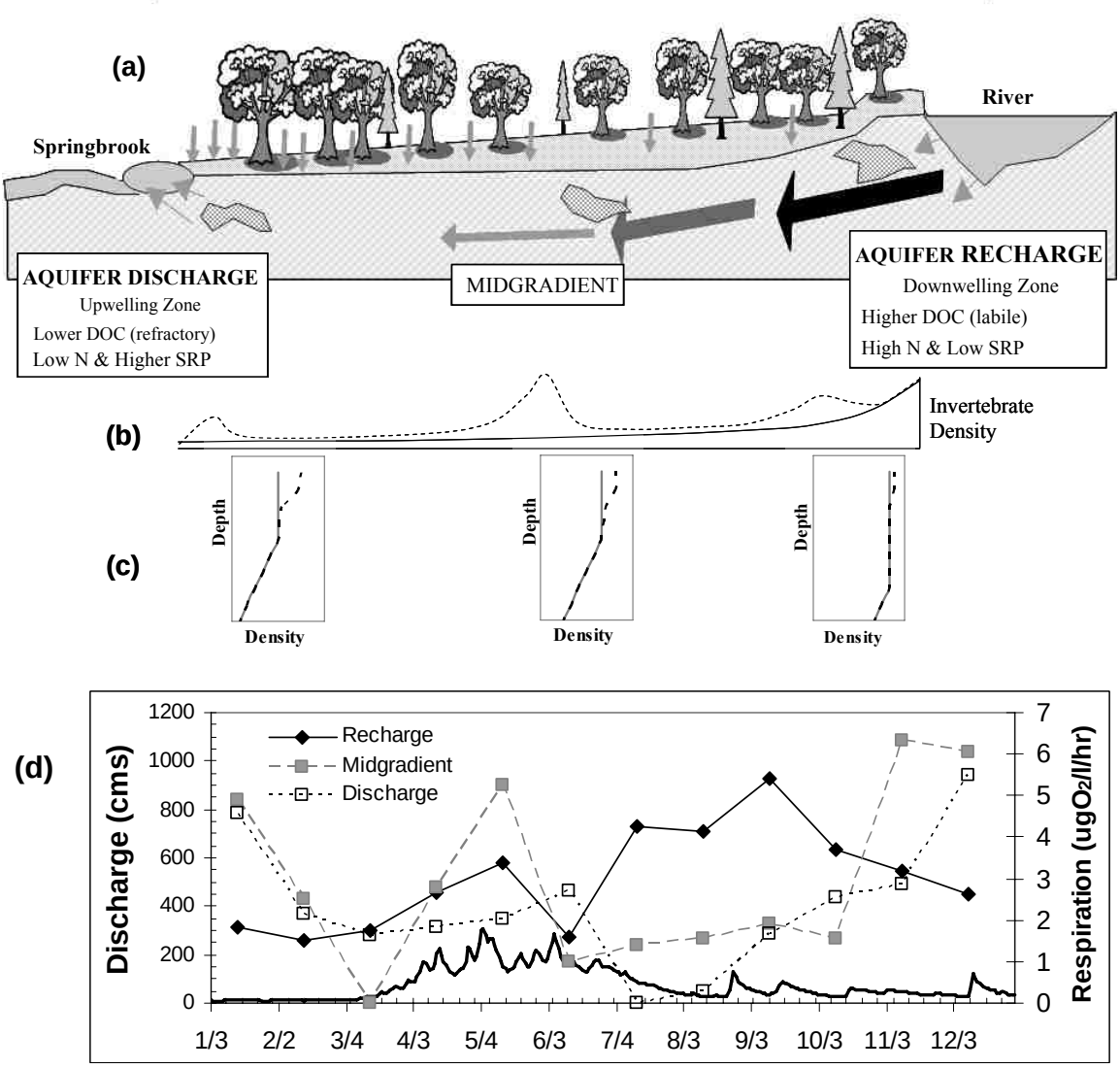

Figure 1: Conceptual model of a lateral flowpath (a). Arrows show potential sources of energy and nutrients along a flowpath, from river DOC (arrows show decreasing concentration and bioavailability), and inputs from soils (vertical arrows), or buried organic matter (polygons). (b) predicted lateral distribution of invertebrate density as a function of distance from the river (solid line), or with density augmented by patches of buried energy sources (dotted line). (c) predicted vertical distribution of invertebrate density as a function of distance from river recharge (solid line) or potential subsidy from overlying terrestrial zone (dotted line). (d) Temporal sequence of potential invertebrate community drivers. Soil line represents river hydrograph in 2004, while symboled lines indicate sediment community respiration for recharge (black diamond), midgradient (gray square) and discharge zones (open square) Data based on 2005-2006 respiration measurements in Reid et al in prep C). See text for additional details on snowmelt pulse and seasonal patterns in channel periphyton.

For simplification, we can represent the integration of these drivers over the annual cycle through hyporheic respiration cycles (Figure 1d, data from Chapter 1). Hence we would expect peaks in invertebrate density in May and August (recharge zones near the river) and peaks in May/Jun and Nov/Dec for longer flowpaths (midgradient, discharge zones), corresponding with respiration peaks.

Hyporheic habitat is an elusive concept, in part due to the sampling difficulties and inaccessibility. Regardless of our conceptual model of an ideal flowpath, defining flowpaths in the field is not straightforward, and flowpaths may change over the course of a year (Poole et al 2006). The few previous studies in floodplain aquifers have focused on gradient analysis (Ward et al 1994) or surface features as indicators of habiat stability (Mosslacher and Ward 1999). Brunke and Gonser (1999) assigned a two-tiered classification for river hyporheic exchange (hyporheic position, based on direction of exchange and depth). Poole's (2006) classification focuses on surficial cues of channel geomorphology and vegetation cover type, however this classification of "hyporheic habitat" has never been evaluated.

In order to tease out the potentially complex spatial and temporal availability of energy resources, we sampled extensively across a medium-size floodplain aquifer, covering the annual cycle for most sites. Parallel to this, we developed a suite of 25 metrics relating to water chemistry, and temperature regime (indicative of cumulative effects of a flowpath), hydrology and sediment organic matter (which is locale-specific), and lastly categorical metrics for range of hyporheic positions and cover types (modified from element vegetation types in Poole 2006).

METHODS

Study site

We conducted this study on the Nyack Floodplain, a 20 km^2 floodplain (10 km long and averages 2 km in width) alluvial reach of the Middle Fork of the Flathead River, in western Montana (48° 27' 30" N, 113° 50' W). The Middle fork is a fifth order gravel-bed river with headwaters in the Bob Marshall-Great Bear Wilderness Complex and is located along the southwest boundary of Glacier National Park (Figure 2a). The floodplain is bounded laterally by valley walls, with bedrock knickpoints at both the

upper and lower ends. The river along the length of the floodplain is anastomosed, with the active channel and parafluvial zone of the river tending toward the northeastern side of the valley. The more mature, orthofluvial floodplain forest and agricultural pasture is to the southwest (see Stanford et al. 2005). Over 30% of the main channel flow is lost to the aquifer at the upstream end of the floodplain (Stanford et al.1994) and various gaining and losing reaches have been documented and modeled throughout the floodplain (Mark Lorang unpub. data, Poole et al submitted). The site has been the focus of research by the Flathead Lake Biological Station for over 20 years, and additional site description is offered in Stanford et al (1994).

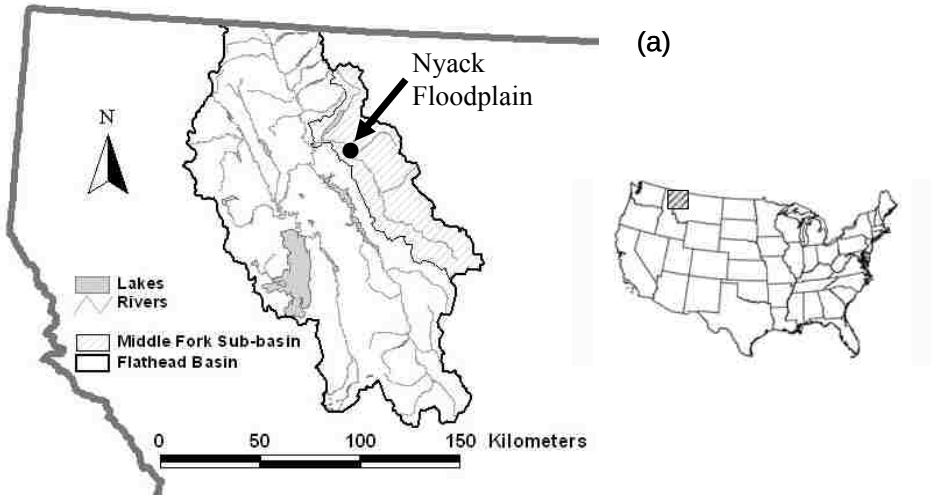

Figure 2 (a): Study site: Nyack Floodplain, Middle Fork Flathead River (MT USA).

Well grid design and installation

The floodplain sampling network consisted of 28 groundwater wells and two surface water sampling locations (Figure 2b). Six of our sampling wells were constructed from three-inch nominal PVC (inside diameter 7.6 cm), installed using a hollow-stem auger drilling rig. An additional 22 invertebrate sampling wells were 2-inch nominal PVC (5.1cm nominal inside diameter), installed using a Geoprobe^{TM}. These wells were located to capture the range of variation among lateral hyporheic positions (Figure 1): aquifer recharge zones, aquifer discharge zones, and midgradient zones (corresponding to infiltration, advection and exfiltration zones, *sensu* Brunke and Gonser 1999, and commonly referred to as areas of downwelling and upwelling). To the extent possible,

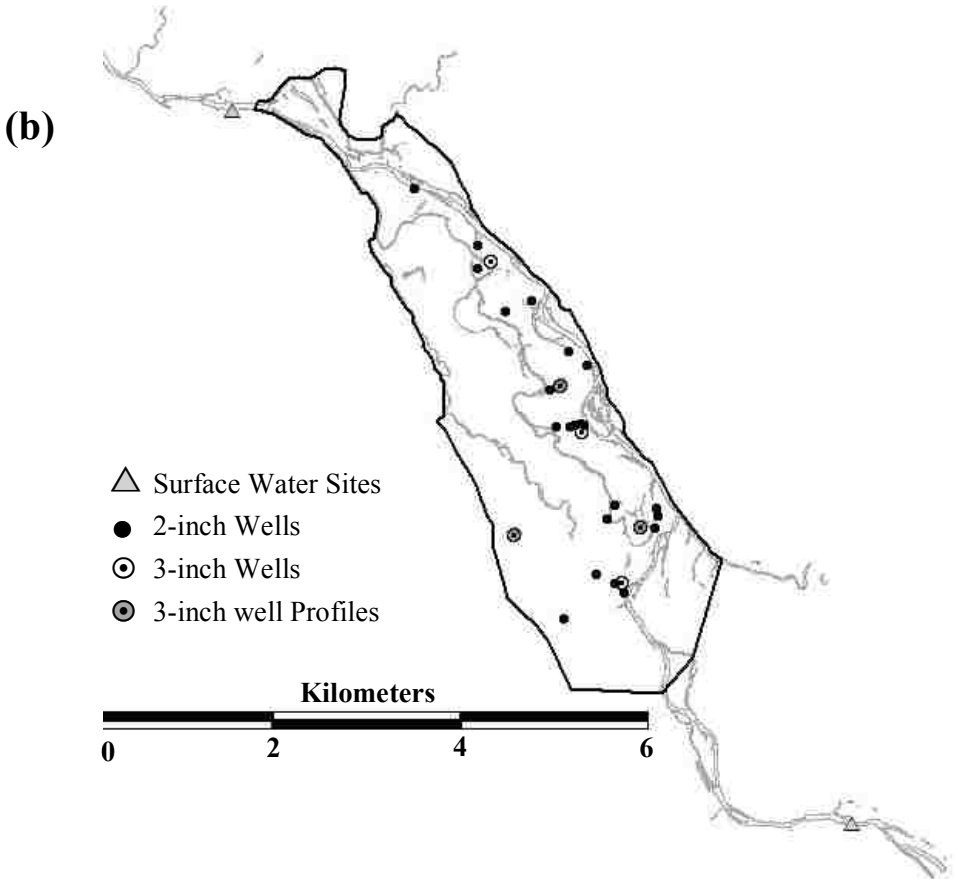

Figure 2 (b). Nyack floodplain well grid. The main channel is furthest to the right, while smaller channel features are spring brooks and other off-channel habitats. Dissolved oxygen sampling locations include 2-inch and 3-inch wells, and surface water sampling points.

well sites were further stratified to represent the upgradient, middle and downgradient regions of the aquifer, and covering the major surface vegetation types (gravel bar, cottonwood and mature conifer forests). Two-inch and three-inch wells were continuously slotted with 100 slot (2.55 mm) and 80 slot (2.04 mm) respectively. The open area extended from just below the soil horizon to total depth, which ranged from 6 to 15 meters for 3" wells and 3 to 5m for 2" wells (see Diehl 2004 for additional details on well design). Since there were some limitations on drill rig portability, especially in more vegetated areas, the floodplain scale well grid is neither random nor entirely systematic. This is balanced by our knowledge that below the soil horizons and surficial channel features, the physical habitat of the subsurface cannot be readily predicted by

passive surface cues. Furthermore, hyporheic position can vary unpredictably within a site over time, depending on river stage and channel activation.

Well and surface water sampling

We collected invertebrates, sediment and organic matter from wells using a hand-operated diaphragm pump (Stanford et al 1994). To isolate 1 meter sampling intervals in the larger 3" nominal wells, we used a flexible hose which was slightly smaller that the well diameter (Tiger Flex, 5 cm dia.). The hose was sealed at the end, the lowest 50 cm interval with intake holes on the side of the hose (2 cm diameter, approximately 25% open area). A 4 cm wide foam packer on either side of this sampling interval was used to isolate this 50 cm interval (see Chapter 1 - Figure 3c). By manipulating the depth of the intake hose, this design allowed for invertebrate and water chemistry sampling at discrete depths along the continuously slotted wells. For the smaller 2" nominal wells we used a similar but scaled-down intake hose design.

We maintained a constant pump discharge between 60-80 liters/min. We sampled 80 liters for each 50cm increment, and pooled increments into 1 meter samples (total 160 liters). Sampling started from a reference depth (RD) unique to each site, which was 10-20 cm below estimated mean low water (based on 2003 water level monitoring: generally this RD was from 1 - 2.6 meters below the land surface). Based on well logs, we observed that the stratified gravel deposits have high vertical substrate heterogeneity. This leads to varying composition of preferential flow zones or pathways, which form suitable habitat for large invertebrates (e.g. stoneflies) intermixed with strata of poorly sorted sand and gravel which greatly limits invertebrate habitat. Establishing a fixed RD for each well was therefore essential for consistency between sampling dates, and to avoid the problems of pump cavitation, low discharge, and low sampling efficiency when water levels receded. We collected pooled 1 meter samples for 1 to 6 meters, depending on the depth of the well. In order to minimize cross-contamination between well intervals at the start of each new interval, we disconnected the intake hose and allowed water to drain back into the well before moving the intake location. Water chemistry samples were taken only from the top 1-meter interval. Occasionally we were able to sample one or two 50 cm increments above RD when high water levels allowed, however these samples

were used for qualitative comparison only. Water, sediment and groundwater invertebrates were collected in a 64 μm NITEX mesh net mounted on a tripod. We concentrated the sample into a bolus net, and we froze the bulk sample in the field with dry ice for later processing. We opted to freeze samples in order to support stable isotope analysis of invertebrates, organic matter, and sediment biofilm (Chapter 6), and also to preserve length-weight relationships. When large amounts of sand were collected, we separated the organic matter and invertebrates from the excess sand via elutriation in the field.

Wells and surface water sites were sampled November 2003 through January 2005 with the highest frequency of sampling during the rising and falling limbs of the hydrograph. We used a stratified (non-random) multi-level sampling design in our well sampling. All wells were sampled for water chemistry on six occasions during the rising and falling limbs of the hydrograph (early Feb, early Apr, late May and late July 2004), and baseflow (Nov 2003 and late Oct 2004). Surface water sites included two main channel locations. A total of 28 wells were sampled for invertebrates. A representative subset, consisting of 9 wells, was sampled monthly from February to October 2004, and once in either December 2004 or January 2005. Sampling frequency was decreased during winter due to the difficulty of access (deep snow) and sampling problems (frozen nets and pumps). Sixteen of the wells were sampled 6 to 7 times, coinciding with water chemistry sampling. Finally, three additional deeper wells were sampled in June and October 2004 and February 2005, in order to better represent vertical fauna profiles.

When invertebrate sampling coincided with water chemistry sampling, we collected the invertebrates first, purging the wells of sediment and invertebrates with the diaphragm pump. Water chemistry samples were drawn from the wells using a 12V electric submersible pump (Whale Submersible 881, Whale Systems Specialists), rather than the diaphragm pump used for invertebrates. The submersible pump discharged at 12 liters per minute, overflowing a 1 liter container containing field probes. We used a YSI 55 Dissolved Oxygen meter (Yellow Springs Instruments) and an Oakton pH/Con10 for pH, specific conductance and temperature. Water was purged for at least 3 minutes prior to taking readings. However, some wells required up to an hour of purging to remove fine sediments before water samples could be taken. DO and other meter readings

generally stabilized within 1 minute of pumping and remained stable regardless of pumping duration. Water was collected in 500ml borosilicate bottles for DOC, and 1 liter polyethylene bottles for NOx, SRP and SO_4. Samples were kept on ice and returned to the lab processing based on standard methods and laboratory-specific protocols. Water samples were analyzed for SRP (molybdate SRP method of Murphey and Riley 1962), DOC (combustion and infrared CO_2 detection on a Tekmar-Dormann carbon analyzer), NO_2/NO_3 (cadmium reduction of Wood et al 1967), and SO_4 using ion chromatography (APHA 1989).

Temperature loggers were installed on smaller diameter PVC inserted into the wells, and the inserts were baffled to isolate respective intervals (Johnson et al 2005). We used Vemco temperature loggers in sites requiring more reliable continuous measurements (near surface water), and iButton loggers were used at other sites, often in vertical arrays of 3 to 6 loggers. The inserts also functioned as well bailers: the column of water inside the well casing was purged when the inserts were drawn out of the well.

Sampling efficiency

Calculating the true density of invertebrates in porous media is difficult. Freeze coring is the only truly quantitative approach, but this method is impractical in deep sediments where repeated sampling is required. Pumping of wells or sandpoints is the only practical approach at large scales or deep sediments. However efficiency of pumping declines over time, presumably as the sampling volume expands and entrainment velocity declines with distance from the well. Several studies have shown large changes in apparent density with increased pumping (Hunt and Stanley 2000, Boulton et al 2003). However if this decline in density is predictable, final invertebrate density could be calculated with a correction factor. We sampled a subset of 10 well intervals representing a range of invertebrate densities. We pumped water in four increments of 20 liters each. For each 20 liter increment, we calculated cumulative density (density at 20, 40, 60 liters) as a proportion of final density (from the full 80 liters) and developed a regression that corrects for pumping efficiency. The regression was used to estimate density at 1 liter (invertebrate density in the immediate vicinity of

the well) as a proportion (Ce) of the final 80 liter sample. We estimated invertebrate density for a m^3 sediment volume, as follows:

$$D = \frac{SD * Ce}{Vol} * \frac{1000l}{1m^3} * \frac{1}{n} \qquad (1)$$

Where D = corrected invertebrate density (#/m^3 sediment), SD = sample density (corrected for meiofauna subsample, see below), Ce = efficiency correction factor, Vol = volume of water sampled [l], and n = sediment porosity (assumed to be 0.4 for preferential flow zones, well sorted gravel - Fetter 2001).

Invertebrate Sample Processing

Invertebrate samples were thawed with running cold water in the lab. Organic matter and invertebrates were separated from mineral sediment by elutriation. Elutriation was repeated until there was minimal evidence of POM remaining in the sand fraction (<<1%). We set aside 10ml of sand from the August samples, which we stained with Rose Bengal and carefully scanned at 25x to estimate efficiency of removal of invertebrates. Typically there were no invertebrates remaining (>99.9% of invertebrates were removed): a few samples had remnants of archiannelids adhering to sand grains, and sites with very high densities of invertebrates had a few copepods or rotifers remaining in the sand fraction.

We rinsed the elutriated fraction through a 500 μm sieve to separate coarse and fine fractions. In contrast to the standard definition of 1mm for meiofauna separation (Higgins and Thiel 1988), the smaller sieve size was chosen to more effectively separate adults of the two dominant copepod genera (*Diacyclops* and *Acnthocyclops*). The coarse fraction was picked at 12x for invertebrates until invertebrates were completely removed. The fine fraction was washed into a 100 ml beaker, diluted to 80-100 ml, and sub-sampled twice with a 5ml Henson-Stimple pipette (pooled to result in a 1/8 to 1/10 sample). Occasionally we diluted to 200-1200 ml, which was required when there was a large volume of organic matter, or invertebrate density was very high. The resulting pooled sample was stained with Rose Bengal for 24hrs, washed of residual stain, and scanned at 25x. For sites that had low density (<30 individuals) or required high dilution, we processed an additional two to six sub-samples. Invertebrates were identified to the

highest practical taxonomic level, as follows: stoneflies were identified to genus or species (depending on size). There are no published descriptions of all of the species of Isocapnia, so we developed a list of traits based on mature nymphs and corresponding adult emergence (see Appendix A). Copepods were identified to species (except for *Parstenocaris*). Mayflies, chironomids, nematodes, ostracods, rotifers, water mites, and amphipods were identified to genus. Annelids, archiannelids and tardigrades were assigned to order or higher. Often this target level of identification could be done during picking; however, for smaller species such as nematodes, cyclopoid copepods, rotifers and chironomids a subset of individuals (generally 10-20) were transferred to a depression slide or permanently mounted for identification. For copepods, this was done comprehensively over the entire sampling period, and was sufficient to estimate overall density by species. For other taxa, this level of identification is only qualitative, and analysis was limited to higher taxonomic order (e.g. Chironomidae, Nematoda, Rotifera etc.) Additional processing steps for SAPOM, CPOM and FPOM organic matter fractions, which was done concurrently with invertebrate processing, are described in detail in Chapter 2.

Analysis

Our analysis focused on 25 variables describing the physiochemical characteristics of each well site (Table 1). For five of the chemical parameters (NOx, SRP, DOC, Specific Conductance (SpC) and pH, we simply calculated a mean based on the six water chemistry sampling events. Note that this mean is probably biased compared to a true mean from continuous data (such as the temperature or oxygen data described below). Sampling was not evenly spaced, with minimal coverage during November through January. Furthermore, the distinctly pulsed nature of floodplains (i.e. the flood pulse in late may, and several minor flood pulses, and the snowmelt/infiltration event) confounds any attempt to estimate true averages, since capturing peak events is not possible without more frequent sampling.

We assigned three categorical variables to each well site. Vegetation cover type was visually estimated from the dominant strata in a 10 meter radius surrounding each well (gravel bar, cottonwood, conifer, grass/agricultural). Cover type is a surrogate for

age of formation, presuming a successional sequence from bare gravel through willow-cottonwood regeneration stand, cottonwood pole stand to mature conifer forest. Concurrent with vegetation development is a change in soil properties from sedimentation and organic matter deposition, hence the grass/agricultural type is probably similar to spruce forest in some regards, based on soil profiles. The second categorical variable was hyporheic position (*sensu* Brunke and Gonser 1999). Recharge zone wells were in areas of presumed river recharge, determined by temperature loggers (diel temperature cycling or annual amplitudes similar to river water), and confirmed by hydrologic investigations (Diehl 2004). Discharge zone wells were located within 10 meters of springs or known areas of bank discharge, determined from potentiometric maps (Diehl 2004). Midgradient zones included all other sites, and were generally located far from surface water and any direct groundwater-surface water exchange. The third categorical variable was well profile, either straight or orthograde, based on the vertical distribution of dissolved oxygen. We assigned a null value for shallow wells where profile could not be determined.

Temperature variables were derived from continuous temperature data, corrected using temperature baths against an ASTM thermometer, with three point calibration. Corrections for the Vemco loggers were generally $\leq$ 0.1 °C. iButton loggers typically overestimated temperature by 0.3 to 0.5 °C (Johnson et al 2005). Accumulated annual degree days was calculated from daily means (using 0.5, one or two hourly measurements depending on site). Where there were short data gaps (1-10 days), we estimated missing data via linear interpolation. In a few cases, we interpolated over 1-3 months, supplemented by data from point measurements taken during well chemistry sampling. Interpolation was reasonable for most of the groundwater data due to low variability and generally predictable temperature trends (rising, falling, and winter temperature trough - many wells near the river remain at about zero for several months). However interpolation is not possible for gaps in surface water data, and was not done for data gaps during the temperature peak. Because of a limitation on loggers, the window for degree day calculation varied by site, drawing from data over a longer time period (2003-2005), and in some cases was fragmented (i.e. we used data from other years for months where data was incomplete). We felt that this was reasonable since monthly degree data

varied on average by only 3 degree days across years, so overall effect over 12 months is ≈1%. Interpolated data had a higher error of 19 monthly degree days across years (i.e. interpolated data compared to measured data from another year). Interpolation was necessary for 5.3% of the data, and we estimate that error from interpolation bias is no more than 3% per site.

We calculated average annual temperature by dividing degree days by 365. Clearly this means that the two variables are related by a constant; however, average temperature was useful in estimating average dissolved oxygen concentration (see below). We observed maximum and minimum temperature from the continuous data and then calculated temperature amplitude (range between max and min, divided by 2. This is an approximation of amplitude in the true sense of a sine waveform, although the annual temperature waveform was not always symmetric about the mean. We visually estimated the time of maximum temperature for both the river and corresponding wells, the latter being delayed as much as three months. This delay was a function of water residence time in the subsurface. This phase shift in temperature between wells and the river source water was therefore used as a coarse surrogate for water residence time. We estimated our phase shift parameter to be accurate within about 5-7 days, hence the estimate is not very reliable for very short residence times.

Dissolved oxygen was measured for most sites on multiple occasions from 2002-2006, in addition to the six water chemistry sampling dates. For each well, we developed a temperature vs. oxygen regression, which was generally linear and significant for all sites (mean $r^2 = 0.68$, ranging from 0.28 to 0.95, $p<0.03$). The slope (Temp/DO sl) was not globally uniform and differs among sites, we believe indicating cumulative respiration over respective river-to-well flowpaths. This slope and intercept (Temp/DO int), combined with the average temperature metric calculated above were in turn used to estimate average DO (essentially estimating a true average DO from continuous data). Using the same regression, we estimated DO maximum and minimum from the corresponding temperature extremes. This site specific relationship between DO and Temperature, and its relationship to community metabolism along flowpaths, is discussed in more detail in Chapter 1.

Organic matter content was estimated from the 2004 frozen invertebrate samples. We recognized two fractions: POM, which is plant derived detritus, was separated from sediment using elutriation, followed by hand removal of invertebrates. Sediment organic matter (SAPOM), equivalent to strongly associated particulate organic matter (SAPOM, *sensu* Pusch 1996, Reid 2007 Chapter 2), is essentially an organic matter coating on fine mineral sediments (sand) pumped from wells. These coatings may consist of cells, biofilm, and sorbed organic matter. POM and SABOM are reported as % of sediment by weight, i.e. organic matter density. More in-depth analysis of sediment organic matter properties at this site, including detailed description of extraction and processing methods, may be found in Chapter 2.

Lastly, we developed three metrics relating to site hydrology. We measured hydraulic conductivity for each well on multiple occasions in 2003, using the residual recovery from drawdown method (Driscoll 1995). Sampling in 2003 employed a high capacity gas-powered diaphragm pump to sample invertebrates, combined with an open ended flexible hose. We monitored pumping time, and prior to terminating the sampling we measured pump discharge as the time to fill a 20 liter bucket. The hose was rapidly withdrawn from the well (noting exact time), an electronic water level logger was inserted into the well, and a series of water level measurements were made (ranging from 10 seconds to 2 minutes post-pumping). We calculated bulk well transmissivity using the following equations:

$$s' = \frac{0.183Q}{T}\left(\log t/t'\right) \qquad (2) \qquad\qquad T = \frac{0.183Q}{\Delta s'} \qquad (3)$$

Where Q is the pump discharge [m^3/d], s' [m] and t' [s] are corresponding measurements of residual drawdown (difference between any given recovering water level and static water level) and time after initiating recharge, while t is total elapsed time during pumping and recovery. Equation 2 shows the relationship between residual drawdown and time as a function of T (and is not directly used). Plotting s' as a function of log (t/t') produces a (usually) linear relationship, the slope of which (Δs') is inserted into equation 3 to solve for T. Hydraulic conductivity (K) was estimated by dividing the computed T value by the open interval of the well (static water level minus the total depth of the well). K values were averaged from 2 to 5 estimates made over the course of sampling in

2003. Note that the K value derived from the residual drawdown method represents the bulk property of the formation penetrated by the screened well interval. Its use to represent properties of the top 1 meter interval may not be appropriate when formation properties are not homogeneous. For 3" wells we obtained K data from Diehl (2004), which was estimated from pneumatic slug tests at discrete 1 meter intervals (Butler et al 2003). We attempted to use a similar approach for 2" wells, but were unable to perform pneumatic slug tests in small wells at shallow depths.

The second hydrologic metric was based on the relationship between water table depth and river discharge. We developed a stage discharge relationship for each well, predicting depth to water to the mean daily discharge (Q in cfs, from USGS gauging station #12358500, 11 kilometers downstream). The relationship was generally linear and significant (mean $r^2 = 0.93$ (+/-0.07), ranging from 0.66 to 0.99, $p < 0.001$). The slope of this relationship (DTW sl) reflects cumulative hydraulic connectivity between respective wells and the river, and is therefore a potential indicator for water residence time in the subsurface. The slope and intercept of this relationship, coupled with the height of the well casing above the ground surface, was used to calculate the depth of the vadose zone. We used a discharge of 12,000 cfs (308 cms – which was the maximum flow during the 2004 flood pulse) to estimate maximum height of the water table for each well. Vadose depth that was negative (typical of gravel bar sites or spring heads) was assigned a value of zero.

We used principle components analysis (PCA; S-plus v. 7.0) as an initial screening of the 25 hyporheic metrics. Invertebrate samples were analyzed for all sampling dates and depths using detrended correspondence analysis (DCA; PC-ORD 5.0). Sample inputs consisted corrected invertebrate densities arrayed as 452 "plots" (individual sampling events specific to well, depth and date) and 33 "species" (taxa occurring in more than one plot, taken to the highest practical resolution as described above). We then compared a subset of the PCA metrics against total invertebrate density and DCA axes 1 and 2. For consistency, all comparisons of hyporheic metrics and invertebrate community metrics were conducted for the first one meter depth interval only.

Results and Discussion

Hyporheic Metrics: Temperature

There is surprisingly little difference between temperature in the river and across the aquifer (Table 1). In general, the aquifer is on average slightly warmer than the river with a higher mean temperature and an excess of up to 500 degree days. We are not sure why the aquifer is warmer, but we speculate that thermal heating of soils and gravels may contribute to this effect. The sites with highest degree days were located on gravel bars at intermediate distances from the river. Alternatively, temperature gain may be a result of mixing with shallow surface water bodies in lateral parafluvial habitats. One well site was significantly colder, and this well was located near a tributary that drains the hillslope water from high elevations. The remaining temperature metrics were somewhat more variable, and based on the initial PCA screening they were highly correlated to the first two metrics discussed (Figure 3, Table 2). The positive relationship between amplitude and maximum temperature, and the negative correlation with minimum temperature, reflects attenuation of the temperature waveform with distance along a flowpath. This is further supported by the correlation with phase shift, as longer flowpaths will have a greater shift in phase between river and aquifer temperatures, and also greater attenuation of the temperature pulse. In our analysis of invertebrate communities, we can therefore reduce our list of temperature variables to temperature amplitude and/or Phase). These temperature patterns are described in more detail in Anderson et al (in prep).

Hydrology

Hydraulic conductivity (K) showed some of the highest variation among all of the variables. The values reported here are within the range of K estimates reported for other well sites by Diehl (2004), but our estimates are somewhat higher than the average of 400 m/d, and are probably less reliable. K was poorly correlated with any of the other metrics (Figure 3, Table 2), perhaps partly due to high variance in our K estimates. The poor correlation is not surprising, since K reflects local hydrologic properties near the well, while chemistry is the result of integrated spatially variable biogeochemical events along flowpaths at much larger scales. K may potentially be a useful property for normalizing

Categorical	**Gravel Bar**	**Cottonwood**	**Conifer**	**Grass**		
Cover Type	9	7	6	3		
	Recharge	**Midgradient**	**Discharge**			
Hyporheic Position	6	10	9			
	NA	**Straight**	**Clinograde**			
DO Profile	5	16	4			
Hydrology	**DTW slope**	**K (m/d)**	**Vadose (cm)**			
Wells	-0.0098 (0.015 to -0.0052)	1021 (84-3087)	36 (0-160)			
Organic Matter	**POM (% mass)**	**SABOM (% mass)**				
Wells	0.81 (0.050-15.4)	0.02 (0.007-0.036)				
Temperature	**Annual Deg. Days**	**Avg T (° C)**	**Ampl T**	**Max**	**Min**	**Phase (days)**
Wells	2461.84 (1901-2734)	6.8 (5.2-7.5)	5.4 (1.3-9.4)	13.0 (7.5-18.8)	2.1 (0.0-4.9)	22 (0-79)
River	2210	6.1	8.2	16.3	0.0	0
Dissolved Oxygen	**Temp/DO slope**	**Temp/DO int**	**avg DO**	**Max**	**Min**	
Wells	-0.56 (-0.08 to -1.14)	9.7 (1.3-15.2)	5.6 (0.7-10.2)	3.1 (1.1-12.5)	8.3 (0.2-6.3)	
River	-0.26	12.70	11.10	8.50	12.7	
Water Chemistry (sd)	**NOx (µg/l)**	**SRP (µg/l)**	**SO_4 (µg/l)**	**DOC (mg/l)**	**SpC (µS/cm^2/s)**	**pH**
Wells	94.9 (54.1)	2.16 (1.01)	6.02 (0.92)	0.65 (0.32)	231 (57.2)	7.87 (0.26)
River	164.5 (76.2)	1.3 (0.5)	4.68 (1.6)	0.82 (0.33)	157 (19.6)	8.24 (0.28)

Table 1: Hyporheic habitat variables, including categorical, hydrology, sediment organic matter content (wells only), and temperature, dissolved oxygen and water chemistry (wells and river). Ranges shown in parenthesis, except for water chemistry variables which are +/- 1 sd. See text for description of variables and derived metrics.

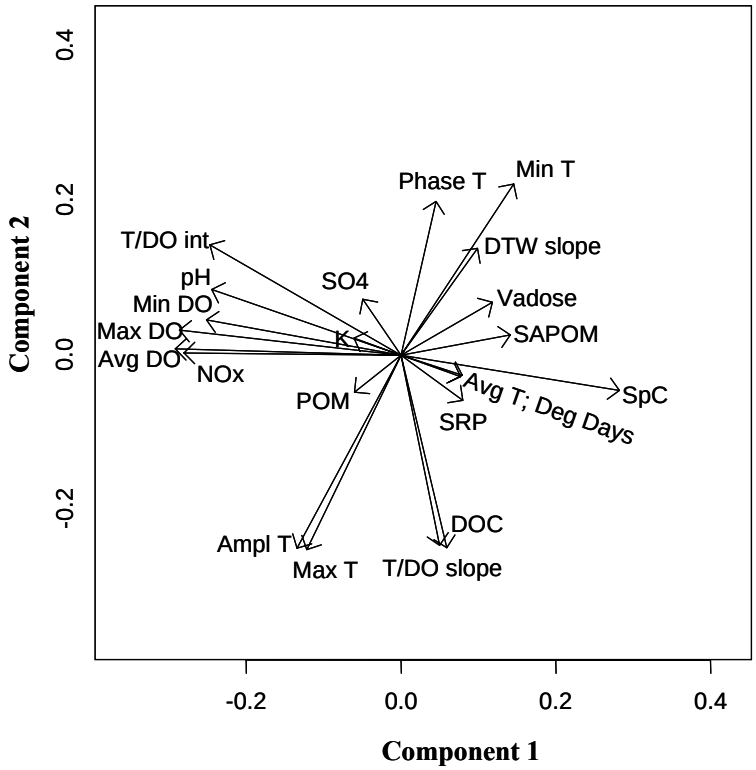

Figure 3: Principle Components Analysis (PCA) biplot of hyporheic variables from Table 1. Variables are described in the text.

		Comp.1	Comp.2	Comp.3	Comp.4	Comp.5
	Standard Deviation	2.71	2.17	1.61	1.25	1.15
	Proportion of Variance	0.335	0.213	0.118	0.071	0.060
	Cumulative Variance	0.335	0.548	0.666	0.736	0.797
Temperature	Degree Days			0.558		-0.253
	Average			0.56		-0.244
	Amplitude	-0.167	-0.392		-0.167	
	Phase Shift		0.311		-0.39	
	Maximum	-0.151	-0.395	0.135	-0.123	
	Minimum	0.182	0.347	0.122	0.234	
DO	Temp vs DO slope		-0.386		0.134	
	Temp vs DO intercept	-0.308	0.224			
	Average	-0.363				
	Minumim	-0.313			0.185	
	Maximum	-0.357				
Hydrology	DTW slope	0.123	0.217	0.13		0.325
	K (m/d)			0.129	0.268	0.666
	Vadose Depth	0.147	0.107		-0.441	
Chemistry	NOx	-0.35				
	SRP				-0.571	0.306
	SO_4			0.113	0.332	-0.254
	DOC		-0.391			
	SpC	0.352				
	pH	-0.305	0.133	0.236		
Organic Matter	POM (%)			-0.232		-0.323
	SABOM (%)	0.176		-0.257		-0.298

Table 2: PCA loadings, showing the first five principle components and explained variance.

invertebrate density, since bulk K may be used to predict the proportion of preferential flow zones (Chapter 1 and Chapter 4). At the 1 meter scale K varies one order of magnitude across the aquifer (Diehl 2004), but there is no systematic pattern of K distribution with depth and along horizontal gradients (Chapter 1). Due to the difficulty in accurately measuring this property we will not use this variable in our analyses, however we note that K may contribute significantly to the variance in the invertebrate density metric.

The slope of the relationship between river discharge and water table (DTWsl) was correlated with the temperature metrics, showing a positive relationship to temperature phase shift. This is not surprising, since we expect a decreasing hydrologic connectivity with the river with an increase in flowpath length. This helps to confirm our observations on the temperature metrics, but also allows us to eliminate some of the redundancy in our metrics.

The vadose zone metric shows no correlation with other variables. The closest covariate is SAPOM, or sediment organic coatings, although there is no significant correlation. Elsewhere we have shown that SAPOM is higher in vegetated types as compared to gravel bar sites (Chapter 2), although this may be a function of sediment age rather than terrestrial aquifer interaction. We will use the vadose depth metric later, to help support our analysis of invertebrate communities and vegetation cover type.

Oxygen and Water Chemistry

There were apparently strong correlations among all of the oxygen metrics, which in turn also show positive or negative correlation with most of the water chemistry variables (Figure 3, Table 2). Oxygen is therefore a very useful reference for the otherwise complex changes in water chemistry variables. The simplest responses to oxygen are linear, negative in the case of NO_x species (Figure 4a, $r^2 = 0.88$, $p<0.001$), and weakly positive for SRP (Figure 4b, $r^2 = 0.11$, log10 transformed, $p = 0.086$). These linear responses probably indicate biogeochemical causation: gradients of denitrification/uptake and desorption (via iron reduction) respectively, in response to declining oxygen concentration. The logarithmic responses of specific conductance

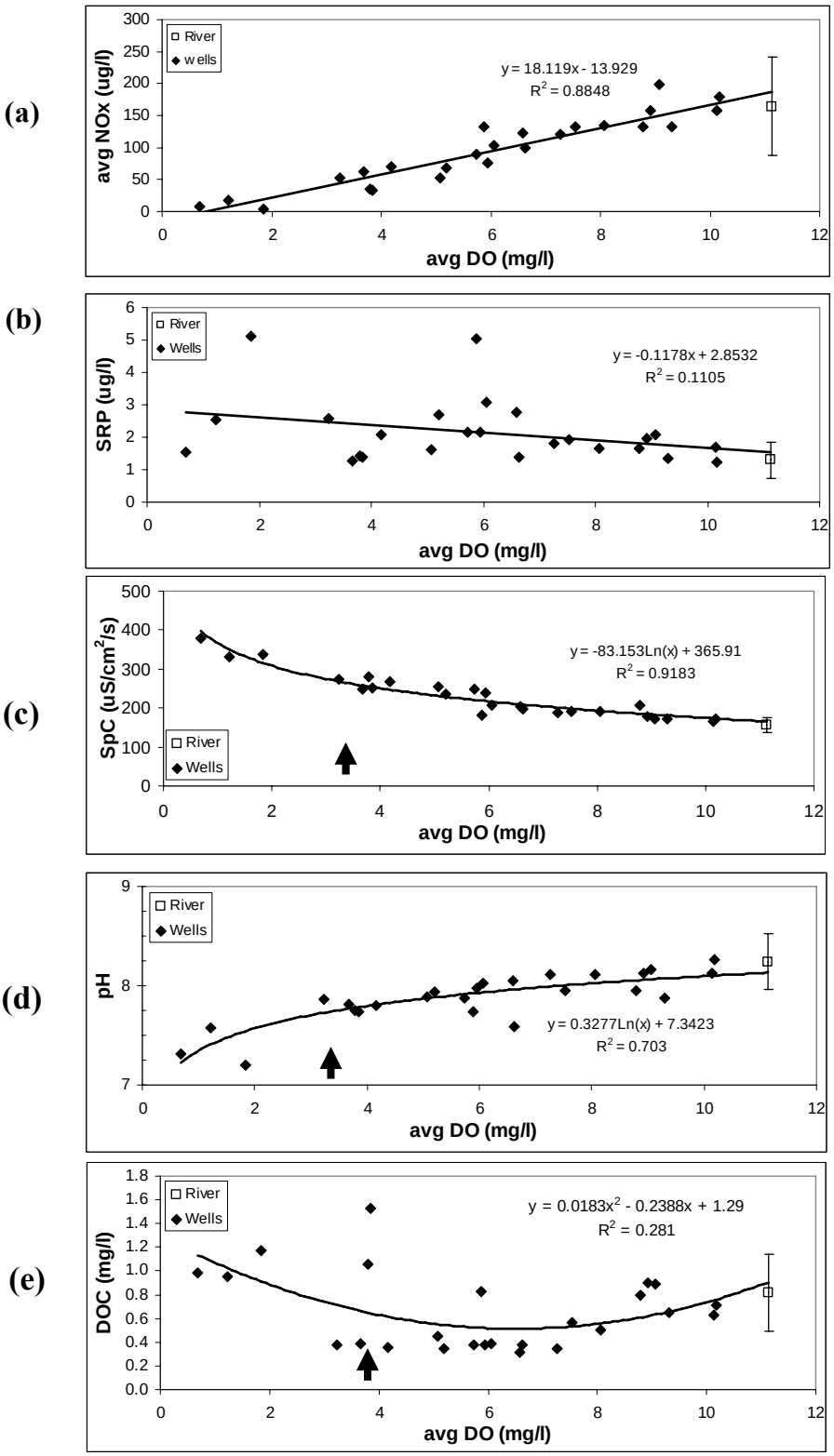

Figure 4: Water chemistry as a function of dissolved oxygen concentration. Open squares are river water, while solid diamonds are groundwater samples. (a) NOx species; (b) SRP; (c) DOC; (d) Specific conductance; (e) pH. Arrows show inflection points, typically near dissolved oxygen of 3-4 mg/l.

(Figure 4c, $r^2 = 0.92$, $p<0.001$), pH (Figure 4d, $r^2 = 0.70$, $p = 0.023$), and %SAPOM ($y = -0.0063*\ln(x)+ 0.0305$, $r^2 = 0.2446$, $p= 0.09$) are actually linear trends through much of the DO range, but with distinct inflection points in the vicinity of 3-4 mg/l. The relationship to pH is likely due to CO_2 evolution through respiration, while specific conductance reflects the increase in dissolved ions (including HCO_3^- from CO_2). The relationship to SAPOM is not known, but may potentially be linked to corresponding changes in DOC concentration and POM metabolism. The relationship between DO and specific conductance and pH is consistent with Brunke and Gonser (1999). Similar relationships have been observed between nitrate and conductivity (Claret et al 2001) and nitrate and oxygen (Claret et al 1997). However, Brunke and Gonser observed the opposite relationships to nitrate and phosphate, possibly because they sampled only shallow hyporheic bed sediments, where oxygen concentration was greater than 72% saturation.

Several of our metrics showed polynomial or U-shaped responses to dissolved oxygen concentration. U-shaped responses indicate more complexity and uncertainty with respect to causation: a U-shaped response is essentially produced by two mechanisms instead of one. We observed U-shaped responses to dissolved oxygen for DOC (Figure 6e, $r^2 = 0.28$) and SO_4 ($y = -0.0381x^2 + 0.4712x + 4.8105$, $r^2 = 0.12$). These responses could also be viewed as asymptotic or exponential through the higher DO range, but again with a more subtle inflection or reversal at 3-5 mg/l O_2. We suspect that in the range of 5-12 mg/l O_2, the declines in DOC indicated uptake, while the increase in SO_4 indicated release/dissolution respectively. We do not suspect causation, but rather correlation with either distance from the river, or sediment contact time since recharge from the river. The reversal at the lower range of DO (<4mg/l) may be directly driven by oxygen concentration. More DOC may be released into solution by breakdown of the abundant POM buried in the sediments. This may be due to an increased number of metabolic pathways for carbon breakdown as the proportion of anaerobic microsites increases. The sulfate relationship is complicated by the competing reactions of dissolution (pyrite or other sulfate minerals) and reduction to hydrogen sulfide. It should not be surprising that the DO-Sulfate relationship is the weakest of the chemical species we investigated.

The relationship between temperature and DO (T/DOsl) shows a correlation with the subset of temperature metrics relating to attenuation of the temperature waveform (Phase, MaxT, MinT, AmpT), as well as the metric for hydraulic connectivity (DTWsl). Collectively these indicate the effect of aquifer residence time on temperature attenuation and cumulative respiration along the respective flowpath. However, none of these variables show a strong relationship to mean DO. In light of the strong relationship between DO and temperature previously shown for individual wells, it is clear that the relationship between temperature and oxygen is apparently site specific. That is, it depends on residence time, and the strong site-specific relationship falls apart when analyzed globally across all sites.

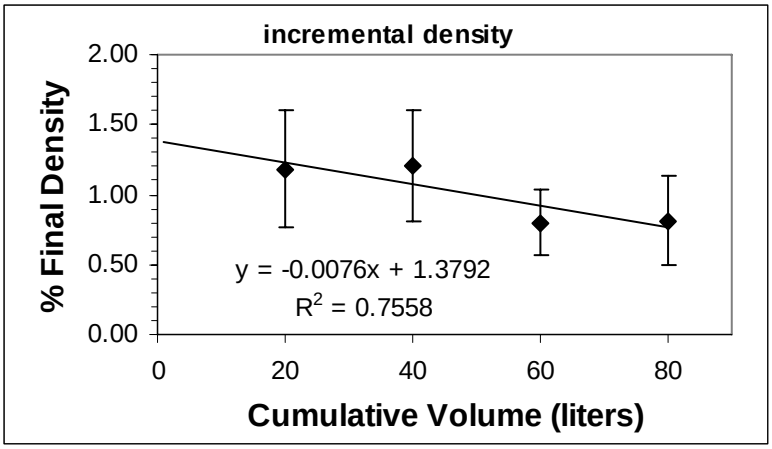

Figure 5: Well sampling efficiency. Invertebrate density (#/l, normalized as a % of the final density) as a function of cumulative sample volume (ln transformed density, p=0.001). True density is approximated by multiplying final density from typical 80 liter sample by the intercept at 1 liter (1.38).

Invertebrate Sampling Efficiency

Invertebrate density estimates were relatively high and variable for the first two 20-liter samples, and only slightly lower and less variable for the final two increments (Figure 5). All ten sites showed this same trend which was consistent across the most abundant meiofauna taxonomic groups (nauplii, cyclopoids, *Bryocamptus*, *Parastenocaris*, archiannelids, bathynellids and rotifers) and was also consistent for the dominant macrofauna (*Stygobromus* and Plecoptera). Collectively the response can be modeled as a linear decline with increased sample volume ($y = -0.0076x+1.3792$, ln transformed to equalize variance, $r^2 = 0.75$, $p = 0.001$). The intercept at 1 liter was used as

the correction factor for pumping volume (Ce = 1.359). This is a surprisingly minor correction compared to other published studies of the effects of sample volume (Boulton et al 2003, 2004). The correction is insignificant compared to the overall 6^{+} orders of magnitude variation in invertebrate density observed across the floodplain since the sites selected for this efficiency trial varied by 4 orders of magnitude.

We developed a simple model to attempt to explain the disparity in sampling efficiency. Knowing the pump discharge (Q), sediment porosity (*n*), well/sandpoint open interval (L) and well radius (r), one can predict the linear velocity and sampling radius around the well. We assumed *n* was 0.3 (gravel/sand ranges from 0.2-0.5 depending or sorting, Fetter 2001), and compared our sampling design (Q = 40 to 80 l/m, L = 50 cm, r = 2.5 cm) to a typical sandpoint or Bou-Rouch method (Q = 1 to4 l/m, L = 15cm, r = 1.25 cm) (Hunt and Stanley 2000). Figure 6a shows the predicted entrainment velocity under a range of pumping rates for each design. The sandpoint sampling, typically employed in shallow hyporheic systems, has a much lower intake velocity that declines rapidly to sub-millimeter per second rates over the course of a typical 5 liter sample. Figure 6b shows an

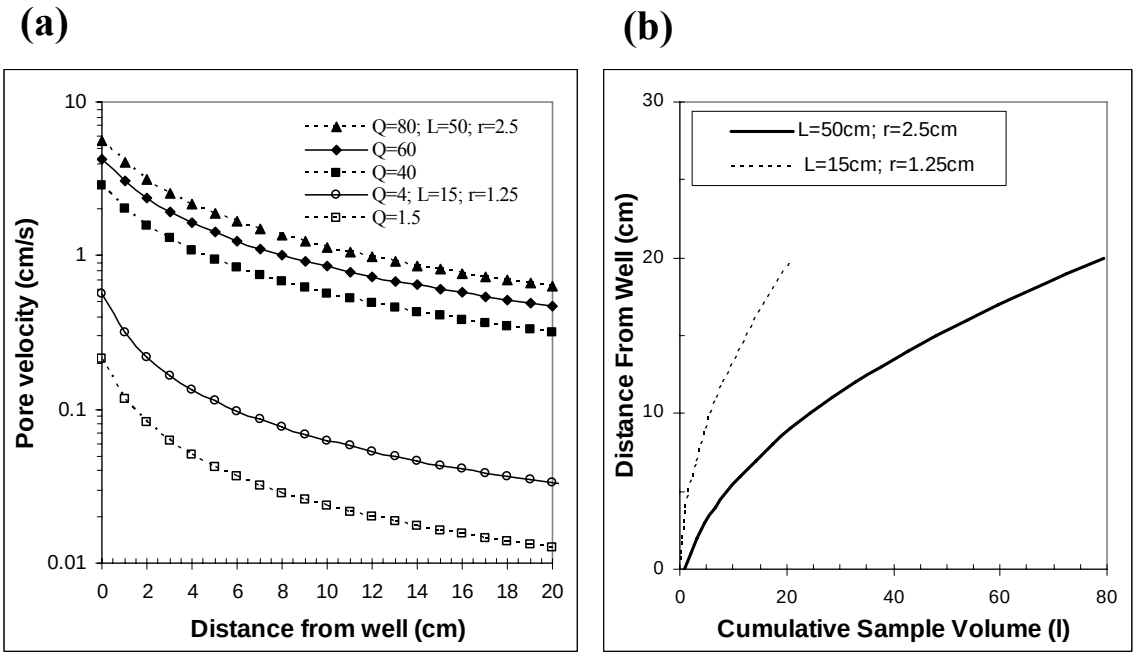

Figure 6: Theoretical well sampling efficiency. (a) Linear pore velocity as a function of pump rate (Q in l/m), sampling interval (L in cm) and well diameter (r in cm). Shown are models for typical sandpoint methods (open symbols) and methods used in this study (solid circles) – Note log scale; see text for assumptions. (b) Sampling radius from well or sandpoint as a function of cumulative volume of water sampled. Typical sandpoint sample of 5 liters will draw from a 10 cm radius, while an 80 liter sample (this study) draws from a 20+cm radius.

estimated sampling radius as a function of sample volume and well design. A typical 5 liter sandpoint sample will entrain water from an approximately 10 cm radius, while an 80 liter well sample will draw from 20 cm beyond the well casing.

We summarize the relative merits of sampling design as follows. First, high pump discharge rate will probably reduce the effects of declining sampling efficiency. Secondly, a larger sampling interval (50 cm vice <15cm) will integrate the effects of vertical substrate heterogeneity. The two are related, since higher pump discharge is more difficult to attain with a small well design. In turn, the effect of small sample interval is probably the main source of variation among sandpoint replicates. Finally, a larger sample volume may also reduce variation by integrating from a larger sample radius around the well. Of course, sandpoints are more useful for sampling small scales while continuously slotted wells may lead to cross-contamination across intervals. We point out that it is relatively easy to manipulate this calculation to design a well or sandpoint that is most appropriate for the given field conditions. Correction for site-specific sampling decay and estimating density at the 1 liter intercept may also be a useful approach for improving comparability between sites. We report our invertebrate densities in terms of sediment volume rather than water volume, since we are interested in scaling up invertebrate populations across the aquifer, and making comparisons with sediment respiration rates (typically normalized by sediment volume).

Invertebrate Communities and Invertebrate Density

Invertebrate density varied over five orders of magnitude for the first 1 meter depth interval, and over 6 orders of magnitude with depth (<1 to over 600,000 individuals/m^3 sediment). A list of common taxa is included in Appendix B. Cyclopoid copepods were overall the most abundant taxa, predominantly *Diacyclops languidoides* and *Acanthocyclops montana*. The harpacticoid *Bryocamptus hiemalis,* was a frequent co-dominant, along with archiannelids (*Troglochaetus*), nematodes (primarily *Monhystera* and *Eudorylaimus*), and rotifers (*Dissotrocha, Rotaria*, and *Lepadella*). Macrofauna were dominated by amphipods (*Stygobromus tritus*) and amphibiont stoneflies (*Paraperla frontalis, Isocapnia grandis, I. integra* and *I. crinita*). In wells near surface waters, stygophiles were a frequent to dominant component, principally the

copepod *Acanthocyclops vernalis*, the mayfly *Ameletus*, and Chironomids (16 genera, but predominantly Orthocladiinae indet. spp.).

Invertebrate community composition and abundance showed the strongest relationships to dissolved oxygen content (Figure 7). Again we see a U-shaped response to mean oxygen; however, the inflection is apparently higher than observed for the biogeochemical metrics (in the range of 6mg/l O_2 for invertebrates, compared to 3-4 mg/l). The categorical variable for cover type is clearly distributed across the spectrum of oxygen and invertebrate density, hence there is no clear general influence of the terrestrial zone.

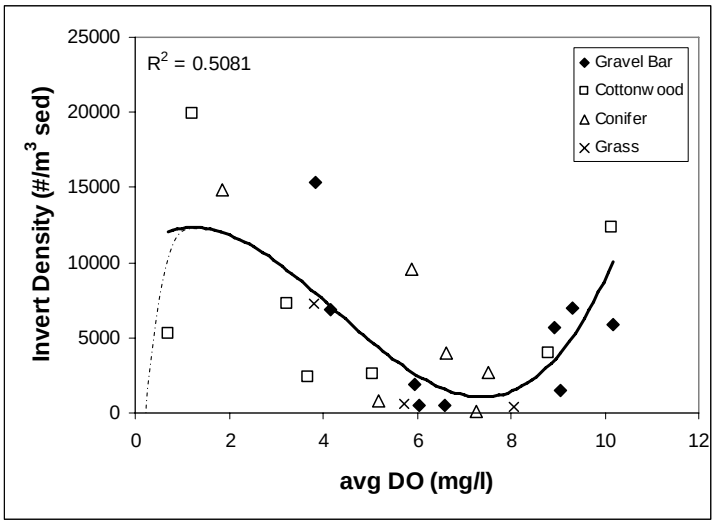

Figure 7: Invertebrate density as a function of dissolved oxygen concentration and vegetation cover type. Dashed line predicts a steep decline in invertebrate densities at extreme low oxygen concentrations.

DCA Axis 1 and 2 explained 0.379 and 0.182 of the invertebrate community variance respectively. We combined invertebrate composition and density for all plots within each site. When we compare the DCA axes with oxygen concentration, we see a gaussian distribution for both axes. In this case, the downward inflection again occurs at about 6mg/l O_2, but the clusters clearly separate only for sites below 3-4 mg/l. Axis 1 for specific taxa are shown in Table 3. The progression in DCA axis 1 from high to low represents a shift in composition from stygophiles, through amphibites and stygobionts. The lowest values represent taxa that dominate in low oxygen zones: the stonefly *P. frontalis*, the copepod *D. languidoides*, and several generalist or psammophilic groups.

Although we did not separate rotifer genera in this analysis, *Lepadella* was also diagnostic for these low oxygen zones. The stonefly *I. crinita* is widespread when mature nymphs are returning to the river, but immature nymphs only occur in these low oxygen zones.

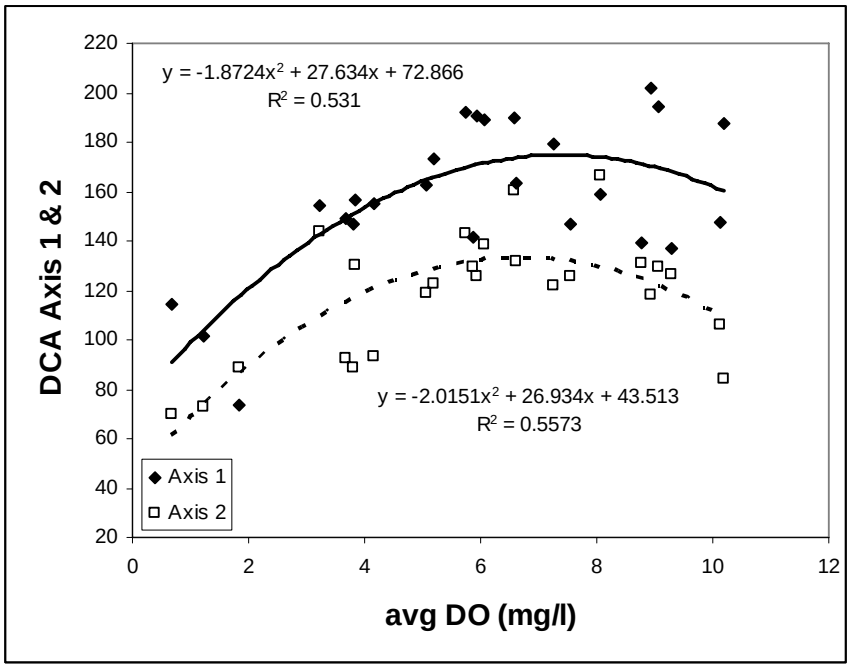

Figure 8: DCA axis 1 (solid diamonds) & 2 (open squares) as a gaussian function of average Dissolved oxygen concentration.

Taxa	Affinity	Axis 1
Acanthocyclops vernalis	SPh	375
Ephemeroptera	SPh	346
Chironimidae	SPh	271
Capniidae (<2mm)	A	270
Bathynellaceae	SB	267
Perlomyia utahensis	A	253
Archiannelid	SB	251
Chloroperlidae (<2mm)	A	244
Acanthocyclops montana	SB	242
Stygobromus tritus	SB	235
Isocapnia spp	A	219
Rotifera	G	180
Isocapnia crinita	A	179
Parastenocaris	G	146
Diacyclops languidoides	SB	139
Paraperla frontalis	A	110
Nematoda	*G*	-32
Bryocamptus hiemalis	G	-36

Table 3: DCA axis 1 for major invertebrate taxa. Declining order reflects trend towards low oxygen sites, and a progression from stygophiles (SPh), through stygobionts (SB) and amphibiont stoneflies (A), to more generalist (G) species, typically psammophilic taxa. The approximate inflection point from Figure 6 is shaded.

Seasonal patterns of invertebrate density

All sites showed a pronounced seasonal variation, typically 2 to 3 orders of magnitude over the annual cycle. Timing of the peak in invertebrate density was variable. It is difficult to specify peaks precisely since there were only 6 to 11 samples per site, and winter coverage was not complete. We did observe 6 general patterns in seasonal abundance. The most common trend (**Group 1**: 7 sites) was a bimodal pattern, with peaks in late June to July, and a second peak, typically larger, in the winter (post October, where sampling coverage was not sufficient to determine precise time). We presume that the first peak may be a delayed response to the river flood pulse, as many, but not all sites have a relatively long residence time (indicated by Phase shift and DTW slope). The second peak is not clear, but may be a response to the oxygen minimum in Sept/Oct (Chapter 1) with a similar phase shift. The second most common pattern (**Group 2**: 5 sites) showed a similar summer peak, but the second peak was absent. Another four sites had an August/September peak; however, there are no consistent features among these sites (**Group 3**). An additional 4 sites had peaks in March and April (**Group 4)**. All of these sites were within 200 meters of each other and were located in a cottonwood stand on an old channel feature. This is the only pattern that suggests a possible influence of floodplain snowmelt (late March to early April) on the subsurface. The soils at these sites are generally deep sand, but other than the geomorphology of this group of wells there are no similar attributes among all sites. Three sites had a peak in invertebrate density in late May, coinciding with the flood pulse, but there were no consistent properties among these sites (**Group 5**). Finally, two sites (**Group 6**) had a distinct winter peak (on or prior to the February sample). Both of these sites were located in discharge zones at the heads of springs. This winter peak was also observed during colonization of one pair of *in-situ* mesocosms (Chapter 4), also located at a spring head, and heretofore unexplained. We suspect that this winter maximum is related to algal productivity in nearby springbrooks (which peaks in late fall), and corresponds with a winter peak in respiration (Figure 1d, discharge zone). Of all the 6 groups, this is one that most clearly shows a potential connection between algal productivity and subsurface invertebrate communities. Jones et al (1995) showed that hyporheic respiration corresponded with algal biomass, at least on the rising limb.

Organic matter

We also observed correspondence between the organic matter variables and invertebrate communities (Figure 8a and b). SAPOM showed a linear relationship to DCA Axis 1 ($r^2 = 0.35$), however there was a much weaker response from Axis 2. DOC had a weaker logarithmic relationship to Axis 1 and 2. POM showed no relationship to invertebrate communities. Collectively these trends indicate that an increase in some forms of organic matter corresponds with an increase in density and taxa typical of low oxygen zones. We note that since metazoans have a limited (to our knowledge) ability to make use of dissolved organic matter, the SAPOM relationship is not only stronger but also more sensible. Elsewhere we show that mineral sediment is the dominant component of invertebrate gut contents (Chapter 6). While the sediment itself offers no particular insight on energy flow in the subsurface, SAPOM (sediment coatings, biofilm) may be an important mechanism for carbon flow through the invertebrate food web.

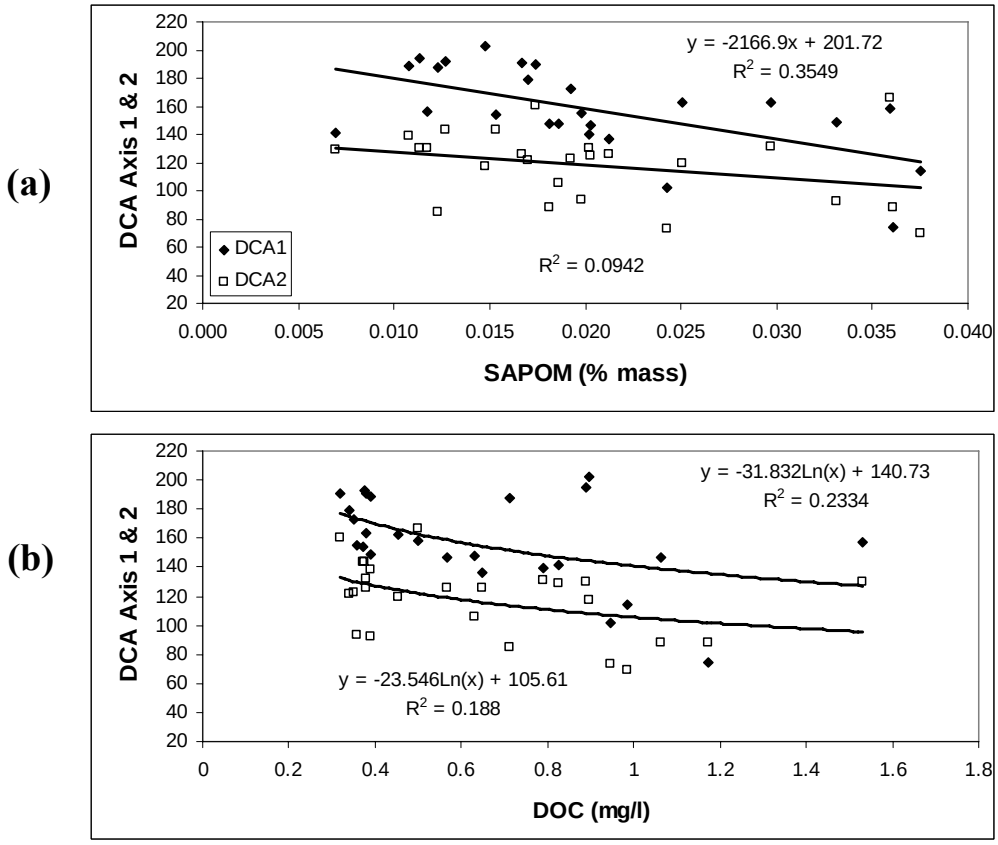

Figure 9: (a) DCA axis 1 (solid diamonds) & 2 (open squares) as a linear function of sediment organic matter (SAPOM fraction). (b) Axis 1 and two as a logarithmic function of average DOC concentration.

Categorical variables: cover type and hyporheic position

We evaluated two of the categorical metrics, cover type and hyporheic position, in terms of their ability to identify invertebrate community attributes. Hyporheic position showed no difference between groups for either DCA axis 1 or 2 (ANOVA, $p = 0.498$ for axis 1, $p = 0.844$ axis 2). There were differences in invertebrate density in response to hyporheic position (Krukal-Wallis, $p= 0.011$). Invertebrate density for aquifer discharge zones (such as spring heads) was significantly lower than recharge or mid-gradient sites (Mann Whitney U-test, $p<0.05$). Cover type showed differences between types for DCA axis 1 only (ANOVA, $p = 0.039$). The differences were solely due to the gravel bar and cottonwood cover types (t-test, $p = 0.0035$). This pattern is reinforced by comparing our cover classes to the metric for vadose depth. Here again, we see a significant difference between cover types (Kruskal-Wallis, $p = 0.053$), which distinguishes gravel bar and cottonwood sites (Mann Whitney U-test, $p = 0.0056$). Gravel bar sites have no real soil development whereas cottonwood stands generally have shallow to deep deposition of well sorted sand. Further along the successional trajectory are conifer forests with deeper soils and distinct silt and clay layers. If there are interactions between the terrestrial zone and the aquifer, regardless of how subtle, cottonwood stands and their sandy soils are the most likely source.

No differences in invertebrate density were observed among cover types (Kruskal-Wallis, $p = 0.54$), which is also clear from Figure 7. None of the other metrics, including the temperature variables, offered any significant predictive power with respect to invertebrate communities. Beyond these relationships, we are reluctant to overanalyze our invertebrate community data. In our list of taxa in Appendix B, we do include general comments on abundance, distribution, affinity (Stygophile, Amphibiont, Stygobiont), and tolerance for low DO. Taxonomic limitations are one impediment. Many of these species are undescribed or cannot be tracked through all life stages. Our collections include two new Bathynellid taxa, a new genus of harpacticoid copepod, a new amphipod species in the genus *Stygobromus,* and 2 indeterminate Orthocladiinae chironomids that may have an amphibiont life history. Animal communities in general are a questionable construct (Tansley 1935) and if anything the subsurface communities are only furthermore so. Subsurface communities are functionally reduced and truncated with high generalization

(Gibert and Deharveng 2002). We expect that the patterns relevant to our question will emerge more strongly from response variables like biomass or production (Chapter 6). Finally, the vertical profiles in invertebrate density, discussed in the next section, in some ways complicate the relationships we have laid out thus far.

Vertical Profiles of Invertebrate Density

In Chapter 1 we described the spatial distribution of oxygen across the Nyack floodplain, including changes with depth. We observed a repeatable pattern where shallow low-oxygen sites always had higher oxygen levels with increased depth. The transition was sharp and typically occurred at 2 to 4 meters depth. This vertical profile, also called an orthograde profile, occurred at about 20% of all wells sites and was distinctly different from the straight DO profiles observed at all other sites. From the patterns described in this paper, we expected that in these orthograde sites invertebrate density would decrease sharply with depth, corresponding with a rise in oxygen. Instead we found that invertebrate density increased exponentially (mean $r^2 = 0.93$) with the peak occurring at the transition zone between low and high oxygen. Since the low dissolved oxygen sites at depth supported some of the highest invertebrate densities at the 1 meter depth, the underlying redox transition was typically an order of magnitude higher density, clearly the highest invertebrate densities in the aquifer. In Figure 10a, we observe that this holds for 3 of the 4 orthograde sites. The outlier was located on an alluvial fan formed by a hillslope drainage, the one well that is farthest from the river channel, and most likely driven by a different groundwater system. Other than its location, we have no direct indication why the vertical correspondence between low oxygen and high invertebrate density is not consistent with the other orthograde wells.

In contrast, sites with straight DO profiles saw a sharp decrease in density with depth. The pattern is logarithmic for 2 of the six wells ($r^2 = 0.94$, includes the alluvial fan well). For the remaining 4 wells, the drop in density occurs in the second meter, and beyond that transition the trend is more or less linear with depth. This sharp decline after the first meter is similar to what we predicted for terrestrial subsidy, shown in Figure 1c. These vertical patterns are similar for macrofauna, except that only two of the orthograde wells show exponential increases in invertebrates with depth (Figure 10b).

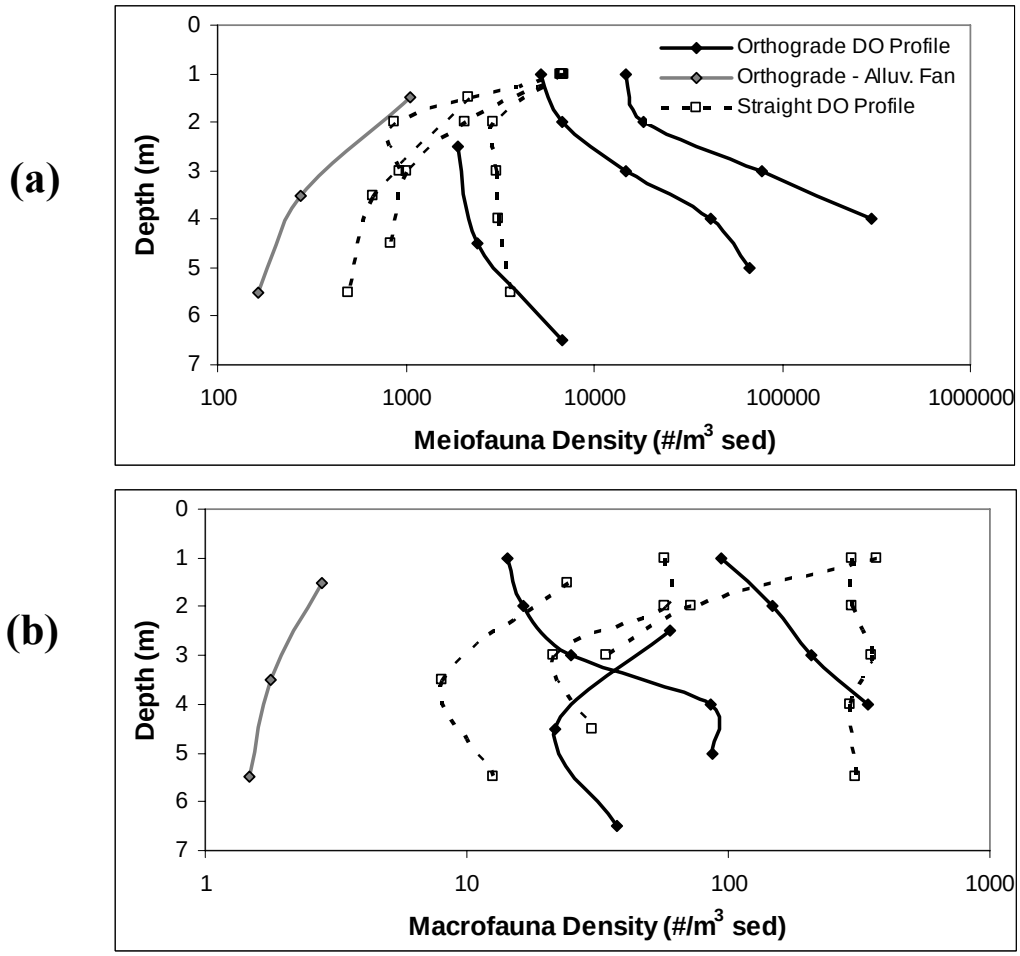

Figure 10: Vertical density distribution of meiofauna (a) and macrofauna (b) for wells of either orthograde or straight DO profiles (x-axis is on a log scale). Meiofauna show an exponential increase with depth for 3 of 4 orthograde profiles, and a logarithmic decline for straight profiles. Macrofauna show less consistent vertical patterns with depth and profile type.

It is not evident from this analysis alone whether the low oxygen zones are a cause or a consequence of high invertebrate density. Metalimnetic oxygen declines in some lakes have been linked to high zooplankton respiration (Minder 1923, Shapiro 1960). Elsewhere these low oxygen layers are attributed to bacterial decomposition (Mitchell and Burns 1979) or methane oxidation (reviewed in Wetzel 2001). There is evidence that some lake rotifer species have population maxima that track with the changing oxycline (Armengol-Diaz 1995). This vertical movement would be very difficult in the aquifer subsurface, due to horizontally stratified coarse and fine sediments. In Chapter 5 we provide experimental evidence that high invertebrate density is a consequence of low oxygen tension. Localized high invertebrate densities occur at the

fine sediment interface, with an increased response when bulk oxygen concentrations are lowest (Chapter 5).

An explanation for these vertical patterns emerges when we look at the changes in invertebrate density over time. Figure 11 shows invertebrate abundance over 4 meters depth through the annual cycle for a typical orthograde well. The transition between low and high oxygen occurs at the 4 meter depth, while the oxygen minimum occurs in late September to early October (Chapter 1). In the top two meters we saw a peak in abundance for meiofauna in late May, and late June for macrofauna. This is the second most common seasonal pattern, as previously described. In the 3rd and 4th meters depth, a second peak appears in late September and early October and is clearly at its maximum in the 4th meter, or the transition to higher dissolved oxygen (2-3 mg/l higher than the surface interval). The stonefly *P. frontalis* and the harpacticoid *B. hiemalis* are particularly abundant at this transition depth (oxycline).

The second peak in the early fall may be indirectly related to the low oxygen minima in overlying sediments. Elsewhere we have shown experimentally that transitions between coarse and fine sediments support dramatically higher invertebrate densities, and that the difference is most strongly magnified in sites with overall low oxygen (Chapter 5). We suspect that the products of anaerobic reactions occurring in fine sediments may be supplied to nearby zones of preferential flow. Methane or short chain fermentation products (or soluble phosphorous), originating from sediments not generally accessible to metazoans, would be oxidized at or near the redox interface, thereby becoming available for grazing. Collectively over the 4 meters depth, the seasonal trend for this site is bimodal, with summer and fall peaks in invertebrate density, similar to the dominant seasonal trend observed in the well network. The implication is that this (potential) anaerobic subsidy of aerobic food webs may propagate to wells far removed from areas of oxygen drawdown, thereby being an important energy source for invertebrates through much of the aquifer.

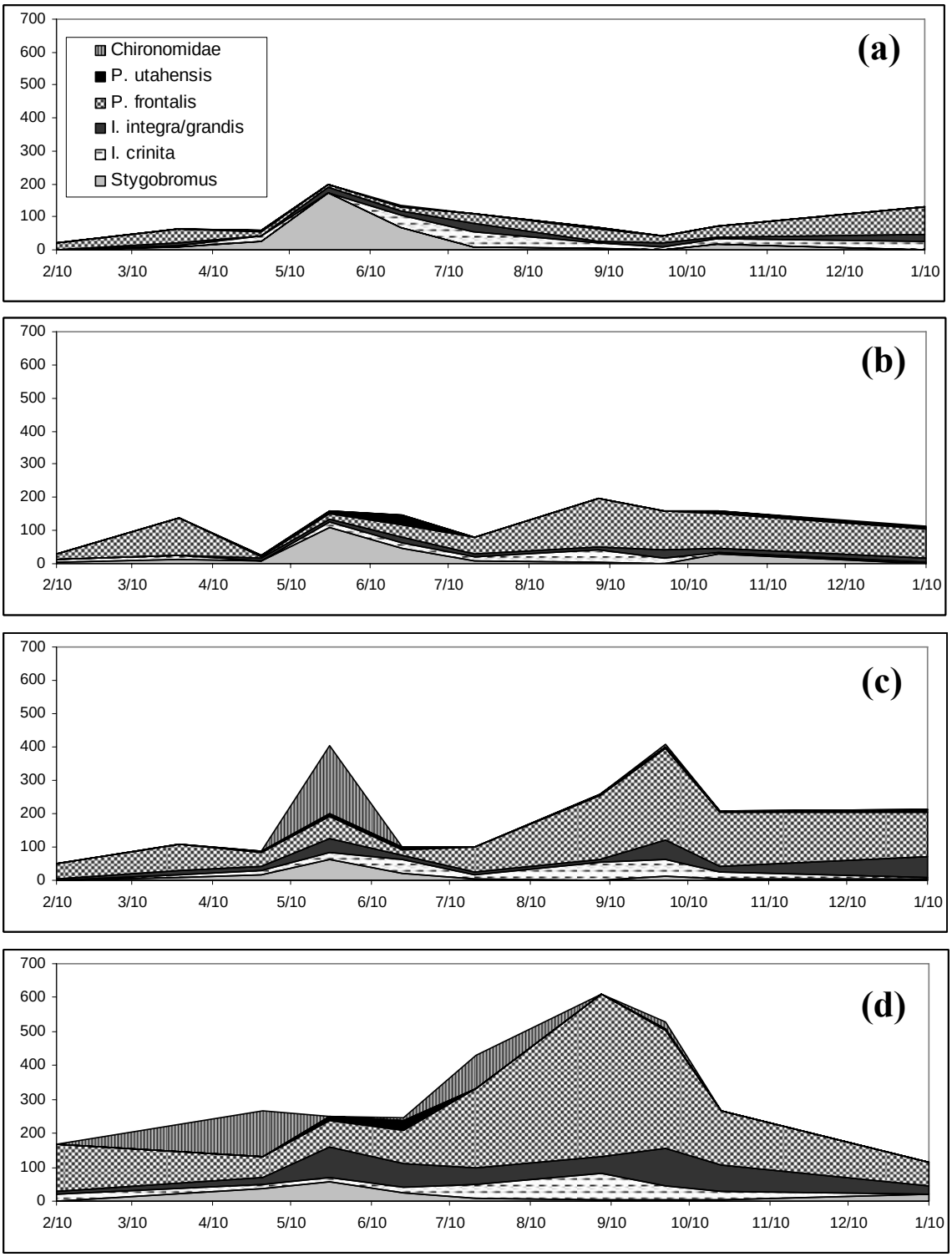

Figure 11: Invertebrate density over time and with depth for major taxonomic groups, for a representative site with clinograde DO profile. Macrofauna density (a through d) shown for depths of 1 through 4 meters below mean low water respectively (all figures are at the same scale). Meiofauna density (e through h) for depths of 1 to 4 meters below mean low water (scale for figure h is 7x higher than e,f and g).

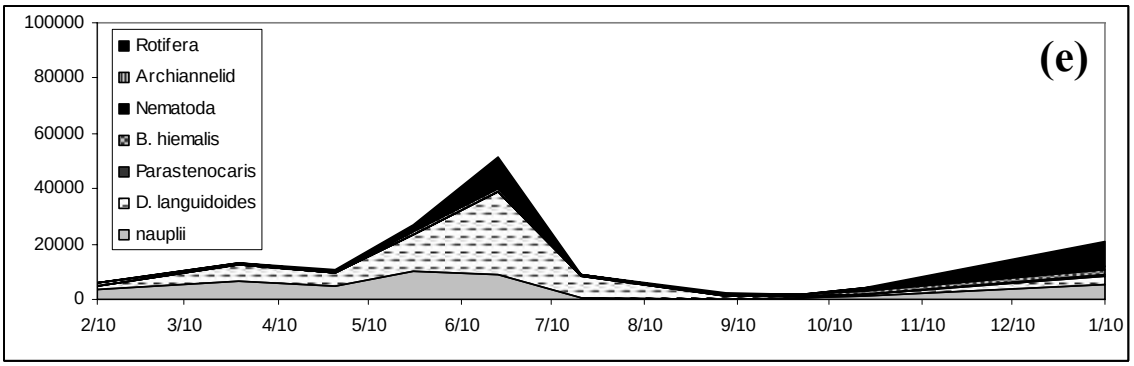
(e)
Rotifera
Archiannelid
Nematoda
B. hiemalis
Parastenocaris
D. languidoides
nauplii
100000
80000
60000
40000
20000
0
2/10
3/10
4/10
5/10
6/10
7/10
8/10
9/10
10/10
11/10
12/10
1/10

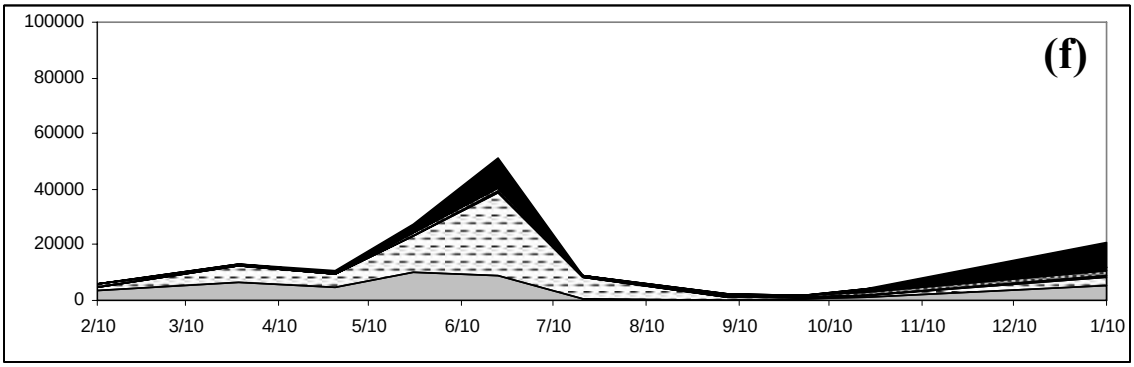
(f)
100000
80000
60000
40000
20000
0
2/10
3/10
4/10
5/10
6/10
7/10
8/10
9/10
10/10
11/10
12/10
1/10

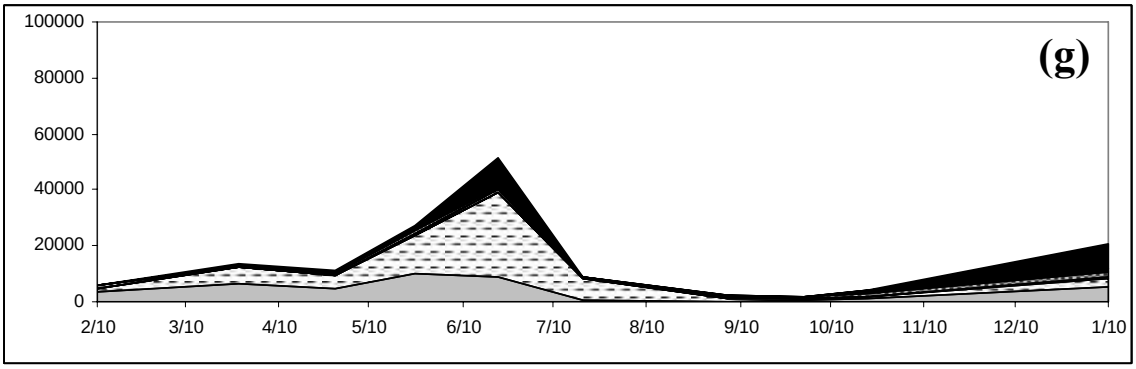
(g)
100000
80000
60000
40000
20000
0
2/10
3/10
4/10
5/10
6/10
7/10
8/10
9/10
10/10
11/10
12/10
1/10

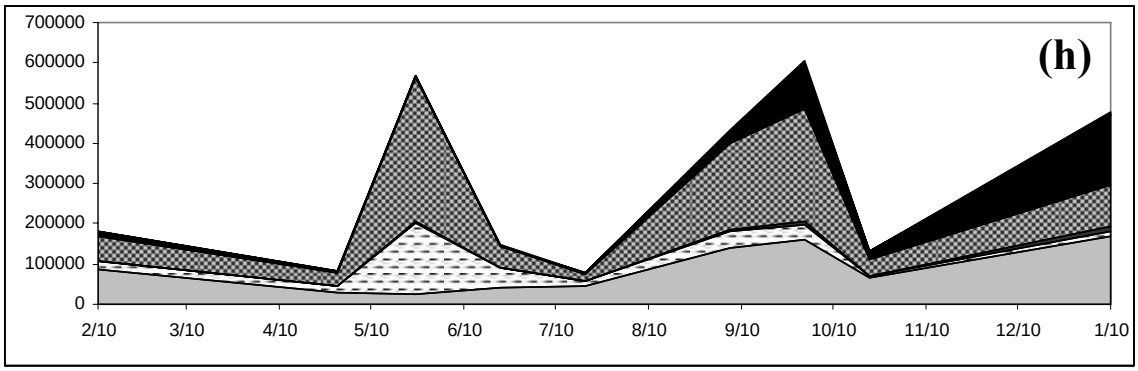
(h)
700000
600000
500000
400000
300000
200000
100000
0
2/10
3/10
4/10
5/10
6/10
7/10
8/10
9/10
10/10
11/10
12/10
1/10

Conclusions

It is clear that oxygen concentration is strongly correlated with patterns of invertebrate density and composition, as well as porewater chemistry. In the same way that pH and temp are master variables in chemical kinetics and temperature is a master variable in organismal biology, there is evidence that oxygen might be considered a master variable in aquatic sediments. However, considering that many of these relationships may be correlation (as opposed to causation), it may be more accurate to describe it as a reference variable to which many other important variables are either correlated or directly influenced by oxygen content.

Oxygen may help define the utility of the concept of flowpaths in the landscape (Fisher et al 2004). The important feature of flowpaths may not be their length, but biogeochemical evolution along flowpaths. Oxygen is the most useful indicator of biogeochemical succession in fluvial sediments. This in turn translates into an indication of metazoan composition and abundance, in somewhat counterintuitive manner: a decline in abundance with falling oxygen, followed by a sharp rise (and presumably falling again when oxygen is very low). These U-shaped response curves indicate that there are two or more variables affecting the dependant variable. Energy resources decline with distance from the source (river) and energy increases again as alternate sources become available with change in redox conditions. The presence of inflection points in most of the geochemical and ecological data indicate that a tipping point occurs in the vicinity of 3-4 mg/l O_2. The seasonal and vertical distribution of metazoans helps support this with high invertebrate abundance at oxygen transition zones and transition periods. These peaks in abundance are seasonal occurring just prior to the oxygen minimum in September-October when redox gradients are strongest. Collectively these patterns indicate that river water and buried organic matter may be major sources of energy to the invertebrate community, the latter realized only under certain redox conditions. Terrestrial subsidy of invertebrate communities, if present, may be too subtle for this spatial scale. However, several indicators do point in this direction. The sharp drop in density of invertebrates at 2 meters depth is the strongest indication, while the differences in communities between gravel bars and cottonwood stands may lend support for a terrestrial-aquifer subsidy. In

the future, these patterns would be best explored by studies of carbon fractionation and bioavailability along the oxygen gradient.

On the mechanistic scale, we believe that the oxygen-driven biogeochemistry within fine sediments may spatially subsidize invertebrate food webs (sensu Polis et al 1997) at the sediment ecotone in three ways (Chapter 6, Figure 16). The first might occur upgradient of the fine sediment interface, by way of sorption of DOC upon fine sediments (Claret et al 1997, Pusch et al 1998). Another might be downgradient of anaerobic zones in fine sediments, where methanogenesis, fermentation, or reduction and mobility of minerals and phosphate become available at the more oxygenated interface. This is similar to Champ's model of what he called an open system (Champ 1979). Finally, there may be spatially disjunct areas of fine sediment interface downgradient of the anaerobic source zone, functioning by the same mechanism. This last situation would correspond with our observations of fall peaks in invertebrate abundance throughout the floodplain well network.

The central role of oxygen in defining the productivity and biogeochemistry in the aquifer leads to the question of what is actually driving dissolved oxygen concentration in the aquifer. Oxygen in the aquifer is largely dependant on initial concentrations in the source water. River oxygen is a balance between saturation kinetics (principally influenced by temperature in surface waters), gas phase equilibrium (Henry's Law), and biotic demand (aquatic respiration). A change in oxygen concentration in the river could result from changing thermal regimes (climate change) and increased biological oxygen demand affected by nutrient loading (generally following land use changes). A change in oxygen in the river source water would affect oxygen in the aquifer, potentially altering productivity in the entire aquifer system. In the short term, productivity might increase following the upstroke in the U-shaped response to oxygen. In the long term, if oxygen drops too much, the limits of low oxygen tolerance by invertebrates may be exceeded and productivity will decline. This unstable response is complicated by the geochemical changes with oxygen, particularly around 3-4 mg/l. An increase in phosphorous or bioavailable carbon would return to the river as groundwater exchange, in turn providing a positive feedback that might further increase oxygen demand in the river, via increased productivity in the river (see Pepin and Hauer 2002).

In this nearly pristine reach of the Middle Fork Flathead, ecosystem decline is a remote possibility. However, the Kalispell aquifer downstream, the site of some of the earliest studies of aquifer ecosystems (Stanford et al 1994), is rapidly urbanizing. The effects of natural terrestrial systems on their underlying shallow groundwaters are only weakly demonstrated here, but the connection is more apparent with urban succession (Datry et al 2003, 2005). Shallow groundwater ecosystems are poorly understood, in part due to the difficulty of sampling and in part because they are not generally appreciated as ecological systems. Yet, they occur at the interface of freshwater resources and human land use, are likely widespread throughout mountain and piedmont regions, and are the overlooked "flowpaths" towards conserving and managing our rivers and surface waters.

REFERENCES

Anderson et al, in prep. Periphyton community dynamics in floodplain lateral habitats.

APHA 1989. *Standard Methods for the Examination of Water and Wastewater,* 17th ed. American Public Health Association, Washington, D.C.

Armengol-Diaz, J., A. Esparcia, E. Vicente, M.R. Miracle. 1995. Vertical distribution of planktonic rotifers in a karstic meromictic lake. *Hydrobiol.* 255/6: 381-388.

Baker, M. A., H.M. Valett, and C.N. Dahm. 2000. Organic carbon supply and metabolism in a shallow groundwater ecosystem. *Ecology* 81(11): 3133-3148.

Baxter, C. V. and F. R. Hauer. 2000. Geomorphology, hyporheic exchange, and selection of spawning habitat by bull trout (*Salvelinus confluentus*). *Can. J. Fish. Aquat. Sci*., 57: 1470-1481.

Boulton, A.J., M.J. Dole-Olivier, P. Marmonier. 2003. Optimizing a sampling strategy for assessing hyporheic invertebrate biodiversity using the Bou-Rouch method: within-site replication and sample volume. *Arch. Hydrobiol.* 156(4): 431-456.

Boulton, A.J., M.J. Dole-Olivier, P. Marmonier. 2004. Effects of sample volume and taxonomic resolution on assessment of hyporheic assemblage composition sampled using a Bou-Rouch pump. *Arch. Hydrobiol.* 159(3): 327-355.

Brunke, M. and T. Gonser. 1997. The ecological significance of exchange processes between rivers and groundwater. *Fresh. Biol.* 37: 1-33.

Brunke, M. and T. Gonser 1999. Hyporheic invertebrates: the clinal nature of interstitial communities structured by hydrological exchange and environmental gradients. *J. N. Am Benthol. Soc.* 18 (3): 344-362.

Butler, J.J., E.J. Garnett, and J.M. Healey. 2003. Analysis of slug tests in formations of high hydraulic conductivity. *Ground Water* 41(5): 620-630.

Champ, D.R., J. Gulens and R.E. Jackson. 1979. Oxidation-reduction sequences in ground water flow systems. *Can. J. Earth Sci.* 16:12-23.

Claret, C., P. Marmonier, J-M Boissiere, D. Fontevieille and P. Blanc. 1997. Nutrient transfer between parafluvial interstitial water and river water: influence of gravel bar heterogeneity. *Freshwat. Biol.* 37: 657-670.

Claret, C., A.J. Boulton, M.J. Dole-Olivier, P. Marmonier. 2001. Functional processes versus state variables: interstitial organic matter pathways in floodplain habitats. *Can. J. Fish. Aquat. Sci*. 58: 1594-1602.

Datry, T., F. Malard, L. Vitry, F. Hervant, J. Gibert. 2003. Solute dynamics in the bed sediments of a stormwater infiltration basin. *J. Hydrol.* 273: 217-233.

Datry, T., F. Malard, J. Gibert. 2005. Response of invertebrate assemblages to increased groundwater recharge rates in a phreatic aquifer. *J. N. Am. Benthol. Soc.* 24(3): 461-477.

Diehl, C.J. 2004. Controls on the magnitude and location of groundwater/surface water exchange in a gravel dominated alluvial floodplain system, northwestern Montana. Unpublished MS Thesis. University of Montana.

Dole-Olivier, M.J. and P. Marmonier. 1992a. Patch distribution of interstitial communities: prevailing factors. *Freshwat. Biol*. 27: 177-191.

Dole-Olivier, M.J. and P. Marmonier. 1992b. Effects of spates on the vertical distribution of the interstitial community. *Hydrobiologia* 230: 49-61.

Driscoll, F.G., 1995. Groundwater and Wells. US Filter, St. Paul Minn. USA.

Fetter, C.W. 2001. *Applied Hydrogeology 4th ed.* Prentice.

Fisher, S.G., R.A. Sponseller and J.B. Heffernan. 2004. Horizons in stream biogeochemistry: flowpaths to progress. *Ecology* 85(9): 2369-2379.

Gibert, J., and L Deharveng. 2002. Subterranean ecosystems: a truncated functional biodiversity. *Biosci.* 52(6): 473-481.

Grimm, N.B. & S.G. Fisher. 1984. Exchange between interstitial and surface water: Implications for stream metabolism and nutrient cycling. *Hydrobiol.* 111: 219-228.

Higgins, R.P. and H. Thiel. 1988. *Introduction to the study of meiofauna.* Smithsonian Institution, Washington D.C.

Hunt, G.W. and E.H. Stanley. 2000. An evaluation of alternative procedures using the Bou-Rouch method for sampling hyporheic invertebrates. *Can. J. Fish. Aq. Sci.* 57: 1545-1550.

Johnson, A. N., B.B. Boer, W.W. Woessner, J.A. Stanford, G.C. Poole, S.A. Thomas, S.J. O'Daniel. 2005. Evaluation of an inexpensive small-diameter temperature logger for documenting ground water-river interactions. *Ground. Wat. Mon. & Rem.* 25(4): 68-75.

Jones, J.B., S. B. Fisher and N.B. Grimm. 1995. Vertical hydrologic exchange and ecosystem metabolism in a Sonoran Desert stream. *Ecology* 76(3): 942-952.

Jones, J.B. and P.J. Mulholland. 2000. *Streams and Ground Waters.* Academic Press, San Diego.

Likens, G.E. and F.H. Bormann. 1974. Linkages between terrestrial and aquatic ecosystems. *Biosci.* 24(8): 447-456.

Marmonier P., M.J. Dole-Olivier, and M. Creuze des Chatelliers. 1992. Spatial distribution of interstitial assemblages in the floodplain of the Rhone River. *Regulated Rivers. Research and Management* 7:75-82.

Minder, L. 1923. Studien über den Sauerstoffgehalt des Zürichsees. *Arch. Hydrobiol. Suppl.* 3: 155-197.

Mosslacher, F. and J.V. Ward. 1999. Distribution of interstitial fauna in a dynamic river floodplain in relation to surficial features and particle parameters. *Mem. Biospel.* 26: 91-99.

Murphey, J. and J. P. Riley. 1962. A modified single solution method for the determination of phosphate in natural waters. *Analytica Chimica Acta* 27: 31-36.

Odum, H.T. 1957. Trophic structure and productivity of Silver Springs, Florida. *Ecol. Mon.* 27(1): 55-112.

Orghidan, T. 1959. Ein neuer Lebensraum des unterirdischen Wassers, der hyporheische Biotop. *Arch. f. Hydrobiol.* 55: 392-414.

Palmer, M.A. 1993. Experimentation in the hyporheic zone: challenges and prospectus. *J. N. Am. Benthol. Soc.* 12: 84-93.

Pepin, D.M. and F.R. Hauer. 2002. Benthic responses to groundwater-surface water exchange in two alluvial rivers in northwestern Montana, *J. N. Am. Benthol. Soc.* 21:370-383.

Polis, G.A., W.B. Anderson and R.D. Holt. 1997. Towards an integration of landscape and food web ecology: the dynamics of spatially subsidized food webs. *Ann. Rev. Ecol. Syst.* 28: 289-316.

Poole, G.C., J.A. Stanford, S.W. Running, C.A. Frissell. 2006. Multiscale geomorphic drivers of groundwater flow paths: subsurface hydrologic dynamics and hyporheic habitat diversity. *J. N. Am. Benthol. Soc.* 25(2): 288-303.

Poole, G.C., J. A. Stanford, S. W. Running, C. A. Frissell and B. K. Ellis. Submitted. Floodplain hydrologic complexity: modeling interactions between river discharge, geomorphology, and hyporheic flow dynamics. *Ecological Applications*.

Pusch, M. 1996. The metabolism of organic matter in the hyporheic zone of a mountain stream, and its spatial distribution. *Hydrobiol.* 323: 107-118.

Pusch, M., D. Fiebig, I. Brettar, H. Eisenmann, B.K. Ellis, L.A. Kaplan, M.A. Lock, M. W. Naegli, W. Traunspurger. 1998. The role of micro-organisms in the ecological connectivity of running waters. *Fresh. Biol.* 40: 453-495.

Shapiro, J. 1960. The cause of a metalimnetic minimum of dissolved oxygen. *Limnol. Oceanogr*. 5: 216-227.

Stanford, J.A. and A.R. Gaufin. 1974. Hyporheic communities of two Montana rivers. *Science* 185: 700-702.

Stanford J.A., M.S. Lorang and F.R. Hauer. 2005. The shifting habitat mosaic of river ecosystems. *Verh. Internat. Verein. Limnol.* 29(1): 123-136.

Stanford, J. A. and J. V. Ward. 1993. An ecosystem perspective of alluvial rivers: connectivity and the hyporheic corridor. *J. N. Am. Benthol. Soc.* 12(1):48-60.

Stanford, J.A. and J.V. Ward. 1988. The hyporheic habitat of river ecosystems. *Nature* 335: 64-66.

Stanford, J. A., J. V. Ward and B. K. Ellis. 1994. Ecology of the alluvial aquifers of the Flathead River, Montana (USA), pp. 367-390. *IN*: Gibert, J., D. L. Danielopol and J. A. Stanford (eds.), *Groundwater Ecology*. Academic Press, San Diego, California, USA. 571 pp.

Strayer, D and G.E. Likens. 1986. An energy budget for the zoobenthos of Mirror Lake, New Hampshire. *Ecology* 67(2): 303-313.

Tansley, A.G. 1935. The use and abuse of vegetational concepts and terms. *Ecology* 16(3): 284-307.

Teal, J.M. 1957. Community metabolism in a temperate cold spring. *Ecol. Mon.* 27(3): 283-302.

Teal. J.M. 1962. Energy flow in the salt marsh ecosystem of Georgia. *Ecol. Mon.* 43(4): 614-624.

Valett, H.M., C.C. Hakenkamp, A.J. Boulton. 1993. Perspectives on the hyporheic zone: integrating hydrology and biology. *J. N. Am. Benthol. Soc.* 12(1): 40-43.

Ward, J.V., J.A. Stanford, N.J. Voelz. 1994. Spatial distribution of Crustacea in the floodplain aquifer of an alluvial river. *Hydrobiol.* 287: 11-17.

Ward, J.V. and M.A. Palmer. 1994. Distribution patterns of interstitial freshwater meiofauna over a range of spatial scales, with emphasis on alluvial river-aquifer systems. *Hydrobiologia* 287: 147-156.

Ward, J.V. and N.J. Voelz. 1994. Groundwater fauna of the South Platte River system, Colorado. pp. 391-423. *IN*: Gibert, J., D. L. Danielopol and J. A. Stanford (eds.), *Groundwater Ecology*. Academic Press, San Diego, California, USA. 571 pp.

Wood, E.D., F.A. Armstrong, F.A. Richards. 1967. Determination of nitrate in seawater by cadmium-copper reduction to nitrite. *J. Mar. Biol. Assoc. U.K.* 47: 23-31.

Chapter 4

AN *IN SITU*, SOLAR POWERED MESOCOSM
FOR MONITORING AND EXPERIMENTATION IN THE HYPORHEIC ZONE.

ABSTRACT

We developed an *in situ* flow-through mesocosm to study the carbon sources of metazoan production in floodplain alluvial groundwater on the Middle Fork, Flathead River (MT). The mesocosms were ultimately designed for multiple purposes relating to system properties of hyporheic zones, including invertebrate density validation, community respiration, and solute dynamics. Eight 440-liter gravel-filled mesocosms were situated in pairs representing a range of lateral hyporheic positions. Flows were maintained at rates comparable to field conditions (mean velocity ≈ 13 m/d). Three pairs of mesocosms were located at remote sites on the floodplain and were powered by solar panels charging deep-cycle lead-acid batteries. One pair was located near commercial power and was operated on AC current. Mesocosms were operated from April 2004 through June 2006, demonstrating the potential for continuous mesocosm operation in a remote location (off of the electrical grid) under adverse environmental conditions (temperatures as low as -30 °C). Invertebrate colonization required at least 6+ months despite multiple seeding. Invertebrate community composition resembled those from well samples, except that macrofauna, particularly the amphipod *Stygobromus* appeared to be significantly under-represented in the mesocosms. Invertebrate density in mesocosms was most comparable to well densities when fine sediments treatments in the mesocosms were used as the basis for comparison. We were unable to explain a strong non-linear decline in invertebrate density along the middle 3 meters of all mesocosms, however we suspect the lack of particulate organic matter in mesocosm sediments. Community respiration rates were high during the initial incubation period. Initially temperature gain due to solar exposure showed a significant departure from subsurface temperatures and required shading and insulation to reduce this artifact. We recommend that in using hyporheic and groundwater mesocosms in ecological studies, investigators should factor in an 8 to 12 month incubation period before initiating sampling or experimentation.

INTRODUCTION

The hyporheic zone, defined by river water penetrating the subsurface and interacting with ground water, was first used by Orghidan (1959) to describe bed sediments below the range of traditional benthic sampling. Since then, hyporheic zone dynamics have been shown to be a strong driver of ecosystem processes in rivers, and there is a rapidly increasing interest in groundwater-surface water interaction (Stanford and Ward 1993, Valett et al. 1993, Stanford 1998, Stanford et al. 2005, Dahm 2006). Hyporheic sediments are difficult to sample compared to surface systems. Lack of adequate methods is one of the greatest challenges of ecological investigations and experimentation in the hyporheic zone (Palmer 1993).

Microcosms and mesocosms have been an important element of ecological research for decades. Their use spans the spectrum between control and realism in experimental studies. On the side of realism, ideally a single variable is manipulated, allowing us to observe system properties in response to the respective treatment (Beyers and Odum 1993). In groundwater, many of these system properties are very difficult to observe. Our mesocosms were designed for multiple purposes leading towards a model of system energy flow of a floodplain aquifer. In this paper, we cover two primary purposes: verification of invertebrate density estimates from well samples by comparing with results from mesocosm substrate (Chapter 3), and assessment of mesocosm performance. The latter objective is accomplished via monitoring of temperature regime, community metabolism, and invertebrate composition and distribution. If the mesocosms provide a reasonable approximation of field conditions, they may be deemed more suitable for studying invertebrate growth and production (Hauer 1993), organic matter decomposition, fine-scale invertebrate distribution, spiraling/uptake rates and nutrient amendments. All of these objectives are difficult to accomplish in the subsurface.

STUDY AREA

The study site was the Nyack Floodplain located on the Middle Fork of the Flathead River (48° 27’ 30” N, 113° 50’ W), a fifth order gravel-bed river with headwaters in the Bob Marshall-Great Bear Wilderness Complex and located along the southwest boundary of Glacier National Park in western Montana, USA (Figure 1a). The

12 km^2 floodplain is 8 km long and averages 1.5 km in width. The floodplain is bounded laterally by valley walls with bedrock knickpoints at both the upper and lower ends. The river along the length of the floodplain is anastomosed, with the active channel and parafluvial zone of the river tending toward the northeastern side of the valley. The more mature, orthofluvial floodplain forest and agricultural pasture is to the southwest. Over 30% of the main channel flow is lost to the aquifer at the upstream end of the floodplain (Stanford et al. 1994) and various gaining and losing reaches have been documented and modeled throughout the floodplain (Stanford et al. 2005, Poole et al. submitted). The site has been the focus of research by the Flathead Lake Biological Station for over 20 years, and additional site description is offered in Stanford et al. (1994).

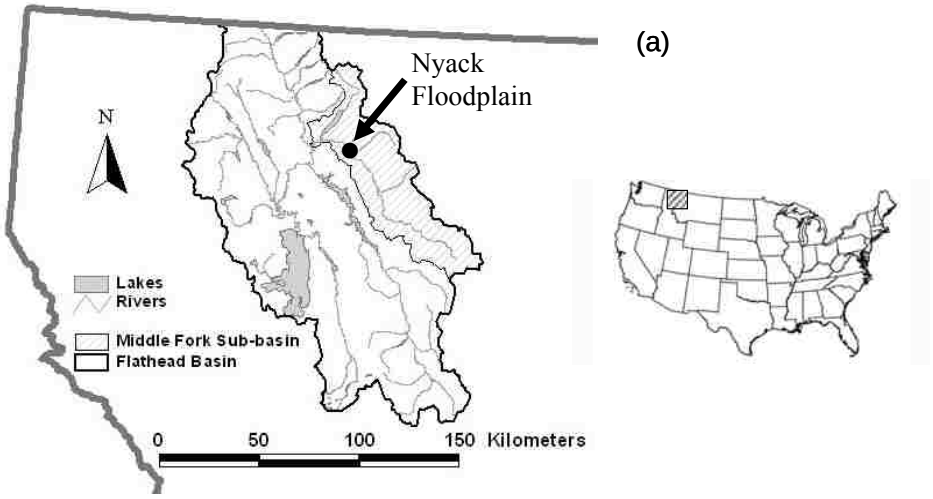

Figure 1 (a): Study site: Nyack Floodplain, Middle Fork Flathead River (MT USA).

METHODS

Mesocosm Design and Construction

We installed four pairs of mesocosms at wells in aquifer recharge, discharge and midgradient zones (Figure 1b & 1c) representing the range of aquifer hyporheic positions (Chapter 1). Within each pair, mesocosms withdrew water from discrete 1-meter intervals at two depths: either shallow (0-1m below estimated mean low water - MLW), or deep (1-2 meters below MLW). Mesocosms M1a and M1b (both shallow due to well

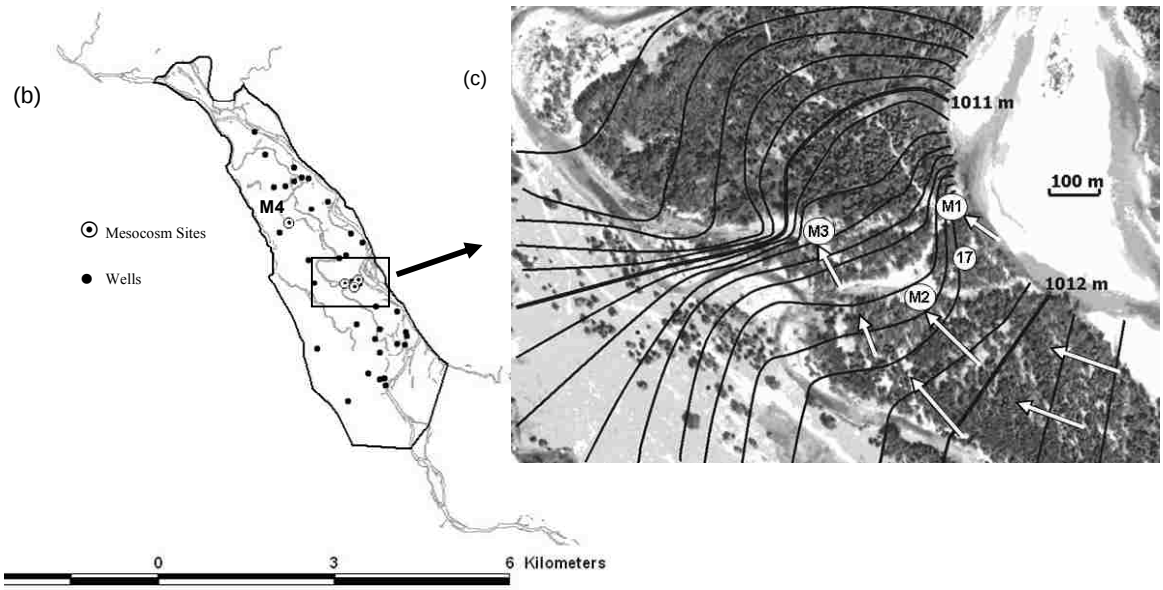

Figure 1 (b). Nyack floodplain: The main channel is furthest to the right, while smaller channel features are spring brooks and other off-channel habitats. Solid black line shows floodplain boundary; **(c)**: Close-up of mesocosm locations for pairs M1 through M3, superimposed on a potentiometric map (contours show water table elevations, and arrows show direction of groundwater flow). Mesocosm sites M1 (Aquifer recharge), M2 (midgradient) and M3 (discharge zone – spring head) are shown.

limitations) were sited in an area of known aquifer recharge, with a subsurface residence time (travel time from river recharge to the well site) estimated at <1.6 days (Johnson 2003). Mesocosms M2a (shallow) and M2b (deep) were located in a cottonwood forest, upgradient of an old channel feature. The aquifer water residence time was approximately 7-19 days, based on temperature cycles. Mesocosms M3a (deep) and M3b (shallow) were located at the head of a spring, draining into a larger orthofluvial springbrook (residence time 45-50 days). Mesocosms M4a (deep) and M4b (shallow) were located farther down the floodplain, at a presumed discharge zone into the same orthofluvial springbrook (residence time ≈ 9 months, estimated from a groundwater flow model and particle tracking, Diehl 2004). A general physico-chemical description of the aquifer at mesocosm sites, including depth, hydraulic conductivity, estimated flowpath length and residence time, and the mean and range of oxygen and temperature of inlet water, are shown in Table 1.

Mesocosm	Zone	Depth (m) [a]	FLOWPATH Length (m) [b]	FLOWPATH τ (days) [c]	TEMPERATURE Mean [d]	TEMPERATURE Range	DO Mean [d]	DO Range	K (m/d)	TREATMENT
M1a	Recharge	1.6	<26	<2	6.8	(1.1-16.1)	9.24	(5.9-11.7)	1008	FPOM
M1b	Recharge	1.6	<26	<2	6.8	(1.1-16.1)	8.96	(5.4-11.7)	1008	Sand
M2a	Midgradient	2.8	91-247	7-19	6.5	(3.3-10.9)	4.17	(2.0-6.8)	214	Sand
M2b	Midgradient	3.8	91-247	7-19	6.5	(4.1-9.5)	5.17	(2.4-6.9)	309	FPOM
M3a	Discharge	1.7	585-650	45-50	6.7	(5.0-8.9)	5.28	(3.7-6.2)	397	Sand
M3b	Discharge	0.7	585-650	45-50	6.7	(5.3-8.7)	4.65	(2.7-6.8)	546	FPOM
M4a	Discharge	4.3	715-845	55-65	6.7	(5.1-9.2)	5.12	(4.1-5.9)	264	FPOM
M4b	Discharge	3.3	1170-1300	90-100	6.7	(5.4-8.8)	5.16	(4.5-6.1)	214	Sand

[a] one meter intake interval, centered on this depth.

[b] flowpath length from river water to location of mesocosm well, estimated using mean velocity of 13 m/d (Diehl 2004).

[c] residence time of water in the river-well flowpath, estrimated from temperature cycle.

[d] mean temperature and dissolved oxygen for inlet water, calculated from monthly data.

Table 1: Physicochemical characteristics of well intervals and respective mesocosms.

Three of the four pairs of mesocosms (M1, M2 and M3) were each driven by a solar charged battery bank, drawing water from wells using variable speed peristaltic pumps (Figures 2 and 3). Two 123 Watt pole-mounted solar panels (Sharp Co.) were used to charge each battery bank, regulated with a Solar Boost 2000E charge controller (RV Power Products, Inc.). Three pairs of six volt lead acid batteries (Deka 8L-16, 390 Amp-hours, Trojan Inc.) were wired in series (for 12 Volts), and then in parallel, providing upwards of 7000 Watt-hours, which is a conservative estimate of the 5-day battery capacity required for continuous pumping in the winter.

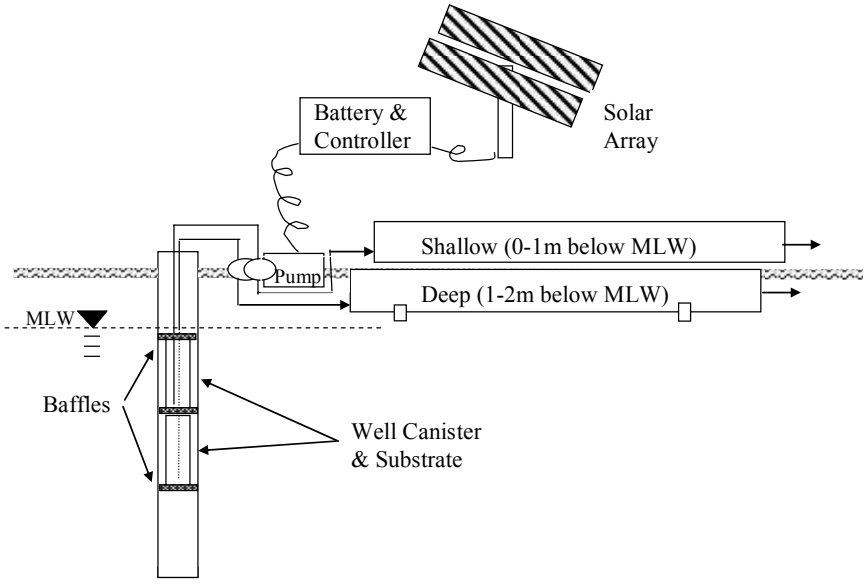

Figure 2: Hyporheic mesocosms: general design. Each site has two mesocosms drawing water from shallow (first 1 meter below mean low water -MLW) and deep (second meter below MLW) depths.

Figure 3: Close-up photos of hyporheic mesocosm components (counter-clockwise from upper left): solar controller, battery bank, peristaltic pump, inlet manifold (viewed through A1 access hatch, before gravel was introduced), sampling hatch with canisters, invertebrate sampling canister (l) and treatment canister (r). Center, paired mesocosms with authors for scale.

Water was pumped to each mesocosm pair using 2 Masterflex Easy-Load II peristaltic pump heads (SS rotors, adjustable occlusion, Cole-Parmer Instrument Co.) mounted on a single 12V DC drive (100-500 rpm, Cole-Parmer). We used Silicone C-flex tubing (L/S 36, 9.7mm ID). The choice of tubing reflects a compromise between optimum gas permeability and pump design: gas permeability and leaching is moderately low, while the relatively high elasticity of the tubing minimizes pump resistance and lowers power consumption, which is especially important with regard to operation of two pump heads on one drive, since the drives are rated for only one pump head. We replaced tubing every 4-6 weeks. We maintained flow rates at 250 ml/min (residence time $\tau \approx 20.3$ hrs) for all mesocosms, except as follows: (1) during winter months (Nov-Feb) flow was maintained at maximum rates (350-400 ml/min, $\tau \approx 8.4$ and 7.4 hrs respectively) to prevent freezing and minimize temperature loss; (2) from Sept 2005-Nov 2005 flow was reduced to 150 ml/min ($\tau \approx 19.6$ hrs) to increase residence time and attempt to better estimate uptake rates of DOC and NOx. Flow adjustment was made to all mesocosms on the same dates, maintained within 10% of target flow rates, and were all within the range of groundwater velocity estimated for the floodplain (Diehl 2004). All mesocosms were in operation continuously from April 2004 through June 2006.

Pump intake water was drawn from canisters positioned at two depths within each well. Canisters were made from 2" nominal PVC (5.1cm), with 7mm holes drilled to approximate 30% open area, and baffled to isolate a discrete 1 m interval within the respective well (Table 1, Figure 2). The canisters were filled with coarse gravel (≈ 17 mm), and 6.4 mm polyethylene intake hose was buried in the gravel, with holes drilled along the length of the respective intake interval. The length of the intake hose varied depending on distance to the well, but was less than 6 meters for all sites, and was covered with insulation to minimize temperature gain. The intake hose was connected to the C-flex tubing with hose clamps. Pump discharge was connected to the mesocosms via another section of polyethylene tubing, in turn connected to a ½" barb, a valve, and 2" reducer coupling, the latter mounted on the end plate of the mesocosm (see below).

Mesocosms were constructed from 20-ft (5.95 meter) sections of 12-inch (30.5 cm inner diameter) Schedule 40 (1.3cm thick) PVC sewer pipe. Sections were cut at the midpoint, and rejoined using the flared end, to allow for disassembly and transport. The size of the mesocosms was determined primarily based on the need for sufficient sediment to sample hyporheic metazoans, which naturally occur at low densities. The ends of the mesocosms were sealed using a slip-on socket flange, with an end plate fabricated from ¼" thick, 16" diameter sheet of black acrylite plastic (inside face), reinforced with ½" plywood (outside face), and secured to the flange with bolts. We used a 2.5cm wide strip of closed cell foam, lined with silicone sealant, to seal the plate to the flange. The end plate is traversed in the center by a short section of 2" PVC pipe, with 2" couplings on both faces (solvent welded and sealed with silicone). The outer coupling was attached to the pump as mentioned above. The inner coupling was attached to a 10cm long hub of 2" pipe, with eight radial spokes of ½" CPVC pipe. The spokes were drilled with holes and functioned as a dispersion manifold (Figure 3).

Two access hatches (20.4 cm square) and six sampling hatches (25.5 cm long by 20.4 cm wide) were positioned along the upper surface of each mesocosm to permit access along the longitudinal gradient of the flowpath. Sampling hatches S1 through S3 and S4 through S6 were spaced 32 cm apart, (with a 84.5 cm gap between S3 and S4 because of the center coupling), and centered at 1.41, 1.98, 2.56, 3.4, 3.98 and 4.55 meters, and clustered in the middle (Figure 3 and 4) to minimize hydrodynamic effects at

the head and tail of the mesocosms (Craig 1993). To seat the hatches, we fashioned 1.3 cm wide flanges out of 3.2 mm acrylite by heating in an oven to soften the plastic and then we conformed the flange to the curve of the hatch opening. We then used solvent to weld the flange to the underside of the hatch opening, which we then secured with pop rivets, and sealed with silicone sealant. The contact with the hatch cover was sealed with 1cm closed-cell foam, attached to the underside of the hatch with adhesive, and further sealed with a thin layer of silicone grease. Gaskets were inspected whenever hatches were opened, and were replaced when necessary (typically 2-3 times per year). Hatches were held in place using a length of bungi cord, looped 8-10 times across non-corrosive screws mounted on the sides of the mesocosms.

We installed two experimentation columns (C1 and C2), located between hatches S2/S3 and S4/S5 respectively (Figure 4). Columns were designed for three purposes: rearing organisms, sediment amendments, and recirculation experiments conducted in canisters isolated from the mesocosm flowfield. The latter function was intended as an

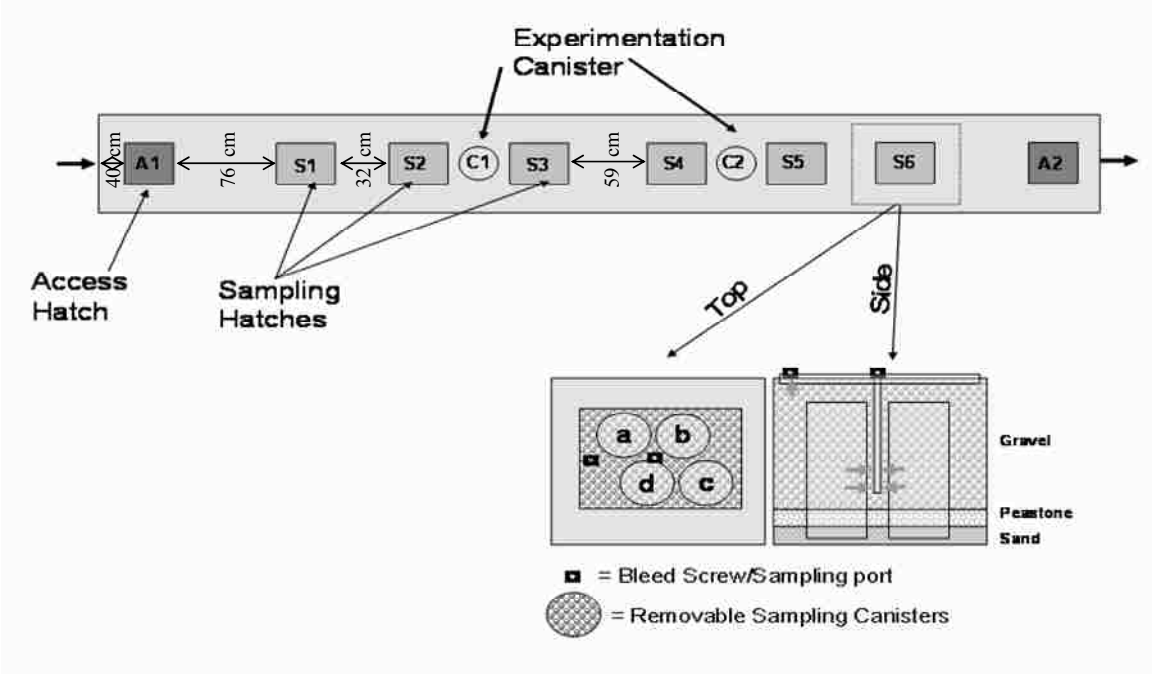

Figure 4: Detail on hatch locations, sampling canisters, and sampling ports. A = access hatch; C = experimentation canister; S = sampling hatch. Hatch locations are not to scale. Water flows from left to right.

alternative to lab-based microcosms and have the advantage of being able to isolate a known quantity of sediment without translocation disturbance and having been incubated in place for long periods of time. Columns were constructed from 40 centimeter lengths of 4" nominal PVC (10.2 cm), installed through a hole in the top of the mesocosms and shaped to fit the bottom of the mesocosm. Holes (7mm) were drilled at 2.5 cm intervals, so that during normal operation the column was exposed to the mesocosm flowfield (open area 30%). (Note: in Chapter 5 we used the columns as the location for sediment amendments.) We added sediment cored from debris jams, with and without organic matter (two treatment types, POM removed via elutriation). Details of this experiment are also in Chapter 5. Some results of this experiment are reported here for the purpose of comparing invertebrate density between the mesocosms and corresponding wells.

Mesocosm outlets had end plates as above, with the 2" coupling attached to an elbow, valve, and 30 cm riser, maintaining the outlet at the highest point of the mesocosm. Mesocosms were installed at a slight pitch oriented towards the head, so that any entrained air would remain in one place at the head of the mesocosm. Bleed screws were installed at the mesocosm head and on all hatches and experimentation columns to purge air after opening and re-closing the mesocosm for sampling (Figure 4).

We were able to run the last mesocosm pair (M4) directly off of AC power using a variable speed AC drive (economy drive, 20-600 rpm, Cole-Parmer Inc.). M4b (shallow depth) was developed from our original prototype mesocosm operated in 2003, and is an older design. The prototype used only the medium gravel fraction, and the treatment columns, installed later, could only be located in the second half of the mesocosm. Otherwise, the design is similar to the remaining mesocosms. This pair was intended for method development and sampling trial runs, and as a qualitative comparison of bimodal vs. coarse substrate types. Because of the limited replication, we cautiously include this last pair in some of our analysis. We note some qualitative differences; however, inclusion of this last pair substantiates our conclusions regarding the other mesocosm pairs.

Substrate

Mesocosms were filled with local sediments simulating a bimodal gravel formation (Huggenberger et al. 1998) typical of alluvial aquifer deposits (Figure 5). We were concerned that the common practice of filling sediment microcosms with bulk sediment would not preserve the sediment structure, principally the interconnected pore space, which we believe is essential for invertebrate habitat. A sorted and layered gravel distribution was therefore chosen to better represent invertebrate habitat and also enable the sampling of multiple substrate types in future experimentation. On the bottom was a 2.5 cm layer of sand (median grain size 250-500 μm) topped by 2.5 cm of fine gravel (average diameter 4.6 ± 2 mm), with the remaining volume (26+ cm) of the mesocosm filled with medium gravel (average diameter 17.6 ± 7.0 mm). All sediments were collected from the floodplain or nearby fluvial gravel deposits and were washed of organic matter and fine particles and sieved to achieve uniform size classes. The sand was collected from overbank deposits and elutriated with well water until there was no visual evidence of POM (< 0.5% AFDM). Substrate was not otherwise sterilized or pretreated.

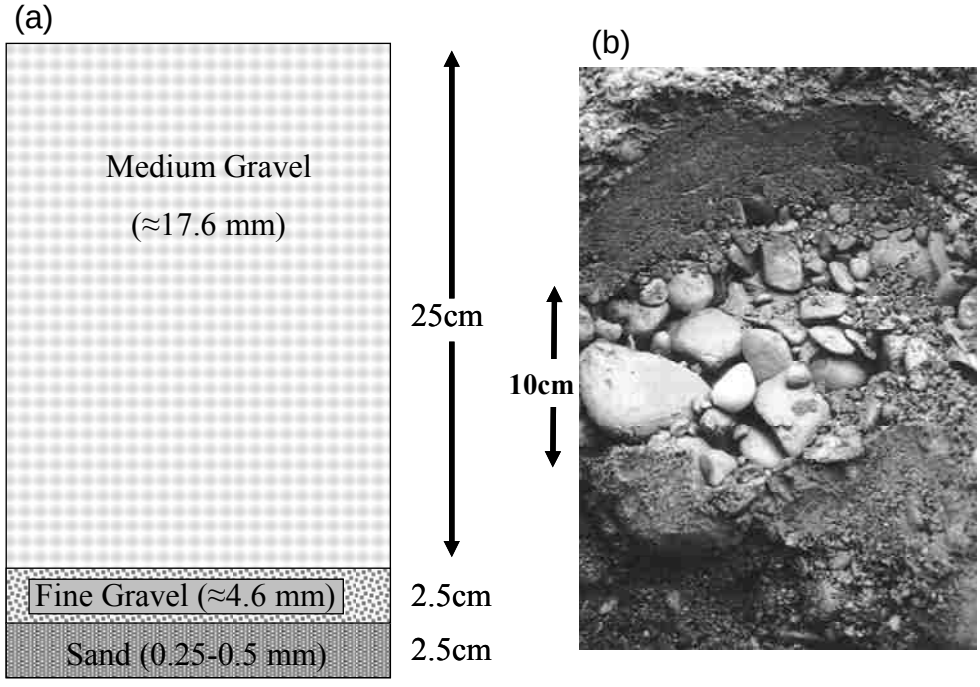

Figure 5: (a) Mesocosm sediment structure; (b) preferential flow zone observed in the field.

Each sampling hatch had four removable sampling canisters (Figure 3 and 4). Canisters were constructed using 25 cm lengths of 3.045 inch diameter (7.76 cm) nylon extruded mesh tubes (Internet Inc., 0.200 inch nominal hole size, 50% open area; RN 7480). The mesh tube slid over a 2" PVC coupling (4.6 cm long), which in turn was capped at the bottom with circle cut from acrylite, and all components connected with silicone sealant. The bottom of each canister was therefore closed, in order to retain gravel and water when the canister was removed for sampling (i.e. only the upper 20.4 cm was exposed to the flowfield). The canister was filled with 1.12 liters of sediment, consisting of a layer of sand (79 ml), fine gravel (79 ml) and medium gravel (960 ml). The top of the fine gravel layer projected about 5mm into the flowfield. Hence most of the fine gravel, and all of the sand, was connected to flow only through vertical dispersion (with 192 sampling canisters, this simplification was necessary). The canisters were slid into 25cm sections of slotted 3" thin-wall PVC (40% open area, cut with a table saw). These canister retainers were designed to hold the mesocosm gravel in place, so that sampling canisters could be removed and replaced with minimal disturbance. The larger treatment canisters (Figure 3, located in the experimentation columns) had a similar design, consisting of 30.5 cm sections of 3.6 inch (9.18 cm) mesh tubes (Internet Inc., 30% open area; RN 2300). Total volume was 1.81 liters of sediment, composed of 120 ml of sand, 120 ml of fine gravel, and 1.58 liters of medium gravel.

Sampling and Baseline Monitoring

Because the mesocosms were located above ground, we observed temperature changes, either gain or loss, depending on air temperature. The advantages of above ground location, and general implications of temperature gain on mesocosm studies, are summarized in the results and discussion sections (mesocosm performance). Groundwater temperature was monitored using iButton data loggers in the well intake canisters, and temperature gain was monitored in two locations along the mesocosm gradient (hatches S2 and S4). An additional Vemco temperature logger was installed at the mesocosm outlets.

Mesocosms were seeded with invertebrates pumped from respective well depths on three occasions: 18 May, 2 June, and 8 July 2004. A 1:16 sub-sample was retained and

processed for later comparison, while the remaining material was poured into hatch A1 of each mesocosm. Since the mesocosms are open or flow-through systems, natural colonization was also anticipated. We monitored invertebrate density and community composition during the colonization phase from June through November 2004. Three canisters were removed along the gradient of each mesocosm at two week intervals. Hatches were alternated (S2, S4, S6 then S1, S3, S5) and canisters rotated (4 canisters in each hatch) so that disturbance to each individual canister was minimized (in post colonization sampling, canisters were left undisturbed for over 1 year). Canisters were removed by fitting a sampling tube (section of 3" thin-walled PVC, bell end down), over the canister retainer. A rubber flange at the bottom, made from the end of a latex glove, acted as a seal. A gasket fashioned out of a 7.7 cm polyethylene foam circle was placed on top of the canister, forming an upper seal that moved with the canister. A loop of nylon line attached to the canister allowed us to draw the sediment canister up into the sampling tube. With practice, we could consistently remove the sediment canister with the sediment and a relatively intact column of water. Specific yield of the canisters was approximately 400 ml. We measured water recovery to verify that 80-95% of the water was retained. Canisters were washed into a bucket of mesocosm water previously strained through a 64 μm Nitex mesh net to remove invertebrates. The sample was agitated and elutriated 3-4 times and elutriate was collected on a 64 μm sieve. The sieve was washed into a Ziploc bag and the sample was frozen for later analysis. The remaining sediment was then sorted on nested sieves and replaced into the sampling canister in layers as described above. Typically, we had to add a small amount of sand to make up for sand lost to the sample during elutriation.

Invertebrate samples were thawed in the lab, placed in a petri dish, and stained with Rose Bengal. Samples were scanned at 25x, and organisms were identified to species (copepods and macroinvertebrates) where possible, or to order for nematodes, rotifers, archiannelids and other less abundant taxa. We estimated invertebrate density based on a canister volume of 1.12 liters. Additional detail on taxonomic composition in the aquifer can be found in Chapter 3.

We used percent similarity index (Krebs 1989) to compare July 2005 invertebrate composition at the order/suborder level between mesocosm and the respective well

interval. We compared our estimates of invertebrate density between respective mesocosms and well intervals (data from Chapter 3) as a function of mesocosm substrate type: bulk gravel from sampling canisters, fine gravel and sand fraction from sampling canisters, and fine sediment/organics from treatment canisters). Our assumption of invertebrate density depends on sampling scale. The values reported in Chapter 3 are bulk values for 1 meter well intervals. At smaller scales the invertebrates are assumed to reside primarily in the zones of preferential flow, the well sorted bimodal gravel with interconnected pore spaces (Huggenberger 1998). Preferential flow zones are only a fraction of any given well interval, which makes comparison between well and mesocosm invertebrate density a challenge. The mesocosm substrate represents primarily the preferential flow zones dominated by coarse gravel. To compare densities, we estimated the percentage of preferential flow zones in the well intervals. We used a binary mixing model (discussed in Chapter 1 and Chapter 3), using the known bulk hydraulic conductivity (K) of the respective well intervals (Diehl 2004 and Chapter 3), and assumed that the end members for poorly sorted gravel and the well sorted gravel have K values of <1 and > 8,000 m/d, respectively. Our estimate of percentage preferential flow zones is sensitive to our assumption of the high end K value. We initially assumed a value of 15,500 m/d, based on extrapolation from the Hazen equation and using a grain size of 17.6 mm (Fetter 2001). Since we have no direct estimates of K for preferential flow zones, and since the Hazen equation is not really appropriate for coarse gravel, the true value is not precisely known. Preferential flow zone K may actually vary across the aquifer depending on degree of sorting and coatings of silt and mud, which we have observed in the field. Hence, our comparison between well and mesocosm invertebrate density has multiple solutions, depending on our K assumption and mesocosm substrate type. We therefore plotted mesocosm versus well invertebrate density as a function of the three substrate types (bulk gravel, fine gravel and the FPOM/Sand treatments), with lines for 1:1 correspondence for a range of K values (4000, 8000, 16000, and 40000 m/d). This approach also allows us to make some conclusions as to which substrate type in the mesocosms provides the most reasonable approximation of the actual substrates in the aquifer. The comparison between mesocosm and well invertebrate density hinges on the assumptions inherent in well sampling. They include

an initial invertebrate density calculation from well water, converted to sediment volume assuming a porosity of 0.4 for all sites, and corrected for decreased efficiency with continued pumping (Chapter 3). We also assumed in Chapter 3 that there was an even contribution of water from the entire well interval (50 cm intake interval). More realistically, most of the water drawn from the well during pumping probably originated from areas of preferential flow, the sampling actually originating from a narrow layer of extended radius from the well, and hence the above calculation may actually overestimate invertebrate density. More details on well invertebrate density assumptions are in Chapter 3. Given that invertebrate density across the well network varies up to 5 orders of magnitude, we are comfortable with these errors, which are less than an order of magnitude.

RESULTS

Mesocosm Temperature

Mean annual inlet temperature was similar for all mesocosms, averaging 6.7 °C. However, the annual temperature range varied from 15 °C in M1 to 3.4 °C for M3 and M4 (Table 1). Annual degree days for inlet water were similar across all mesocosms and averaged 2434 (± 44) degrees. Because the mesocosms are above ground and exposed to air temperature and sunlight, internal temperature cycled considerably. In the summer of 2004, we observed warming in excess of 7 °C (Figure 6a). Meanwhile the groundwater temperature for the respective wells did not show this cycling behavior. We reduced the effect of temperature cycling and temperature gain through progressive improvements in insulation and shading structure. Mesocosms were initially insulated with a layer of Reflectix insulation (8 mm thick layered reflective material). We subsequently added a layer of ½" bubble wrap (13mm) in August. A large 3m x 7m concrete curing blanket was added in December 2004 to help prevent freezing. Finally, greenhouse enclosures were constructed over the mesocosms to maintain warm air temperature in the winter and shaded with tarps in the summer. With this insulation, in 2005 the average absolute value of temperature gain or loss was only 1.1 °C (± 1.0), with an amplitude no greater than 2

°C (Figure 6b). In the case of mesocosm M1, we were able to maintain flow year round, even during winter air temperatures of -30 °C and inlet water temperatures less than 1 °C.

One of the potential consequences of temperature gain is the effect on community metabolism. During the first six months of operation, we observed summer respiration rates that were approximately three to four times higher than rates in the following summer (Figure 7; data from Chapter1). This coincides with the period of increased temperature gain (such as in Figure 6), and temperature gain predicted community respiration much more effectively than average temperature (Chapter 1). We can not separate the effects of temperature gain from the disturbance and recovery trajectory of newly established mesocosm communities. However, the general implication from the respiration data is that the initial incubation time for hyporheic sediment may be on the order of 6 months or more.

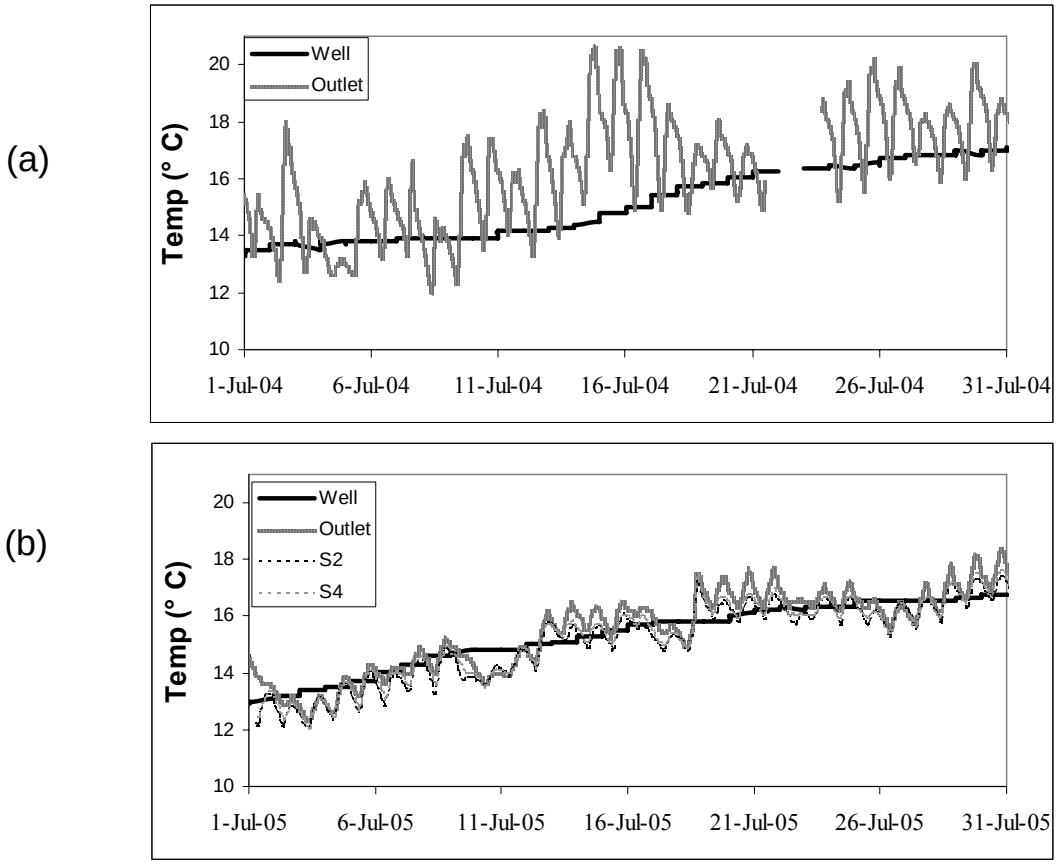

Figure 6: Example of temperature artifacts within mesocosm M1: (a) Inlet vs. outlet temperature in July 2004, prior to insulation; (b) Inlet, outlet and middle of gradient (hatches S2 and S4) for July 2005, post insulation.

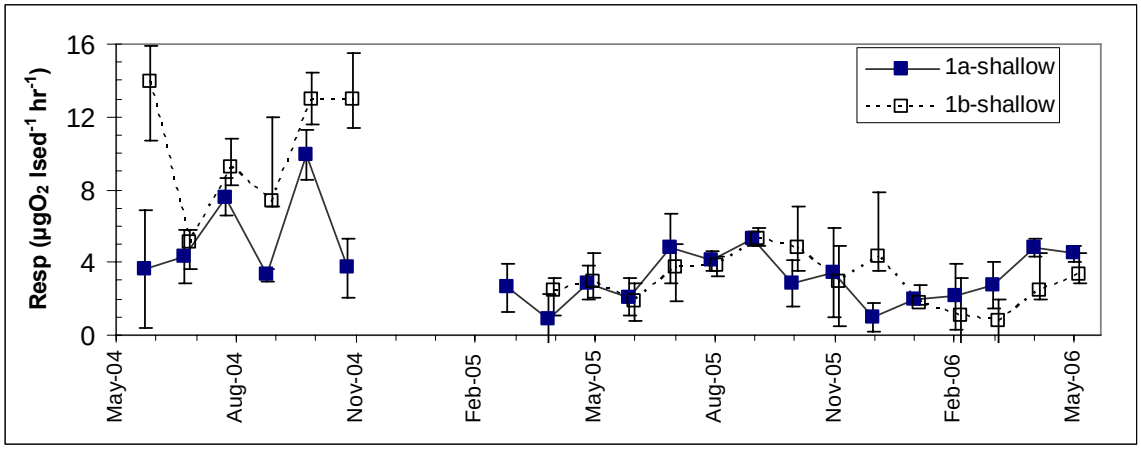

Figure 7: Example of community respiration artifacts for mesocosm 1 (recharge zone). Both mesocosms sampled water at the 1 meter depth interval. Unusually high and variable respiration rates occurred during the first six months of operation (gap in data due to DO probe malfunction at cold temperatures).

Invertebrate Colonization

Invertebrate colonization was much slower than we anticipated, despite several early seeding events (Figure 8). Rate of colonization depended on site, with the recharge zone site (M1) approaching an apparent steady state in density and taxonomic composition within 2-3 months. On the other end of the spectrum, site M4, which is located on the longest flowpath length of all the sites, required somewhere between 8-12 months to reach steady state. Finally, we observed an unexpected spike in density in the November 2004 sample for one pair of mesocosms (M3), which led to the decision to abandon plans to use mesocosms to directly estimate invertebrate production in the short term. The event coincided with the construction of a beaver dam on a nearby springbrook, which may have altered the local flowfield through changes in hydraulic head. Nonetheless, this change in the near-mesocosm environment does provide insight into the subtle changes that may occur naturally in the subsurface.

Community Composition

Invertebrate community composition in the mesocosms was very similar to taxa observed in respective well intervals in July 2005, at least at a coarse level of order/suborder (Figure 9). Percent Similarity Index (PSI) between well and mesocosms taxa was 62.7 ± 8.1%. We excluded mesocosm 4b because it only had coarse substrate,

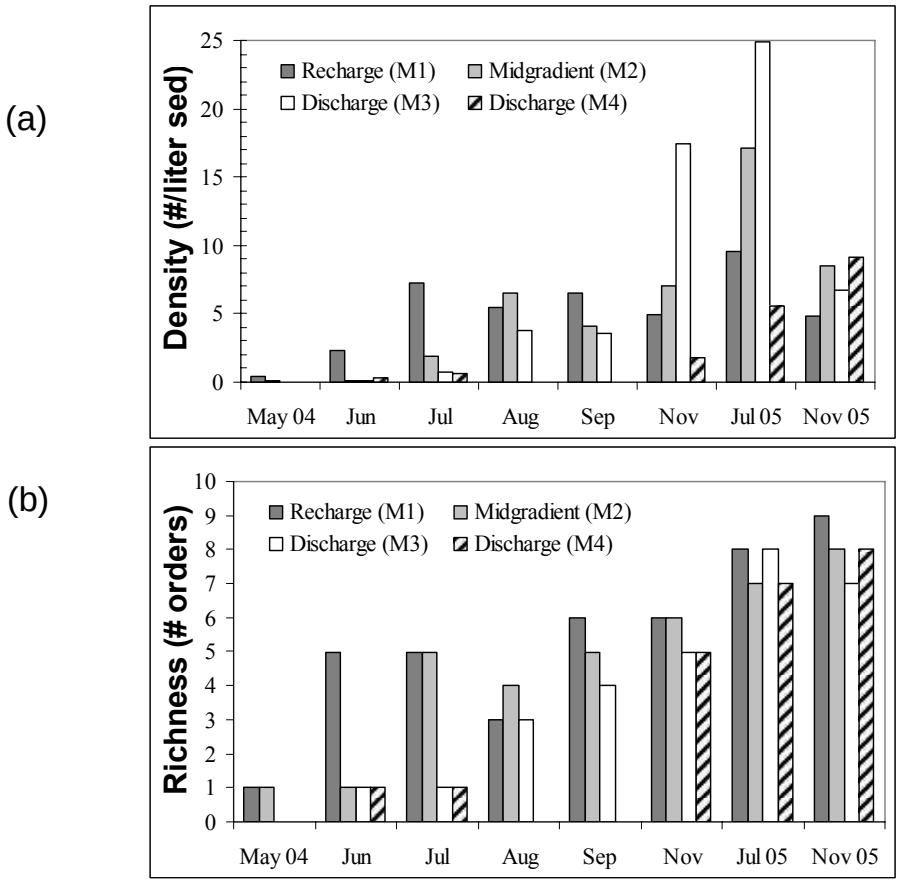

Figure 8: Invertebrate colonization dynamics: (a) invertebrate density; (b) taxonomic-order richness.

but it is noteworthy that PSI of this site was by far the lowest, at 25.1%. The density of *Stygobromus* amphipods, bathynellid crustaceans and ostracods was significantly lower in mesocosms compared to wells ($p<0.05$; Wilcoxon Signed Ranks Test). Combined macrofauna (amphipods, stoneflies, chironomids and mayflies) in mesocosms across all sampling dates (n = 332 samples) was very low, and bathynellid crustaceans were entirely absent from all mesocosm samples, despite the fact that bathynellids averaged 7.5% of the seeded invertebrates.

There was a strong gradient in invertebrate density along the length of the mesocosms in July and November 2005 (Figure 10 shows the average gradient, with error bars showing variance among sites). Invertebrate density decreased on average by a factor of 5, which we did not expect and had not previously observed during sampling in November 2004 (not shown). The slope appears linear on a log scale, hence the actual

gradients are curvilinear and quite strong (evident in the high variance in the middle sampling stations). The gradients were either concave or convex depending on the individual mesocosm, with no predictable pattern among sites.

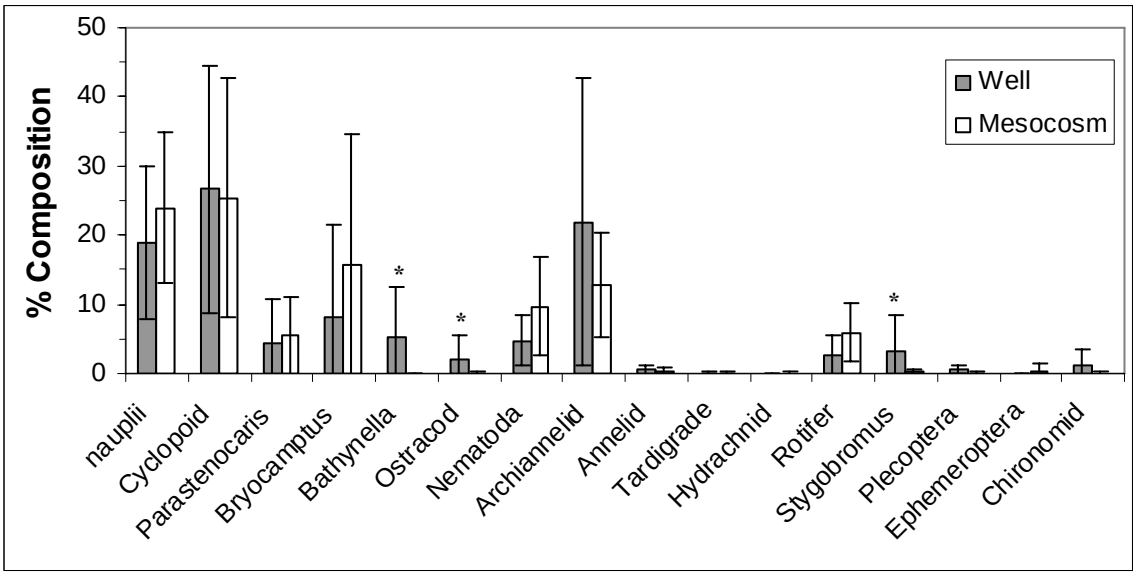

Figure 9: Comparison of invertebrate composition between mesocosms and respective well intervals. Error bars indicated +/- 1 sd. Asterisks indicate significant difference ($P<0.05$, Wilcoxon Signed Rank Test).

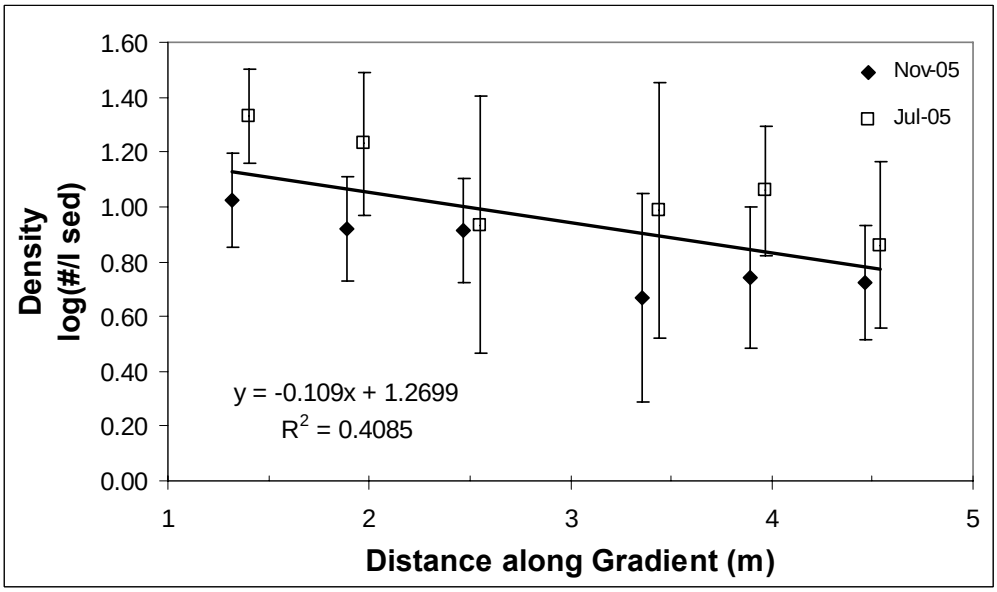

Figure 10: Invertebrate density gradients in July and November 2005. Decline in invertebrate abundance was consistent and non-linear for each respective site and sampling date: error bars represent variation among sites (± 1 SD).

Comparison to Invertebrate Communities from Well Sampling

Comparison of mesocosm invertebrate density to respective well intervals is complicated by choice of substrate and basic assumptions on the size of preferential flow zones and available habitat in the aquifer. The high response to the experimental POM treatments (see Chapter 5) affords an opportunity to more effectively compare mesocosm invertebrate density to the corresponding well intervals, since the treatments bracket the high end of invertebrate density. This comparison depends on both the substrate type in mesocosms and the percentage of preferential flow zones within the corresponding well intervals. Mesocosm substrate is essentially a representation of the preferential flow zones in the aquifer. For example, with an assumption of K ≈ 16,000 m/d for preferential flow zones, if measured a bulk hydraulic conductivity = 400 m/d over the total well interval, the preferential flow zones would comprise 2.5% of the well interval. As a result, and density estimates are adjusted by a factor of 40. Preferential flow zones in the field are, in turn, somewhat variable in a qualitative sense ranging from well sorted coarse gravel to mixed coarse and fine gravel, and occasionally coarse gravel with a coating of silts and organic matter. Because of this variability, the assumed hydraulic conductivity of 16,000 m/d for the preferential flow zone is not truly known. The mesocosm substrate, while more controlled, also affords some uncertainty with respect to estimating density of invertebrates. We initially estimated mesocosm invertebrate density assuming that organisms were evenly distributed across coarse/medium gravel and sand. We recalculated invertebrate density for the mesocosm sampling canisters using a lower volume of 142 ml, which would be the conservative density estimate if all of the invertebrates were clustered in the fine gravel (the bottom 5 cm in Figure 5a). Finally, the treatment canisters employed in Chapter 5 have invertebrate densities calculated from the narrow interface at the fine sediment boundary, the organisms being excluded from the interior fine sediments due to small pore size and a mesh net. Therefore, this comparison between well and mesocosm samples is a problem with multiple solutions, depending on preferential flow zone K, and substrate type. In Figure 11, we show mesocosm invertebrate density compared to well invertebrate density for both the coarse substrate (diamonds – bulk gravel from mesocosms sampling canisters) and fine substrate (triangles - combining the FPOM and sand treatment canisters from Chapter 5). The plot

is centered on an assuming preferential flow zone K of 8,000 m/d. Additional 1:1 lines of correspondence are shown for K values ranging from 4,000 m/d through 40,000 m/d. The mesocosms density calculated from bulk gravel consistently underestimates well density, while the estimates based on Sand/FPOM treatment canisters overestimate well density and with higher scatter. The recalculated density estimates for fine gravel are clustered within the most reasonable range of assumptions of preferential zone K (8,000-16,000 m/d). We note that the mesocosm density calculations consistently underestimate well invertebrate density for mesocosm 2a (indicated by the oval in Figure 11), except for the case of the sand treatment. This site consistently has the lowest oxygen levels.

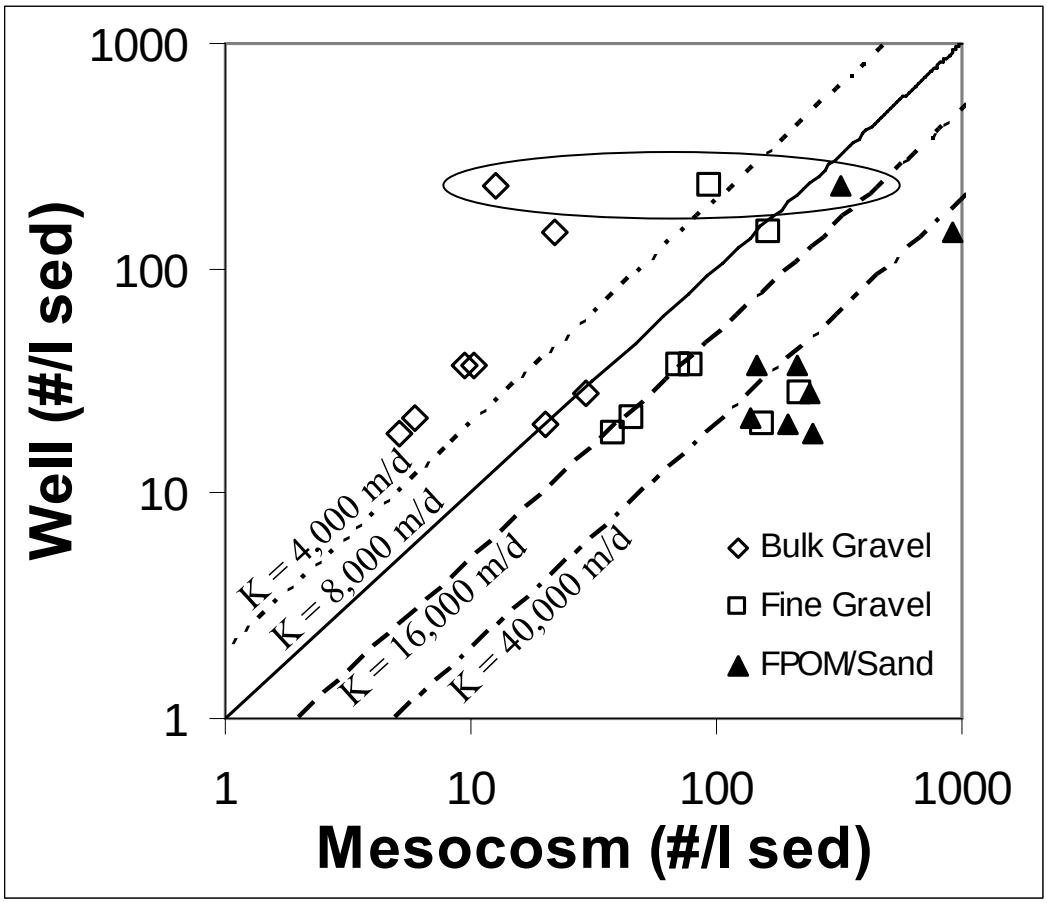

Figure 11: Invertebrate density comparison between mesocosms and corresponding well intervals, depending on calculation assumptions. Symbols indicate mesocosm invertebrate density calculated from: (1) bulk mesocosm gravel (diamonds); (2) sand and fine gravel fraction only (open squares); (3) treatment canister (triangles - combined FPOM and Sand treatments - see text). Well invertebrate density calculations are normalized for % preferential flow zone, based on measured hydraulic conductivity for each site, and lines indicates 1:1 correspondence with the assumption of K for preferential flow zones: K=8,000 m/d, solid line; 4000 m/d, dotted line; 16,000 m/d, dashed line; 40,000 m/d, alternating line. Mesocosm M2a outliers are shown inside the oval (see text).

DISCUSSION

Mesocosm Performance, Assumptions and Limitations

Because the mesocosms were designed for multiple purposes, they are admittedly not ideally suited for any given one. In this section, we comment extensively on assumptions and limitations of our design and sampling methods in context with the few alternative hyporheic microcosms and mesocosms in the published literature. The discussion is intended more from the perspective of lessons learned and future directions, rather than a critical review. Because of the challenges in sampling and experimenting with groundwater systems *in situ*, at best most our approaches are essentially indirect. One of the advantages of using experimental microcosms and mesocosms is that we have more direct access to the system and perform manipulations. Results within the mesocosms can be used to develop methods that would be very difficult to refine through trial and error in the field. In our case, while the mesocosms did not perform as originally anticipated, we were still able to observe general system properties, and adapt our experimental approach accordingly (Chapter 5).

Ecological microcosms are typically either batch reactors or more commonly packed bed reactors (in closed recirculation), and they are often employed as supporting evidence in hyporheic and groundwater studies (Jones et al. 1995, Baker et al. 2000, Craft et al. 2002, Crenshaw et al. 2002, Marshall and Hall 2004). There are very few published accounts of the use of larger mesocosms in the subsurface. One approach used a stainless steel chamber that is driven into the aquifer (Korom et al. 2005). These inserted mesocosms were essentially a more contained version of the push-pull method, where solutes are introduced with a conservative tracer, and are resampled after a period of incubation. Above ground pipes or troughs (Sobczak and Findlay 2002) allow for greater access and control, but may have less realistic sediment structure. Based on our experiences, successes and failures, and in context with the literature, we offer several important considerations for employing microcosms and mesocosms. Investigators are cautioned to pay attention to the replication of system conditions when interpreting and scaling up the results. Most important among the many potential system variables is the temperature regime, the grain size distribution of substrate, the disturbance from handling

and transport of sediment, the choice of appropriate flow rate for the respective grain size, and the potentially long incubation time before steady state conditions are achieved. There are also problems with sampling along very fine gradients and problems of interpretation in scaling up to natural systems.

Temperature regulation is generally not a problem for microcosms, which are typically used in temperature baths in the lab or are buried in the stream bed. But slow hyporheic processes might not be visible in microcosms. Scaling up to larger mesocosms requires a design that minimizes temperature gain. Community respiration is strongly affected by temperature gain or temperature cycling, more so than by mean temperature. This artifact might in turn confound estimates of uptake rates of solutes (Sobczak and Findlay 2002), as well as microbial and invertebrate growth rates.

Choice of grain size is important. Most studies use batch material collected from natural systems. This may reflect an accurate distribution of grain sizes and organic matter content. But, fluvial sediments may have high heterogeneity due to sorting, and the most important physical formations such as preferential flow zones may represent a very low percentage of overall sediment. When sediment is thus structured, it is perhaps impossible to preserve the arrangement when the sediment is transferred to a container, often after being homogenized. Sediment structure and size distribution should also determine the flow rate (Chapter 5). It is unrealistic to force high flow rates through a fine substrate that would, under gradients observed in the field, have low flow. And it is also unrealistic to maintain low flow rates in coarse sediments. This is not generally a problem with artificial substrates used in the field, or when a head tank is used to regulate flow (Sobczak and Findlay 2002). In these cases, the average velocity will be strongly regulated by sediment permeability, which varies by orders of magnitude. In contrast, hydraulic gradient probably varies by << 50%. When flow in artificial systems is regulated by a pump, there is a much higher likelihood that flow rate may be mismatched with intrinsic permeability and flow may be forced through sediments at unnaturally high rates.

For nutrient sampling along gradients, there are the scaling and sampling problems of strong chemical gradients existing over short distances (particle scale) superimposed on weak gradients over large spatial distances (flowpath scale). This is

perhaps the primary challenge in subsurface ecology. Marshall and Hall (2002) encountered this problem in their microcosms, and resorted to a somewhat subjective approach of selecting sample points to represent trends along microcosm gradients. Given the methodological challenges in subsurface science, this is perhaps an acceptable approximation of gradients. Use of resin capsules (see Chapter 5) to evaluate relative loading rates was unorthodox, but effective and relatively inexpensive. The capsules estimate loading rate, a combination of flow rate and concentration of the respective ions. We caution that the use of resin capsules can only indicate relative differences in loading rate, since they are selective in their sorption and exchange of ions, and the selectivity changes with time as ions are sorbed (see Sherrod et al. 2002 for an example of these limitations). We also cannot eliminate the possibility that leaching of synthetic resins from the capsules might stimulate or alter nutrient cycling. An alternative approach employs semi-permeable polycarbonate membranes, also known as peepers or dialysis samplers (Crocker and Meyer 1987, Lewandowski and Hupfer 2005). This sampling method allows for passive equilibration of chemistry, integrated over a period of time, thereby reducing sample variance. However, this method is selective depending on the time period of deployment and unlike resin capsules they do not amplify ions that are typically observed in very low concentrations. We feel that improvement lies in the use of increased replication and smaller sample size, coupled with either of the two approaches just described. For nutrient sampling along gradients, we might need 2-3 replicates using very small sample volumes for each port because of the minute and centimeter scale of sample variance (e.g. Odum 1957).

We cannot explain the non-linear declines in invertebrate density along the mesocosm gradients, and this is perhaps the most significant caveat with respect to interpretation of our mesocosm work. Declines in invertebrate abundance along aquifer flowpaths are not nearly this strong (Chapter 3). We offer several explanations that bear further testing. First, since the mesocosms are open systems, and a high rate of invertebrate colonization could result in a skewed distribution oriented towards the mesocosm inlet. Given the slow rate of colonization during the initial phase of operation and that these gradients were not observed until later on, we think that this possibility is unlikely. We could test for this by installing in-line sieves and periodically checking them

over the annual cycle to evaluate colonization dynamics. During April and May, we observed mature nymphs of amphibiont stoneflies in the inlets, in one case (M2a) occurring in large enough numbers to clog the inlet. We subsequently installed coarse strainers during these periods, which were cleaned weekly. The problem of stonefly attraction to permanent wells is discussed in Chapter 3. We were able to reduce or eliminate the problem by using baffles to seal the well from the atmosphere. However unlike the sampling wells, for reasons that we cannot explain the baffles on the mesocosm wells were not as successful at reducing stonefly emigration. It is possible that the stoneflies were attracted to or disoriented by the flow environment created by the continuous pumping of water for the mesocosms.

Most of the stoneflies survived the pumping, but it is still possible that dead animals subsidized the food web at the head of the mesocosm. Because the slope of the non-linear gradients persisted in the November samples, albeit at a lower overall level (Figure 9d), we do not think that a DOC subsidy, either from decaying stoneflies, a soil water pulse, would result in this skewed distribution. We also think that it is unlikely that a continuous loading of aquifer DOC (and subsequent sorption to the sediments at the head of the mesocosm) would explain these patterns. Internal spiraling, however short the uptake length, would gradually even out the distribution of energy or nutrient resources through the mesocosms. Additionally, we have not observed a consistent pattern of net DOC uptake in the mesocosms (unpubl. data). These assumptions could be readily tested using spiraling studies with labeled tracers, which is one of the long-term objectives for the use of the mesocosms.

We have shown that the loading rate of particulate matter is higher at the inlet for a single sampling event in November 2005. However, the steady state distribution of loosely associated benthic organic matter (LAPOM, *sensu* Pusch and Schwoerbel 1994), and the quality of the LAPOM (which is strongly correlated with invertebrate density on the treatments) does not correspond with background gradients of invertebrates (Chapter 5). Possibly the difference is expressed in the more strongly attached sediment organic matter (SOM), such as sediment coatings and biofilm, which might be available as sediment passes through invertebrate guts. Perhaps the most likely explanation is the lack

of POM in mesocosm sediments, which may lead to a depletion of energy resources that cannot be made up for with DOC loading.

Our results show that incubation time required to attain steady state conditions (relative to the annual cycle) may be very long, on the order of 8 to 12 months or more. This is apparent from the invertebrate colonization, and may also be true for, or a result of, biofilm development, which was not measured. Biofilm in streams show nonlinear patterns of diversity with an increase and decline to lower levels followed by a slow rise with longer term development of structure (Jackson et al. 2001). This succession sequence occurs over several months in surface systems and may be much more drawn out in the subsurface. Elsewhere we show that system respiration rates during the first six months of operation were as much as twice as high and much more variable compared to the longer term respiration observed over the course of two years (Chapter 1). Incubation time may at best be unclear, given that we never approached natural densities of amphipods, ostracods, bathynellids, and probably stoneflies. We conducted some preliminary growth trials with stonefly nymphs, (mentioned briefly in Chapter 6). The failure to observe any significant growth over 6 months indicates that some important elements or of the true subsurface environment are missing (such as POM).

Scaling up to natural systems from artificial systems is complicated, and has been the subject of some intense debate (summarized in Chalcraft et al. 2005). In the subsurface, the advantages of artificial systems clearly outweigh the disadvantages, and in a sense are sometimes the only option for study and experimentation. We made an effort to compare between mesocosm and natural systems in several ways, including the temperature and invertebrate composition already mentioned. We also showed favorable comparisons with respect to community respiration estimates (see Chapter 1). Finally, we compared community composition between mesocosms and respective well intervals and the results were favorable, at least at a coarse taxonomic resolution.

REFERENCES

Baker, M. A., H.M. Valett, and C.N. Dahm. 2000. Organic carbon supply and metabolism in a shallow groundwater ecosystem. *Ecology* 81(11): 3133-3148.

Benke, A. C., F. R. Hauer, D. L. Stites, J. L. Meyer and R. T. Edwards. 1992. Growth of snag-dwelling mayflies in a blackwater river: the influence of temperature and food. *Archiv f. Hydrobiologie* 125(1):63-81.

Beyers, R.J. and H.T. Odum. 1993. *Ecological Microcosms.* Springer-Verlag, New York.

Brunke, M. and T. Gonser. 1997. The ecological significance of exchange processes between rivers and groundwater. *Freshwat. Biol.* 37: 1-33.

Chalcraft, D.R., C.A. Binckley and W.J. Resetarits. Experimental venue and estimation of interaction strength: comment. *Ecology* 86(4): 1061-1067.

Craft, J.A., J.A. Stanford and M. Pusch. 2002. Microbial respiration within a floodplain aquifer of a large gravel-bed river. *Fresh. Biol.* 47: 251-261.

Craig, D.A. 1993. Hydronamic considerations in artificial stream research. In: Lamberti, G.A. and A.D. Steinman eds. Research in artificial streams: applications, uses and abuses. *J. N. Am. Benthol. Soc.* 12(4): 313-384.

Crenshaw, C.L. and H.M. Valett. 2002. Effects of coarse particulate organic matter on fungal biomass and invertebrate density in the subsurface of a headwater stream. *J. N. Am. Benthol. Soc.* 21(1): 28-42.

Crenshaw, C.L., H.M. Valett and J.R. Webster. 2002. Effects of augmentation of coarse particulate organic matter on metabolism and nutrient retention in hyporheic sediments. *Fresh. Biol.* 47: 1820-1831.

Crocker, M.T. and J.L. Meyer. 1987. Interstitial dissolved organic carbon in sediments of a southern Appalachian stream. *J. N. Am. Benthol. Soc.* 6(3): 159-167.

Dahm, C. 2006. Presidential address. North American Benthological Society, Anchorage, AK.

Diehl, C.J. 2004. Controls on the magnitude and location of groundwater/surface water exchange in a gravel dominated alluvial floodplain system, northwestern Montana. Unpublished MS Thesis. University of Montana.

Fetter, C.W. 2001. *Applied Hydrogeology 4th ed.* Prentice.

Findlay 1995. Importance of surface-subsurface exchange in stream ecosystems: The hyporheic zone. *Lim. Ocean.* 40(1): 159-164.

Findlay, S. and W. Sobczak. 1996. Variability in the removal of dissolved organic carbon in hyporheic sediments. *J. N. Am. Benthol. Soc.* 15(1): 35-41.

Hauer, F.R. Artificial streams for the study of macroinvertebrate growth and bioenergetics. In: Lamberti, G.A. and A.D. Steinman eds. Research in artificial streams: applications, uses and abuses. *J. N. Am. Benthol. Soc.* 12(4): 313-384.

Huggenberger, P., E. Hoehn, B Beschta, and W. Woessner. 1998. Abiotic aspects of channels and floodplains in riparian ecology. *Fresh. Biol.* 40: 407-425.

Jackson, C.R., P.F. Churchill and E.E. Roden. 2001. *Ecology* 82(2): 555-566.

Johnson, A.N. 2003. Preliminary hydrogeological and ground penetrating radar investigation of preferential flow zones in a gravel dominated floodplain, northwest Montana. Unpublished MS Thesis. University of Montana.

Jones, J.B., S. B. Fisher and N.B. Grimm. 1995. Vertical hydrologic exchange and ecosystem metabolism in a Sonoran Desert stream. *Ecology* 76(3): 942-952.

Korom, S.F., A.J. Schlag, W.M. Schuh and A.K. Schlag. 2005. In situ mesocosms: dentrification in the Elk Valley Aquifer. *Gr. Wat. Mon. & Rem.* 25(1):79-89.

Krebs, C.J. 1989. *Ecological Methodology*. Harper and Row, New York.

Lewandowski, J and M. Hupfer. 2005. Effect of macrozoobenthos on two-dimensional small scale heterogeneity of porewater phosphorous concentrations in lake sediments: a laboratory study. *Limnol. Oceanogr.* 50 (4): 1106-1118.

Malard, F. and F. Hervant. 1999. Oxygen supply and the adaptations of animals in groundwater. *Fresh. Biol.* 41: 1-30.

Marshall, M.C. and R.O. Hall. 2004. Hyporheic invertebrates affect N cycling and respiration in stream sediment microcosms. *J. N. Am. Benthol. Soc*. 23(3): 416-428.

McIntire, C.D. 1993. Historical and other perspectives of laboratory stream research. In: Lamberti, G.A. and A.D. Steinman eds. Research in artificial streams: applications, uses and abuses. *J. N. Am. Benthol. Soc.* 12(4): 313-384.

Orghidan, T. 1959. Ein neuer Lebensraum des unterirdischen Wassers, der hyporheische Biotop. *Arch. f. Hydrobiol.* 55: 392-414.

Palmer, M.A. 1993. Experimentation in the hyporheic zone: challenges and prospectus. *J. N. Am. Benthol. Soc.* 12: 84-93.

Poole, G.C., J. A. Stanford, S. W. Running, C. A. Frissell and B. K. Ellis. Submitted. Floodplain hydrologic complexity: modeling interactions between river discharge, geomorphology, and hyporheic flow dynamics. *Ecological Applications*.

Pusch, M. and J. Schwoerbel. 1994. Community respiration in hyporheic sediments of a mountain stream (Steina, Black Forest). *Arch. Hydrobiol.* 130(1): 35-52.

Pusch, M., D. Fiebig, I. Brettar, H. Eisenmann, B.K. Ellis, L.A. Kaplan, M.A. Lock, M. W. Naegli, W. Traunspurger. 1998. The role of micro-organisms in the ecological connectivity of running waters. *Fresh. Biol.* 40: 453-495.

Sherrod, S.K., J. Belnap and M.E. Miller. 2002. Comparison of methods for nutrient measurement in calcareaous soils: ion-exchange resin bag, capsule, membrane and chemical extraction. *Soil Sci.* 167(10): 666-679.

Sobczak, W., J. Cloern, A. Jassby, B. Cole, T. Schraga and A. Arnsberg. 2005. Detritus fuels ecosystem metabolism but not metazoan food wens in San Francisco estuary's freshwater delta. *Estuaries* 26(1): 124-137.

Sobczak, W.V and S. Findlay. 2002. Variability in bioavailability of dissolved organic carbon among stream hyporheic flowpaths. Ecology 83(11):3194-3209.

Stanford, J. A. 1998. Rivers in the landscape: introduction to the special issue on riparian and groundwater ecology. *Freshwater Biology* 40(3):402-406.

Stanford, J.A. and A.R. Gaufin. 1974. Hyporheic communities of two Montana rivers. *Science* 185: 700-702.

Stanford, J. A. and J. V. Ward. 1993. An ecosystem perspective of alluvial rivers: connectivity and the hyporheic corridor. *J. N. Am. Benthol. Soc.* 12(1):48-60.

Stanford, J.A. and J.V. Ward. 1988. The hyporheic habitat of river ecosystems. *Nature* 335: 64-66.

Stanford, J. A., J. V. Ward and B. K. Ellis. 1994. Ecology of the alluvial aquifers of the Flathead River, Montana (USA), pp. 367-390. *IN*: Gibert, J., D. L. Danielopol and J. A. Stanford (eds.), *Groundwater Ecology*. Academic Press, San Diego, California, USA. 571 pp.

Valett, H.M., C.C. Hakenkamp, A.J. Boulton. 1993. Perspectives on the hyporheic zone: integrating hydrology and biology. *J. N. Am. Benthol. Soc.* 12(1): 40-43.

Ward, J.V., F. Malard, J.A. Stanford and T. Gonser. 2001. Interstitial aquatic fauna of shallow unconsolidated sediments, particularly hyporheic biotopes. In: H. Wilkens, D.C. Culver and D.F. Humphreys, eds. *Ecosystems of the world: Subterranean Ecosystems*. Elsevier, Amsterdam.

Chapter 5

EFFECTS OF SUBSTRATE, ORGANIC MATTER AND OXYGEN
ON INVERTEBRATE DENSITY AND BIOMASS:
A MESOCOSM EXPERIMENT IN THE HYPORHEIC ZONE.

ABSTRACT

Previous observations from a floodplain aquifer indicate areas of high invertebrate density in or adjacent to areas of very low dissolved oxygen, but with no direct correlation with energy resources such as buried organic matter. We hypothesized that anaerobic reactions in patches of buried fine sediments and wood provide an indirect energy supply to spatially focused invertebrate production in adjacent, more oxygenated areas. We added wood-jam sediment with and without organic matter to a coarse gravel flow field within replicated mesocosms, to generate hypoxia plumes and evaluate the effect on biogeochemistry and invertebrate populations. While the treatments did not create hypoxia plumes or affect downgradient invertebrate densities, we observed localized 20-80 fold increases in density, and a 5-45 fold increase in biomass at the treatment interface (i.e. in direct contact with fine sediments). Density showed a strong U-shaped response curve to dissolved oxygen, increasing with both low and high inlet concentrations of DO. Biomass response strength was higher for the organic matter treatment. The biomass response curve showed a potential U-shaped response in the organic matter treatment. We observed metal precipitates on the downgradient surface of the organic matter treatments, indicating the potential activity of iron reducing bacteria within the treatment. Both treatments had increased ammonium, decreased nitrate, and a higher concentration of fine sediments and loosely associated particulate organic matter (LAPOM) at the treatment interface. The experiment suggests that fine sediments with or without particulate organic matter may be sufficient to explain areas of high invertebrate production in the aquifer. Organic matter is a more likely explanation for the U-shaped response curve to DO, although the indirect effect may be limited to fine sediment interfaces. The experiment also provides evidence that low DO conditions in the aquifer are a cause and not a consequence of high invertebrate density and production.

INTRODUCTION

Coupling between biogeochemical species is increasingly recognized in stream ecology, with some of the most dramatic work at the catchment scale (Bernhardt and Likens 2002, Brookshire and Valett 2005). This large scale work is empirical, but the relationships are fundamentally a reflection of integrated biogeochemical processes at small scales. These small-scale processes are microbially mediated, and are strongly influenced by the patchiness of sediment grain size distribution (Pusch et al. 1998). Microbial metabolism and behavior of chemical species will vary with grain size, and strongly so between aerobic and anaerobic sediments. In an analogous situation in soils, DOM loading is spatially separated from denitrification. Sites with high DOM loading high also have high flow velocity and oxygen concentration, whereas denitrification occurs in low flow, anaerobic sites. (Siemens et al. 2003). The physical basis of aerobic/anaerobic coupling at large scales is problematic. Anaerobic microsites and/or hyporheic exchange is the somewhat generic answer, but at what point does a high flow system such as a stream become influenced or dominated by low-flow sediment based hyporheic systems? The question of hyporheic contribution to whole stream metabolism is a central theme in hyporheic zone studies (Grimm 1984, Fisher 1995, Baker et al. 1999). The core question, the physical basis for aerobic-anaerobic coupling, although alluded to by Findlay has not systematically been addressed in streams.

The hyporheic zone, defined by river water penetrating the subsurface and interacting with ground water, was first used by Orghidan (1959) to describe bed sediments below the range of traditional benthic sampling. Since then, hyporheic zone dynamics have been shown to be a strong driver of ecosystem processes in rivers, and there is a rapidly increasing interest in river groundwater-surface water interaction (Stanford and Ward 1993, Valett et al. 1993, Stanford 1998, Dahm 2006). The hyporheic zone is generally considered a transition or ecotone between the channel and phreatic groundwater (Brunke and Gonser 1997). We believe that large hyporheic systems such as fluvial aquifers should be considered ecotypes in their own right, rather than transitional zones. Considered as a system, floodplain aquifers are isolated from solar energy and probably limited by carbon bioavailability. Our research identifies three potential sources of energy to hyporheic systems: river-derived organic carbon, infiltrating soil organic

carbon, or buried and stored particulate organic carbon. These energy sources are indicated by patterns of invertebrate density (Chapter 3), and spatial patterns of dissolved oxygen distribution (Chapter 1).

Elsewhere we have shown that hyporheic invertebrate density and production in the aquifer show an inverse parabolic or U-shaped response to dissolved oxygen concentration (Chapter 3, Chapter 6). Metazoan density decreases with declining oxygen and increased distance from the main channel. However invertebrate populations in the aquifer increase dramatically at DO < 3mg/l (16% of sampling wells), with the highest densities at the oxycline (higher oxygen transition zone below low oxygen zones). Our observations suggest that low oxygen zones may actually be energetically favorable for some invertebrates. Moreover, hyporheic stoneflies may actively seek out low DO zones out as part of the amphibiont life cycle

In the field, the aquifer adjacent to these zones has hydraulic conductivity exceeding 500 m/d (Diehl 2004), yet have consistently low dissolved oxygen, low nitrate and in some cases low sulfate concentrations (Chapter 1, Chapter 3). The biogeochemical pattern of oxygen, nitrate and sulfate depletion is similar to groundwater redox zonation in response to organic matter loading (Figure 1). This pattern was described by Champ et al. (1979) and is frequently observed in the field of applied subsurface contaminant bioremediation (Wiedemeier et al. 1999). At our study site, the source of energy for these low DO hotspots has not been identified. Most of oxygen depleted "hotspots" are 10's of meters in size, and appear to be located within or downgradient of buried wood jams, or

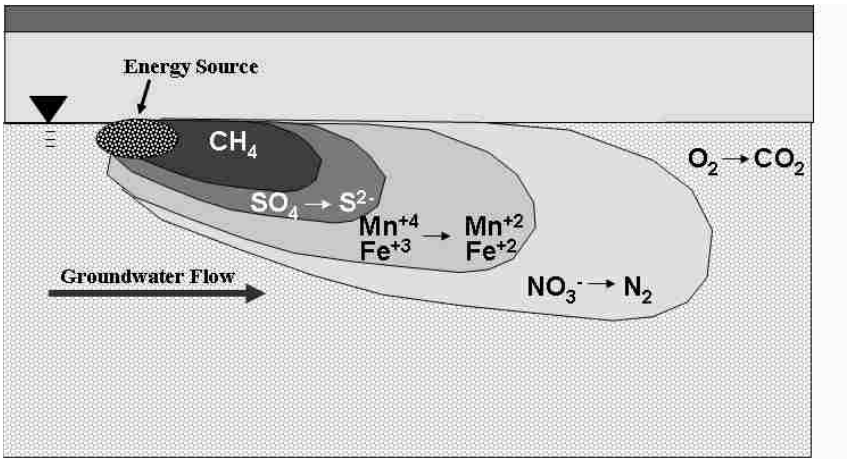

Figure 1: Terminal electron acceptor zones in response to an anthropogenic carbon source. (modified from Champ 1978). Naturally occurring redox gradients observed in floodplain aquifers may be a result of buried organic matter.

abandoned channel features. This partly supports the idea of the importance of buried carbon. Yet the occurrence of low oxygen zones in areas of high hydraulic conductivity, and relatively short residence time, is counterintuitive (presuming that abandoned channels are areas of deposition of fine sediment).

We hypothesized that anaerobic reactions in patches of buried fine sediments and organic matter, either from wood jams or abandoned channel deposits, spatially subsidize invertebrate productivity in adjacent, more oxygenated areas of the aquifer. This is a difficult problem in the field, requiring an extensive nested well grid and intense sampling at multiple scales. We used an array of *in situ* flow-through hyporheic mesocosms as a first step, to address the smaller scale aspects of this problem. We added wood-jam sediment with and without organic matter to a coarse gravel flow-field within replicated mesocosms, pumping groundwater at near-aquifer flux rates. In response to the treatments, we predicted that redox plumes would form down-gradient of each treatment site, with the magnitude of the plume depending on the amount of organic matter present (Figure 2a). These plumes would in turn correspond with deflections in DO, DIC, invertebrate community composition and density, depending on position within these gradients (Figure 2b). We expected a positive deflection in invertebrate density, DIC and

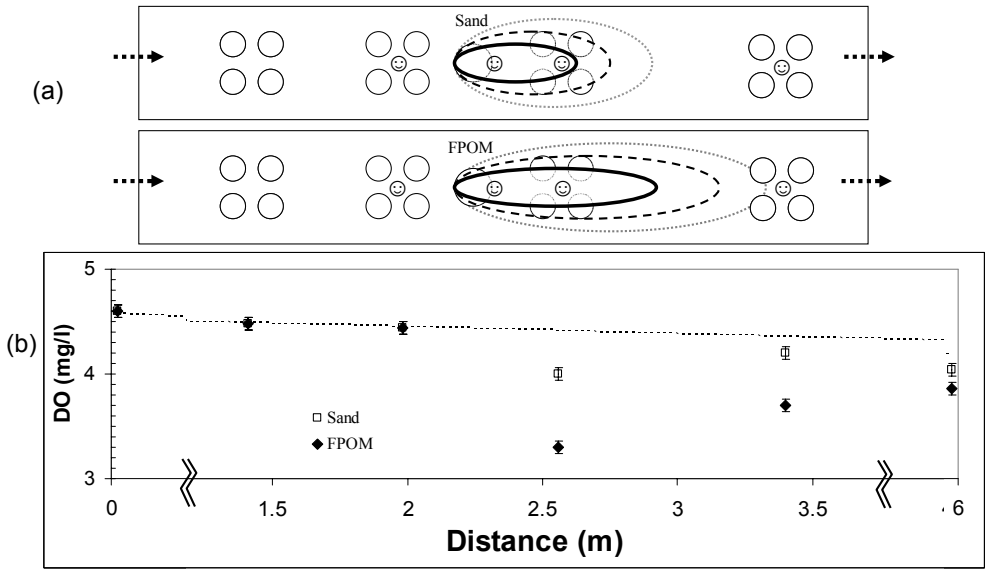

Figure 2: (a) Experimental Design for paired FPOM and sand treatments. Circles represent treatment canisters (large) and sampling canisters (small). Resin capsule locations shown by symbols. Predicted redox plumes for depletion of oxygen (dotted line) nitrate (dashed line) and sulfate (solid line) are shown for fine sediment treatment (top) and sediment with organic matter treatment (bottom). (b) Predicted response along mesocosm gradient (e.g. downward deflection in dissolved oxygen).

ammonium downgradient of each treatment, and a corresponding negative deflection in oxygen and nitrate. Our mesocosm sites represented a range of DO concentrations, which allowed us to evaluate the interaction between oxygen and sediment distribution. The results of this work are intended to inform the sampling scales and refine methods to be used in the more complex problem of field sampling.

STUDY SITE

The study site was the Nyack Floodplain located on the Middle Fork of the Flathead River (48° 27' 30" N, 113° 50' W), a fifth order gravel-bed river with headwaters in the Bob Marshall-Great Bear Wilderness Complex. The site is located along the southwest boundary of Glacier National Park in western Montana, USA (Figure 3a). The 12 km^2 floodplain is 8 km long and averages 1.5 km in width. The floodplain is bounded laterally by valley walls with bedrock knickpoints at both the upper and lower ends. The river along the length of the floodplain is anastomosed, with the active channel and parafluvial zone of the river tending toward the northeastern side of the valley. The more mature, orthofluvial floodplain forest and agricultural pasture is to the southwest. Over 30% of the main channel flow is lost to the aquifer at the upstream end of the floodplain and various gaining and losing reaches have been documented and modeled throughout the floodplain (see Fig 4, Stanford et al. 2005, Poole et al. submitted). The site has been the focus of research by the Flathead Lake Biological Station for over 20 years, and additional regional and site description is offered in Stanford et al. (1994, 2005) and Whited et al. (in press).

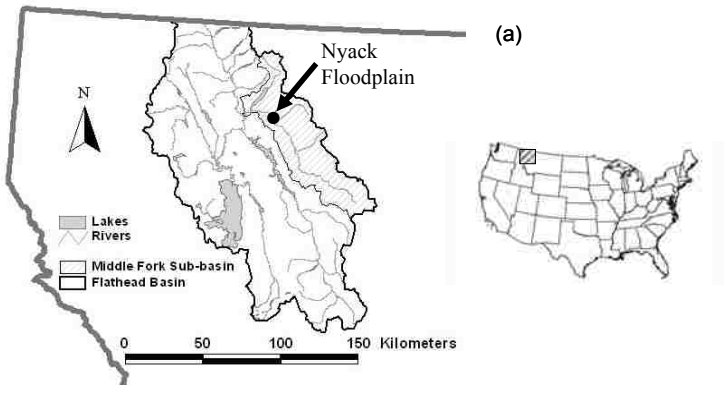

Figure 3 (a): Study site: Nyack Floodplain, Middle Fork Flathead River (MT USA).

METHODS

Mesocosm Design and Substrate

We installed four pairs of mesocosms at wells in aquifer recharge, discharge and midgradient zones (Figure 3b, 3c). Within each pair, mesocosms withdrew water from discrete 1-meter intervals at two depths: either shallow (0-1m below estimated mean low water - MLW), or deep (1-2 meters below MLW). Additional description of mesocosm sites, construction, and baseline performance are discussed in Chapter 4.

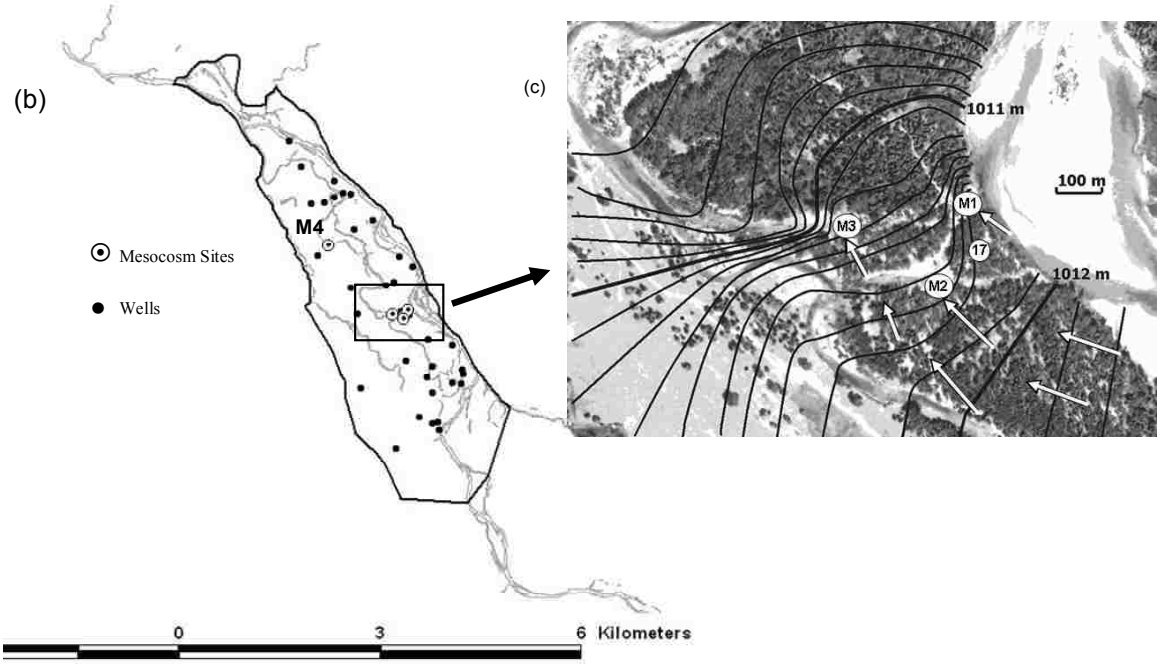

Figure 3 (b). Nyack floodplain: The main channel is furthest to the right, while smaller channel features are spring brooks and other off-channel habitats. Solid black line shows floodplain boundary; **(c)**: Close-up of mesocosm locations for pairs M1 through M3, superimposed on a potentiometric map (contours show water table elevations, and arrows show direction of groundwater flow). Mesocosm sites M1 (Aquifer recharge), M2 (midgradient) and M3 (discharge zone – spring head) are shown, in addition to well #17.

Mesocosms were filled with local sediments simulating a bimodal gravel formation (Huggenberger et al. 1998). We were concerned that the common practice of filling sediment microcosms with bulk sediment would not preserve the sediment structure, principally the interconnected pore space, which we believe is essential for invertebrate habitat. A sorted and layered gravel distribution was therefore chosen to

better represent invertebrate habitat and also enable the sampling of multiple substrate types in future experimentation. On the bottom was a 2.5 cm layer of sand (median grain size 250-500 μm) topped by 2.5 cm of fine gravel (average diameter 4.6 ± 2 mm), with the remaining volume (26+ cm) of the mesocosm filled with medium gravel (average diameter 17.6 ± 7.0 mm). All sediments were collected from the floodplain or nearby fluvial gravel deposits. We washed and sieved the material to achieve uniform size classes. The sand was collected from overbank deposits, and elutriated with well water until there was no visual evidence of POM (< 0.5% AFDM). Substrate was not otherwise sterilized or pretreated.

Sediment Amendment: Experimental Design and Sampling

We compared the effects of debris jam sediment, with and without organic matter, upon redox zonation and invertebrate density along mesocosm gradients. Material was collected from an actively accreting wood jam using a soil auger. Pooled sediment from 18 cores was separated into two halves. One half was left intact (FPOM treatment: 2.46 ± 0.21 % AFDM). In the other half, the organic matter was removed by elutriation until no organic matter was visible ("Sand" treatment: 0.058 ± 0.03 % AFDM). We added 1.41 liters of each treatment to a mesh bag (250 μm Nitex). We randomly assigned the two treatments pairwise to each corresponding mesocosm pair, resulting in treatments pairs at each of four mesocosm sites. Treatments were installed in experimentation canister C1 (Chapter 4, Figure 4), replacing the existing gravel in the respective canisters.

We sampled gradients of invertebrate density and composition, and biochemical gradients of oxygen, DIC, at hatches S1 through S6. Two invertebrate canisters were sampled from each hatch in July 2005. Invertebrate samples were thawed in the lab, placed in a petri dish, and stained with Rose Bengal. Samples were scanned at 25x, and organisms were identified to species (copepods and macroinvertebrates) where possible, or to order for nematodes, rotifers, archiannelids and other less abundant taxa. We estimated invertebrate density based on a canister volume of 1.12 liters for background sampling canisters and 0.39 liters for the treatment canisters (78% of the canister volume was displaced by the treatment substrate). All individuals were measured to the nearest 40 μm for biomass estimates, and nematodes and rotifers were also classified into

morphological groups for volumetric biomass estimates. Biomass of dominant taxa was calculated from a combination of published length weight regressions, and our own regressions for amphipods, stoneflies and copepods. For remaining taxa we used a volumetric approach, using length to width proportions, (assuming a specific gravity of 1.05, and dry mass of 15%, following Strayer and Likens 1986). Total biomass was calculated from the sum of individual taxa. We calculated average invertebrate mass of meiofauna by dividing total biomass by density for each treatment. Additional detail on taxonomic composition in the aquifer can be found in Chapter 3. The length-weight and length-volume regressions can be found in Chapter 6.

We re-sampled invertebrates in November 2005, revising our procedures as follows. We sampled only one canister per hatch in November, however we also sampled the treatment canister, using stainless steel sleeve. The mesh cylinder containing the treatment was then removed, washed gently with DI water to collect any invertebrates on the surface of the treatment, and set aside. The remaining sediment and water was processed as per the sampling canisters. We used DI water to process all samples, and retained the elutriate (water passing the 64 μm sieve). For a subset of canisters (S1, S3, S5 and the treatment canisters C1) we filtered this elutriate to estimate the density of fine particles and loosely associated particulate organic matter (LAPOM, *sensu* Pusch and Schwoerbel 1994). The elutriate was agitated and a 500 ml sub-sample was collected and filtered in the field onto a pre-weighed glass fiber filter (0.7 μm). We used a hole punch to sub-sample the filter, and ashed the filter for one hour at 500 °C for AFDM. We used a Fisons NA1500 elemental analyzer for CN analysis of the sub-sample. Following the November sampling we estimated the loading rate of fine particles and LAPOM by installing filters in-line with the outlets and inlets of the mesocosms. 45mm filters (0.7 μm, Whatman, Inc) were retained in Swin-Loc filter holders, and attached to the ends of acid washed outlet risers (the original risers were contaminated with algal growth). Flow rate was monitored hourly, and the filter was retained in place for 24 hours or until we observed a decrease in flow due to clogging. We repeated the procedure for the mesocosm inlets. Filters were returned to the lab, and processed for LAPOM, dry mass and CN ratio using the same procedures used for the invertebrate canisters.

We developed a modified micro-Winkler technique to measure dissolved oxygen (DO) concentration along mesocosm gradients. Sample collection along flowing gradients at the scale of the mesocosms required rapid sampling and high precision among samples. Ideally, the investigator must minimize the amount of sample water drawn, so as not to affect sampling at adjacent sites through changes in flow patterns. Earlier trials using a conventional Winkler bottles required too much time to fill bottles, and resulted in high variance relative to the known inlet and outlet concentrations (using standard 250 ml Winkler). Syringe titrations of 3ml and 5ml also proved to be far too variable among replicates. We developed a scaled-down Winkler titration using 2 dram (8.65 ± 0.065 ml) vials, with a polyethylene polyseal screw-cap (BioQuip Co.), which effectively displaced air and when closed. A 10 cm section of Norprene tubing that was previously attached to the inside face of each hatch allowed for water to be drawn from the center depth of the mesocosm (Figure 4). A sampling hose with hose clamp was attached to the outside of each sampling port, and three vials were filled per sampling port (S1-S6; Figure 4), starting from S6 hatch and working forward. Sample bottles were overflowed three volumes before sealing, ensuring that no air bubbles were trapped inside. Samples were fixed in the field, stored on ice and titrated within 12 hours. Scaled down reagents were as follows: 40 µl of 2.15 M $MnSO_4$ and 40 µl of 0.9 KI (with NaOH and NaN_3), followed by 80 µl of 25% H_2SO_4. The last reagent resulted in a pH somewhat less than 1.5, which is lower that the recommended pH of 2. We found that higher pH led to a much slower and often incomplete dissolution of precipitate, and contributed considerably to the variance. If air bubbles appeared after the first two reagents were added, the samples were discarded. Replicate 2 ml aliquots were titrated using 0.025 M Sodium Thiosulfate, diluted 50:1, and starch indicator. Standards (1.313 mM $KH(IO_3)_2$) were run before and after titrating each mesocosm sequence, until consistent results were obtained (both to standardize the Thiosulfate and also to ensure consistent observation of the endpoint). With practice, we were able to reduce the standard deviation among replicates to 0.02-0.08 mg/l. Dissolved inorganic carbon (DIC) was sampled using the same polyseal vials and sampling procedures for DO. Vials were stored on ice and transported to the lab, and analyzed within 24 hours for DIC using a combustion and infrared analyzer (Oceanographics International, Model 3300).

Due to the very high variability observed during preliminary sampling of oxygen and DIC gradients, we settled on an alternative and somewhat unconventional approach to sampling nutrients along mesocosm gradients in response to the treatments. We used PST-1 ionic exchange resin capsules (Unibest Inc.), which are mixed bed (anion and cation) resins enclosed in a rigid polyester shell of uniform surface area. Ion exchange resins are frequently used in soil science (Skogley and Dobermann 1996), either *in situ* or to expedite ion extraction through batch processing of soil samples in the lab. When used *in situ,* resins sorb ions at rates determined by diffusion properties of the medium and suite of ions present. Ions extracted from the resins are presumed to represent relative nutrient availability to plants. We know of no example of their use in flowing aquatic environments, however the principle remains the same. We reasoned that the capsules exchange ions in a manner similar to ion exchange observed in sediment biofilm (Freeman et al. 1995), with rates depending on the flux rate and the concentration of ions in solution. Upon extraction, the concentration of ions would therefore reflect the relative loading rate of the respective species. Note that resins have differential affinities for various ions, and this method provides only a qualitative comparison among and within sites. Resin capsules were installed in December 2004, and were located at 10cm depth in hatches upgradient (S2) and downgradient (two capsules at S3 and one at S4) and directly adjacent to and downgradient of the treatment (C1 – see Figures 2a, and Chapter 4 Figure 4). One capsule at S3 was removed from each mesocosm in early March (day 70), and the remaining capsules were harvested in April (day 120). Each capsule was placed in an acid washed polyethylene bottle with 25ml of 2M KBr, and mounted on a shaker table for 6 hours. The extraction was repeated three more times, pooled into a single bottle, and frozen until analysis. We analyzed for NH_4^+, NO_x (cadmium reduction), SRP and SiO_2^{2-} on a Seal Analytical Autoanalyzer 3 (APHA 1998).

Following the experiment, the treatments were removed, and hydraulic conductivity of the treatments was estimated in the lab using a falling head permeameter (Fetter 2001). We evaluated the grain size distribution of the treatments via dry sieving, and measured silt and clay content using a modified pipette method (Gavlak et al. 2003). We recovered organic matter from the FPOM treatments using elutriation and AFDM as

before, and calculated the overall loss of organic matter relative to the original concentration.

Results

Biogeochemical Response

We observed no obvious deflection in oxygen or DIC gradients in the 3rd-4th weeks of June 2005 (Figure 4a and 4b), seven months after the treatment was initiated. Nor did we observe changes in invertebrate density along gradients in July 2005 as we had predicted (Figure 4c).

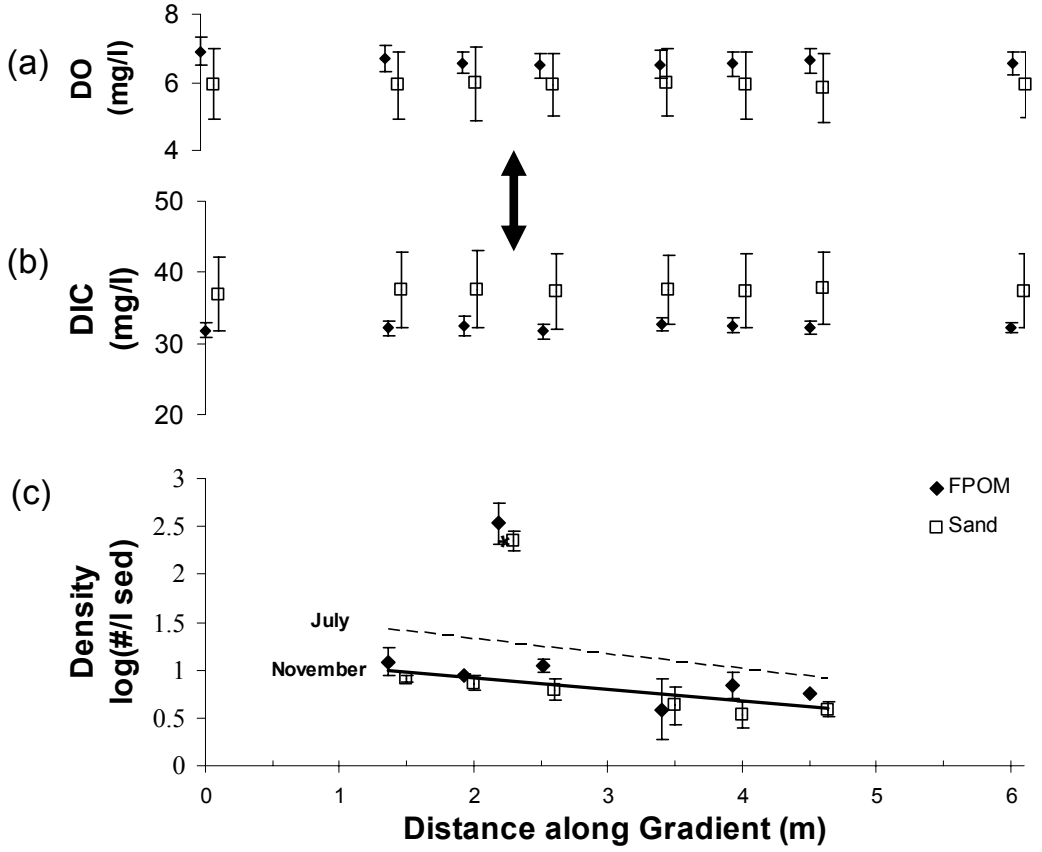

Figure 4: Mesocosm respiration and invertebrate gradients in response to treatments: (a) Dissolved oxygen (May 2005) (b) DIC (June 2005) and (c) invertebrate density (July and November 2005) in response to the treatments for mesocosms M1, M2 and M3. Error bars indicate ± 1 SE. Arrow show treatment location. Both treatments were significantly different from Background and canister blanks (Kruskal-Wallis $p<0.001$).

Ionic resin capsules demonstrated that there were treatment effects on nutrient chemistry, but generally only at the sampling sites directly downgradient of the treatments, at the treatment interface (Figure 5). Relative nitrate loading at the interface was significantly different from the gradient for both treatment types ($p=0.041$, Kendall's W). Nitrate is clearly lower for the FPOM treatment, and lower at 3 of 4 sites for the sand treatment. The fourth sand treatment (M2a) had a high relative outlier, but overall NOx concentrations at all sampling points in this mesocosm were almost an order of magnitude lower than all other sites. This site also has consistently lower bulk DO concentrations (Chapter 4). Omitting this outlier results in a consistent decrease in nitrate, regardless of treatment type, at least at the scale of the fine sediment interface. We also observed an increase in relative ammonium loading for both treatments (Figure 5b), at

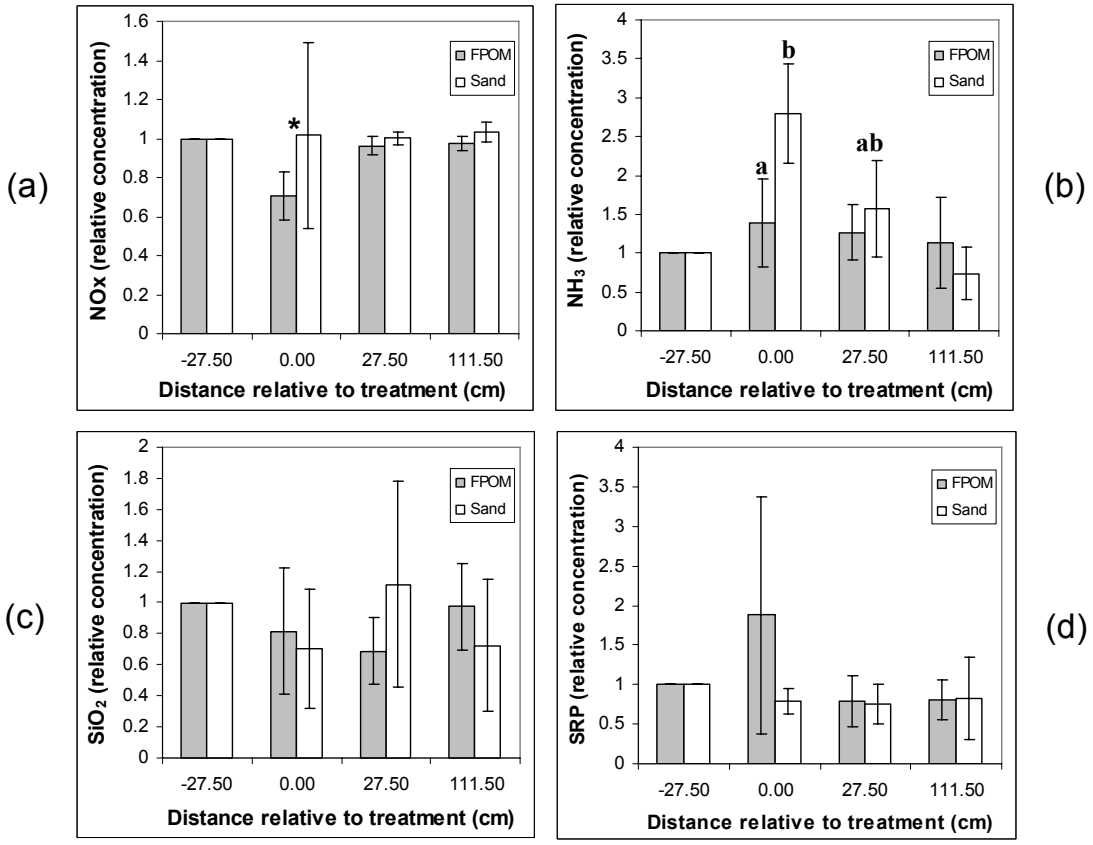

Figure 5: Mesocosm biogeochemistry gradients in response to treatments: (a-b) DIN; (c) SiO2 (d) SRP. Qualitative results are based on extractions from ionic resin capsules, and are normalized by the upgradient site for each respective mesocosm (hence the -27.5 cm distance = 1). Capsules located at distance zero were downgradient of and in direct contact with the treatments. Error bars indicate +/- 1 sd. * $p < 0.05$ Kendall's W; ab $p \leq 0.05$ Wilcoxon signed ranks test.

both the treatment interface, and at the S3 hatch (27.5 cm downgradient of the treatment $p \leq 0.05$, Wilcoxon Signed Ranks Test). At the furthest downgradient site (111.5 cm), NH_4^+ loading returned to background levels. The sand treatment had a significantly stronger ammonium loading response than the FPOM treatment at the treatment interface only ($p=0.021$, Kruskal Wallis). SRP was also higher on average at the FPOM treatment site, but the difference was not consistent and not significant with respect to the small sample size. We observed no obvious effect on SiO2 relative loading, indicating a negligible effect of mineral dissolution with increase in residence time that might have been caused by the treatment.

Based on the resin capsule results, we re-sampled mesocosm canisters for invertebrate density in November 2005, at about the time of the oxygen minima (Chapter 1). This time, we sampled the FPOM and sand treatment canisters, in addition to the canisters along the mesocosm gradient. Upon removal of the treatment canisters, we observed visual evidence of the biogeochemical effects of the treatments (Figure 6a): concentric rings of iron hydroxides (orange) and either manganese hydroxides or iron sulfides (black) on the FPOM treatment. We observed this pattern at three of four treatment pairs, with the strongest effect at M3b (lowest oxygen levels of all FPOM treatments). This effect has also been observed in the field, at a nearby fluvial aquifer on the Swan River (MT, USA). On the Swan River, we found a layer of ferricrete: coarse gravel with large pore sizes, cemented together and with a thick coating of presumably iron and manganese oxides (Figure 6b).

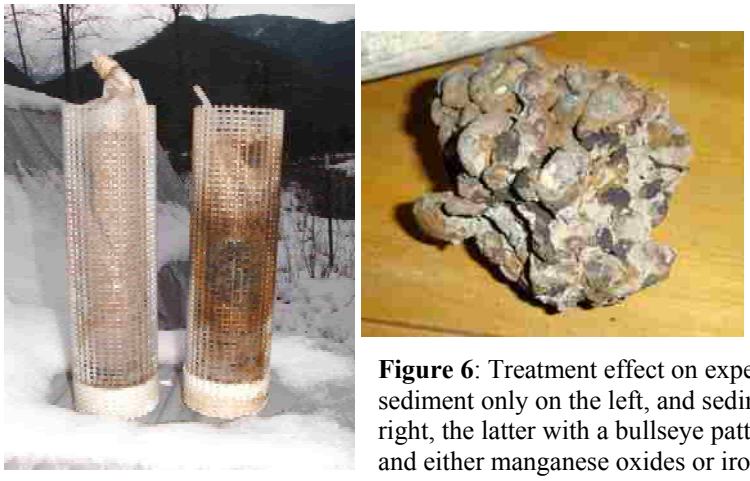

Figure 6: Treatment effect on experimentation canisters: (a) fine sediment only on the left, and sediment with organic matter on the right, the latter with a bullseye pattern of iron hydroxides (orange) and either manganese oxides or iron sulfides (black). (b) Coarse sediment ferricrete from the nearby Swan River aquifer, showing coarse grains with high pore space, cemented and coated with iron and manganese oxides.

Invertebrate Response

Invertebrate densities were significantly higher in the treatment canisters than background levels along the mesocosm gradient (Figure 4c), with densities up to 2.5 orders of magnitude higher (p=0.012, Wilcoxon Signed Ranks Test). Since the treatment canisters were larger and of different design than the sampling canisters, we also compared treatment canisters against canister blanks, to control for canister design (not shown). The blanks were the same design as the treatment canisters, but with coarse gravel only, and located in the second experimentation column (C2, Chapter 4 Figure 4). We saw no difference between the blanks and background levels. We divided the treatment density by the background levels (average density across the gradient) for each mesocosm, which produced an index of treatment strength (e.g. normalized for each mesocosm). This treatment strength in invertebrate density shows a strong U-shaped response as a function of average oxygen concentration (Figure 7). The pattern is generally consistent regardless of the period over which the independent variable for oxygen is averaged. The strongest fit to a curve is evident when using the two month running average for DO concentration. There is no clear difference between the two treatments within this curve.

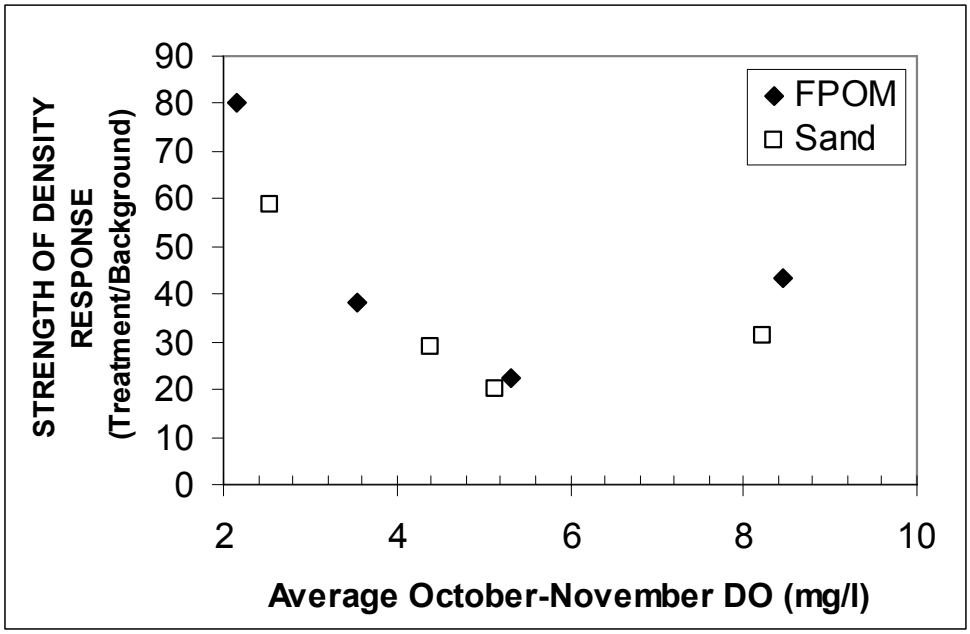

Figure 7: Strength of invertebrate density response (treatment/background) as a function of average oxygen concentrations. U-shaped pattern in response to extremes in oxygen concentration is similar to patterns observed for invertebrate production in the floodplain well grid.

Invertebrate community composition was influenced by substrate type (Figure 8). The two treatments collectively had significantly fewer Archiannelids and more rotifers than background levels ($p<0.05$, Wilcoxon Signed Ranks Test), the latter primarily the bdelloid genera *Dissotrocha* and *Rotaria*. Differences between the two treatment types are less clear due to the small sample size, however the sand treatment consistently had higher densities of harpacticoids (*Parastenocaris* sp and *Bryocamptus hiemalis*) and had lower average densities of cyclopoid copepods and nematodes.

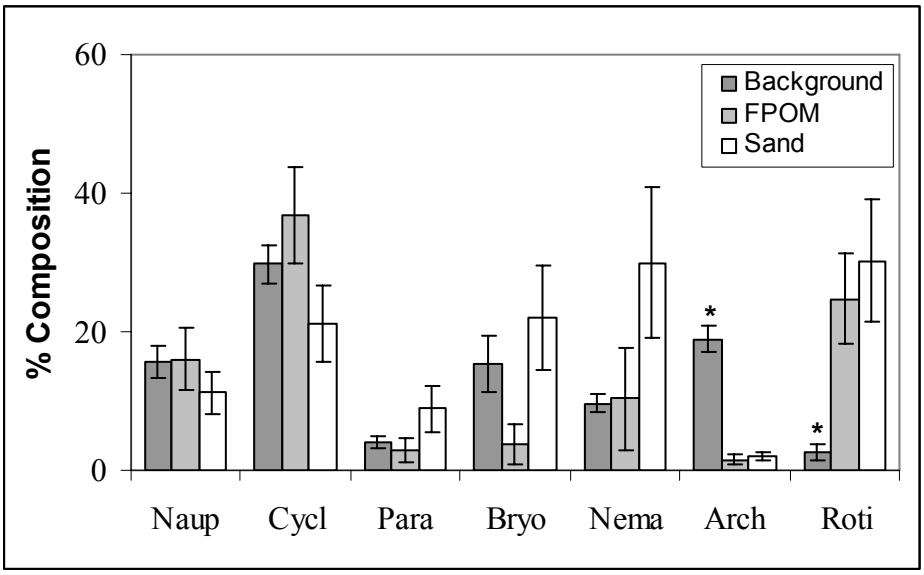

Figure 8: Invertebrate community composition within treatment canisters, compared to sampling canisters (background) in November 2005. Dominant taxa include: Naup = copepod nauplii; Cycl = Cyclopoid copepods; Para = *Parastenocaris sp*; Bryo = *Bryocamptus hiemalis;* Nema = *Nematodes;* Arch = *Archianellid;* Roti = *Rotifers*. Error bars indicate ± 1 SE. Asterisk indicates significant difference ($p<0.05$, Wilcoxon Signed Ranks Test).

Invertebrate biomass showed somewhat different patterns. Intrepretation of biomass patterns is complicated by the rare occurrence of macroinvertebrates, which individually outweighed the meiofauna composition for any given sample. We omitted macroinvertebrates (amphipods, stoneflies, chironomids and mayflies) from our analysis to avoid a skewed mass distribution. Our biomass calculation refers to meiofauna fraction (although technically adults of the cyclopoid *Acanthocyclops* would be considered macrofauna based on retention in a 500um sieve, we included these copepods as meiofauna). Dividing the biomass of invertebrates at treatment canisters by background levels to get a treatment response strength (Figure 9a), we found that the FPOM

treatments had consistently higher biomass response than the sand treatments (p=0.02, Kruskal Wallis Test). Dividing the biomass estimate by the density estimate for respective treatment canisters and sampling canisters provided an estimate of the average mass of the meiofauna (Figure 9b). Average meiofauna mass does not consistently differ between treatment pairs, and falls within the range of mass distributions observed in the sampling canisters. However the average meiofana mass for treatment and background samples declined significantly with a decline in DO (Figure 9b).

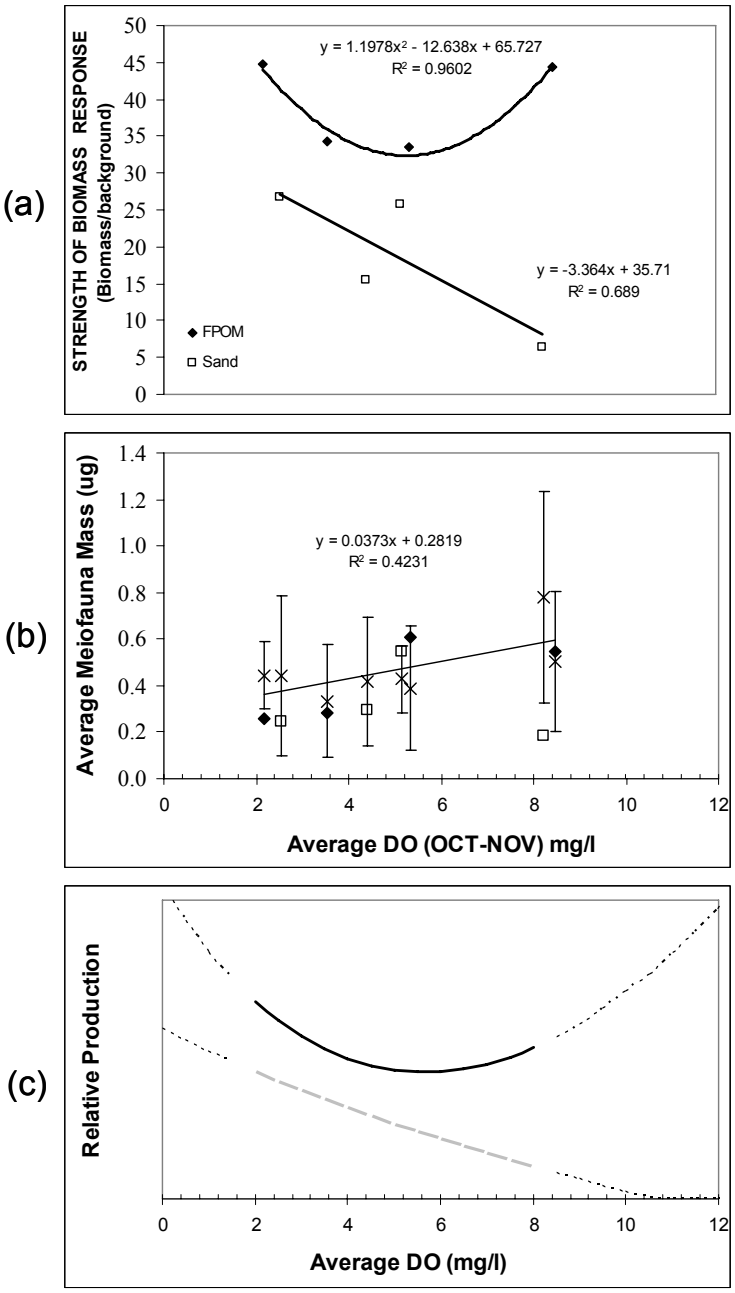

Figure 9: Response to treatments as a function of dissolved oxygen levels during DO minimum (October - November): (a) Strength of biomass response above background levels; (b) Average individual mass for meiofauna. (c) Model of relative production of meiofauna as a function of DO, assuming that P/B is proportional to $M^{2/3}$, and using the biomass and individual mass relationships in (a) and (b). Dark line is the FPOM treatment, gray line is the sand treatment, and dotted lines represent extrapolation beyond the range of empirical observations in (a) and (b).

When we compared invertebrate density among the three substrates against the several properties of the LAPOM dislodged during sampling, we observe a positive correlation with dry mass, % LOI, ash-free dry mass and C:N ratio. The last two properties, shown in Figure 10a and 10b, showed the strongest relationships and minimal outliers. We estimated the movement of particles through mesocosms inlets and outlets on a single day in November 2005. Flux rate and concentration of particles was generally higher for inlet water than outlet water, although the difference was not significant or consistent. Inlet water averaged 7.6 ± 6.3 µg POC/l, and outlets had 2.1 ± 1.6 µg POC/l, or a flux of 2.3 mg C/d and 0.3 mg C/d respectively. Inlet water suspended particles also had a higher C:N ratio and higher %LOI. Despite this imbalance, and the strong correlation between LABOM and invertebrate density, we saw no clear gradients within the mesocosms for any of these LAPOM properties that might correspond with the steep gradients in invertebrate density. In fact, 5 of 8 mesocosms had a consistent pattern where LAPOM %LOI decreased, then increased, in the sequence of hatches from S2 to S4 to S6.

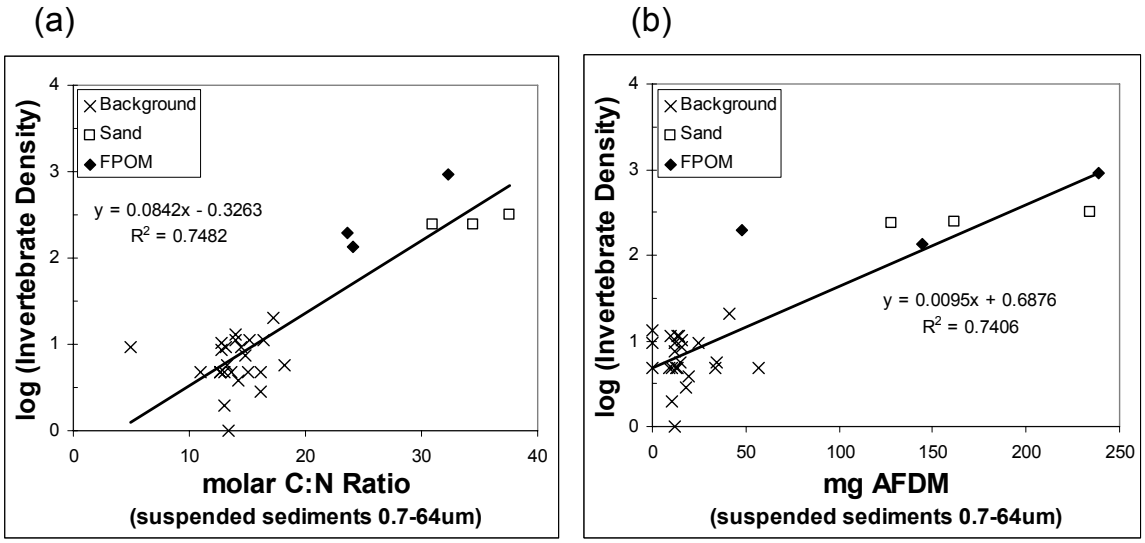

Figure 10: Invertebrate density in response to properties of loosely associated benthic organic matter (LAPOM - 0.7um-64um): (a) molar C:N ratio; (b) mg ash-free dry mass.

Hydraulic conductivity of the treatment material ranged from 0.002 m/d to greater than 150 m/d (the maximum permeability that we could measure, based on blank permeameter trials without sediment). There was no consistent difference between

treatment types, despite several replicates and repacking of the permeameter. Median grain size of both the sand and FPOM treatments was similar (64-125 um), however the distribution of grain sizes differed. The sand treatment had significantly higher percentages of sediment in the 150 and 250 μm sieves, while the FPOM treatment had higher percentage of sediment in the clay and silt fractions ($p=0.02$, Kruskal Wallis Test). Despite the difference in bulk sediment properties, there was no difference in the effect of LAPOM between treatments (Figure 10). Final organic matter content in the FPOM treatments was 2.12 ± 0.22 %. Average decrease in organic matter in the treatments was 16.8% (3.77g), or an exponential decay rate of -2.4×10^{-4} per day.

Discussion

Effects of Experimental Substrate

Although we anticipated that the sand treatment without organic matter would produce a response, we did not expect that the strength of the invertebrate density response would rival the corresponding FPOM treatment. We were originally at a loss to explain this, since, in the most general sense, invertebrates cannot get energy from mineral sediment. On a more subtle level, there are important similarities among the two treatments, which may outweigh the gross difference in bulk organic matter. Both treatments had high LAPOM relative to background levels. The treatment fine sediments potentially acted as mechanical filters for the suspended particles that we have shown are moving through the system (Recent work on this by Andy Pakman's group at Northwestern, pers comm.). Secondly, mineral soil will have biofilm and organic matter coatings (Chapter 2). Collectively, the biofilm and mineral surfaces offer high surface area for sorption of dissolved compounds (Claret et al. 1997, Push et al. 1998), mineral ions, and both DOM and minerals (flocculation, chelation). Presumably this particulate phase is available for consumption by larger invertebrates (Benke et al. 1992). Guts of subsurface invertebrates are often filled with mineral sediment (Chapter 6). Essentially the organic matter filtration and sorption capacity of fine sediments may be essential to invertebrate energetics. But the ultimate organic matter source (POM) may contribute energy either locally (FPOM treatment) or remotely (sand treatment) via breakdown of POM to more mobile/soluble DOM.

Finally, and related to the previous points, There is a balance between flow rate and total surface area in sediment based systems with advective transport of water. Extremes in grain size may have high flow but low surface area, and vice versa. We predict that an optimum will occur in an intermediate grain size, realizing the benefits of high flow rates and high sediment surface area (Figure 11). This model is essentially an extension of the model proposed by Findlay (1995, Figure 2), with the recognition that both axes of his graph are more or less regulated by grain size distribution. Assuming evenly sorted, uniformly shaped material, there is an apparent optimum grain size in the fine sands (0.5-1mm diameter). Hydraulic conductivity, estimated from the empirical equation of Hazen 1911 (in Fetter 2001) is increasing rapidly at this point but approaching an asymptote. At the same time, total surface area per unit volume (shown here for a representative volume of $1m^3$) is falling rapidly to a low asymptote. This optimum grain size is not far from the median grain size of 250-500 μm we observed in both treatment canisters.

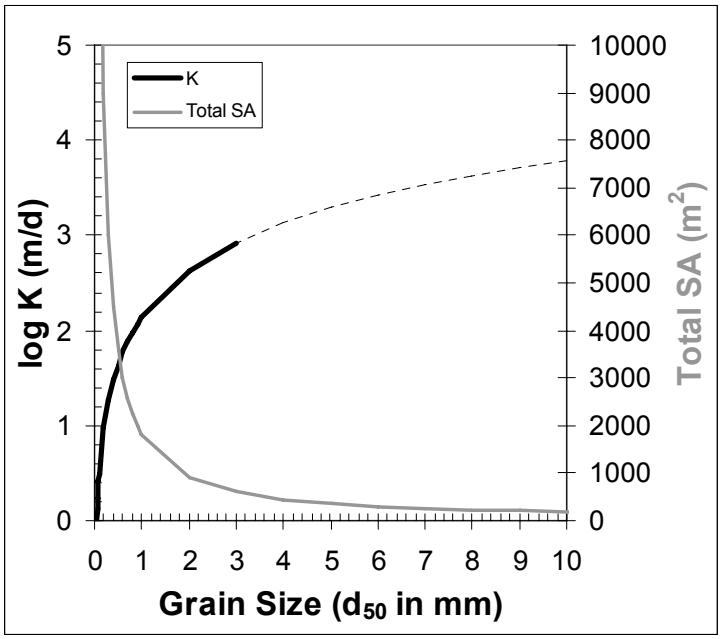

Figure 11: Model of sediment permeability (K) and surface area in response to grain size. The model predicts an optimum grain size of 0.5-1 mm (sand), where flux rate and volumetric surface area are maximized. The model assumes uniform grain size. Hydraulic conductivity (K) is estimated using the Hazen Approximation K= Cdj50 (Hazen 1911). Note that Hazen's empirical relationship is valid only up to a d50 of 3mm.

This model is a modification of the one proposed by Findlay (1995), predicting that a higher proportion of hyporheic exchange may not necessarily result in higher biogeochemical activity. Of course our model is an over-simplification, on two major counts. Biofilm architecture can alter flow properties and surface area with its complicated three dimensional structure (Neu and Lawrence 1997), and also be shaped by flow regime (Battin et al. 2003). Secondly, organic matter content is likely correlated with sediment size as material is sorted and deposited by the river. Smaller mineral particles will have lower settling velocity following Stoke's Law, and will show higher rates of co-deposition with organic matter under field conditions.

Interpretation of the effects of the treatments depends on the response variable. We observed no treatment differences when using density, but there were clearly different effects on meiofauna biomass. This does not get us to our original observation on production rates in the aquifer, however we can make an informed speculation based on our limited data set. Assuming that the biomass patterns hold through the annual cycle, we can model relative production in response to oxygen concentrations by multiplying mean annual biomass (approximated by Figure 9a) by an estimated P/B ratio. For any given organism, P/B is roughly proportional to the average mass at maturity to the 2/3 power (Banse and Mosher 1980). Using the average mass to oxygen relationship (Figure 9b), we can estimate this P/B across the same range of oxygen values, and project a relative production in response to oxygen concentrations (Figure 9c). This is a very coarse approximation of relative production patterns only, and we limit our interpretation to the observation that the organic matter treatment, based on its U-shaped curve, may have a stronger potential to explain invertebrate production in the aquifer. Changes in average mass with oxygen contribute little to the overall shape of these predicted patterns. The model is relatively insensitive to the choice of scaling exponent (i.e. ¾ power scaling predicted by metabolic theory, Ernest et al. 2003, or approximately ½ power scaling observed in respirometry trials, Chapter 6).

Additional evidence that fine sediments, with or without organic matter, may explain the production patterns observed in the field, lie in the comparisons between wells and mesocosms. In terms of community composition, the absence of archiannelids, and presence of rotifers, is a feature common to both our treatments and aquifer hotspots

(Chapter 3). The FPOM/sand treatments were also the only substrates that could reasonably predict invertebrate densities from wells in the low oxygen site (M2 – see Figure 11 in Chapter 4). The two other calculations based on coarse gravel and fine gravel layers in the background sampling canisters significantly underestimated invertebrate density for this site. This leads to the question of why do the recalculated sampling canisters (based only on the fine sediment interface, as a fraction of layered gravel/sand) produce density estimates that are consistently lower than the FPOM/sand treatments (also calculated based on the volume at the fine sediment interface). They both represent fine substrates, but the spatial context is different. The FPOM/Sand treatments are directly exposed to a coarse gravel flow-field, while the fine sediment of the background sampling canisters is on the edge of and oriented parallel to the axis of flow. There are several lines of evidence that indicate that the spatial context may be important to the biogeochemical gradients, and further, that oxygen may be a major factor regulating the effects of sediment structure and sediment heterogeneity.

Oxygen as a biogeochemical regulator in aquatic sediments

It is clear that oxygen concentration is strongly correlated with patterns of invertebrate density, biomass, and possibly size spectra (average body mass). Our experiment provides strong evidence that low DO is a cause rather than a consequence of high invertebrate density (i.e. low DO is not the result of invertebrate respiration). In the case of biomass and probably production, oxygen concentration may interact with sediment quality and the presence of particulate organic matter. The experimental design did not allow us to sample oxygen in sediment porewater at very small spatial scales and within the treatments. However the resin capsule data and visual evidence of iron oxyhydroxides support the notion of a steep redox interface between coarse and fine sediments. Most likely the organic matter in the sediments supplied an energy source for iron reducing bacteria, the reduced iron becoming mobile, only to subsequently become immobilized at the coarse sediment interface. The invertebrate data also suggests that the effects of biogeochemistry within fine sediments appear to be limited to the fine sediment interface and the immediate vicinity of this interface. This does not quite correspond with our field observations and the original problem as stated in the introduction: the co-

occurrence of low oxygen, high hydraulic conductivity, and high invertebrate density and production. The disparity may be due to treatment strength. In the field, there may be natural zones of preferential flow that also have very high contact area with anaerobic fine sediments. A buried wood jam or channel fill deposit may create a large obstruction with a coarse gravel flow-field, whereas our treatments are relatively small and obstructed only about 30% of the flow-field. We propose that a stronger treatment that completely or nearly completely obstructs the flow may be required to show such an effect upon oxygen concentrations downgradient of the treatment. Alternatively, an approach based on modeling, using a range of scenarios of permeability, path size, and spatial context, might be used to evaluate potential treatment strength. This approach was used quite successfully to model the physical factors that control seepage and stagnation zones beneath lakes (Winter 1978).

We believe that the biogeochemistry within fine sediments may spatially subsidize invertebrate food webs (*sensu* Polis et al. 1997) at the sediment ecotone in three ways (see Chapter 6, Figure 15). One mechanism might be upgradient of the fine sediment treatment, by way of immobilization of DOC (Pusch et al. 1998). Another might be downgradient of anaerobic zones, where metabolic production of methanogenesis, fermentation, or reduction and mobility of minerals and phosphate, become available at the more oxygenated coarse sediment interface. This is similar to Champ's model of what he called an open system, but may actually be simple mixing (Champ 1979). Finally, there may be spatially disjunct areas of fine sediment interface downgradient of the anaerobic byproducts, also functioning as immobilization sites. This last situation corresponds with the observations in the aquifer well network.

Our problem of anaerobic subsidy mechanisms is one of sampling scale: none of the mesocosm sites were truly anoxic, but only hypoxic at best. The fact that low oxygen levels, not necessarily complete depletion of oxygen, can regulate biogeochemistry, fits with the idea that anaerobic microsites can make significant contributions to overall system behavior. As we explain in the introduction, the physical basis for this is rarely spelled out in the aquatic literature. We know from soil science that bulk oxygen concentration will affect the percentage of anaerobic microsites within soil aggregates, depending on the aggregate size and composition (Glinski and Stepniewski 1985).

Our results run contrary to a popular notion that anoxia is averse to invertebrate populations, or is somehow not a beneficial (sensu Findlay 1995). Hypoxia and/or proximity to anoxic conditions may actually increase system productivity and energy flow. The availability of particulate organic matter to higher trophic levels may be dependant on aerobic/anaerobic biogeochemistry, hence regulated by oxygen. Rarely is oxygen used as an independent variable, probably because of the difficulty in manipulating it. We feel that the strong influence of oxygen upon density, biomass, mean body size and production is noteworthy, despite the limited set of observations and sample size. Aside from temperature, oxygen may be among the few variables that may control body size distribution. Body size spectra have long been known to show repeatable but poorly explained patterns across systems (Sheldon et al. 1972, Strayer 1986, 1991). Whatever controls the distribution of individual mass controls system energetics, since individual mass is the basis of allometric scaling in metabolic theory (Brown et al. 2004).

Conclusions

While not conclusive, our experiment showed multiple lines of indirect evidence for buried POM on aquifer invertebrate food webs, including effects on invert biomass but not density. The exponential decay of invertebrates along mesocosm gradients, in a system where POM has been removed, may also be related. But POM availability is not straightforward, and may depend on the effects of fine sediment with which it typically co-occurs, and the physical context, in the case of the treatments in the middle of a coarse flow-field. The sediment interface has a strong effect on invertebrate dynamics, density, community composition. The properties of the fine sediments are in turn probably regulated by bulk oxygen content surrounding the areas of fine sediments, since most of our measurements showed strong often non-linear patterns in response to oxygen concentration.

REFERENCES

APHA 1998. *Standard Methods for the examination of water and wastewater, 20th ed.* Washington DC.

Baker, M. A., H.M. Valett, and C.N. Dahm. 1999. Acetate retention and metabolism in the hyporheic zone of a mountain stream. *Limn. Oceanogr.* 44(6): 1530-1539.

Baker, M. A., H.M. Valett, and C.N. Dahm. 2000. Organic carbon supply and metabolism in a shallow groundwater ecosystem. *Ecology* 81(11): 3133-3148.

Banse, K. 1982. Mass-scaled rates of respiration and intrinsic growth in very small invertebrates. *Mar. Ecol. Prog. Ser.* 9: 281-297.

Battin, T.J., L.A. Kaplan, J. D. Newbold, C.M.E. Hansen. 2003. Contributions of microbial biofilms to ecosystem processes in stream mesocosms. *Nature* 426: 439-442.

Benke, A. C., F. R. Hauer, D. L. Stites, J. L. Meyer and R. T. Edwards. 1992. Growth of snag-dwelling mayflies in a blackwater river: the influence of temperature and food. *Archiv f. Hydrobiologie* 125(1):63-81.

Bernhardt, E. and G.E. Likens. 2002. Dissolved organic carbon enrichment alters nitrogen dynamics in a forest stream. *Ecology* 83(6): 1689-1700.

Beyers, R.J. and H.T. Odum. 1993. *Ecological Microcosms.* Springer-Verlag, New York.

Brookshire, E.N.J., H.M. Valett, S.A. Thomas and J.R. Webster. 2005. Coupled cycling of dissolved organic nitrogen and carbon in a forest stream. *Ecology* 86(9): 2487-2496.

Brown, J.H., J.A. Gillooly, A.P. Allen, V.M. Savage and G.B. West. 2004. Toward a metabolic theory of ecology. *Ecology* 85(7): 1771-1789.

Brunke, M. and T. Gonser. 1997. The ecological significance of exchange processes between rivers and groundwater. *Fresh. Biol.* 37: 1-33.

Champ, D.R., J. Gulens and R.E. Jackson. 1979. Oxidation-reduction sequences in ground water flow systems. *Can. J. Earth Sci.* 16:12-23.

Claret, C., P. Marmonier, J-M Boissiere, D. Fontevieille and P. Blanc. Nutrient transfer between parafluvial interstitial water and river water: influence of gravel bar heterogeneity. Fresh. Biol. 37: 657-670.

Clinton, S.M., R.t. Edwards, and R.J. Naiman. 2002. Forest-river interactions: influence on hyporheic dissolved organic carbon concentrations in a floodplain terrace. *J. Am. Wat. Res. Assoc.* 38(3): 619-621.

Craft, J.A., J.A. Stanford and M. Pusch. 2002. Microbial respiration within a floodplain aquifer of a large gravel-bed river. *Fresh. Biol.* 47: 251-261.

Crenshaw, C.L. and H.M. Valett. 2002. Effects of coarse particulate organic matter on fungal biomass and invertebrate density in the subsurface of a headwater stream. *J. N. Am. Benthol. Soc.* 21(1): 28-42.

Crenshaw, C.L., H.M. Valett and J.R. Webster. 2002. Effects of augmentation of coarse particulate organic matter on metabolism and nutrient retention in hyporheic sediments. *Fresh. Biol.* 47: 1820-1831.

Crocker, M.T. and J.L. Meyer. 1987. Interstitial dissolved organic carbon in sediments of a southern Appalachian stream. *J. N. Am. Benthol. Soc.* 6(3): 159-167.

Dahm, C. 2006. Presidential address. North American Benthological Society, Anchorage, AK.

Datry, T, F. Malard, L. Vitry, F. Hervant and J. Gibert. 2003. Solute dynamics in the bed sediments of a stormwater infiltration basin. *J. Hydrol.* 273: 217-233.

Datry, T., F. Malard and J. Gibert. 2005. Response of invertebrate assemblages to increased groundwater recharge rates in a phreatic aquifer. *J. N. Am. Benthol. Soc.* 24(3): 461-477.

Diehl, C.J. 2004. Controls on the magnitude and location of groundwater/surface water exchange in a gravel dominated alluvial floodplain system, northwestern Montana. Unpublished MS Thesis. University of Montana.

Ernest, S.K.M., B.J. Enquist, J.H. Brown, E.L. Charnov, J.F. Gillooly, V.M. Savage, E.P. White, F.A. Smith, E.A. Hadly, J.P. Haskell, S.K. Lyons, B.A. Maurer, K. J. Niklas and B. Tiffney. 2003. Thermodynamic and metabolic effects on the scaling of production and population energy use. *Ecol. Lett.* 6: 990-995.

Fetter, C.W. 2001. *Applied Hydrogeology 4th ed.* Prentice.

Findlay 1995. Importance of surface-subsurface exchange in stream ecosystems: The hyporheic zone. *Lim. Oceanogr.* 40(1): 159-164.

Findlay, S. and W. Sobczak. 1996. Variability in the removal of dissolved organic carbon in hyporheic sediments. *J. N. Am. Benthol. Soc.* 15(1): 35-41.

Freeman, C., P.J. Chapman, K. Gilman, M.A. Lock, B. Reynolds and H.S. Wheater. 1995. Ion Exchange mechanisms and the entrapment of nutrients by river biofilms. *Hydrobiol.* 297: 61-65.

Galas, J., T. Bednarz, E. Dumnicka, A. Starzecka and K Wojtan. 1996. Litter decomposition in a mountain cave water. *Arch. Hydrobiol.* 138(2): 199-211.

Gavlak, R., D. Horneck, R.O. Miller, J. Kotuby-Amacher. 2003. Soil, plant and water reference methods for the western region. Western Region Extension Publication WREP 125, 2nd ed. University of Alaska.

Glinski, J. and W. Stepniewski 1985. *Soil Aeration and its Role for Plants*. CRC Press, Boca Raton FL.

Huggenberger, P., E. Hoehn, B Beschta, and W. Woessner. 1998. Abiotic aspects of channels and floodplains in riparian ecology. *Fresh. Biol.* 40: 407-425.

Jackson, C.R., P.F. Churchill and E.E. Roden. 2001. *Ecology* 82(2): 555-566.

Johnson, A.N. 2003. Preliminary hydrogeological and ground penetrating radar investigation of preferential flow zones in a gravel dominated floodplain, northwest Montana. Unpublished MS Thesis. University of Montana.

Jones, J.B., S. B. Fisher and N.B. Grimm. 1995. Vertical hydrologic exchange and ecosystem metabolism in a Sonoran Desert stream. *Ecology* 76(3): 942-952.

Malard, F. and F. Hervant. 1999. Oxygen supply and the adaptations of animals in groundwater. *Fresh. Biol.* 41: 1-30.

Marshall, M.C. and R.O. Hall. 2004. Hyporheic invertebrates affect N cycling and respiration in stream sediment microcosms. *J. N. Am. Benthol. Soc*. 23(3): 416-428.

Neu, T.R., and J.R. Lawrence. 1997. Development and structure of biofilms in river water studied by confocal laser scanning. *FEMS Micr. Ecol.* 24(1): 11-25.

Newbold, J. D., Mulholland, P. J., Elwood, J. W. & O'Neill, R. V. Organic carbon spiralling in stream ecosystems. *Oikos* 38, 266-272 (1982).

Orghidan, T. 1959. Ein neuer Lebensraum des unterirdischen Wassers, der hyporheische Biotop. *Arch. f. Hydrobiol.* 55: 392-414.

Polis, G.A., W.B. Anderson and R.D. Holt. 1997. Towards an integration of landscape and food web ecology: the dynamics of spatially subsidized food webs. *Ann. Rev. Ecol. Syst.* 28: 289-316.

Poole, G.C., J. A. Stanford, S. W. Running, C. A. Frissell and B. K. Ellis. Submitted. Floodplain hydrologic complexity: modeling interactions between river discharge, geomorphology, and hyporheic flow dynamics. *Ecological Applications*.

Pusch, M. and J. Schwoerbel. 1994. Community respiration in hyporheic sediments of a mountain stream (Steina, Black Forest). *Arch. Hydrobiol.* 130(1): 35-52.

Pusch, M., D. Fiebig, I. Brettar, H. Eisenmann, B.K. Ellis, L.A. Kaplan, M.A. Lock, M. W. Naegli, W. Traunspurger. 1998. The role of micro-organisms in the ecological connectivity of running waters. *Fresh. Biol.* 40: 453-495.

Sheldon, R.W., A. Prakash, W.H. Sutcliffe Jr. 1972. The size distribution of particles in the ocean. *Limnol. Oceanogr.* 17(3): 327-340.

Sherrod, S.K., J. Belnap and M.E. Miller. 2002. Comparison of methods for nutrient measurement in calcareaous soils: ion-exchange resin bag, capsule, membrane and chemical extraction. *Soil Sci.* 167(10): 666-679.

Siemens, J., M. Haas, M. Kaupenjohann. 2003. Dissolved organic matter induced denitrification in subsoils and aquifers? *Geoderma* 113: 253-271.

Skogley, E.O. and A. Dobermann. 1996. Synthetic ion-exchange resins: soil and environmental studies. *J. Environ. Qual.* 25: 13-24.

Sobczak, W., J. Cloern, A. Jassby, B. Cole, T. Schraga and A. Arnsberg. 2005. Detritus fuels ecosystem metabolism but not metazoan food wens in San Francisco estuary's freshwater delta. *Estuaries* 26(1): 124-137.

Sobczak, W.V and S. Findlay. 2002. Variability in bioavailability of dissolved organic carbon among stream hyporheic flowpaths. *Ecology* 83(11):3194-3209.

Stanford, J. A. 1998. Rivers in the landscape: introduction to the special issue on riparian and groundwater ecology. *Freshwater Biology* 40(3):402-406.

Stanford, J.A. and A.R. Gaufin. 1974. Hyporheic communities of two Montana rivers. *Science* 185: 700-702.

Stanford, J. A. and J. V. Ward. 1993. An ecosystem perspective of alluvial rivers: connectivity and the hyporheic corridor. *J. N. Am. Benthol. Soc.* 12(1):48-60.

Stanford, J.A. and J.V. Ward. 1988. The hyporheic habitat of river ecosystems. *Nature* 335: 64-66.

Stanford, J. A., J. V. Ward and B. K. Ellis. 1994. Ecology of the alluvial aquifers of the Flathead River, Montana (USA), pp. 367-390. *IN*: Gibert, J., D. L. Danielopol and J. A. Stanford (eds.), *Groundwater Ecology*. Academic Press, San Diego, California, USA. 571 pp.

Strayer, D and G.E. Likens. 1986. An energy budget for the zoobenthos of Mirror Lake, New Hampshire. *Ecology* 67(2): 303-313.

Strayer, D. 1986. The size structure of a lacutrine zoobenthic community. *Oecologia* 69: 513-516.

Strayer, D. 1991. Perspectives on the size structure of lacustrine zoobenthos, its causes, and its consequences. *J. N. Am. Benthol. Soc.* 10(2): 210-221.

Strayer, D., S. May, P. Nielsen, W. Wollheim and S Hausam. 1997. Oxygen, organic matter, and sediment granulometry as controls on hyporheic animal communities. *Arch. Hydrobiol.* 140(1): 131-144.

Tillman, D.C., A. Moerke, C. Ziehl and G. Lamberti. 2003. Subsurface hydrology and degree of burial affect mass loss and invertebrate colonization of leaves in a woodland stream. *Fresh. Biol.* 48: 98-107.

Valett, H.M., C.C. Hakenkamp, A.J. Boulton. 1993. Perspectives on the hyporheic zone: integrating hydrology and biology. *J. N. Am. Benthol. Soc.* 12(1): 40-43.

Ward, J.V., F. Malard, J.A. Stanford and T. Gonser. 2001. Interstitial aquatic fauna of shallow unconsolidated sediments, particularly hyporheic biotopes. In: H. Wilkens, D.C. Culver and D.F. Humphreys, eds. *Ecosystems of the world: Subterranean Ecosystems*. Elsevier, Amsterdam.

Wiedemeier, T.H., H.S. Rifai, C.J. Newell, and J.T. Wilson. 1999. *Natural attenuation of fuels and chlorinated solvents in the subsurface*. Wiley.

Winter, T.C. 1978. Numerical Simulation of Steady State Three-Dimensional Groundwater Flow Near Lakes. *Wat. Resour. Res.* 14(2): 245-254.

Chapter 6

CARBON ENERGY FLOW IN A FLOODPLAIN AQUIFER ECOSYSTEM

ABSTRACT

We developed an energy budget for the hyporheic invertebrate community of a large floodplain aquifer, including the production and respiration of invertebrate and microbial communities. We also estimated loadings of carbon inputs from rivers, soils, and buried organic matter, as the three primary energetic drivers of the groundwater ecosystem. Our budget is founded on an extensive hyporheic invertebrate population dataset, closed chamber invertebrate respirometry, an annual cycle of community respiration measurements, mesocosm and microcosm experiments, stable isotope analysis and invertebrate gut contents. The invertebrate respiration scaling exponent was 0.474 (+/- 0.068 95% CI) across six orders of magnitude in body mass, significantly lower than ¾ power scaling predicted by metabolic theory. Cyclopoid copepods dominated invertebrate production, followed by the harpacticoid *Bryocamptus hiemalis*, *Stygobromus* amphipods, and amphibiont stoneflies. Invertebrate community production ranged form 20.9 to 4200 mgC/m^3 sediment/year, with a U-shaped response to mean dissolved oxygen revealing high production at both low and high oxygen concentrations. Production declined exponentially with depth for most sites. However, there was an exponential increase at the oxycline below low DO areas leading to the oxycline supporting the highest levels of production in the aquifer. Aerobic microbial community production ranged from approximately 1200 to >2000 mgC/ m^3 sediment/year. Similarly to the invertebrate fauna, the microbial community also exhibited a U-shaped production curve to oxygen concentration. System RQ ranged from ≈ 0 to 9.5, indicating a significant contribution of anaerobic production to system energy flow. Invertebrate stable carbon isotope signatures showed strong levels of depletion among most taxa ($\delta^{13}C$ -25‰ to -70‰), indicating a methane contribution of 10% to 99% of invertebrate energy flow. We documented multiple lines of evidence for DOC (soil, river) and buried POM carbon sources, however POM was by far the largest carbon reservoir in the aquifer at ≈ 10^8 (to 10^{10}) mg C/ m^3 sediment. Energy from POM breakdown was the only source sufficient to explain microbial and invertebrate production, as well as a steady state DOC concentration in the aquifer. These results indicate a significant anaerobic subsidy of aerobic food webs in the aquifer, probably driven by the large reservoir of buried organic matter and localized zones of anaerobic conditions.

INTRODUCTION

Raymond Lindeman, building upon the earlier concept of community economics (Thienemann 1926), was the first to systematically treat entire ecosystems from an energetics approach. Lindeman's "Trophic–Dynamic" energy budget for a small late-succesional pond (Lindeman 1942a) inspired a generation of ecologists, a handful of whom conducted system energy flow budgets for other ecosystems: a coral atoll (Odum and Odum 1955), a large subtropical springbrook (Odum 1957), a small temperate cold spring (Teal 1957), a salt marsh (Teal 1962), a small stream (Fisher and Likens 1973), fish migration in a larger stream continuum (Hall 1972), a small forest-stream catchment (Gosz et al. 1978) and a millpond (Strayer and Likens 1986). There are several things that we note from this rather complete list. First, this approach has not been applied very often. Second, it has not been attempted in quite some time. Lastly, these are some of the most frequently cited works in the field of ecology. While the reasons behind the apparent lapse in the systems energetics approach would make for interesting discussion, our purpose here is merely to apply an old but effective method in examining one of the worlds least understood ecosystems. Our system is a floodplain aquifer, the large lateral extent of the hyporheic zone within a mountain valley.

The hyporheic zone of rivers and streams, first described by Orghidan (1959), is generally considered a transition or ecotone between the channel and phreatic groundwater (Brunke and Gonser 1997). The assessment of hyporheic zone function is almost always focused unidirectionally upon the significance to surface water systems (Grimm and Fisher 1984, Valett et al. 1994, Baxter and Hauer 2000, Jones and Mulholland 2000, Pepin and Hauer 2002), or occasionally on the terrestrial zone (Tremoliers 2002, Harner and Stanford 2003, Mouw and Alaback 2003). The discovery of subsurface stonefly nymphs in highly porous floodplain sediments kilometers from the river channel (Stanford and Gaufin 1974) changed the scale of thinking, and dramatically demonstrated the large spatial extent of the hyporheic zone (Stanford and Ward 1988). We believe that large hyporheic systems such as fluvial aquifers should be considered ecosystems in their own right, rather than transitional zones. Large populations of groundwater obligate species occur in bounded floodplain groundwater, the aforementioned stoneflies being among the many specialized taxa of the hyporheic

community. This fluvial aquifer community is probably a repeatable feature among mountain and piedmont valley groundwater systems throughout the world (Stanford and Ward 1993).

Ecological studies of fluvial aquifers are almost exclusively limited to three study systems: The Rhone River in France (Dole-Olivier et al. 1994), The Lobau wetland of the Danube aquifer (Pospisil 1994, Danielopol et al. 2000), and the Flathead River System in Montana, USA (Stanford et al. 1994). Although considered impractical for subsurface systems (Danielopol et al. 2000), we demonstrate herein that the traditional study of whole system energy flow can be highly successful in explaining subsurface invertebrate communities. Fluvial aquifers represent a unique opportunity to look at population biology and systems ecology of an extreme system. Considered as a system, floodplain aquifers are isolated from direct solar energy, and are probably limited by carbon bioavailability. Among groundwater ecosystems in general, the energy inputs and mass fluxes of fluvial aquifers are likely high compared to karstic and epikarstic systems. Alluvial aquifer substrate, although heterogenous and difficult to sample, is much more uniform over large spatial and geochemical gradients than groundwater systems in fractured rock. There is also the potential role of aquifers in the still largely unexplored concept of a hyporheic continuum (Ward and Palmer 1984, Stanford et al. 1993, Ward and Voelz 1994). Fluvial aquifers are probably an energetically important feature in this continuum, and a major biogeographical link for highly endemic groundwater organisms.

We developed an energy budget for a 20 km^2 floodplain aquifer ecosystem, with a particular focus on determining the energetic drivers of the invertebrate community. We estimated the loadings of carbon inputs from the river, soils, and buried organic matter, as the three primary energy sources of the groundwater ecosystem. This paper represents a synthesis of work relating to this objective, starting with Chapter 1, an overview of dissolved oxygen systematics across a floodplain aquifer. Here we provided indirect evidence for the three potential energy sources based on spatial and temporal patterns of oxygen concentration and community respiration rate: (1) input of energy from the river, the extent of influence depending on seasonal respiration rates, as mediated by temperature; (2) possible indirect influence of soil based energy sources, through change in river stage and a rising water table; (3) concentrated patches of energy, probably

associated with buried organic matter or debris jams. In Chapter 2 we show the highly skewed distribution of buried plant detritus (POM) in the aquifer, and the potential relationship between POM decomposition and SAPOM (sediment coatings, biofilm). Chapter 3 demonstrates the invertebrate response in the context of 25 attributes of hyporheic habitat. We found that oxygen covaried with many of these attributes, while invertebrate populations had an unusual U-shaped (inverse modal) response to oxygen concentration. In Chapters 4 and 5 we used *in situ* experimental mesocosms to demonstrate the interaction between sediment, organic matter, and bulk oxygen concentrations, in turn explaining the U-shaped patterns in invertebrate density and biomass.

In addition to this previous work, we include detailed information on several smaller scale sampling efforts and experimental work not previously reported. We feel that to understand an ecosystem, especially one as unexplored as ours, this detail is an essential part of the process. These smaller details can help reduce uncertainty and add some support for our many assumptions, and are not meant as distraction. Progressively through this paper the level of detail is reduced, system properties emerge, and finally we can describe the ecosystem and its drivers in a simple yet uncompromising manner.

METHODS

Study site

The study site was the Nyack Floodplain located on the Middle Fork of the Flathead River (48° 27' 30" N, 113° 50' W), a fifth order gravel-bed river with headwaters in the Bob Marshall-Great Bear Wilderness Complex. The river channel is the southwest boundary of Glacier National Park in western Montana, USA (Figure 1a). The 12 km^2 floodplain is 8 km long and averages 1.5 km in width. The floodplain is bounded laterally by valley walls with bedrock knickpoints at both the upper and lower ends. The river along the length of the floodplain is anastomosed, with the active channel and parafluvial zone of the river tending toward the northeastern side of the valley. The more mature, orthofluvial floodplain forest and agricultural pasture is to the southwest. Over 30% of the main channel flow is lost to the aquifer at the upstream end of the floodplain and various gaining and losing reaches have been documented and modeled

throughout the floodplain (see Fig 4, Stanford et al. 2005, Poole et al. submitted). The site has been the focus of research by the Flathead Lake Biological Station for over 20 years, and additional regional and site description is offered in Stanford et al. (1994, 2005) and Whited et al. (in press).

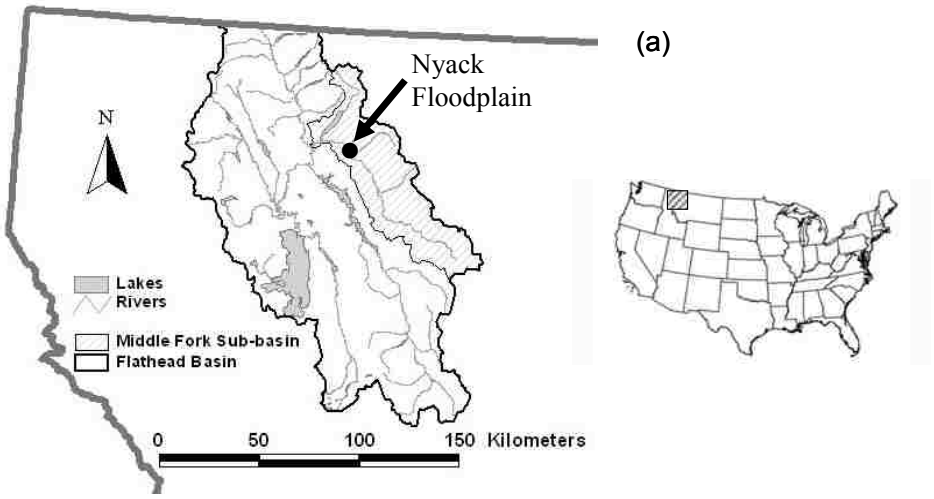

Figure 1 (a): Study site: Nyack Floodplain, Middle Fork Flathead River (MT USA).

Invertebrate Sampling, Enumeration and Biomass Estimation

We sampled invertebrates, organic matter and sediment using a hand operated diaphragm pump. Twenty-five sampling wells (Figure 1b), representing a range of hyporheic positions and terrestrial cover types across the floodplain, were sampled at multiple depths of 1 meter each. Samples were collected in a 64 µm Nitex mesh net, transferred to a Ziploc bag, and frozen in the field using dry ice. Details on well design, installation, discrete interval sampling, sample processing and correction for pump efficiency are in Chapter 3.

Samples were thawed in the lab, separated into two fractions using a 500 µm sieve, and sorted and identified at 6-12x for macrofauna and 25x for meiofauna. We measured body lengths (head to end of abdomen or last segment, excluding spines, cerci, or rami) for all organisms with a calibrated ocular micrometer (resolution 0.2 mm at 6x, 80 µm at 12x, 40 µm at 25x). We transferred amphipods to a watch glass, and individually moved them above the meniscus with a probe, where they could be measured consistently in an extended state. For stoneflies that were damaged due to sampling we measured width of head capsule and derived a head-width to length

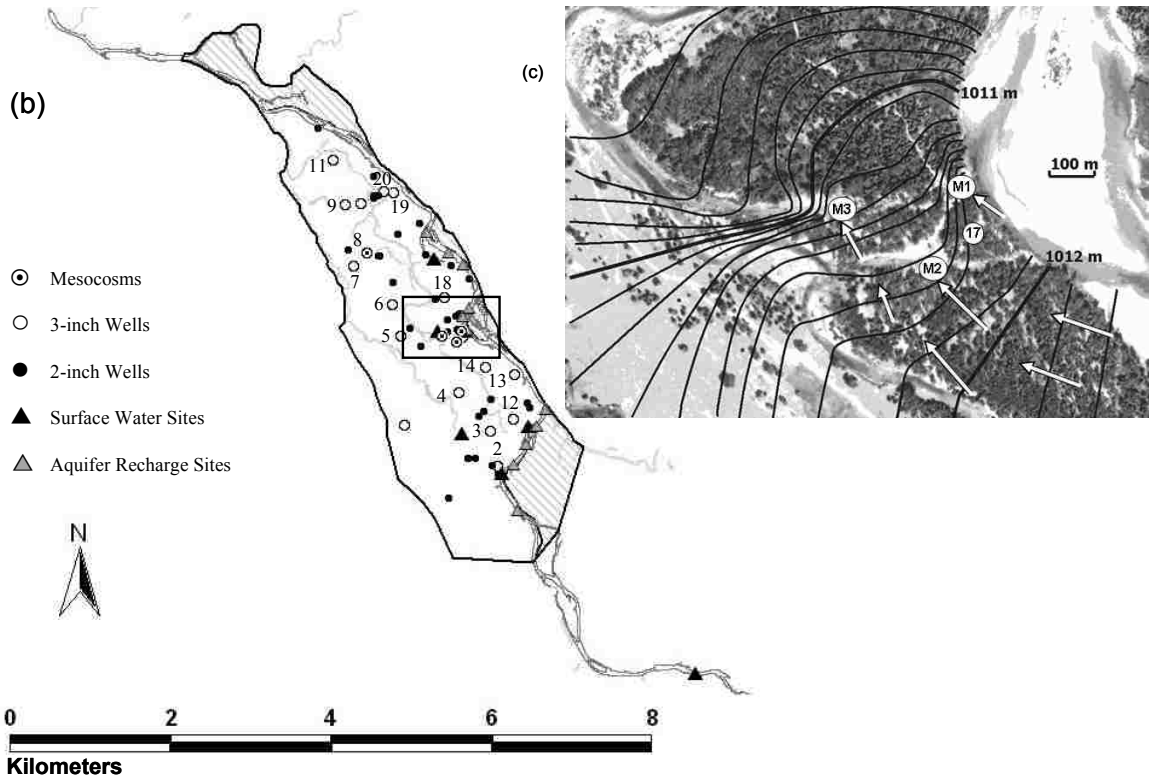

Figure 1 (b). Nyack floodplain: The main channel is furthest to the right, while smaller channel features are spring brooks and other off-channel habitats. Sampling locations include 2-inch and 3-inch wells, and surface water sampling points. Three inch well network is labeled in two longitudinal transects, from south to north (wells 2 through 11 and 12 through 20 respectively). Solid black line shows floodplain boundary used for system RQ contouring, while excluded areas (blanking) are cross hatched. **(c)**: Close-up of mesocosm locations for pairs M1 through M3, superimposed on a potentiometric map (contours show water table elevations, and arrows show direction of groundwater flow). Mesocosm sites M1 (Aquifer recharge), M2 (midgradient) and M3 (discharge zone – spring head) are shown, in addition to well #17.

relationship to account for all specimens. We measured urosome length for all copepods. While greater resolution is typically employed in studies of size distribution of single species, we opted for a lower resolution due to the large number of body length measurements conducted over 500+ samples. This resolution was typically < 6% of the size range of the dominant organisms, and represents a minor source of error. We measured widths in addition to lengths for some taxa (Chironomidae, Annelida) to improve biovolume calculations. Some rotifers could only be identified generally to the order Bdelloidea, and were assigned to one of two classes depending on whether they preserved in an extended or contracted state. Nematodes were assigned to one of three classes for biovolume calculations, based on relative body width (approximately 5-10

μm, 20-40 μm, and 40-80 μm respectively). We measured body lengths for all meiofauna in each sub-sample until we reached 30 measurements for a given taxa, after which we simply counted the remaining organisms (typically we reached this limit only for cyclopoids, nauplii, and *Bryocamptus,* and occasionally for Nematodes, Rotifers and Archiannelids).

We developed length-mass regressions for all taxa and/or classes (as defined above). For both the largest taxa and most abundant taxa (i.e., all stoneflies, amphipods, cyclopoids, the harpacticoid *Bryocamptus,* and smaller size classes of the mayfly *Ameletus*), we developed size-mass regressions directly through measuring and weighing. We pooled animals into size classes (bin sizes <10% of adult mass), transferred to tin capsules or pre-weighed foil vessels. Capsules were dried at 60 °C for 24 hours, and weighed on a Sartorius microbalance to 1 μg. We plotted weight against geometric mean of body length for each size class, and fitted a curve (generally a power function). Our most comprehensive length-mass relationships were based on abundant frozen material; however, there is the potential for some mass loss, often taxon specific depending on preservation method (Stanford 1973, Dumont 1975). We therefore collected additional material in January 2007, and developed similar regressions for fresh material (cyclopoids and *Stygobromus* amphipods). This latter step was intended not only to validate regressions based on frozen material, but also to improve estimates of mass-specific respirometry (discussed below).

For less abundant taxa, we estimated mass using biovolume (Strayer and Likens 1986, Pearre 1980, McCauley 1984). Using a Leica stereomicroscope with a SPOT imaging system (Diagnostic Instruments Inc.), we measured length and width(s) for the following taxa: *Parstenocaris*, Archiannelids, Bathynellids, Ostracods, Tradigrades, Rotifers, and Nematodes. For each individual, we calculated biovolume from organismal geometry (cyclindrical, ellipsoid etc.), and developed a length vs biovolume regression (typically a power function, but occasionally linear). We estimated dry mass assuming a specific gravity of 1.05, and a fresh to dry mass conversion of 0.15 (Strayer and Likens 1986) or 0.115 for crustaceans (Dumont et al. 1975). For comparison, we repeated this volumetric procedure and compared it to length-mass regressions for cyclopoids and

Bryocamptus. Finally, we also compared our results against published regressions (Smock 1980, Culver et al. 1985, Meyer 1989, Benke et al. 1999).

Stable Isotopes

We processed major animal taxa removed from freshly thawed June and October samples for stable isotope analysis (dual $\delta^{13}C$ and $\delta^{15}N$ analysis). Ideally we sought to represent 3^{+} wells from each category in our initial classification (i.e. cover type, hyporheic position); however, we were often constrained to sites where animals were abundant. We included some sites with lower abundance, keeping in mind the pitfall of unequal sample sizes (less total organisms in the isotopic analysis, and hence higher potential error do to individual variance, especially with the more mobile macrofauna). Samples were processed from both the 1^{st} and 2^{nd} meter depth intervals where animals were abundant, or we combined intervals where organisms were less abundant. We also treated separately organisms from the oxycline intervals for sites with orthograde oxygen profiles (transition zone between low and high oxygen - 2 sites).

Macrofauna included the amphipod *Stygobromus*, amphibiont stoneflies *Paraperla*, *Kathroperla*, *Isocapnia* spp and *Perlomyia*, and a limited number of the dipteran family chironomidae and the mayfly *Ameletus*. We also processed additional stoneflies collected in 2004 during well sampling, as adults or mature nymphs emerging from wells. Sample size for macrofauna was generally 5-10 organisms, although occasionally as few as 1 for mature stonefly nymphs, or more than 200 for the more abundant amphipods. Macrofauna were removed from thawed samples, quickly rinsed in DI water, transferred to glass vials and dried at 60 °C for 24 hours. Since sample material was small and much material is lost during milling, samples were ground by hand within the glass vials, using a small blunt spatula that was acid-washed, DI rinsed and dried with compressed nitrogen. We transferred 600 to 1200 μg of material to 5x7 mm tin capsules, weighed to the nearest μg using the Sartorius microbalance. For most amphipod samples, we processed two tin capsules, the second was acidified directly inside the capsule to remove inorganic carbonates. Since sample sizes were generally small, we found that acidification in the glass vials made it nearly impossible to recover enough material to transfer to tin capsules. We added one drop of 0.1N HCL to the second tin after

weighing. Visual observation of acidification trials indicated that carbonate was removed within 1 minute (bubbling ceased), after which we added 9-10 drops of DI water for dilution, and re-dried material at 60 °C. Because acidification resulted in brittle containers, we placed the acidified and dried capsule in a larger 7x9 tin capsule before final compressing and shipping for analysis (^{13}C single isotope). We developed a correction for amphipod samples that were not acidified (due to small sample size) based on a linear regression of untreated vs. treated subsamples.

For meiofauna, we processed cyclopoid copepods (combined taxa *Acanthocyclops* spp and *Diacyclops* spp), and a limited number of *Bryocamptus* harpacticoids and Bathynellaceae crustaceans. A large number of individuals, generally 50-200, were required due to the very small individual mass (1-10 μg). Additional processing steps were required to remove sediment and attached particulate organic matter from the animal material. We initially transferred individuals to a watch glass with sample water, hand picked organic matter from any body attachment using forceps, and removed remaining organic matter using a small pipette. This was followed by a series of dilutions with DI water to minimize external contamination of the specimens. The concentrated animals were then transferred to a tin capsule using a pipette, dried at 60 °C for 24 hours, and weighed and processed as for macrofauna. All samples were processed by UC Davis Stable Isotope Laboratory for dual analysis, and reported as per mil difference from PDB belemnite ($\delta^{13}C$) and atmospheric nitrogen ($\delta^{15}N$).

We processed DOC and POC from various sources on the floodplain to establish $\delta^{13}C$ and $\delta^{15}N$ end members for the invertebrate food web. Water extractable DOM (Baker et al. 2000, Chantigny 2003) was obtained from soil columns, collected using a 20cm PVC soil core (8" nominal, with beveled edge, Figure 2). The corer was driven into soil with a sledge hammer to a depth of 50 cm, extracted intact using a shovel, and capped with a PVC hub fitting. The base of the hub was modified with a ¾" threaded nylon elbow fitting and barb followed by attachment to flexible tubing functioning as a drain. Three replicate cores were collected in September-November 2005, from 2-3 sites of each of three cover types (pole cottonwood, mature conifer forest, and parafluvial gravel bar). We closed the drain and added 5 liters of DI water to the top of each core, which was sufficient to saturate the soil (percolating and removing air, but with no

standing water). After incubation under field conditions for 24-48 hours, we opened the drain and collected leachate in an acid-washed 150 ml erlenmyer flask. Specific yield varied among cores, but generally 50-150 ml was collected. The three replicates were pooled for each site, and a 40ml sub-sample was filtered in-line with a 60ml syringe (Whatcom 0.7 μm GFF) and transferred to a borosilicate septum vial.

We collected DOC from the main channel using a syringe and in-line filter as above. River samples were collected during base flow and flood pulse; May, August and October 2004, and May, September and October 2005. We also collected river DOC and groundwater DOC with greater frequency, tracking through the snowmelt, rising limb and flood pulse in 2006. We collected samples using the syringe and filter as above, from one main channel site and three mesocosm sites (see Chapter 3) and two depths (five total groundwater samples per event – one site is limited by a shallow well). We collected these samples approximately every two weeks from Mid-March through early May 2006. All samples were preserved with 0.5ml saturated $HgCl_2$, and shipped to Colorado Plateau Stable Isotope Lab for ^{13}C DOC and DIC isotope analysis.

Coarse and fine particulate organic matter was taken from October well samples. POM samples were limited to 10 sites where organic matter was high and all animals could be reasonably removed. Sediment organic matter (SAPOM, including biofilm, cells, and sediment coatings) samples were processed for all 25 sites, and 1 to 4 depths, using elutriated sand. Detailed methods for extracting and processing POM and SAPOM for stable isotopes are in Chapter 2.

Gut Contents

We examined gut contents of major taxa (*Stygobromus*, *Paraperla*, *Isocapnia* spp., Cyclopoid spp., Chironomidae). We used specimens from representative well sites (aquifer recharge, discharge, low oxygen zones) collected in 2003 and preserved in 95% ethanol. We used the alcohol preserved samples because we were concerned that frozen material collected in 2004 would produce unrealistic results, since frozen animals are not fixed immediately, are concentrated to unnaturally high densities in the sample containers and thus results may be influenced by within container predation or evacuation prior to freezing. We dissected whole guts of macrofauna following Cummins (1973), although in

some cases we were able to directly disperse and mount gut contents on glass slides instead of collecting on gridded cellulose filters. Meiofauna (copepods) were slide-mounted whole in glycerin, as groundwater fauna were usually semi-transparent and did not require clearing. We conducted a qualitative visual estimate of the % composition of major contents, including amorphous detritus, mineral sediment, animal fragments, fungal hyphae, and plant material. We used this qualitative approach because most (typically >95%) of all gut contents consisted of amorphous material and mineral sediment. While the latter may have organic matter coatings (SAPOM, see Chapter 2), it was not feasible to estimate the SAPOM organic matter fraction by way of biovolume.

Respirometry

We conducted closed-chamber micro-respirometry on hyporheic *Diacyclops* and *Acanthocyclops* copepods, the stygobiont amphipod *Stygobromus*, and the epigean mayfly *Ameletus*. We used a multichamber system manufactured by Unisense Inc., consisting of a retractable picoelectrode (OX-MR, Unisense Inc., Revsbech 1989) and specially designed glass chambers 500 µl and 1000 µl. The chambers had removable ground glass stoppers and capillary pore (0.7x13mm) to allow insertion of the electrode (Bang et al. submitted). Eight chambers were mounted in a rack, allowing for synchronous and repeated respirometry measurements on replicated chambers. The apparatus includes a small magnetic stirring mechanism, PA 2000 picoammeter, and software interface (MicOx). The chamber volume was calibrated to the nearest µl by weighing (water filled chambers minus dry chambers), ensuring that chamber-stopper pairs were conserved among trials. All trials were conducted with the rack, chambers, and probe continuously submerged in a temperature bath. We used two-point calibration for the microsensor. Zero oxygen was calibrated using a special calibration chamber consisting of a 2 ml glass vial and stopper similar to the organismal chambers, but with the stopper modified with a semi-permeable polyethylene chamber. The inner chamber was slightly longer than the extended microsensor allowing the sensor to fit inside the larger glass chamber. The outer glass chamber was filled with 0.017 M $Na_2SO_3^-$, while the inner chamber was filled with autoclaved de-oxygenated water (see below). We allowed 2 hours for zero calibration (Note: the chamber holds zero oxygen for several

days). The second point calibration was with the sensor retracted and within the temperature bath at O_2 saturation for 5 °C and local barometric pressure, which was verified with a YSI 550A dissolved oxygen meter, Yellow Springs Instruments).

Organisms, sediment, and organic matter along with several liters of excess well water were collected from 4 wells between early February and late March 2006. Samples were transported to the lab and refrigerated at 4 °C. Prior to respirometry, we separated a few representative organisms with a pipette and placed them in glass vials filled with filtered well water for a minimum of a 24 hour starvation period. All respirometry trials were conducted at 5 °C, which was reasonably close to all of the well temperatures at the time of collection, which is also close to mean groundwater temperature for the respective wells (6.1-6.9 °C). We then conducted respirometry measurements on 3-6 organisms per trial with each specimen in individual chambers. Each trial was conducted at three oxygen concentrations (approximately 1-3, 4-6, and 7-10 mg/l O_2). Oxygen concentration per trail was more continuous than categorical due to the difficulty of setting precise oxygen conditions in small chambers, and because of biological oxygen demand of the organism over the course of the experiment. We used filtered well water (Whatcom 0.7 μm GFF) as the respirometry medium. All chambers, transfer syringes and stirring apparati, and two 150 ml vials filled with filtered well water were autoclaved prior to the experiment. The two vials were then partly submersed in the temperature bath. One was aerated for 20^+ minutes with an aquarium aerator to achieve saturated O_2 conditions. The second was aerated with reagent grade nitrogen gas to achieve a zero O_2 concentration. We then filled glass syringes with either the no or saturated oxygen water, and injected either into respective chambers to achieve final O_2 concentrations of approximately 2, 5, and 8 mg/l. Each chamber had a small glass-coated magnetic stirrer (500 ul chambers). The 1000 ul chambers also had a circular glass guard and stainless steel screen (MetNet, Unisense Inc.) to separate organisms from the stirrer. We verified that chambers were free of all gas bubbles on the stirring mechanisms or against the sides of the vial before introducing the animals.

Copepods were transferred to the glass chambers using a pipette and larger organisms using forceps. We took care not to injure the animals or dilute the chamber with additional water. We then dropped the stopper into the chambers, ensuring that no

air bubbles remained in the capillary pore. Any bubbles could usually be removed by injecting additional low oxygen water into the stopper. The remaining 1 or 2 chambers were used as blanks, mixed in the same manner, but with no organisms. The blanks allowed for correction for sensor fouling, drift, sensor oxygen consumption and potential diffusion of water into the chambers from the bath (negligible according to Bang et al. submitted). We verified that animals were alive and active at the start and end of each experiment; however, it was not possible to monitor animal activity during the experiments as they could not be observed while in the bath. We took an initial oxygen reading in all chambers, then allowed 6-8 hours for the animals to acclimate to the transfer and new oxygen regime. Following this period, we measured oxygen concentration in each chamber every twelve hours over a 36 hour period. Immediately prior to a series of measurements, we activated the stirring mechanism at low speed for one minute to ensure uniform oxygen throughout the chambers. We avoided continuous stirring due to the potential for damaging organisms and because magnetic stirring interfered with the sensor when used in the smaller (500 ul) chambers. For each measurement we used a 2 minute delay (for sensor response curve) and a 3 minute oxygen measurement (three minute running average). Oxygen consumption was calculated as the change in concentration over the sampling interval (12+/- hours) multiplied by the chamber volume and subtracting the blank. We converted respiration rates to watts, assuming a density of 1.43 g/l O_2, and 20.1 J/l O_2, and regressed respiration rate against invertebrate mass within species and across all taxa.

Respirometry was scaled to the population level using relationships established by metabolic theory (Brown et al. 2004, Savage 2004). We derived the mass scaling exponent (γ) and normalization constant (i_0) collectively across all taxa from the regression of individual biomass (M, in g dry mass) against respiration rate in watts (I), which we normalized for temperature via the Boltzmann factor: $I = i_0 M^{\gamma} e^{E/kT}$. We had no *a priori* assumptions regarding a ¾ power scaling exponent (Gillooly et al. 2001, Ernest et al. 2003, Brown et al. 2004). Instead we used the slope γ and intercept $C = \ln(i_0)$ from the above expression plotted in ln units (Brown et al. 2004). We converted standard metabolic rate to field metabolic rate using a factor of 2.5 (Savage et al. 2004). We then

estimated population respiration for each taxa using the Taylor expansion second order correction term for mass and temperature variance (Savage 2004):

$$R_{pop} = \langle M^{\gamma} \rangle \langle e^{-E/kT} \rangle \approx i_0 \langle M \rangle^{\gamma} e^{-E/k\langle T \rangle}(1+G_1 +F_1 +F_1G_1)$$

where <M> is annual mean mass of individuals within a population and <T> is mean temperature (°K). We assumed an average activation energy (E) of 0.62 eV (Gillooly et al. 2001), and a Boltzmann constant of 8.62×10^{-4} eV/K. The functions F_1 and G_1 account for population and temperature distribution respectively (equations 16 and 20 in Savage 2004). These functions require an estimate of the relative standard deviation $r_x = \sigma/\langle x \rangle$ for both temperature and mass. We calculated r_M directly from our biomass distributions, and estimated r_T from mean monthly temperature data (see Chapter 3). We converted from watts to mg O_2 as above and report data in units of mg C/m^3/year, assuming an RQ ≈ 1 for aquatic animals (Elliott and Davison 1975) and a molar ratio of 0.375. We combined cyclopoid copepods into one population due to the difficulty of distinguishing population size distribution for immature stages.

Secondary Production

Direct production estimates for each of the sites was not possible due to the mobility and non-random distribution of large organisms, low densities per well site, the difficulty in obtaining evenly spaced samples throughout the year, and the lack of identifiable cohorts for most of the taxonomic groups. We estimated population production from population respiration (Teal 1962) for each taxonomic group using equation 6 for short-lived (<2yr) poikilotherms in McNeill and Lawton (1970): log P = 0.8262 * log R -0.0948. We assumed 11 kcal/g C (Salonen et al. 1976). We also used two additional allometric scaling equations (e.g. (1) in Plante and Downing (1989), based on lake populations, and eq (3) in Morin and Bourassa (1992) based on stream populations) as secondary estimates of population production. Inputs to these equations include population biomass, mean annual temperature, and either max individual mass (eq1 - determined from our population data), or mean individual mass (eq 3 - calculated by dividing population biomass by density).

DOC Bioavailability

We estimated relative bioavailability of DOC from soils and river water using recirculating sediment chambers (Figure 2). We used 1.12 liter sediment canisters extracted from mesocosms in April and May (see Chapter 4 for details on design and sediment structure). The canisters were carefully transferred to a sterilized bucket filled with well water from respective sites, and transported to the lab (approx 1 hour) for trials. We drilled holes in the bottom of canisters to allow for recirculation and inserted canisters into 3" nominal PVC pipe fitted with a slip cap and recirculation loop (norprene tubing, Cole-Parmer Inc.). The chamber design was similar to chambers used in other hyporheic sediment respirometry (Baker et al. 2000, Crenshaw et al. 2002b, Craft et al. 2002). However, instead of a reservoir to replace water lost from sampling (e.g. an external Erlenmeyer flask), we modified the chamber to include a machined piston with o-rings, lubricated with silicon grease (Figure 2). The chamber was airtight yet collapsible or expandable to accommodate addition of treatments or removal of sample water. This design was essential due to the very low respiration rates and possible source of error from adding make-up water. We placed the chambers in a temperature bath filled with unfiltered well water maintained at 6 °C (+/- 0.1). Water to the chambers was re-circulated in an open circuit (all chambers exchanging water with the bath) ≈ 25 ml/min for 48 hours to minimize the effects of disturbance on respiration rates.

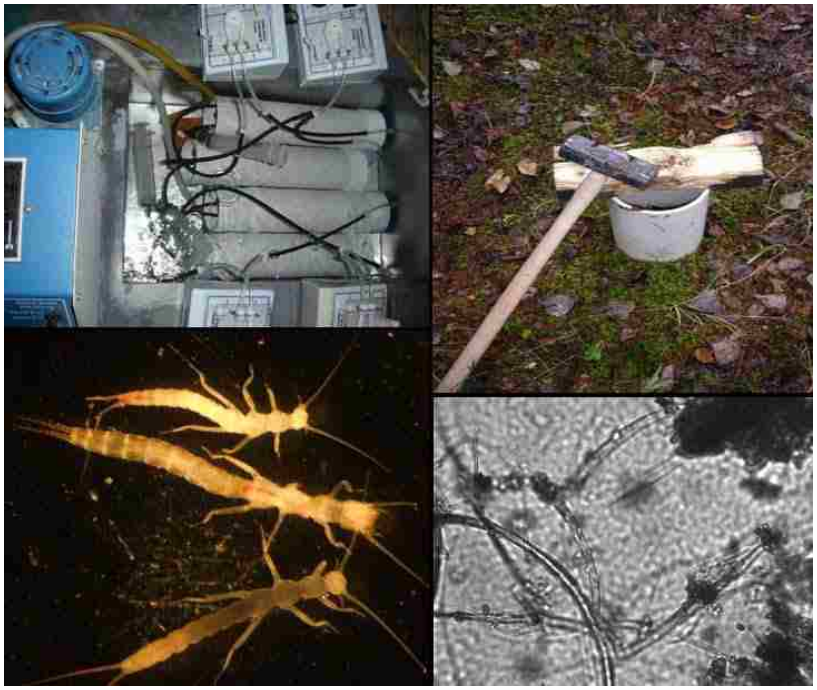

Figure 2: (Clockwise from upper left) Sediment chambers and respirometry setup for DOC bioavailability experiment; Soil core (fully driven, prior to extraction); Fungal hyphae from stonefly guts; Hyporheic stoneflies *Isocapnia crinita* (top), *Paraperla frontalis* (middle – approx 2 cm long) and *Isocapnia grandis* (bottom). Note orange amorphous material in mid and hindguts.

We conducted six trials using canisters from mesocosms M1, 2 and 3 (Figure 1c) in April and May 2006. For each trial, we ran four chambers extracted from the same mesocosm hatch (see Chapter 4), with four simultaneous treatments of DOC extracted from: cottonwood soil, conifer soil, groundwater (from respective mesocosm site, as a control), and river water (collected during the rising limb in April). Soil DOC was from pooled material collected for $\delta^{13}C$ analysis in November 2005 described above (and frozen during the intervening time). Upon initiating each experiment, we installed the piston to close the chamber. After 30 minutes of recirculation within the chamber and using a syringe, we added 60 ml of a DOC treatment type to a respective chamber making certain that any gas bubbles were removed from the syringe prior to treatment additions. We drew our initial sample after two hours, to allow for complete mixing of the treatment. Based on salt tracer experiments during preliminary trials we estimated residence time at 35 minutes with 99% mixing at about 120 minutes. During this mixing period, we monitored respiration rate using a Read-OX 4H Respirometer (Sable Systems Inc.) with 1/8" flow-through oxygen electrodes (model 8-730, Microelectrodes Inc.). We verified that there were no initial spikes in respiration that might be missed during the period of mixing; however, electrode drift prevented us from using the electrodes over the 24 hour course of the experiment. Sample water was withdrawn from chambers using a 60 ml syringe, again ensuring no air bubbles, and sample water was injected into 9 ml glass polyseal vials (Bioquip Inc). We sample water by overflowing 3 volumes and collected three replicates per treatment. These vials were fixed and analyzed for dissolved oxygen using the micro-Winkler technique described in Chapter 4, resolution ≈ 0.04 mg/l). We conducted our final sample at 24 hours, using the same procedure. Following the experiment, we measured the volume of water remaining in canisters (specific yield) to calculate total oxygen consumption.

We also sampled 40 ml of DOC during this experiment to estimate bioavailability. Previous studies do not distinguish between sorption and metabolism as confounding factors in the "uptake" of DOC. We predicted that we could separate these two mechanisms of DOC removal using an analysis of $\delta^{13}C$ in both DOC and DIC. With the distinct end members for the bath (groundwater) and the respective treatment, we could calculate metabolism from the shift in $\delta^{13}C$ DIC corresponding with a shift in $\delta^{13}C$

DOC. Unfortunately the analysis of the carbon samples was delayed for 9 months, and we consider the results unreliable. Here we report on DOC bioavaiability indirectly, via sediment oxygen demand.

Anaerobic Respiration and System RQ

We calculated inorganic carbonate species from pH and alkalinity data (APHA 1989) for each well in the network (Figure 3b) during the DO minima in late October 2004. Since inorganic carbon is primarily HCO_3^- at aquifer pH of 7.5-8, we assumed that both bicarbonate and CO_2 (aq) reflected increases from biogenic respiration and mineral dissolution. We calculated the gain in dissolved carbonate species from source water in the river, which is relatively constant and at saturation. We subtracted the carbonate potentially contributed by calcite dissolution using molar equivalents of Ca^{2+} and Mg^{2+} gain, and assume that the residual gain was biogenic. This will likely underestimate the net gain of calcite inorganic carbon due to a variety of geochemical processes such as ion exchange with iron, which in turn may precipitate with sulfides or complex with carbonates. Both will occur under reducing conditions and in the pH range of the aquifer. We also estimated the loss of O_2 between source water in the river and respective well sites. The oxygen source water is much more variable over diel and seasonal cycles (see Chapter 1), so we estimated source water DO using well water temperature and the site specific oxygen/temp relationships (see Chapter 3), (i.e. the oxygen concentration in the river for the corresponding well water temperature). This assumes that temperature is conservative, which may be reasonable for short flowpaths. But, there is more error for longer flowpaths from cumulative heat exchange with sediments.

We divided the gain in CO_2, reflected in the CO_2 and HCO_3^- species, by the uptake of O_2 as a general indication of the relative contribution of anaerobic and aerobic respiration. We call this "system respiratory quotient" (system RQ), which is essentially equivalent to RQ reported for sediment respiration by Crenshaw et al. (2002b). RQ in the traditional sense relates to organismal metabolism of various carbon substrates, while system RQ indicates an excess of anaerobic respiration in an entire sediment community. We used Surfer v7.0 (Golden Surfer Software) to contour RQ isopleths across the floodplain (see Chapter 3). We excluded areas of the floodplain where water chemistry

data was lacking, which generally included the eastern boundary of the river and mid channel gravel bars (cross-hatching in Figure 2b). We estimated system RQ for the floodplain by dividing the contoured system RQ volume by the surface area of he floodplain. This is similar to estimating mean depth in lakes.

Energy Budget

In addition to the invertebrate production and respiration calculations, we estimated the microbial contribution to system energy flow and potential pools and fluxes of dissolved and particulate organic matter. The microbial respiration data were taken from our community respiration measurements from our hyporheic mesocosms (Chapter 1), subtracting the contribution of metazoans. We estimated microbial production by rearranging the production-respiration relationship in Model II of del Giorgio and Cole (1998): $BP = 0.131 * BR^{1.64}$, where BP and BR are bacterial production and respiration respectively, in μg C/l/hr. We estimated the maximum contribution of anaerobic respiration from our system RQ calculation (RQ-1) * $BR_{aerobic}$. Anaerobic production was then calculated using the same equation for aerobic production. All calculations were in mg C/m^3 sediment per year. We estimated microbial contribution to decomposition from the microbial production, subtracting metazoan assimilation (production + respiration).

DOC inputs were estimated from mean DOC concentrations (Chapter 3). Flux was calculated from Darcy's law, assuming an average linear velocity of 13 m/d (Diehl 2004) and a porosity of 0.3 (mixed sand/gravel, Fetter 2001). We determined the minimum travel distance and residence time of riverine DOC using the annual respiration cycle from mesocosms (Chapter 1). POM and SAPOM pools were taken from data reported in Chapter 2. Energy flow from POM, via biodegradation and/or conversion to DOC (Findlay and Sobczak 2000) was estimated from the decomposition rate observed in the mesocosms experiments (0.00024 d^{-1}; Chapter 5).

We estimated energy outputs from egestion, emergence and decomposition of invertebrates. Loss from emergence/emigration of insects was assumed to be bounded by the maximum biomass achieved by stoneflies, the mayfly *Ameletus* and chironomids in the aquifer. Egestion was calculated from production, net production efficiency (NPE) and assimilation efficiency (AE) using eq. 2 in Marshall and Hall (2004). Invertebrate

production data was from our calculations based on metabolic theory and respiration. NPE was calculated for each site from production and respiration data. AE was taken from literature values (Benke and Wallace 1980) and estimated to be near the high end for detritivores (0.2). Invertebrate contribution to decomposition was estimated as total production minus loss from emergence. Qualitative trophic relations were determined from invertebrate gut contents, stable isotopes, and production data. Progressive efficiency (PE *sensu* Lindeman 1942a) was calculated as per Kozlovski (1968).

We constructed our budget to represent four representative hyporheic community types, based on patterns of community respiration and invertebrate distribution and density:

- **Type I**: aquifer recharge zones, where stygophiles occur (although not exclusively), and where respiration shows a summer pattern corresponding with temperature (Chapter 1). These areas are identified by a temperature minimum near zero (Tmin; Chapter 3).
- **Type II**: midgradient zones, usually low production, a winter respiration out of phase with Type I sites (Chapter 1) and without direct influence from the river channel. This is essentially a broad category where there are no distinct changes in invertebrate or biogeochemical gradients.
- **Type III**: Low oxygen zones, with high invertebrate density and distinct species composition (Chapter 3). The transition from Type II sites occurs at about 3-4 mg/l O_2, but is most clearly defined below 2 mg/l.
- **Type IV**: Transition zones below areas of low oxygen, in orthograde DO profiles (Chapter 1). These are areas of extremely high hyporheic invertebrate density and production, and frequently have significant populations of amphibiont stoneflies (Chapter 3).

RESULTS

Biomass Calculations

Length-weight regressions in Table 1 for meiofauna and Table 2 for macrofauna are based on a combination of volumetric methods and length mass relationships with

Table 1: Mass calculations for meiofauna, using volumetric and length-weight regressions.

Species	Max Mass (ug DM)	Meth *	Volume Estimation	Mass ** (ug DM)	r^2	n	Length (mm) min	Length (mm) max
nauplii (<0.08 mm)		Vol	$V=4/3*\pi*(L/2)^3$				0.04	0.08
nauplii (>0.08 mm)	0.187			**$m=2.5968*L^{1.6349}$** †			0.14	0.31
Cyclopoid (>0.65 mm)	25.1	Fresh		**$m=6.1475*L^{2.9929}$**	0.93	69	0.66	1.71
Copepodite (<0.65 mm)		Froz		**$m=4.366*L^{2.0875}$** ‡	0.85	151	0.31	0.64
Parastenocaris	0.048	Vol	$V = L*\pi*(w/2)^2$	**$m = 0.1329*L$**	1.00	4	0.25	0.3
Bryocamptus hiemalis	1.04	Froz		**$m = 1.717*L^{1.5254}$** §	0.82	105	0.24	0.62
Bathynellaceae	6.472	Vol	$V=L*\pi*(w_1/2+w_2/2+w_3/2)^2$	**$m = 1.1834*L^{2.6046}$**	0.97	21	0.44	1.54
Ostracoda	8.36	Vol	$V=4/3*\pi*L*w*h$	**$m = 11.59*L^{2.5566}$**	0.99	28	0.23	0.92
Nematoda 1	1.36	Vol	$V = L*\pi*(w/2)^2$	**$m = 0.063*L$**	1.00	13	0.41	1.6
Nematoda 2	1.52	Vol	$V = L*\pi*(w/2)^2$	**$m = 0.126L^{2.2722}$**	0.76	20	0.54	2.1
Nematoda 3	1.84	Vol	$V = L*\pi*(w/2)^2$	**$m = 0.2363*L^{2.757}$**	0.77	15	0.72	2
Archiannelid	1.37	Vol	$V=l*w*h$	**$m = 1.2125L^{3.0819}$**	0.67	16	0.36	0.84
Tardigrada	0.236	Vol	$V = L*\pi*(w/2)^2$	**$m = 4.5833*L^{2.9031}$**	0.73	15	0.14	0.32
Bdelloid		Vol	$V=L*\pi*(w_1/2+w_2/2+w_3/2)^2$	**$m = 1.5435*L^{2.3935}$**	0.70	20	0.160	0.280
Bdelloid (contracted)	0.498	Vol	$V=L*\pi*(w_1/2+w_2/2+w_3/2)^2$	**$m = 7.9695*L^{2.4328}$**	0.69	16	0.107	0.505
Lepadella	0.154	Vol	half ellipsoid: $V = 4/3*\pi*(L/2*w^2/4)/2$	**$m = 7.5285*L^{2.4182}$**	0.90	13	0.080	0.180
Notholca	0.069	Vol	$V = 0.13(3abc+4c^3)$; b=0.65a; c=0.2a ††	**$m = 8.64045*L^3$**	ns	7	0.133	0.158
Cephalodella	0.138	Vol	ellipsoid: $V = 4/3*\pi*(L/2*w^2/2)$; b,c=0.348a	**$m = 9.9855*L^3$**	1.00	6	0.150	0.303

*** Methods include volumetric (Vol), and length mass regression using fresh (Fresh) or frozen (Froz) material.**

**** Conversion of volume to mass assumes specific gravity of 1.05, and 0.125 conversion to dry mass for crustaceans (0.15 for other taxa)**

† From Culver et al 1985

‡ Corrected by a factor of 1.25, since frozen underestimates by 20% at edge of 1.6 size class

§ Used uncorrected mass based on regression of frozen material, since it agrees with volumetric (large sizes) and nauplii (small sizes)

†† Modified from (McCauley 1984) in Downing And Rigler 1984

Table 2: Mass calculations for macrofauna, using volumetric and length-weight regressions.

Species	Max Mass (ug DM)	%Comp *	Mass (ug DM)	r^2	n	min (mm)	max (mm)	%C (sd)	C:N (sd)	n
Kathroperla perdita	21137.7		**$m = 0.0598*L^{4.1338}$**	0.96	5	8.3	23.3	0.52(0.02)	5.22(0.5)	8
Paraperla frontalis	8308.0		**$m = 0.1663*L^{3.7456}$**	0.84	27	4.6	16.6	0.50(0.04)	4.69(0.59)	121
Isocapnia spp.			**$m = 0.274*L^{3.7045}$**	0.85	44	2.2	15.0			
Isocapnia crinita	8257.0	11.5						0.51(.026)	5.09(0.65)	90
Isocapnia grandis	10287.5	31.7						0.50(0.04)	4.88(1.10)	57
Isocapnia integra	2090.2	40.6						0.47(0.06)	5.36(0.61)	29
Isocapnia vedderensis		16.2						0.49	4.52	2
Perlomyia utahensis	658.3		**$m = 0.5047*L^{3.2262}$**	0.96	22	1.9	9.0	0.54	7.67	10
Plecoptera (< 2.1mm)			**$m = 0.51975*L^{3}$ ****			0.5	2.1			
Stygobromus tritus	578.2		**$m = 3.5038*L^{2.9713}$ †**	0.87	18	2.1	4.7	0.38(0.041)	7.43(3.06)	557
Chironomidae	18.0 §		‡					0.49	5.95	41
Ameletus sp.	4085.3		**$m = 2.9847*L^{2.8918}$**	0.96	49	1.8	12.0	0.46	5.81	3

*** Per cent composition based on adult emergence data from 2002-2003 (Reid unpubl data).**

**** Estimated by fitting a volumetric equation to capnniids < 2.1mm and chloroperlids < 4.6mm: V = L*w*h; w=0.1L; h=0.33w**

† Adjusted by a factor of 1.91 due to underestimate of dry mass from frozen material

‡ Estimated from the volumetric equation: V = L*π*(w/2)2; Assuming a specific gravity of 1.05, and wet to dry mass conversion of 0.15

§ Calculated from average weight of all pupae collected

fresh or frozen material. For length mass regressions, we had much more material available to cover a far greater range in size classes, and we corrected these regressions with data from fresh (unpreserved) specimens. We found that in some cases frozen material (in some cases stored frozen up to 1 year), sometimes underestimated mass determined from volumetric approaches, fresh material, and published regressions. Cyclopoid weight was 20-60 % lower (greater error for larger size classes) and *Stygobromus* mass was 50-55% lower using frozen material. For copepodite copepods we applied a 20% correction to compensate for small size classes below of fresh material regression. For *Stygobromus* we applied a 55% correction for out frozen material regression, which otherwise included a much larger range in size classes. We used uncorrected regression from frozen material for the harpaticoid *Bryocamptus* because it agreed well with volumetric estimates of mass. We do not know the potential underestimate of stonefly mass from frozen material, and our length-weight regressions for stoneflies were somewhat lower than regressions for the most closely related taxa (family Capniidae and Chloroperlidae, Benke et al. 1999). Mass loss from various preservation methods is variable, and probably taxa specific (Stanford 1973, McCauley 1984). Most regressions are based on organisms preserved in formalin, and frozen material is generally assumed to be comparable in terms of minimal mass loss (Dumont et al. 1975, Campbell and Chow-Fraser 1995). We consider the possible underestimate of stonefly mass in our energy flow calculations.

Respirometry

Mass vs metabolic rate showed a strong linear trend across taxa (Figure 3, Table 3; $p<0.001$), while the scaling exponent of 0.474 (+/- 0.068, 95% CI) was significantly different from either 2/3 (Banse and Mosher 1980) or ¾ power scaling (West et al. 2004). This is possibly due to decreased metabolic rate for meiofauna (Banse 1982), and general lower metabolic rate for groundwater organisms (Hervant et al. 1998, Malard and Hervant 1999). Within taxa, scaling exponents were highly variable and the regressions were only marginally significant for all groups, except *Stygobromus* (Table 2). The normalization constant ($i_0 = 2.00 \times 10^6$) is taken from the logarithm of the intercept of the regression (Brown et al. 2004). It is slightly below the range for major organismal groups

(p=0.06), which range from 7.65 x10^6 for unicells through 2.94 x10^6 for mammals (Brown et al. 2001). Within taxonomic groups, the normalization constant is highly variable and the normalization constant for *Stygobromus* (3.55x10^9) is significantly higher than this range (p=0.018). Results were very sensitive to the assumption of activation energy, which may range from 0.41-0.74 eV among major organismal groups (Gillooly et al. 2001). If we adjust our assumed E of 0.62 eV to 0.74 eV (comparable to unicells and invertebrates) our respiration estimates fall by two orders of magnitude.

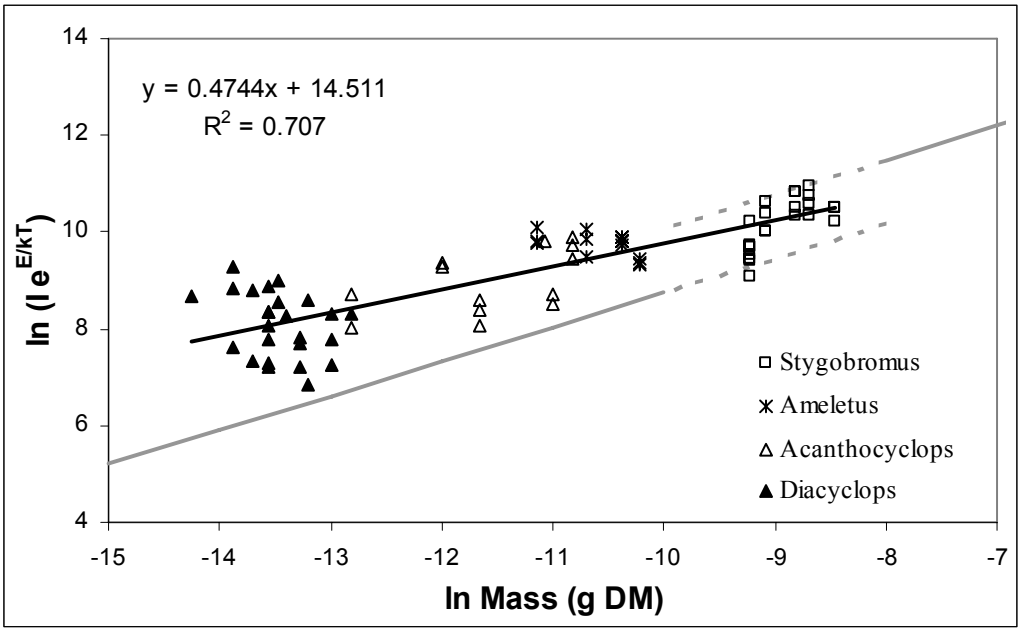

Figure 3: Mass scaled respiration rate across four hyporheic taxa (ln Watts, normalized for temperature). Gray lines show mass scaled metabolic rate for unicells and invertebrates, based on ¾ power scaling (from Brown et al 2004). Dotted gray lines are projections beyond the range of empirical data.

Species	b	a	n	r^2	p
Diacyclops spp	-0.672	-0.97	27	0.112	0.101
Acanthocyclops spp	0.484	14.56	13	0.278	0.064
Stygobromus tritus	1.321	21.99	23	0.513	<0.001
Ameletus sp.	-0.348	6.07	14	0.260	0.052
Combined	0.474	14.51	77	0.747	<0.001

Table 3: Taxon specific respiration scaling of the form ln (B) = a + b ln (m), where B is respiration rate (Watts) and m is organismal mass (g dry wt). Species specific scaling exponents (b) differ significantly from predicted 2/3 or ¾ power exponents: overall scaling exponent is approximately ½ power. Normalization constant i0 is calculated from the intercept (a; see text).

When oxygen was included in the regression model (stepwise regression with partial correlation) there was no significant effect ($p = 0.399$). We did not observe a threshold respiration response to oxygen (critical pO_2) as we expected, although we were not able to establish initial oxygen concentrations below 3mg/l for taxa other than *Stygobromus* (0.5-9 mg/l). Generally our observations indicate compensation for declining oxygen, at least over short time periods. This "regulator" strategy towards declining oxygen tension is typical for groundwater adapted organisms (Danielopol et al. 1994). Hypogean organisms generally have a lower critical PO_2 than epigean organisms (Hervant et al. 1998). Chironimids in lake benthos adapted to feeding on benthic methanotrophs have a threshold response at about 3 mg/l (Hamburger et al. 1994), which corresponds with the biogeochemical changes we have observed occurring at 3-4 mg/l O_2 (see Chapter 3).

We did not correct for the possible loss of organismal mass during the starvation and respiration period. This loss can be considerable for small organisms (Lampert 1984); however, we assumed that for groundwater organisms with low food density and low metabolic rate this was probably not a significant source of error for the duration of the experiments we conducted.

Invertebrate Production

Invertebrate production was dominated by Cyclopoid copepods (mean 54.2 $mgC/m^3/yr$, range 0.14 – 381.5), followed by the harpacticoid *Bryocamptus* (mean 22.4 $mgC/m^3/yr$, range 0.06 – 710.6). Next were the stonefly *Isocapnia* spp (mean 20.4 $mgC/m^3/yr$, range 0 – 91.6), *Paraperla* (mean 9.4 $mgC/m^3/yr$, range 0 – 84.7), and the amphipod *Stygobromus* (mean 7.9 $mgC/m^3/yr$, range 0 – 50.5). Macrofauna production was lower than meiofauna production, typically by a factor of ≈ 5. A complete list of production for major taxonomic groups and all sites is listed in Appendix 6-A. Production scaling based on respirometry produced results that are midway between the estimates based on Morin and Bourassa (1992) and Plante and Downing (1989) for most taxa (Figure 4). There is generally less than one order of magnitude difference among methods. It is apparent from the slope of our respirometry data (Figure 3) that our data predicts unusually low metabolic rates for larger organisms (i.e., above the range of our

measurements) and unusually high rates for smaller organisms (i.e., below the range of our data). This concurs with our mass scaling exponent of -0.53 for production, based on the respirometry scaling exponent (following the assumptions laid out by Dickie et al. 1987). Our production scaling exponent is significantly lower than published scaling exponents, which range from -0.17 to -0.37 (Banse and Mosher 1980, Plante and Downing 1989, Morin and Bourassa 1992, Brown et al. 2004). From the comparison of production estimates, we do find that larger taxa (*Stygobromus* and the plecoptera), respirometry predicted about 8 to 11 times lower respiration than the other methods. *Stygobromus* was included in our respirometry trials, and we presume that the lower than expected amphipod and stonefly production are probably more accurately predicted by our respiration rates.

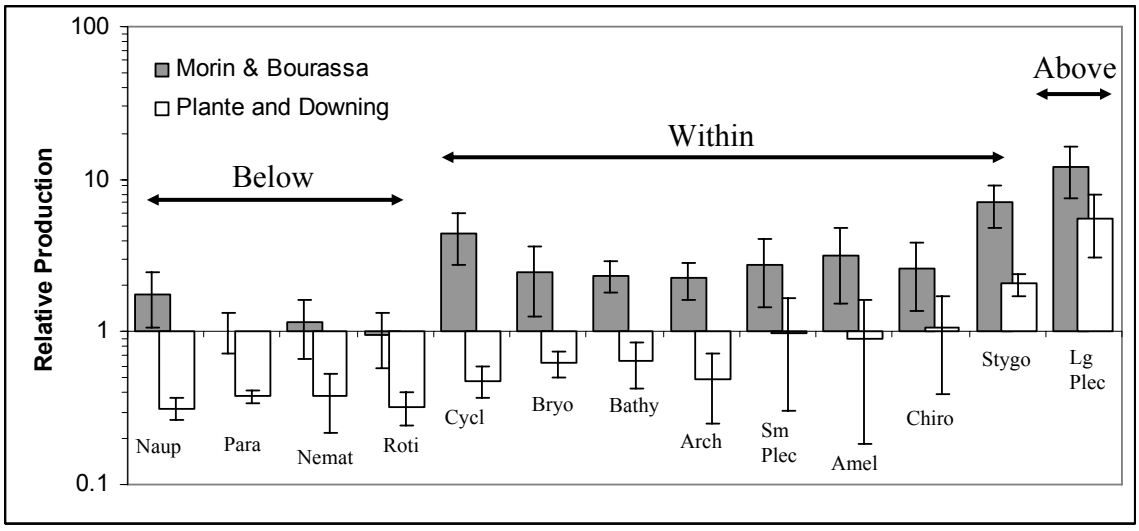

Figure 4: Comparison of production calculations for major taxa. Production scaling based on stream populations (Morin and Bourassa 1992) and lake populations (Plante and Downing 1989) are normalized against production calculated from respirometry and metabolic theory. A relative production of 10 indicates a 10 fold higher estimate than that predicted from respiration rates, while 1 indicates close correspondence. Arrows indicate species groups that are below, within, and above the range of individual mass used for respirometry trials. Taxa, arranged in order of mean mass, include copepod nauplii (Naup), the harpacticoid *Parastenocaris* (Para), Nematodes (Nemat), Rotifers (Roti), cyclopoid copepods (Cycl), the harpacticoid *Bryocamptus hiemalis* (Bryo), bathynellid crustaceans (Bathy), the polychaet archiannelid *Troglochaetus* (Arch), small plecopotera (sm Plec, arbitrarily seperated bue to inability to distinguish species, but generally <3mm), the mayfly *Ameletus* (Amel), Chironomids (Chiro), the amphipod *Stygobromus* (Stygo) and larger plecoptera (*Isocapnia, Perlomyia and Paraperla* - lg Plec)

The same concern is apparent from comparison of production estimates of the micrometazoans, which was below the range of our respirometry scaling. In this case,

there is the potential for overestimating production. Since the Plante and Downing equation from lake populations includes small metazoans like rotifers, it is more likely that our respirometry predictions are in error. For most of these taxa production is on average < 2 mg C/m^3/yr, and the effect of these taxa as a potential source of error is minimal. However, nauplii and nematode production average 15.5 and 8.0, respectively. Their contribution is significant; however, we do have good data for cyclopoid respiration. Also the lake allometry underestimates our rates by about 65%, which is not far from the underestimates of the slightly smaller micrometazoans. Epp and Lewis (1980) observed a scaling exponent of 1 for nauplii respiration, which if true for the subsurface may support our predictions (see also Riisgard 1998). For consistency in comparison across sites, we used the production rates predicted from respirometry. However, it is likely that in the smaller size classes the production predictions from metabolic rate represent the upper boundary rather than the lower.

When we compare total production for each site to the mean DO concentration, we find a familiar U-shaped curve (Figure 5). Production declines with decreasing oxygen concentration increased sharply at about 5mg/l. This is the same trend we observed with population density (Chapter 1). However, the range is reduced from about 5 orders (density) down to about 3 orders (production) magnitude of variation among

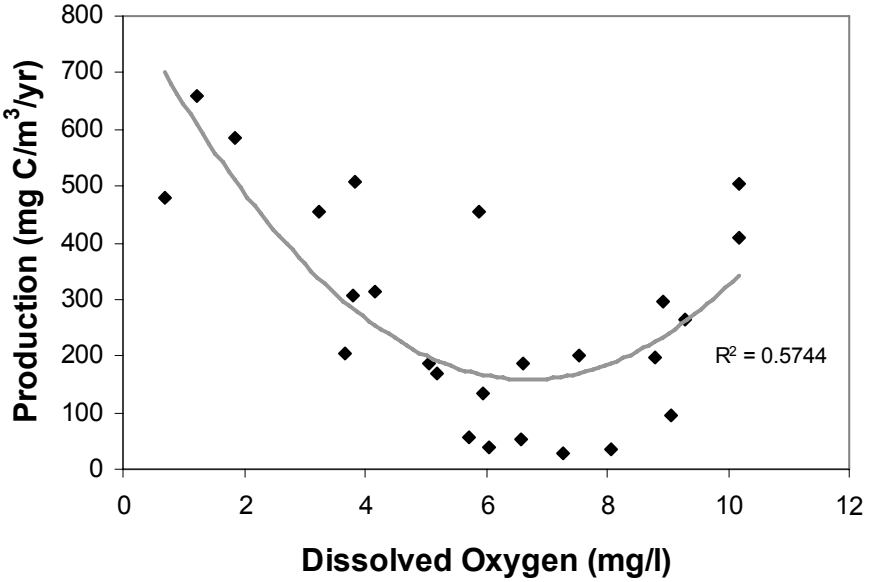

Figure 5: Total annual invertebrate production in response to mean annual dissolved oxygen concentration for the first 1 meter depth interval.

sites. When we examine vertical profiles of production with depth, we also see comparable patterns (Figure 6). Sites with orthograde oxygen profiles (solid symbols) show an exponential increase in production with depth, occurring approximately at the oxycline. Where oxygen does not change much with depth, production profiles in the parafluvial zone (i.e., high GW-SW interaction near the river channel) show somewhat straight patterns, while more remote sites in the orthofluvial zone show exponential declines in production with depth.

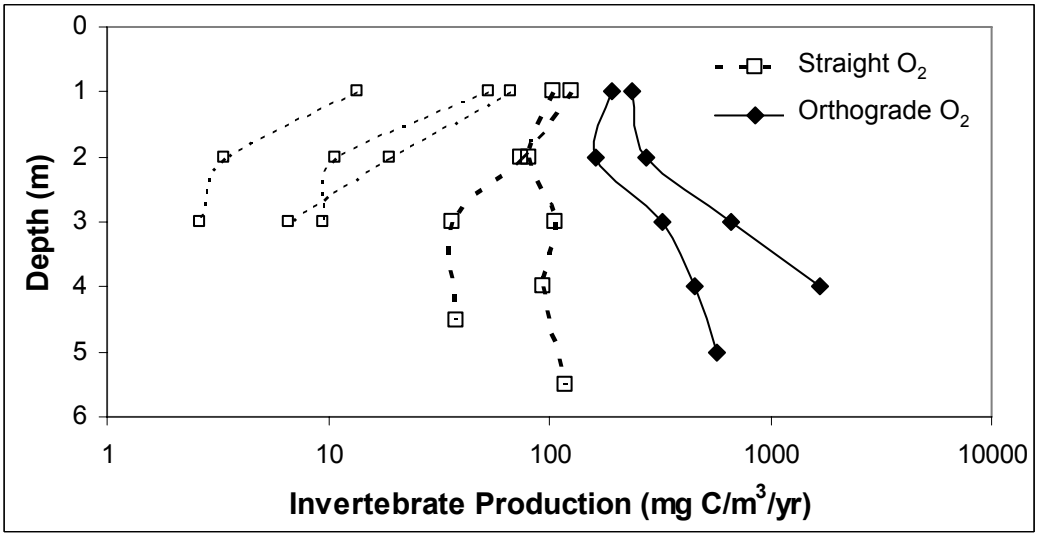

Figure 6: Invertebrate production in response to depth below the water table, for representative clinograde (increasing O2 with depth) and orthograde profiles. The x-axis is log scale. Production data was available for 4 of the six sites in Reid 2007 Chapter 3 (large symbols), and additional straight DO profiles were included for sites with sampling beyond 2m depth. The straight profile sites reflect a range of distances from the river, with the two sites previously reported (large squares) occurring in the parafluvial zone near the main channel, and the remaining sites (small squares) in older formations underlying conifer forest, and more remote from the river.

We found no correlation between invertebrate production and organic matter (POM or SAPOM). Invertebrate production shows a positive correlation with DOC (Figure 7a); however, the progression from aquifer recharge (open squares) to midgradient zones (triangles) to low DO zones (diamonds) is not a linear progression. Since DOC probably contributes little directly to invertebrate energetics, we cannot presume causation here. The more likely mechanism is indicated by Figure 7b, which shows cumulative respiration along a flowpath (calculated from temperature phase shift and DO gain for respective sites in Chapter 3) showing a positive relationship to DOC.

Therefore both invertebrate production and high DOC may be the result of cumulative metabolism along a flowpath. The relationship is not straightforward, depending on the energy resources intercepted by respective flowpaths. The respiration/DOC regression is also not a linear sequence, and the uniformly low DOC in midgradient zones may be the result of mixing and dilution.

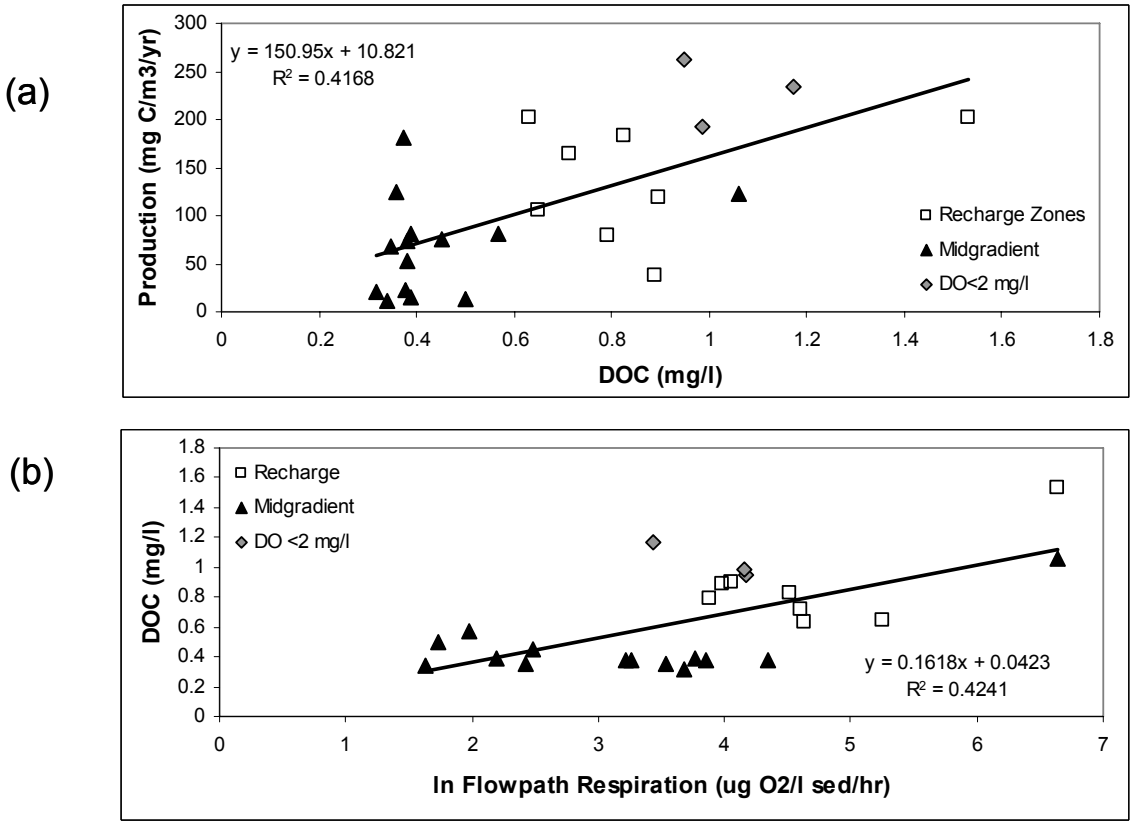

Figure 7: Relationship between community respiration, DOC concentration and invertebrate production. (a) Invertebrate production tracks positively with DOC, however the progression from aquifer recharge – midgradient – low DO zones is not a linear progression. (b) Cumulative respiration along a flowpath shows similar positive relationship to DOC. The uniformly low DOC in midgradient zones may be the result of mixing and dilution.

Gut Contents

Gut contents of the major taxa consisted primarily of mineral sediment and amorphous organic matter (Table 4). In macrofauna guts we observed fungal hyphae, and in the stonefly *I. crinita* up to 20% of material by volume was hyphae. We have also observed hyphae in cylopoid guts on separate occasions. Despite the abundance of FPOM in the field, plant material (excluding unidentifiable amorphous material) was a very

small fraction (<1%) of invertebrate gut contents. We only observed one occurrence of predation, an ostracod in the gut of the predator stonefly *Paraperla*. Otherwise there were no apparent trophic differences among taxa. Mineral sediment grain size was typically 1-10 μm for meiofauna, up to 200 μm for macrofauna. Amorphous detritus (i.e, no evident cellular structure) was typically stained orange in low DO sites (see Figure 2). Hyphomycetes were commonly mixed within this orange amorphous material.

Species	# Ind	# sites	Sediment	Amorph	Hyphae	Animal	Plant
Bryocamptus hiemalis	10	1	60	40			
Cyclopoid spp	32	4	74.2	25.8			
Chironomidae	4	1	45	50	5		
Isocapnia crinita	10	5	58.5	12	19.5		
Isocapnia grandis	4	2	52.5	47.5	7.5		0.25
Paraperla frontalis	20	5	51.8	44.4	1.1	2.5	0.2
Stygobromus tritus	14	4	58.6	41.4			
TOTAL			**61.8**	**34.1**	**2.9**	**0.5**	**0.1**

Table 4: Qualitative survey of invertebrate gut contents for major taxa (weighted average). Mineral sediment grain size was typically 1-10 μm for meiofauna, up to 200+ μm for macrofauna. Amorphous detritus (no evident cellular structure) was typically stained orange in low DO sites (visible in guts in Figure 2), and was mixed with aquatic hyphomycetes. Evidence of animal predation by the "predator" *Paraperla* was limited to a single ostracod, which was an uncommon taxa in our well samples.

In conducting our gut dissections, we observed that nearly ¾ of all *I. crinita* guts were empty except for a thick lining of cells that appeared to be attached to the gut walls. The guts of *I. crinita* were very delicate and difficult to remove intact, compared to other stonefly taxa. Conspecifics collected at the same sites had normal contents, so differences in food availability are an unlikely explanation. We did not factor this into our estimates of mean gut contents; however, there is a possibility that this species may host bacteria as endosymbionts. Although there is no clear mechanism here, this observation corresponds with the occurrence of *I. crinita* nymphs in low DO zones, and the unusually depleted carbon stable isotope signatures discussed below.

Stable Isotopes

End members for $\delta^{13}C$ for river and soil DOC fell within a narrow range of -21‰ to -26‰ (Table 5, Figure 8). There was a significant difference between river water at baseflow and soil DOC from mature orthofluvial sites (cottonwood and conifer cover

types; t-test, p<.001). At flood pulse, river DOC approaches a soil signature, which is expected with erosion and entrainment of sediment when discharge increases. At base flow the river signature is closer to periphyton, which is 16.5 (+/- 3.0 ‰) (Michelle Anderson, pers comm). Also noteworthy is that the gravel bar and regeneration stands, in the more flood-prone active parafluvial zone have intermediate "soil" DOC signatures most similar to river DOC at flood pulse (there is no actual soil development at these sites). Soil DOC signatures are similar to published values (Dawson et al. 2002).

	POM $\delta^{13}C$	$\delta^{15}N$
High DO (> 3mg/l)	-25.65 (+/- 0.68)	-2.51 (+/- 2.73)
Low DO (< 3mg/l)	-29.04 (+/- 3.49)	-0.31 (+/- 1.46)
	SAPOM $\delta^{13}C$	**$\delta^{15}N$**
June	-26.4 (-24.4 to -37.7)	4.28 (1.9 to 6.22))
October	-26.0 (-21.2 to -42.0)	3.51 (-0.81 to 6.69)
	DOC $\delta^{13}C$	
River Baseflow	-22.0 (+/- 1.09)	
River Flood Pulse	-23.7 (+/- 0.85)	
Soil	-25.0 (+/- 0.71)	

Table 5: Summary of stable isotope end members for river and soil DOC, particulate organic matter, and sediment organic matter (SAPOM: biofilm, organic coatings etc..). POM and SAPOM data from Chapter 2.

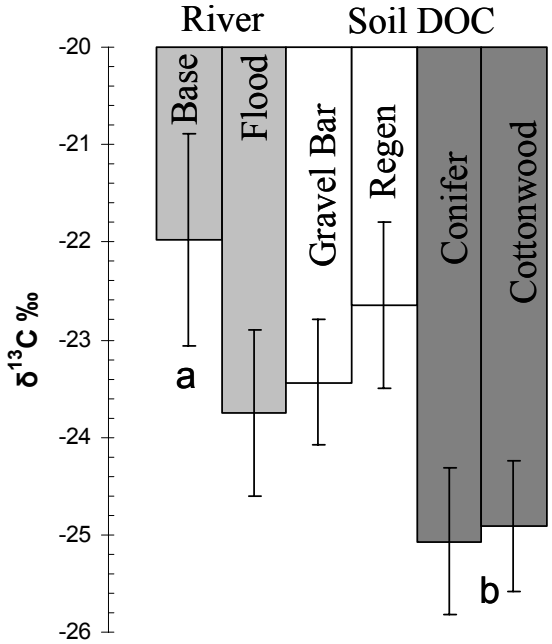

Figure 8: Stable isotope δ13C end members for river and soil DOC. Water extractable soil DOC from mature vegetation (Cottonwood and Conifer) was significantly different from river DOC at base flow (p<.001).

Table 5 also shows carbon and nitrogen signatures for SAPOM and POM (data from Chapter 2). By comparison, POM and SAPOM $\delta^{13}C$ signatures are strongly clustered around -25‰. POM in low oxygen sites a somewhat more depleted to -29‰. SAPOM signatures had a river signal (-21 to -22‰) for a few sites in October. Some of these enriched sites are in aquifer recharge zones, however a few are on longer flowpaths (Chapter 2). A few sites in low oxygen zones had more depleted SAPOM signatures ranging from -26 to -42‰, which is well beyond the range of any of the other organic carbon end members. Our lowest values occurred at the oxycline in October coincidental with peak development of the orthograde oxygen profile (see Chapter 1). Fractionation associated with methanogenesis can result in highly depleted ^{13}C values between -60‰ (heterotrophic methanogenesis) and -120‰ (autotrophy) (Whitticar 1999). Methanogenesis has not been documented in the aquifer; however, if it occurs methanotrophs are likely near concentrations of buried organic matter (e.g., buried wood jambs) that result in an interface between low and high DO. An alternative explanation for the depleted $\delta^{13}C$ signatures is chemoautotrophic oxidation of sulfate (e.g. *Thiobacillus*), which can fractionate carbon and has signatures 25‰ lighter than ambient inorganic carbon (Ruby et al. 1997). Such microbial communities are known to occur in cave groundwater (Vlasceanu et al. 1997).

Dual isotope signatures of invertebrates showed a very large range for both carbon and nitrogen isotopes (Figure 9). All taxa had mean $\delta^{13}C$ that were more depleted than local end members. Hence most animals have signatures that more depleted (often far more depleted) than any local food resources, except for SAPOM in low DO zones. The stonefly *I. crinita* had a mean $\delta^{13}C$ signature of -59.8‰, and ranged as low as -70.9‰. The stoneflies are very mobile throughout the floodplain aquifer. However the depleted signature in *I. crinita* was apparent even in pre-emergence nymphs and adults collected in high oxygen wells near the river. Chironomids from two aquifer recharge sites also had depleted $\delta^{13}C$ signatures ≈ -54‰. These apparently undescribed taxa (Orthocladiinae, see Chapter 3) may be the equivalent of the amphibiont stoneflies, only more cryptic. The amphipod *Stygobromus* had the least depleted carbon signatures of all the taxa, which corresponds with gut observations that they are excluded from low oxygen zones (Chapter 1). Invertebrate nitrogen signatures showed a trophic position

expected for the predator stoneflies, elevated 2 to 4‰ above the lowest level (*Isocapnia* spp). The detritivores (*Stygobomus* and copepods), as generalist organisms that feed on particles or microbes were approximately one trophic position above the predator stoneflies. When we look at less mobile meiofauna, we see that there are significant differences in $\delta^{13}C$ that correspond with DO concentration (Figure 10). Copepods in low DO sites had signatures similar to the possible methane end member, while high DO sites were on average much closer to the -25‰ for most of the organic carbon end members.

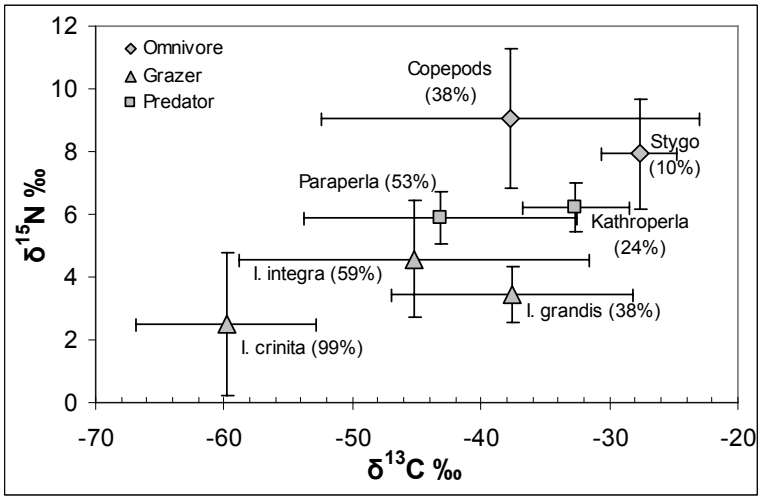

Figure 9: Stable isotope biplot for major invertebrate taxa (+/- sd). All taxa have 13C signatures that are more depleted than DOC or POM end members, and the extreme shift for some organisms indicate the possible contribution of methane to energy flow in the invertebrate food web (via methanotrophs). Per cent contribution of methane is shown in paratheses, assuming end members of -60 ‰ (methane) and -25 ‰ (DOC/POM).

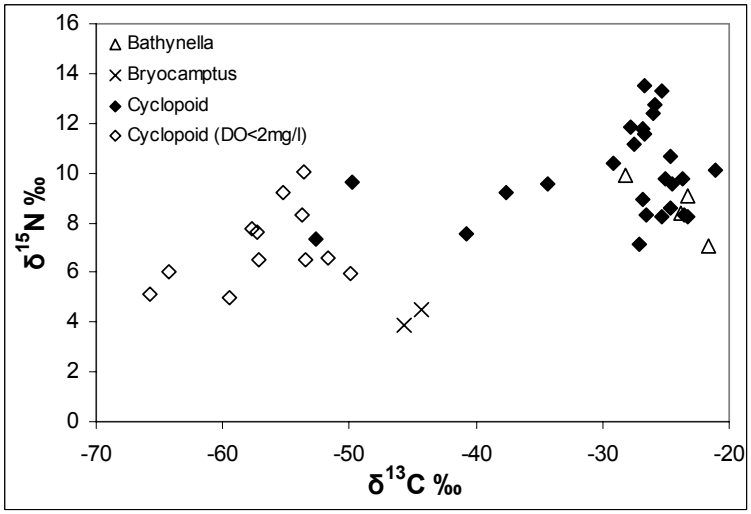

Figure 10: Stable isotope biplot for meiofauna. A significant difference in δ13C signatures as a function of mean dissolved oxygen concentration is especially apparent for these smaller and presumably less mobile organisms.

The SAPOM values (Chapter 2) are an approximation of isotopic signatures of the biofilm food base. Another method of estimating microbial isotopic signatures is from the $\delta^{13}C$ of DIC, assuming that this signature reflects respired carbon from the microbial community (Coffin and Cifuentes 1993). In Figure 11 it is apparent that this assumption is not likely valid, since the DIC $\delta^{13}C$ signatures are far more enriched than any organic carbon signature. This is most likely due to the dissolution of calcite, which will have a carbon signature close to 0‰. However when we track the DIC signature through snowmelt flood pulse cycle (Figure 11), we observe deflection in the DIC signature towards the lighter carbon signal, which indicates an increased contribution of biogenically respired carbon. Although this does not offer any direct indication of carbon sources, it does indirectly through the timing in shifts of DIC $\delta^{13}C$. Site M1 (aquifer recharge zone) shows a potential increase of organic carbon respiration in early April indicating potential riverine DOC sources for short flowpaths during the rising limb of the hydrograph. Site M2 (midgradient, low DO zone) shows an earlier shift in community metabolism, coinciding with floodplain snowmelt in late March. The shallow site (M2a)

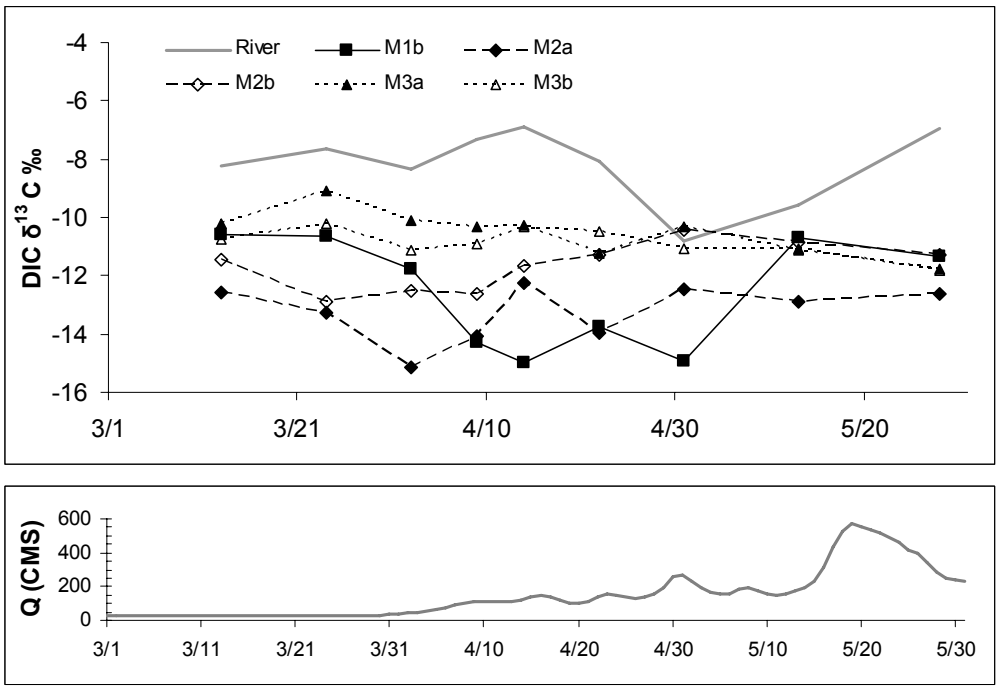

Figure 11: DIC 13C for surficial groundwater at mesocosm sites (Figure 1), tracked through the sequence of floodplain snowmelt (late march early April), rising limb (late April - May), through flood pulse (mid May). Mesocosm pairs represent an aquifer recharge zone (M1b), midgradient (M2a shallow and M2b deep) and longer flowpath near a spring head (M3a shallow and M3b deep). A decrease in δ13C (lighter DIC, downward deflection) indicates and increase in organic matter metabolism.

has a more pronounced shift than the deeper site (M2b). We expected that these trends would also be reflected in the time series of DOC $\delta^{13}C$ for these same sites; however, our samples were potentially contaminated by a cleaning solvent used by the analytical lab, and the results are not reliable. The DIC $\delta^{13}C$ data also provides an end member for estimating $\delta^{13}C$ of sulfate chemoautotrophs, if present in the aquifer. With a fractionation of ≈ -25‰ from a baseline of ≈ -15‰, these organisms would have a signature of about -40‰. This may potentially explain some $\delta^{13}C$ depletion in the aquifer invertebrates, but is not sufficient to explain the highly depleted values observed in Figure 9 and 10.

DOC Bioavailability

Respiration rates ranged from 6.8 μg O_2/l sed/hr (site M1, conifer soil DOC) to 101.5 μg O_2/l sed/hr (site M3, river DOC). The high end respiration response was comparable to the lowest response to acetate amendment observed by Craft et al. (2002). We saw no consistent effect of treatment upon respiration rates, the lowest rates per site were typically the river water DOC and the highest were from cottonwood soil DOC. However, the difference was not significant (Mann-Whitney U test, $p = 0.423$). There were far greater differences among sites (ANOVA, t-test, $p = 0.002$). The lowest respiration rates were from site M1 (Figure 1c, aquifer recharge zone), while the highest rates were from sites M2 shallow (a low DO zone), and M3 deep (near a spring head). We cannot discount the effects of time. The experiment was conducted over 4 weeks, and conditions may have changed among sites during the hydrograph rising limb.

DISCUSSION

Energy Budget

The invertebrate contribution to energy flow (respiration, production, egestion) show clear differences among the hyporheic groups (Table 6a). The sequence from Group I (aquifer recharge zones) through Group II (midgradient) to Group III (low DO zones) follows the same U-shaped pattern in Figure 5, as we expected. Group IV (orthograde DO; transition to higher oxygen) has the highest rates of energy flow through the invertebrate community, also expected from Figure 6. Net production efficiency (NPE) was the lowest for Group IV, probably due to the increased dominance of

organisms with smaller body size in low oxygen zones (see Chapter 4). The consequence of this lower NPE is a proportionally greater contribution of egested organic matter for potential recycling through the microbial food web in Group III and Group IV sites.

Group	Production	Respiration	Egestion	NPE	P/B	PE
1	341 (± 151)	322 (± 170)	2653 (± 1282)	0.53 (± 0.032)	20.3 (± 36.1)	0.029
2	169 (± 126)	149 (± 127)	1271 (± 1012)	0.56 (± 0.048)	6.0 (± 4.4)	0.023
3	575 (± 89.3)	661 (± 167)	4942 (± 1016)	0.47 (± 0.026)	7.6 (± 3.9)	0.015
4	2112 (± 1408)	3221 (± 2566)	21331 (± 15887)	0.41 (± 0.026)	8.8 (± 4.0)	

Table 6 (a): Summary of invertebrate contribution to system energy flow for 4 major hyporheic groups: (1) aquifer recharge; (2) midgradient; (3) low DO; (4) oxycline (see text for more complete description). Production, respiration and egestion are in units of mg C/m^3 sediment/year (+/- 1 sd, calculated across sites within each group). NPE = net production efficiency; P/B = community production to biomass ratio; PE = progressive efficiency (*sensu* Lindeman 1942).

	Aerobic			Anaerobic		Total
Group	Production	Respiration	System RQ	Production	Respiration	Decomposition
1	1928 (± 440)	8406 (± 3416)	2.0 (± 1.4)	3688 (0-14900)	8541 (0 - 29300)	4953
2	1206 (± 612)	6314 (± 4177)	1.8 (± 0.9)	1388 (0-4966)	5211 (0 - 15000)	2276
3	2016 (± 1094)	8637 (± 5950)	5.8 (± 3.2)	30122 (11597-66758)	41247 (25000 - 73000)	30902

Table 6 (b): Microbial contribution to system energy flow. All rates are in units of mg C/m^3 sediment/year (+/- 1 sd, calculated within each group over the annual cycle). Ranges are shown for estimated anaerobic production and respiration. Mesocosm respiration data is from Chapter 1, based on mesocosms 1, 2 and 3 (Figure 1c). Mesocosm site M2 represents a low oxygen zone (group 3), however we lack data for the oxycline below a typical low DO zone (group 4).

Group	SOURCE	SS mass (g/m^3)	Loading (g/m^3/yr)
1	**Groundwater DOC**	0.866 (± 0.287)	1233 (± 408) *
2		0.445 (± 0.189)	634 (± 270) *
3		1.035 (± 0.121)	1473 (± 172) *
	River DOC	0.831 (+/-0.29)	1576 (+/-550) §
	Cottonwood Soil	11.8 (± 17.6)	0.228 (± 0.338) §
	Conifer Soil	9.3 (± 4.5)	0.178 (± 0.087) §
	POM	$1.69x10^5$ (10^4-10^7) **	$1.22x10^4$ (10^3-10^5) †
	SAPOM	$2.97x10^4$ (±1.2 $x10^4$) ††	(>$6x10^4$) ‡

*** DOC loading = [DOC] * v * 1 m^2 * n; n = 0.3; v = 13m/d**

**** POM median across all sites**

† Based on decay rate of 0.00024 per day

†† Concentration extracted from core, shown on m3 basis for comparison

‡ Assuming turnover ≤ 6 months

§ Assumes one time pulse of a time span ≤ 1 week

Table 6 (c): Carbon inputs to system energy flow, including groundwater and soil DOC, and POM/SOM. Shown are steady state concentrations (SS mass) and loadings (rates calculated as indicated by symbols). All units are in gC/m3 sed/year (vice mg C in Table 8a and 8b). Parentheses indicates +/- 1 sd (over annual cycle for groundwater DOC, and among site variation for soil cores and SOM) or range (POM).

We note that lacking direct estimates of organismal and community NPE, this pattern would not be apparent if we assume P/R is not different from 1 (Humphreys 1979). Community production to biomass ratio was lowest in Group II, which are the lowest energy sites. Odum (1969) predicted that mature ecosystems will express less energy flow per unit biomass (lower P/B). Group II sites were typically in older formations with conifer cover types, hence older, more stable, energy depleted sites might be considered mature groundwater systems.

Microbial energy flow is based on respiration estimates from in situ mesocosms (Chapter 4), which have limited replication but much more comprehensive coverage over the annual cycle. Again we see the general U-shaped response curve with high rates in Group I and Group III, and lower rates in Group II (Table 6b). System RQ contouring across the floodplain shows a pattern similar to oxygen contouring (see Chapter 1), with a general increase in RQ along the axis of the floodplain, and distinct hot-spots of high RQ. Average system RQ across the aquifer is 3.5 in October, suggesting that there is 2.5 times as much anaerobic respiration as aerobic. Since we performed this calculation only for October, the RQ estimate is probably a maximum value for the annual cycle. Group III sites had the highest system RQ (5.8), which translates to anaerobic respiration and production rates that are an order of magnitude higher than Group I and II sites.

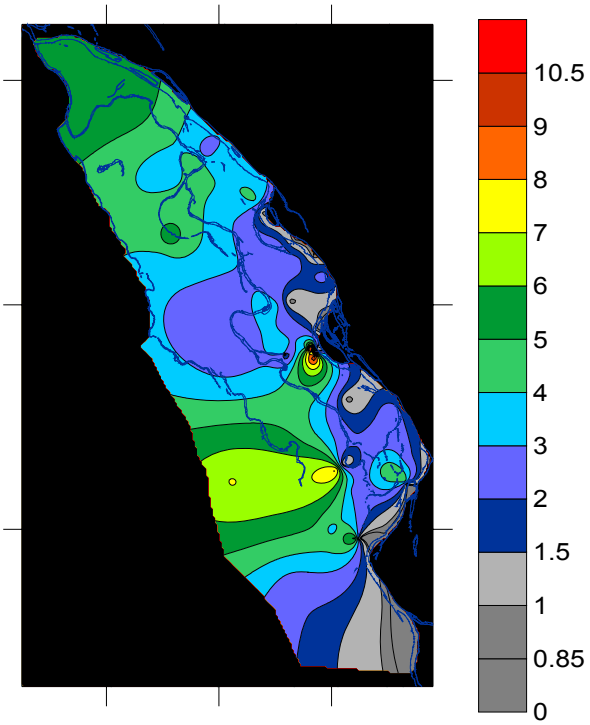

Figure 12: System respiratory quotient (Sys RQ), contoured across the floodplain aquifer for the top 1 meter depth interval, October 2004. Sys RQ is calculated as a ratio of the gain in inorganic carbon (primarily HCO3-) divided by the loss in Oxygen for every well site, with the river at saturation used as the source concentration (see text). An RQ>1 indicates potential anaerobic respiration. Note that zones of high Sys RQ correspond with low DO hotspots documented in Chapter 1.

Our organic matter estimates are reported in terms of percentage carbon by weight of fine sediments. This also leads to an overestimate of volumetric organic matter density, since much of the aquifer consists of mixed sand and gravel with occasional deposits of more sorted sand-sized material. Also, silt/clay layers, which are uncommon but may dominate below 10 meters at the downstream end of the floodplain (Diehl 2004), may harbor much more organic matter than reported here. Such formations are probably difficult to extract via well pumping. We estimate that fine sandy sediments may comprise roughly 10-40% of the aquifer, the high end being roughly the porosity of well sorted gravel with sand potentially forming the matrix.

The organic carbon POM pool (1.69×10^5 gC/m^3, range 6.4×10^4-1.3×10^7) is clearly greater than the SAPOM pool (2.97×10^4 gC/m^3) by an average of 1 order of magnitude. This is a low estimate, considering the assumption of 10% sand and not accounting for larger wood particles. Conversely, smaller material may be more available for decay. Based on a general estimate of POM decay in the aquifer of -2.4×10^{-4} per day (Chapter 5), the POM pool may supply 1.22×10^4 gC/m^3/year. Considering the patchiness of particulate organic matter, local contributions of POM to energy flow can be 3 orders of magnitude higher than this average loading rate. By comparison, the DOC concentration in the aquifer is on average 0.65 mg/l (+/- 0.32), which is slightly less than DOC of the source water (main channel). Assuming an average linear velocity of 13 m/d (Diehl 2004) and a porosity of 0.3, annual loading of DOC is approximately 926 gC/m^3/year (+/- 427), which is far lower than the potential carbon loading from the POM pool. This potential energy source may be analogous to a battery, storing energy for aquifer food webs for long periods of time and contributing to the stability of groundwater ecosystems (Wetzel 1995).

Carbon inputs from DOC also follow the U-shaped pattern (Table 6c) in terms of both average concentration and annual loading. In comparison, the pool of buried POM and SAPOM are very large potential energy sources compared to DOC inputs. The loading of POM (rate of loss of POM, either complete metabolism or loss via DOC) is clearly the largest potential input to system energy flow. Soil DOC is probably a minor contribution to system energy flow, as its steady state concentration, based on maximum

mass released from soil columns and potential loading, are a very small fraction of the annual DOC loading and POM reservoir.

A sample energy budget for Group I sites illustrates the relationship among the invertebrate energy flow, microbial energy flow, and organic matter loading (Figure 13). We point out that with respect to DOC, this sample budget reflects site specific inputs for representative regions of the aquifer. It is not intended to reflect whole aquifer inputs of riverine DOC. This scale of analysis would require scaling across the aquifer and modeling (Poole et al. in prep), which is beyond the scope of this paper. Degradation of POM and turnover of SAPOM cannot be distinguished from loading of DOC, and DOC in turn may be either metabolized or sorbed or incorporated as SAPOM (including biofilm).

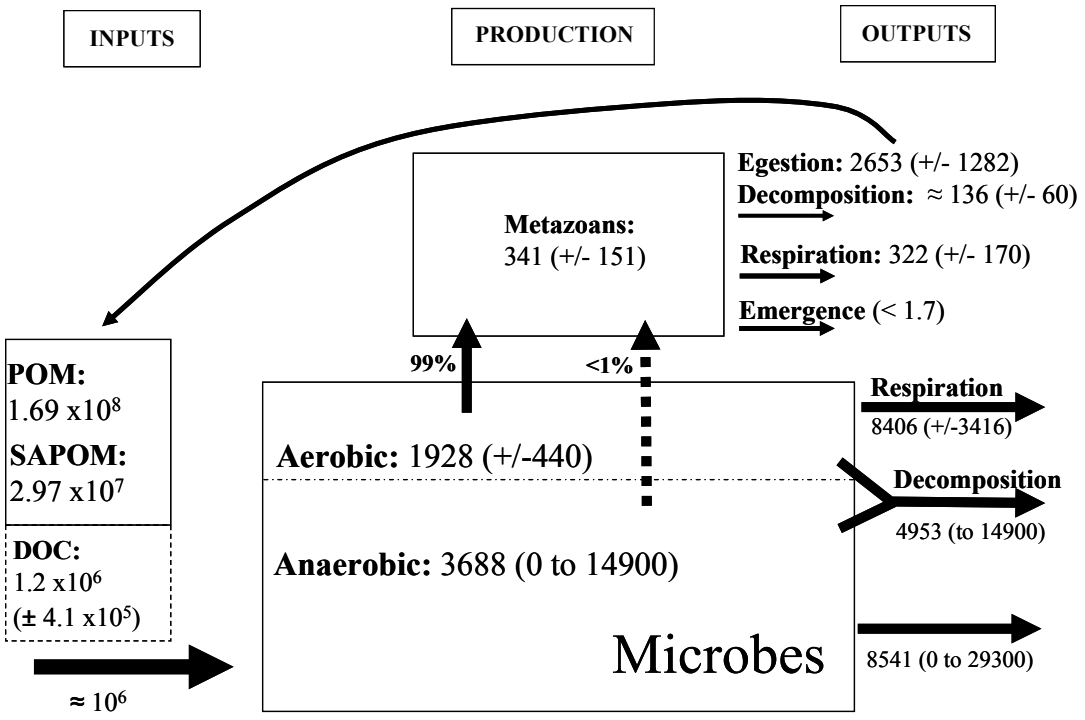

Figure 13: Sample energy flow diagram for group I sites, using data from Table 8. Shown are rates (production, fluxes, or decomposition), with POM/SAPOM pool shown for comparison. All units are in mg C/m3/year. Trophic transfers are shown as percentage of production contributed by anaerobic vs. aerobic energy (estimated from stable isotopes).

From this budget there is potentially two orders of magnitude more organic matter inputs, via POM degradation and or DOC loading, than energy flow through invertebrate and microbial communities in Group I and II sites. For group III sites there is still a 10-

fold excess of organic matter inputs to system energy flow. We do not have an estimate of energy flow for the microbial community for group IV, however if it is proportional to the increase in invertebrate energy floe, the organic matter inputs should still be sufficient to account for system energy flow. Loss of energy from the system due to insect emergence is negligible. Recycling of organic matter from invertebrate egestion and detritus may contribute to microbial metabolism, however it is probably no more than 5% of microbial energy flow assuming 100% utilization.

Trophic Basis for Production

Our general conclusions on the invertebrate trophic base are that SAPOM (mineral sediment, biofilm, sorbed DOM) and amorphous material mixed with hyphae are the dominant inputs. Cummins (1973) considered mineral substrate as a potential food resource, and here it probably outweighs any advantage in mechanical damage to cellular material (Brown 1960). Consumption of lithoautrotrophs may also be a factor. Poulson (1964) reviewed work by Caumartin (1959) and Gounot (1960) showing that invertebrate richness was higher in groundwater systems with red clays as opposed to gray clays. These clays are linked to a facultative autotrophic ferrobacterium which uses iron carbonate as a substrate. Consequently there were high ferrobacteria densities on the mineral sediment. Regardless of the trophic mechanism, the isotopic signatures for SAPOM in low DO zones are the only possible end members that can explain the highly depleted $\delta^{13}C$ signatures and relatively enriched $\delta^{15}N$ of the invertebrates.

The high frequency of fungal hyphae within invertebrate guts corresponds with observations by Ellis et al. (1998) in the Kalispell aquifer (downstream from our study site). Fungi were common in wells on longer flowpaths, and fungal biovolume exceeded bacterial biovolume at some sites. They also sampled The Nyack aquifer during their study, and found a much lower contribution of fungi to the microflora at the Nyack site.

We cannot resolve the origin of amorphous material based on our work. But, we do know that plant detritus is of limited direct importance to invertebrate energy flow, except possibly in the nearly completely decomposed forms. Nonetheless, the observation that invertebrate populations are independent of POM density (Chapter 3) indicates that despite the presence of hyphae, amorphous material and plant detritus may not have a

common origin. $\delta^{15}N$ signatures for POM include amorphous material collected from low DO well sites. The POM $\delta^{15}N$ isotope signatures are too low to explain most invertebrate signatures, except for the grazer stoneflies. POM $\delta^{13}C$ signatures never approach the range of depleted values observed in the stoneflies.

It is also clear that predation is probably a limited component of energy flow in this system. We cannot reject the possibility that predation would emerge in importance when a larger spatial and temporal sample of the predator stonefly *Paraperla* is examined. We did observe that the C:N ratio of *Paraperla* declined with an increase in body size, indicating a potential increase in consumption of animal matter with size. While there is evidence that predation is a viable feeding strategy in the subsurface (Simon et al. 2003), our results correspond with the generalizations of Gibert and Deharveng (2002): subsurface communities are trophically simplified, omnivory prevailing over predation.

These trophic observations are linked to dissolved oxygen distribution in the floodplain. Only the SAPOM stable isotope end members from low oxygen zones can explain invertebrate signatures. Orange amorphous material with hyphae of uncertain assimilative value was a diagnostic feature in guts at low oxygen sites. Iron-associated bacteria may provide a facilitating role in oxygen depleted or transition zones. Examples include the ferrobacteria associated with iron carbonates described above and the iron reducing bacteria that were likely stimulated by our mesocosm organic matter amendment experiments (see Chapter 5). Adams (2006) collected stoneflies from some of the wells at our site, and found that the denitrifyiers *Pseudomonas* and *Acidovorax* accounted for as much as 51% of all sequenced strains in *Isocapnia* guts, and 20% of strains in the guts of predator stonefly *Paraperla*. The general pattern of invertebrate distribution may provide the strongest evidence for the trophic basis of production (Findlay 1995). The clumped distribution of invertebrates across the aquifer argues against general bacterial grazing as a feeding strategy. However invertebrate density and production corresponds directly with low oxygen zones, and possibly indirectly to the highly skewed POM distribution (Chapter 2). Peaks in microbial biomass and ETS-activity correspond with low DO in some stream sediments (Claret et al. 1997), and hence grazing efficiency of microbes is potentially maximized in low DO zones.

One of the strongest lines of evidence for an anaerobic trophic basis for invertebrate production is the methane isotopic signal. There is an increasing recognition of the importance of methane to lake food webs (Bunn and Boon 1993, Bastviken et al. 2003, Kelly et al. 2004), and growth in zooplankton on methanotroph cultures may meet or exceed growth in strictly aerobic cultures (Kankaala et al. 2006). Chironmids in lake benthos are adapted to waiting out periods of anoxia, subsequently showing significant population increase at the re-oxygenation during lake turnover (Frank 1982). Amphibiont stoneflies at our site occur almost exclusively in low oxygen or transition zones with peak populations during the oxygen minima in September (Chapter 3). Whether they wait out hypoxia or hover somewhere at the boundary, there is strong evidence that stoneflies selectively feed where $\delta^{13}C$ is highly depleted, and where methanotrophic bacteria are most likely to occur. Energy resources in low oxygen zones of aquifers may be the reason for stonefly migration into aquifers and thus a significant driver behind amphibiont life histories. We observed two indeterminate species of Orthocladiinae that frequent low oxygen zones tens of meters from the river channel (Chapter 3). Although data are limitied, we observed chironomids to have depleted $\delta^{13}C$ signatures. Both the amphibiont stoneflies and these two Orthocladiinid midges may benefit from an anaerobic subsidy originating from methanogenesis. Both may fill the analogous ecological niche as chironomids in lake benthos. However, the stoneflies have greater ability at dispersal and are more widely associated with low oxygen throughout the aquifer.

A less likely and as yet unexplored alternative to anaerobic subsidy, may originate from sulfur autrotrophs, which also may produce depleted $\delta^{13}C$ signatures. Mutualistic sufide oxidizing bacteria are the dominant energy pathway in hydrothermal vent invertebrates (Jannasch 1984). Similar chemoautotrophic microbial communities have been discovered in cave groundwaters (Sarbu 2000), although they are not as productive or diverse as vent communities. Our observations on the weakly developed and often empty guts of *I. crinita* warrant further investigation of potential endosymbionts.

Sources of Energy: Soil DOC, River DOC or Buried POM

Riverine DOC is a major energy source for small hyporheic systems (Jones et al. 1995). However, in our large floodplain aquifer system, the evidence for riverine DOC is

the weakest of the three potential energy sources. This was surprising, since we know that large volumes of river water are gained and lost over the length of the floodplain (Diehl 2004, Stanford et al. 2005). The theoretical travel time and distance of riverine DOC, based on the annual aerobic respiration cycle, was on average ≈ 100 meters, and ranged from 27 meters to 332^{+} meters (Figure 14). Transport of riverine DOC was lowest in the winter, higher in the spring and fall, with an outlier of extensive transport during the late flood pulse in June (>2 times the typical travel distance). Direct input of river DOC is limited to aquifer recharge zones (identified in Chapter 1). Overall we estimate that this input affects probably < 5% of the aquifer, although river DOC may be an important subsidy for some of the most energetically active parts of the aquifer (high DO recharge zones, such as shown in Figure 5).

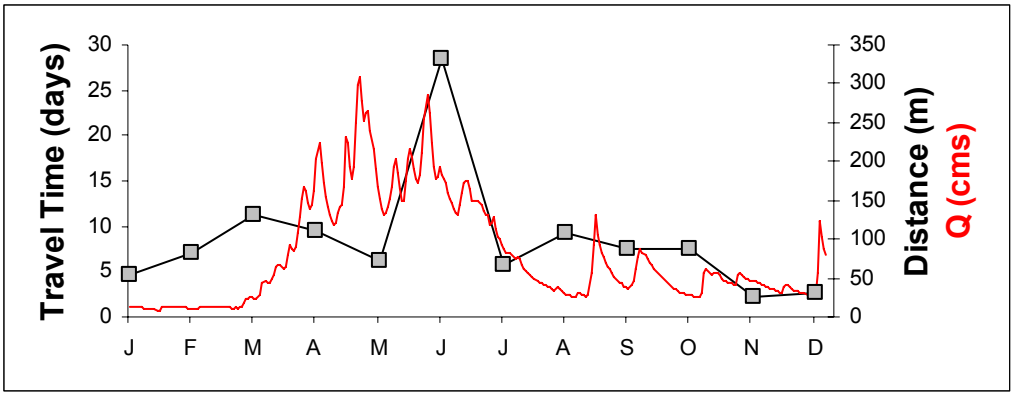

Figure 14: Metabolism of riverine DOC. Gray squares indicate maximum travel time (primary y-axis) and travel distance (secondary y-axis) of riverine DOC, assuming sole carbon source for metabolism. Respiration rate is based on maximum of 5 days of recharge zone rates, followed by midgradient rates until complete metabolism, for respective monthly intervals. Hydrograph (red) shown for comparison.

The most direct indication of riverine carbon sources is the SAPOM isotope signature. We observed a temporary shift to the river DOC signature in some aquifer recharge sites in October baseflow (Chapter 2). Failure to observe these signatures at the same sites in June indicates a high turnover rate of SAPOM (< 6 months); however due to the shift in riverine DOC signature during the flood pulse, we cannot distinguish river DOC from other carbon end members during this time period. The summer respiration cycle at mesocosm M1 (Figure 1c, aquifer recharge) suggests a strong connection to river channel productivity (Chapter 1). The connection is also supported by DIC $\delta^{13}C$ time series for the same mesocosm (Figure 11). It is not clear whether this cycle is driven by

carbon bioavailability or is solely due to temperature. The one convincing piece of evidence for a larger scale riverine DOC subsidy is the winter respiration cycle in midgradient aquifer sites (M2 and M3, Figure 1c). In Chapter 1, we speculated that in winter low temperatures in the river and aquifer recharge zones resulted in deeper penetration of river DOC. As a result, we saw that respiration rates rose in the fall and peaked in the winter at these midgradient sites (M2 & M3), corresponding with a drop in respiration in the site near the river (M1). Finally, we saw that the most common temporal patterns in subsurface invertebrate density included a peak in density in June and July following the flood pulse; although, most sites also had a second winter density peak, (Chapter 3). Time series sampling of groundwater DOC along a river recharge flowpath might provide a clearer indication of the extent of riverine DOC input, except during flood pulse.

We have not considered the transport and fate of riverine particulate organic matter, including algal cells. There is very limited evidence for transport of fine organic matter through sediments (Findlay 1995), although some transport has been demonstrated in shallow bed sediments by standpipe traps (Leichtfried 1988). Our single estimate of POM flux out of mesocosms indicates that POM transport is 2-3 orders of magnitude lower than DOC flux (Chapter 5). We did observe filamentous algae in two parafluvial wells in May and June, immediately following the flood pulse. These wells were in sites of active scour and deposition. In the Kalispell aquifer, downstream from our study site, Ellis et al. (1998) observed river diatoms in wells up to 350 meters from the main channel, and green algae and cyanobacteria up to 4800 meters from the main channel. We cannot exclude the possibility of sample contamination. We have observed that PVC wells are only semi-opaque, and enough light is transmitted through the plastic to support visible algal growth in the humid environment inside well risers.

The evidence for a terrestrial subsidy of aquifer energy flow is somewhat stronger. First, we saw significantly higher SAPOM content in shallow (1m) versus deep (2m) groundwater. The difference was only significant in June, indicating a seasonal turnover of organic matter at shallow depths, possibly corresponding with the flood pulse. We saw strong vertical gradients in both invertebrate density (Chapter 3) and production, consistent with our predictions for the effects of terrestrial subsidy. Invertebrate

population density peaked in one cluster of well sites immediately following floodplain snowmelt, which was also consistent with our terrestrial subsidy predictions (Chapter 3). DIC $\delta^{13}C$ signatures indicated a potential respiratory response to snowmelt at 1 mesocosm pair, with the strongest response in the shallow interval (mesocosm M2, Figure 11). Conversely, our bioavailability experiment showed no clear evidence of increased respiratory response to soil DOC, based on limited replication, particularly on the temporal scale. Baker et al. (2000) observed strong temporal declines in aquifer DOC and O_2 following a flood pulse, which she attributes to the region of seasonal saturation (ROSS). Our monthly well sampling did not have enough temporal resolution to document any short term spikes in DOC. We did observe spikes in O_2 following flood events (i.e. rising water table), and in one case saw a large decline in O_2 at mesocosm M1 (Figure 1c) during the pulse. But long-term O_2 trends showed a steady decline to a minimum in October (see Chapter 1). But, based on mass balance of DOC leached from soil columns, DOC loading from soils will be a very small input compared to the continuous loading of DOC in the aquifer. We suspect that there is a weak and patchy subsidy of shallow groundwater that is not obvious at the level of invertebrate populations, unless following a dramatic recharge event.

We also cannot exclude the potential direct contribution of the rooting zone to shallow groundwater. In an Australian karst stream Jasinska (1996) observed *Eucalyptus* root mats at depths of 10-18 meters. Invertebrate populations were concentrated on these mats, while root detritus and mycorhizae were frequently in the gut contents. We have occasionally observed live roots in the vicinity of the water table, and senescent roots accounted for up to 16% of POM (Chapter 2). Fresh root material rarely appeared in our POM samples except for a wetland site with very shallow depth to saturated soils. We did not observe root material in guts, although hyphae were present. We observed significant differences in invertebrate density and community structure between gravel bar and cottonwood sites (Chapter 3). Given the depth and degree of magnitude variation in water table, and the stresses upon plant roots under saturated anoxic conditions (Glinski and Steniewski 1985), we think that direct root interaction with the aquifer is possible, but is probably unrelated to the low DO hotspots in the aquifer.

The major source of energy flow to the aquifer ecosystem is probably buried POM. The relationship between POM and oxygen, respiration, and invertebrate production is indirect, and not easily established. In other systems there is considerable evidence for microbial response to POM in the subsurface (Galas et al. 1996, Crenshaw et al. 2002b), although the direct cause of microbial respiration is confounded by the transferability and lability of DOC and POC (Findlay and Sobczak 2000). Invertebrate response to buried particulate organic matter is sometimes positive (Strayer et al. 1997, Crenshaw et al. 2002a, Tillman et al. 2003) but often only weakly so. In the Nyack aquifer, there is no direct correlation between organic matter content and invertebrate density or organic matter content and production. We observed extremes of high organic matter and low invertebrate density and vice versa (Chapter 3). Experimentally we showed that the indirect effects of organic matter on invertebrate populations may depend on the interaction with fine sediments and oxygen (Chapter 5). Our replication was limited due to the size of each experimental unit, so our conclusions here are less certain. In paired treatments of fine sediment, with and without POM, invertebrate density responded strongly to both treatments, but only at the fine sediment interface. At that interface, invertebrate biomass and estimated production had a significantly higher response to the organic matter treatment. We also observed that invertebrate density in mesocosms showed strong exponential declines along longitudinal gradients. We were not able to explain this decline, but in view of the experimental results we suspect that the absence of POC may have led to a reduction in carbon energy sources spiraling through the mesocosms. Finally, we observed a significant positive relationship between POC content (e.g., plant detritus) and SAPOM (Chapter 2). The difference was only apparent in vegetated well sites (conifer/cottonwood) and not the unvegetated sites (parafluvial - gravel bars), indicating the importance of sediment age and cumulative effects of POC decay.

At larger spatial scales, Kaplan and Newbold (2000) predicted that buried organic matter will produce local sites of oxygen demand visible in vertical sediment profiles. We observed similar profiles of low DO hotspots, extending vertically from the top of the water table down to 2-4 meters (Chapter1). The spatial extent of these low oxygen zones is not precisely known, but based on the depth of the plumes and elongate elliptical

plume shapes typical of unconsolidated sediments, they were probably on the order of 10-100^{+} meters in length. They were at their largest extent in October covering up to 10% of the floodplain well grid, but remnants persisted throughout he annual cycle. The low DO hotspots did not correspond directly with any patterns in hydraulic conductivity, buried organic matter, or geomorphic context. However the highly skewed distribution of POC (Chapter 2), about 10% of sites having POC density orders of magnitude higher that average, is similar to the skewed oxygen distribution. Potentiometric maps did not indicate an impaired flowfield that might drive the system to anoxia (Well 17 in Figure 1c represents one of these hotspots). Several low DO sites occurred near the heads of recently abandoned channel formations near the active channel (i.e., avulsion nodes), and some sites were clearly downgradient of buried debris jams. Others sites were located kilometers from the main channel in much older orthofluvial formations. One of these sites was on an alluvial fan. Combining our experimental and field observations, we believe that buried POM is the most likely explanation for these low oxygen zones; however, the effect of POM may be indirect. The plume of hypoxia may extend well outside the range of the conditions that generated the plume. This is entirely likely in groundwater system with relatively rapid flow rates. The shallow oxygen depleted zones typically had larger seasonal temperature amplitudes than the deeper transitional zone of the oxycline, indicating that there may be greater flux of water in shallow low DO zones. As noted by Jones et al. (1995), the combination of high flux rates and high substrate heterogeneity can produce very biogeochemically reactive systems.

The Anatomy of a Biogeochemical Hot Spot

The low oxygen zones are clear examples of biogeochemical hot spots (McClain et al. 2003), with dynamic biogeochemistry and strong gradients. We have also shown that these hot spots influence microbial energy flow, and corresponding with high energy flow in the invertebrate communities. Moreover these areas appear to be sought out by amphibiont stoneflies and midges as sources of energy. Buried particulate organic matter is probably necessary condition as we discussed, but it is not sufficient. The high reactive surface area of fine sediment may also be required, as indicated by our experimental treatments (Chapter 5). However, finer sediment will also have reduced flows and hence

reduced loading rates. The middle ground here may be deposits of well sorted sand, which have relatively high permeability and also high surface area (Figure 11 in Chapter 5). Well sorted alluvial sands and buried organic matter from channel fill (e.g. Figure 15) is potential explanation for low DO zones.

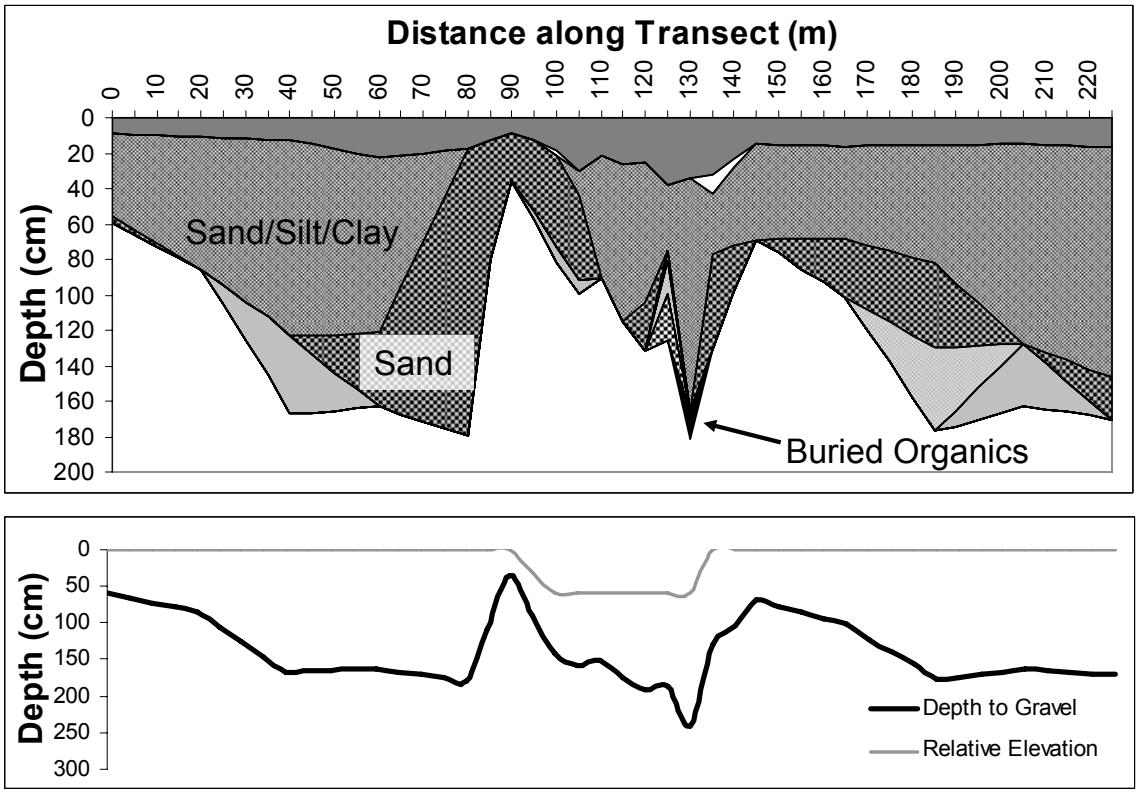

Figure 15: Soil catena along a 220 meter transect. The transect bisects a paleochannel in the orthofluvial zone, showing zones of well sorted sand, mixed sediment, buried organic matter as infill, all overlying gravel.

Our observation of aerobic invertebrates, coupled with anaerobic conditions, contradicts the assumption that invertebrate production declines with oxygen concentration (Downing 1984, Findlay 1995, Smock et al. 1992). There must be an energetic benefit to these low DO zones. We believe that the biogeochemistry within fine sediments may spatially subsidize invertebrate food webs (*sensu* Polis et al. 1997) at the sediment ecotone in three ways (Figure 16). One mechanism might be immobilization of DOC (Findlay 1995, Pusch et al. 1998) upgradient of a fine sediment formation. Another spatial subsidy may occur downgradient of anaerobic zones, where metabolic production of methane, sulfide, fermentation products, or the reduction and mobility of minerals and

phosphate, become available at the more oxygenated interface. This is similar to Champ's model of what he called an open system (Champ 1979). Finally, there may be spatially disjunct areas of fine sediment interface downgradient of the anaerobic source, functioning as an offsite reactive surface (otherwise the same mechanisms). This last scenario corresponds with our observations in the aquifer well network, where presence of sites of large anaerobic generation could not be correlated to properties such as hydraulic conductivity or organic matter. If methananogenesis is the primary anaerobic mechanism for this subsidy, as some of our data suggests, then this last mechanism may also reflect the interaction between sediment, higher oxygen and increased nitrogen availability downgradient of the anoxic zone. There is evidence from lake systems that methanotrophy may be inhibited at high DO, in part via the activity of nitrogen fixers (Rudd et al. 1976). Determining the anatomy of these biogeochemical hotspots, their cause and mechanism, is a problem of smaller sampling scale we that which we persued, requiring a much finer grid of nested multilevel wells.

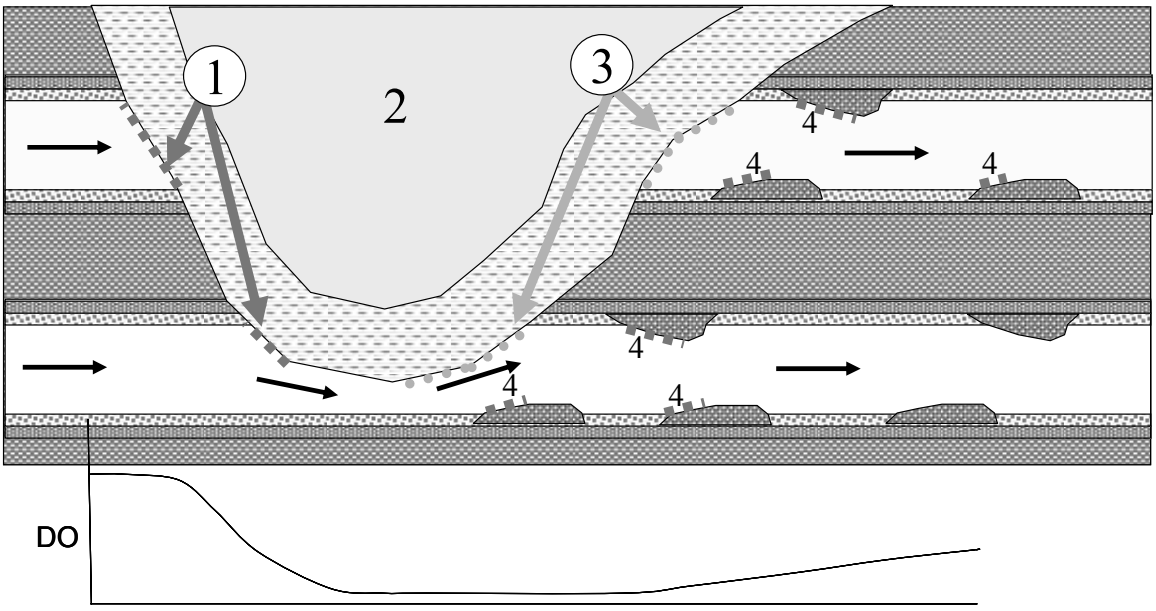

Figure 16: Conceptual model of mechanisms whereby fine sediment (channel fill or wood jam) can influence invertebrates in adjacent preferential flow zones. Biogeochemical and physical processes in fine sediment could subsidize invertebrate food webs at upstream (receiver or sorption surface) and downstream (redox) interfaces, potentially propagating downgradient. (1) Upgradient reciever – sites of DOC immobilization; (2) Highly reduced channel fill or wood jam sediments – sites for fermentation, methanogenesis, iron reduction, and a source of fine sediments and iron carbonates; (3) Downgradient redox interface – sites of chemical oxidation, flocculation, methanotrophy and microbial uptake; (4) Downgradient receiver – fine sediment patches, sites of sorption or uptake of chemical species or DOC originating from upgradient reduced zone.

None of the sampling sites were truly anoxic, but only hypoxic. The fact that low oxygen levels, not necessarily complete depletion of oxygen, can regulate biogeochemistry, fits with the idea that anaerobic microsites can make significant contributions to overall system behavior. We know from soil science that bulk oxygen concentration will affect the percentage of anaerobic microsites within soil aggregates, depending on aggregate size and composition (Glinski and Stepniewski 1985). Hypoxia and/or proximity to anoxic conditions, in addition to seasonally fluctuating redox gradients, may actually increase system productivity and energy flow. Groundwater organisms are known to be well adapted to weathering out periods of anoxia (Malard and Hervant 1999). These adaptations may also enable them to exploit energy resources resulting from hypoxia and anoxia. The availability of organic matter to higher trophic levels may be dependant on aerobic/anaerobic biogeochemistry, hence regulated by oxygen dynamics. Rarely is oxygen used as an independent variable, probably because of the difficulty in manipulating it. In aquatic sediments and along aquatic flowpaths, oxygen may be the master variable that regulates system function and productivity.

Assumptions and Limitations

There are two major sources of uncertainty in our energy budgets: (1) problems of sampling scale with habitat heterogeneity, and (2) the application of scaling relationships to a low energy system where empirical data is limited. We discussed the scale/heterogeneity issue in detail earlier (Chapter 1 and Chapter 4). In short, bimodal gravel distributions (coarse well sorted gravel layers sandwiched by upwardly fining and poorly sorted sediments; Huggenberger et al. 1998) are comprised of two distinct formations, with different biogeochemistry, invertebrate density (near zero in poorly sorted material) and sampling efficiency. We assume that all metazoan populations are restricted to the well sorted, high porosity gravel of preferential flow zones and burrow no more than a few centimeters into sands or poorly sorted material (Pennak 1940, Strayer 1985). However, preferential flow formation is only a small fraction of the overall sediment profile, typically only one or possibly two 3-5cm thick formations for every 100 cm depth (see Chapter 1 and Chapter 4). We sampled wells at 1 meter depth intervals (pooled 50 cm intervals), which is the smallest practical interval due to the

depth of wells, sampling efficiency at high pump discharge (Chapter 3), and is consistent with our goal of large spatial coverage. When water is sampled in bulk from such formations, most of the water and organisms comes from the most conductive formations. Hence, all of our water chemistry reflects properties of preferential flow zones with perhaps some contribution from adjacent fine sediments. We report invertebrate population density and production in units of m^3 bulk sediment. But, populations may be 20x to 40x more concentrated within preferential flow zones and comparison between sites presumes that these zones are a random and repeatable feature across the floodplain aquifer. Along the same lines, our estimates of organic matter content are in units of %C content of fine sediments by weight (Chapter 2). We assume that POM corresponds with fine sediments and is sorted out from coarse sediments during initial deposition. This means that the large pool of particulate matter may not be directly accessible to invertebrate populations or microbes in preferential flow zones. This spatial discontinuity can also be viewed in terms of its implications for spatial subsidy of invertebrate energy flow. We consider this spatial uncertainty in more detail in our discussion of the energy budget below. Here we point out that the spatial scale is the major source of uncertainty in our energy budget, outweighing any confidence intervals based solely on the raw population data.

There are few population studies of subsurface organisms, and save for shallow hyporheic zones (Smock et al. 1992) production of subsurface organisms has never been accomplished. The use of the empirical allometric relationships presumes that subsurface organisms scale in the same manner as epigean organisms. Therefore, we rely primarily on our measurements of standard metabolic rate as the approximate lower bound and the calculations based on lake and stream populations as an upper limit. While the respiration equation of McNeill and Lawton (1970) includes populations of several poikilotherms that have lower area specific rates (i.e. low density), the regression does not include micrometazoans. The smallest taxa by specific mass are the chironomids *Anatopynia* and *Calospectra* (From Teal 1957), and in using this equation we are admittedly projecting beyond the range of empirical data. The general model from Morin and Bourassa (1992) is based on stream benthic invertebrates. Although taxa are not specified, their minimum individual mass was 800µg, which is well above all of the micrometazoans and some of

the dominant macroinvertebrates in this study (i.e. *Stygobromus*). Their equation is based on mean mass of a population, as opposed to the maximum mass (Plante and Downing 1989) or mass at maturity (Banse and Mosher 1980). It is not clear that these differences in basic assumptions can account for the differences in mass scaling exponents: -0.34 for Morin and Bourassa (1992), -0.17 for Plante and Downing (1989), -0.37 for Banse and Mosher (1980), and -0.25 for metabolic theory (Brown et al. 2004). The equation in Plante in Downing (1989) is perhaps the most realistic, in that it includes lake benthos and micrometazoans ("zooplankton," including benthos, although a list of taxa and specific mass are not provided.). Their temperature correction, which is small compared to mass and population biomass, is based on lake surface temperature and thus may not be at all related to benthic temperature. The three different scaling equations provide somewhat different results, depending on body size. Given the general lack of understanding of groundwater ecosystems, this level of uncertainty is acceptable.

Our respiration estimation of standard metabolic rate is the low end of invertebrate metabolism. Lampert proposed that studies of field populations would be more effective in measuring respiration during normal feeding activity, even if conducted in the lab (Lampert 1984). However, the food substrate is poorly known for these organisms and attempts to determine growth rates of the stoneflies *Isocapnia* and *Paraperla* on natural sediment under field conditions were unsuccessful (B. Reid, unpubl data). Lampert also showed that under food limiting conditions (which is likely in the aquifer) a small error in respiration measurements can lead to a large error in the production estimate. Our use of a constant of 2.5 for converting standard to field metabolic rates is based on mammal populations (Savage et al. 2004), and it is not known whether invertebrates, much less groundwater invertebrates, would scale proportionally. This is perhaps a very general problem when applying metabolic theory to field populations, which we feel has not been adequately addressed. We recommend the recently translated work by Pavlova (2006) on marine zooplankton energetics, as an example of how to systematically approach this problem: calculating the proportion of time organisms engage in various activities, correcting for the effects of container size on movement, and relating metabolic rate to activity. Savage et al. (2004) appear to conflate basal and standard rates, and the two may differ by a factor of 1.5 to 2.3 or more

depending on body size (Pavlova 2006). We know only that our respirometry trials were performed under conditions best described as standard rate (limited movement), and that animals observed in culture dishes with native sediment have clearly much higher activity than in the respirometry chambers. In groundwater systems, a low estimate may not be too unreasonable. Our conversion factor of 2.5 is clearly very approximate.

Projecting respiration and production outside the range of our measurements is a potential source of error. As indicated in Figure 5, the stoneflies are above our range and nauplii, rotifers and other micrometazoans are below our range. Figures 4 and 5 suggest that this would result in an underestimate of macrofauna respiration and production and an overestimate for micrometazoans. For macrofauna, our lower than expected rate for the amphipod *Stygobromus*, is comparable to the underestimate for the largest stoneflies (Figure 4). There is ample evidence from the literature that hypogean organisms have lower mass specific metabolic rates than comparable epigean taxa (Malard and Hervant 1999, see also Huppop 1985 for a comprehensive review). If we substitute the upper estimates from lake and river population scaling, our conclusions from patterns in Figure 5 through 7 are not altered, but actually enhanced since the stoneflies almost exclusively occur in low oxygen and transition zones (see Chapter 3).

We assumed that invertebrate and microbial metabolic activity was not reduced by very low oxygen tension. This assumption is supported by evidence from microbial communities (Longmuir 1954) and our respirometry trials indicated no short-term effects of low oxygen on invertebrate aerobic respiration rate. Over longer time scales, there is evidence that invertebrates in lake benthos may remain active (euryoxybiotic) and survive 120+ days under anaerobic conditions (Lindeman 1942b), although Lindeman observed 50% mortality after 50 days. We did not make similar observations of invertebrate activity in our system. Very rarely we observed encystment of cyclopoid copepods (Moore 1939) which might indicate prolonged dormancy of organisms. The encysted copepods did not clearly correspond with environmental conditions such as low oxygen. Invertebrate respiration under low oxygen conditions may be supplemented by anaerobic fermentation reactions, with a subsequent oxygen debt incurred during posthypoxic recovery (Hervant et al. 1998, Malard and Hervant 1999). We assumed here that there was minimal decline in invertebrate metabolism during low oxygen tension,

and that the contribution of fermentation reactions to system metabolism was ultimately balanced through payment of the oxygen debt.

The production to respiration relationship in del Giorgio and Cole (1988) is derived from bacterioplankton communities. It is not known how well it is transferable to aquatic sediments; however, when we calculate production efficiency (BGE, eq 3 in del Giorgio and Cole 1988) we arrive at a BGE of 12.4 (for longer flowpaths) to 17.3 for the low oxygen hotspots. This is not too different from 0.24 BGE reported for stream benthos (Bott and Kaplan 1985) and somewhat below 0.3 (Meyer et al. 1987, and used by Ellis et al. 1998). Our estimate of BGE is well within the range for less productive lakes listed in del Giorgio and Cole (1988).

Comparison to Other Systems:

Perhaps one of the greatest values of the analysis of ecosystem energy flow is the potential to compare vastly different systems in terms of common units. The choice of dimensions for energy units is probably important to the organism of interest, and Hall (1972) demonstrated that in stream channels of varying depth, conclusions may differ depending on whether the analysis is made on an aerial vs. volumetric basis (i.e. factoring for depth of water). But in general most systems can be readily reduced to two dimensional units (benthos, or aerial productivity). Our subsurface system is the only true three-dimensional system studied from an energy perspective, rendering comparison difficult. However if we assume that energy flow is restricted to preferential flow zones, which comprise approximately 5% of the vertical stratigraphy, we can compress our cubic meter units to square meters by dividing by a factor of 20. Even without this correction our system has 1000x times less energy than Root Spring (Teal 1957), and groundwater ecosystems are probably among the lowest energy systems yet studied. Our groundwater system also differs from other study systems in that it is restricted to one trophic level, which is perhaps not unrelated to our first observation. Our groundwater system also exhibits a very low trophic transfer efficiency. Our transfer efficiencies are in the range of 1.5 to 3% (Table 6a). In contrast, a progressive transfer efficiency of 10% (as recalculated by Kozlovski 1968) appears to be conservative across many of the systems previously studied. Finally, we demonstrate the importance of anaerobic metabolism to

higher food webs, this previously unreported spatial subsidy being possible where sediment heterogeneity interacts with relatively high flux rates of water and solutes. This complicates the notion of ecosystems, in that internal heterogeneity may result in emergent properties not otherwise evident if systems are studied as a whole, without consideration for such internal variation. There is clearly some value in including additional ecosystems in the portfolio of system energy flow studies, our groundwater example thus providing the extreme range for comparison.

As evident from the introduction, our work does not significantly expand upon the all too short list of energy flow studies. However it does afford an opportunity to return to Lindeman's original trophic dynamic concept. Perhaps one of the most cited papers in ecology, we contend that is also one of the most mis-cited papers, the term "trophic-dynamic" having become descriptive jargon for food webs. Lindeman of course was talking about energy flow at the scale of trophic levels, and clearly states in his introductory paragraph the concept of trophic energy flow over successional time. In this strict sense, all of the energy flow studies are snapshots in time, and do not represent a successional chronosequence. The true trophic dynamic properties of ecosystems have never been fully explored, and Eugene Odums's "Strategies of Ecosystem Development" (Odum 1969) is perhaps the only major theoretical addition to Lindeman's concept. Our work is also technically a snapshot in time. However in representing various parts of the aquifer in our sampling, we have developed a general understanding of system energetics as it relates to age of aquifer formations (i.e. young gravel bar vs. mature conifer forest). Since we are dealing with the subsurface, the idea of succession is not as intuitive as it is for vegetation development. Instead, succession in the subsurface can be defined in terms of energy inputs. An initial pulse of particulate carbon is buried in a new gravel bar, and that energy resource is depleted over time (a slowly draining battery). There is probably much more to succession in the subsurface than this, most likely related to the development of geochemical complexity and diagenesis over time, rather than faunistic or floristic succession. The major point here is that the successional trajectory in the subsurface is the reverse of the surface systems that are more familiar to us. Energy dissipates from high to low, rather than accumulating from low to high (or to some steady state). A rough calculation based on the average POM density in the aquifer and its

estimated exponential rate of decay indicates that this initial energy pulse is depleted in about 100 years. In the infrequent patches with high organic matter density, buried POM is a battery that may last perhaps a little more than 10,000 years. This is approximately the age of Quaternary alluvium, the inactive glacial terraces which often comprise most of the sediment in glaciated alluvial valleys.

Conclusions

Clearly this research effort is based on some significant assumptions, often translated from systems such as lakes and stream benthos with properties only similar to groundwater ecosystems, but loosely constrained by field and experimental data. Our conclusions represent a framework. And, from this framework we can hopefully ask more relevant questions about the function of one of the world most poorly described ecosystems. Floodplain aquifers are probably a widespread and repeatable feature in mountain and piedmont valleys throughout the world (Stanford and Ward 1988). The biogeography of the deep hyporheic stoneflies *Isocapnia* and *Paraperla* (Stewart and Stark 2002) provide strong support for the occurrence of these systems in western North America. In western Montana, surficial groundwaters overlap with high human population density, the flat low-lying areas typically having the most intense land use (Figure 17). The site of some of the earliest studies of alluvial groundwater (Stanford et al. 1994) is one of the most rapidly urbanizing areas in the state (Swanson 2003). We have already mentioned several potential areas for future work: employing tracer and spiraling studies in mesocosms, organic carbon speciation (particularly as a function of DO gradients), more comprehensive spatial and temporal studies of gut microflora (e.g. Adams 2006), and time series of groundwater DOC isotopes.

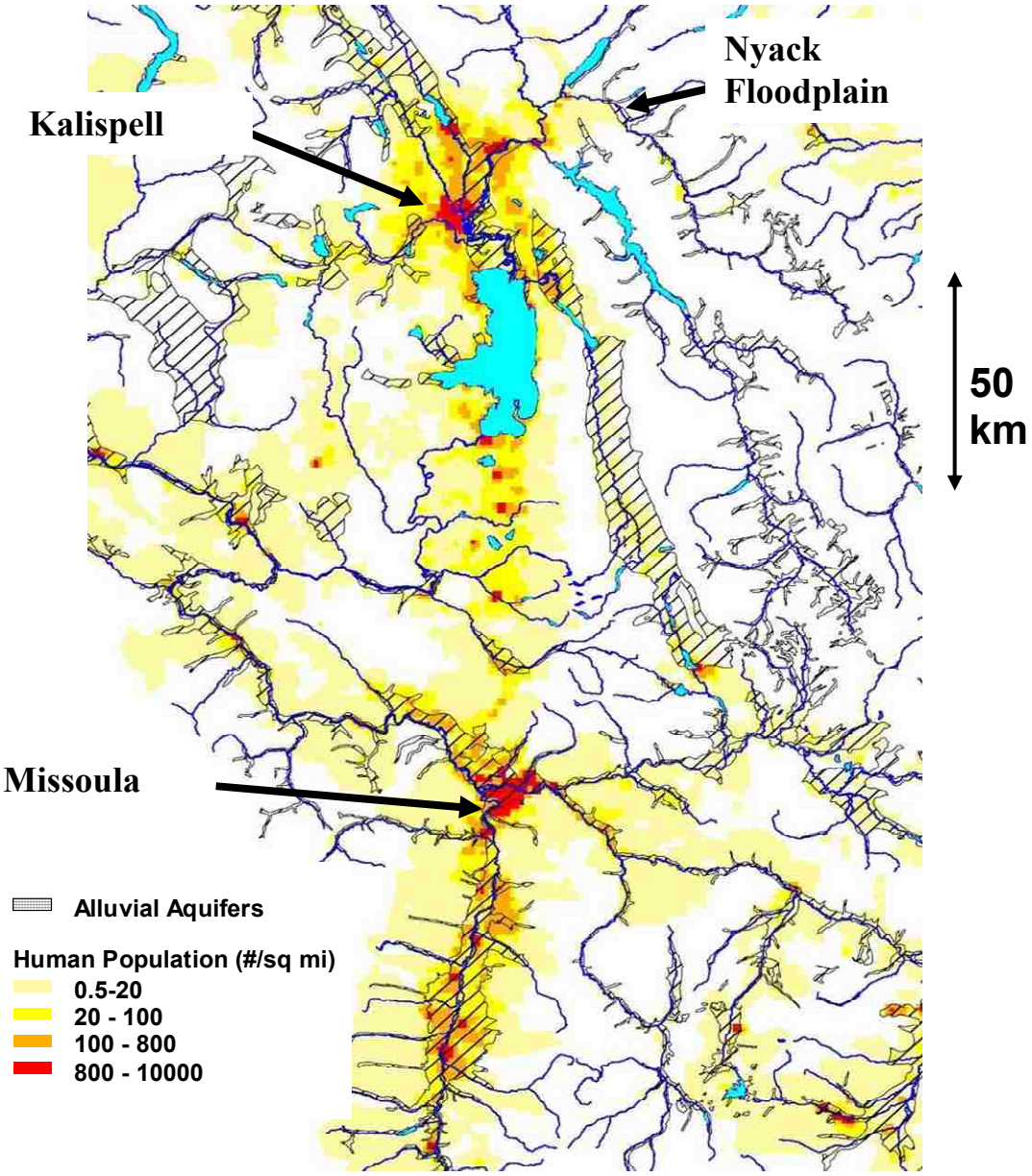

Figure 17: Alluvial aquifers in western Montana, with an overlay of human population density. In mountain and piedmont valleys, alluvial aquifers overlap with urban land use. The Kailspell aquifer is the site of some of the first studies of large hyporheic systems. The greatest impacts to natural landscapes often coincide with shallow groundwater water resources.

We close this paper with a few ecosystems scale and landscape scale questions that have a strong bearing on the conservation and management of surficial groundwaters and floodplain aquifers:

1. How does the terrestrial zone influence the subsurface in different climatic regimes (i.e. with increased precipitation recharge in temperate rain forest)?

2. How are these linkages altered in urbanized landscapes?
3. How widespread are this systems (based on the range of deep hyporheic stoneflies) and are there distinct biogeographic differences in species or system function?
4. What is the long term prospect for these shallow groundwater ecosystems, largely undocumented, in light of projected urbanization pattern in the west?
5. What is the mechanism for the shift in biogeochemistry and invertebrate communities at 3-4 mg/l O_2?
6. To what extent will compromise of these aquifer systems (such as through a reduction in DO) feed back on the rivers and watersheds. Can a reduction in main channel DO (from biological oxygen demand or temperature rise) alter biogeochemical cycling of entire river-aquifer systems?
7. How does the lifespan of buried carbon energy interact with free flowing rivers (reburial of POM) at the landscape scale? Will alluvial aquifer systems suffer from depletion of buried organic matter energy, a system with dead or dying batteries as a result of river regulation?

REFERENCES

Adams, S. A. 2006. Microbes, stoneflies and fish: trophic interactions in aquatic ecosystems. MS Thesis, University of Montana.

APHA 1989. *Standard Methods for the Examination of Water and Wastewater,* 17th ed. American Public Health Association, Washington, D.C.

Baker, M. A., H.M. Valett, and C.N. Dahm. 2000. Organic carbon supply and metabolism in a shallow groundwater ecosystem. *Ecology* 81(11): 3133-3148.

Bang, A., Frederiksen, T.M., Bruhn, A.,. Meilvang, A.S & Grønkjær, P. 2004. A simple and sensitive closed respirometer for small aquatic organisms. For submission to "*Limnology and Oceanography: Methods*".

Banse, K. 1982. Mass-scaled rates of respiration and intrinsic growth in very small invertebrates. *Mar. Ecol. Prog. Ser.* 9: 281-297.

Banse, K. and S. Mosher. 1980. Adult body mass and annual production/biomass relationships of field populations. *Ecol. Mon.* 50(3): 355-379.

Bastviken, D., J. Ejlertsson, I. Sundh, L. Tranvik. 2006. Methane as a source of carbon and energy for lake pelagic food webs. *Ecology* 84(4): 969-981.

Baxter, C. V. and F. R. Hauer. 2000. Geomorphology, hyporheic exchange, and selection of spawning habitat by bull trout (*Salvelinus confluentus*). *Can. J. Fish. Aquat. Sci*., 57: 1470-1481.

Benke, A.C., A.D. Huryn, L.A. Smock, J.B. Wallace. 1999. Length-mass relationships for freshwater macroinvertebrates in North America with particular reference to the southeastern United States. *J. N. Am. Benthol. Sci.* 18(3): 308-343.

Benke, A.C., J.B. Wallace. 1980. Trophic basis of production among net-spinning caddisflies in a southern Appalachian stream. *Ecology* 61: 108-118.

Bott, T.L. and L.A. Kaplan. 1985. Bacterial biomass, metabolic state and activity on stream sediments: relationship to environmental variables and multiple assay comparisons. *Appl. Environ. Microbiol.* 50: 508-522.

Brown, D.S. 1960. The ingestion and digestion of Chloeon dipterum. L. *Hydrobiol.* 16: 81-96.

Brown, J.H., J.A. Gillooly, A.P. Allen, V.M. Savage and G.B. West. 2004. Toward a metabolic theory of ecology. *Ecology* 85(7): 1771-1789.

Brunke, M. and T. Gonser. 1997. The ecological significance of exchange processes between rivers and groundwater. *Freshwat. Biol.* 37: 1-33.

Bunn, S.E. and P.I. Boon. 1993. What sources of organic carbon drive food webs in billabongs? A study based on stable isotope analysis. *Oecologia* 96: 85-94.

Campbell, L. and P. Chow-Fraser. 1995. Differential effects of chemical preservatives and freezing on the length and dry weight of *Daphnia* and *Diaptomus* in an oligotrophic lake. *Arch. Hydrobiol.* 134(2): 255-269.

Caumartin, V. 1959. Quelques aspects noveaux de la microflore cavernes. *Annales de Speleogie* 14: 147-157.

Champ, D.R., J. Gulens and R.E. Jackson. 1979. Oxidation-reduction sequences in ground water flow systems. *Can. J. Earth Sci.* 16:12-23.

Chantigny, M.H. 2003. Dissolved and water-extractable organic matter in soils: a review on the influence of land use and management practices. *Geoderma* 113: 357-380.

Claret, C., P. Marmonier, J-M Boissiere, D. Fontevieille and P. Blanc. 1997. Nutrient transfer between parafluvial interstitial water and river water: influence of gravel bar heterogeneity. *Freshwat. Biol.* 37: 657-670.

Coffin, R.B. and L.A. Cifuentes. 1993. Approaches for measuring stable carbon and nitrogen isotopes in bacteria. In: P.F. Kemp, B.F. Sherr, E.B. Sherr and J.J. Cole, eds. *Handbook of methods in aquatic microbial ecology.* Lewis, Boca Raton, FL.

Craft, J.A., J.A. Stanford and M. Pusch. 2002. Microbial respiration within a floodplain aquifer of a large gravel-bed river. *Fresh. Biol.* 47: 251-261.

Crenshaw, C.L., H.M. Valett, J.L. Tank. 2002a. Effects of coarse particulate organic matter on fungal biomass and invertebrate density in the subsurface of a headwater stream. *J. N. Am. Benthol. Soc.* 21(1): 28-42.

Crenshaw, C.L., H.M. Valett and J.R. Webster. 2002b. Effects of augmentation of coarse particulate organic matter on metabolism and nutrient retention in hyporheic sediments. *Fresh. Biol.* 47: 1820-1831.

Culver, D.A., M.M. Boucherle, D.J. Bean, J.W. Fletcher. 1985. Biomass of freshwater crustacean zooplankton from length-weight regressions. *Can. J. Fish. Aquat. Sci.* 42: 1380-1390.

Cummins, K.W. 1973. Trophic relations of aquatic insects. *Ann Rev Entom.*18:183-207.

Danielopol, D.L., M. Creuzé des Châtelliers, F. Moeszlacher, P. Pospisil, R. Popa. 1994. Adaptation od Crustacea to Interstitial Habitats: A Practical Agenda for Ecological Studies. *IN*: Gibert, J., D. L. Danielopol and J. A. Stanford (eds.), *Groundwater Ecology*. Academic Press, San Diego, California, USA. 571 pp.

Danielopol, D.L., P.P. Pospisil, J. Dreher, F. Mosslacher, P. Torreiter, M Geiger-Kaiser, A. Gunatilaka. 2000. A groundwater ecosystem in the Danube wetlands at Wien (Austria). In: Wilkens, H., D.C. Culver and W.F. Humphreys, Eds. *Ecosystems of the World 30: Subterranean Ecosystems.* Elsevier.

Dawson, T.E., S. Mambelli, A.H. Plamboeck, P.H. Templer and K.P. Tu. 2002. Stable isotopes in plant ecology. *Ann. Rev. Ecol. Syst.* 33: 507-59.

del Giorgio, P.A. and J.J. Cole. Bacterial growth efficiency in natural aquatic systems. *Ann. Rev. Ecol. Syst*. 29:503-541.

Diehl, C.J. 2004. Controls on the magnitude and location of groundwater/surface water exchange in a gravel dominated alluvial floodplain system, northwestern Montana. Unpublished MS Thesis. University of Montana.

Dickie, L.M., S.R. Kerr, P.R. Boudreau. 1987. Size-dependent processes underlying regularities in ecosystem structure. *Ecol. Monogr.* 57(3): 233-250.

Dole-Olivier, M.J., P. Marmonier, M. Creuzé des Chateliers, & D. Martin.1994. Interstitial Fauna Associated with the Alluvial Floodplains of the Rhône River (France). *IN*: Gibert, J., D. L. Danielopol and J. A. Stanford (eds.), *Groundwater Ecology*. Academic Press, San Diego, California, USA. 571 pp.

Downing, J.A. 1984. Assessment of secondary production: the first step. In: Downing, J.A. and F.H. Rigler, Eds. A Manual on Methods for the Estimation of Secondary Productivity in Fresh Waters. Blackwell.

Dumont, H.J., I.V. de Velde, S. Dumont. 1975. The dry weight estimate of biomass in a selection of cladocera, copepoda and rotifera from the plankton, periphyton and benthos of continental waters. *Oecologia* 19:75-97.

Elliott, J.M. and W. Davison. 1975. Energy equivalents of oxygen consumption in animal energetics. *Oecolgia* 19: 195-201.

Ellis, B.K., J. A. Stanford and J. A. Ward. 1998. Microbial assemblages and production in alluvial aquifers of the Flathead River, Montana, USA. *J. N. Am. Benthol. Soc.* 17(4): 382-402.

Epp, R.W. and W.M. Lewis. 1980. The nature and ecological significance of metabolic changes during the life history of copepods. *Ecology* 61(2): 259-264.

Ernest, S.K. M., B.J. Enquist, J.H. Brown, E.L. Charnov, J.H. Gillooly, V.M. Savage, E.P. White, F.A. Smith, E.A. Hadly, J.P. Haskell, S.K. Lyons, B.A. Maurer, K.J. Niklas, B.Tiffney. 2003. Thermodynamic and metabolic effects on the scaling of production and population energy use. *Ecol. Lett.* 6: 990-995.

Fetter, C.W. 2001. *Applied Hydrogeology 4th ed.* Prentice.

Findlay, S. 1995. Importance of surface-subsurface exchange in stream ecosystems: The hyporheic zone. *Limnol. Oceanogr.* 40(1): 159-164.

Findlay, S. & W. Sobczak. 2000. Microbial communities in hyporheic sediments. In: Jones, J.B. & P.J. Mulholland, eds. *Streams and Ground Waters.* Academic Press, San Diego.

Fisher, S.G. and G.E. Likens. 1973. Energy flow in Bear Brook, New Hampshire: an integrated approach to stream ecosystem metabolism. *Ecol. Mon.* 43: 421-439.

Frank, C. 1982. Ecology, production and anaerobic metabolism of Chironomus plumosus L. larvae in a shallow lake: I. Ecology and production. *Arch. Hydrobiol.* 94(4): 460-491.

Galas, J., T. Bednarz, E. Dumnicka, A. Starzecka and K Wojtan. 1996. Litter decomposition in a mountain cave water. *Arch. Hydrobiol.* 138(2): 199-211.

Gibert, J., and L Deharveng. 2002. Subterranean ecosystems: a truncated functional biodiversity. *Biosci.* 52(6): 473-481.

Giere, O. 1993. *Meiobenthology*. Springer-Verlag, Berlin.

Gillooly, J.F., J.H. Brown, G.B. West, V.M. Savage, E.L. Charnov. 2001. Effects of size and temperature on metabolic rate. *Science* 293: 2248-2251.

Glinski, J. and W. Stepniewski 1985. *Soil Aeration and its Role for Plants*. CRC Press, Boca Raton FL.

Gosz, J.R., R.T. Holmes, G.E. Likens, F.H. Bormann. 1978. Flow of energy in a forest ecosystem. *Sci. Am.* 238(3): 93-102.

Gounot, A.M. 1960. Recherches sur de limon argileux souterrain et sur son role nutritif pour les Nipharges. *Annales de speleogie* 15: 501-526.

Grimm, N.B. & S.G. Fisher. 1984. Exchange between interstitial and surface water: Implications for stream metabolism and nutrient cycling. *Hydrobiol.* 111: 219-228.

Hall, C.A.S. 1972. Migration and metabolism in a temperate stream ecosystem. *Ecology* 53(4): 585-604.

Hamburger, K., P. C. Dall, C. Lindegaard. 1994. Energy metabolism of *Chironomus anthacinus* (Diptera: Chironomidae) from the profundal zone of Lake Esrom, Denmark, as a function of body size, temperature and oxygen concentration. *Hydrobiol.* 294: 43-50.

Harner, M.J., & J.A. Stanford. 2003. Differences in cottonwood growth between a losing and a gaining reach of an alluvial flood plain. *Ecology* 84: 1453-1458.

Hervant, F., J. Mathieu, G. Messana. 1998. Oxygen consumption and ventilation in declining oxygen tension and posthypoxic recovery in epigean and hypogean crustaceans. *J. Crust. Biol.* 18(4): 717-727.

Huggenberger, P., E. Hoehn, B Beschta, and W. Woessner. 1998. Abiotic aspects of channels and floodplains in riparian ecology. *Fresh. Biol.* 40: 407-425.

Humphreys, W.F. 1979. Production and respiration in animal populations. *J. Anim. Ecol.* 48(2): 427-453.

Huppop, K. 1985. The role of metabolism in the evolution of cave animals. *NSS Bulletin* 42(2): 136-146.

Jannasch, H.H. 1984. Chemosynthesis: the nutritional basis for life at deep-sea vents. *Oceanus* 27: 73-78.

Jasinska, E.J. and B. Knott. 2000. Root-driven faunas in cave waters. In: Wilkens, H., D.C. Culver and W.F. Humphreys, Eds. *Ecosystems of the World 30: Subterranean Ecosystems.* Elsevier.

Jones, J.B., S. B. Fisher and N.B. Grimm. 1995. Vertical hydrologic exchange and ecosystem metabolism in a Sonoran Desert stream. *Ecology* 76(3): 942-952.

Jones, J.B. and P.J. Mulholland. 2000. *Streams and Ground Waters.* Academic Press, San Diego.

Kankaala, P., S. Taipale, J. Grey, E. Sonninen, L. Arvola, R. Jones. 2006. Experimental $\delta^{13}C$ evidence for a contribution of methane to pelagic food webs in lakes. *Limnol. Oceanogr.* 41 (6): 2281-2827.

Kaplan, L.A. and J.D. Newbold. 2000. Surface and Subsurface Dissolved Organic Carbon. In: Jones, J.B. and P.J. Mulholland, eds. *Streams and Ground Waters*. Academic Press, San Diego USA.

Kelly, A., R.L. Jones, and J. Grey. 2004. Stable isotope analysis provides fresh insights into dietary separation between *Chironomus anthacinus* and *C. plumosus*. *J. N. Am. Benthol. Soc.* 23(2): 287-296.

Kozlovski, D.G. 1968. A critical evaluation of the trophic level concept. I. Ecological efficiencies. *Ecology* 44(1): 48-60.

Lampert, W. 1984. The measurement of respiration. In: Downing, J.A. and F.H. Rigler, Eds. *A Manual on Methods for the Estimation of Secondary Productivity in Fresh Waters.* Blackwell.

Leichtfried, M. 1988. Bacterial substrates in gravel beds of a second order alpine stream (Project Ritrodat-Lunz, Austria). *Int. Ver. Theor. Angew. Limnol. Verh.* 23: 1325-1332.

Lindeman, R.L. 1942a. The trophic-dynamic aspect of ecology. *Ecology* 23: 399-418.

Lindeman, R.L. 1942b. Experimental simulation of winter anaerobiosis in a senescent lake. *Ecology* 23(1): 1-13.

Longmuir, I.S. 1954. Respiration rate of bacteria as a function of oxygen concentration. *Biochem. J.* 57: 81-87.

Malard, F. and F. Hervant. 1999. Oxygen supply and the adaptations of animals in groundwater. *Fresh. Biol.* 41: 1-30.

Marshall, M.C., R.O. Hall. 2004. Hyporheic invertebrates affect N cycling and respiration in stream sediment microcosms. *J. N. Am. Benthol. Soc.* 23(3): 416-428.

McCauley, E. 1984. The estimation of the abundance and biomass of zooplankton in samples. In: Downing, J.A. and F.H. Rigler eds. *A Manual on Methods for the Assessment of Secondary Productivity in Fresh Waters*, 2nd ed. Blackwell Scientific, Oxford.

McClain, M.E., E.W. Boyer, C.L. Dent, S.E. Gergel, N.B. Grimm, P.M. Groffman, S.C. Hart, J.W. Harvey, C.A. Johnston, E. Mayorga, W. H. McDowell, G. Pilay. 2003. Biogeochemical hot spots and hot moments at the interface of terrestrial and aquatic ecosystems. *Ecosystems* 6: 301-312.

McNeill, S. and J.H. Lawton. Annual production and respiration in animal populations. *Nature* 225: 472-474.

Meyer, E. 1989. The relationship between body length parameters and dry mass in running water invertebrates. *Arch. Hydrobiol.* 117(2): 191-203.

Meyer, J.L., R.T. Edwards, R. Risley. 1987. Bacterial growth on dissolved organic carbon in a blackwater river. *Micr. Ecol.* 13: 13-29.

Moore, G.M. 1939. A limnological investigation of the microscopic benthic fauna of Douglas Lake, Michigan. *Ecol. Mon.* 9(4): 537-582.

Morin, A. and N. Bourassa. 1992. Modèles empiriques de la production annuelle et du rapport P/B d'invertèbrès benthiques d'eau courante. *Can. J. Fish. Aquat. Sci.* 49: 532-539.

Mouw, J.E.B.& P.B. Alaback. 2003. Putting floodplain hyperdiversity in a regional context: An assessment of terrestrial-floodplain connectivity in a montane environment. *J. Biogeogr.* 30: 87-103.

Odum, E. P. 1969. The strategy of ecosystem development. *Science* 164: 262-270.

Odum, H.T. and E.P. Odum. 1955. Trophic structure and productivity of a windward coral reef community on Eniwetok Atoll. *Ecol. Mon.* 25 (3): 291-320.

Odum, H.T. 1957. Trophic structure and productivity of Silver Springs, Florida. *Ecol. Mon.* 27(1): 55-112.

Orghidan, T. 1959. Ein neuer Lebensraum des unterirdischen Wassers, der hyporheische Biotop. *Arch. f. Hydrobiol.* 55: 392-414.

Pavlova, E.V. 2006. *Movement and Energy Metabolism of Marine Planktonic Organisms*. Universities Press, India.

Pearre, S. Jr. 1980. The copepod width-weight relation and its utility in food chain research. *Can. J. Zool.* 58: 1884-1891.

Pennak, R.W. 1940. Ecology of the microscopic metazoan inhabiting the sandy beaches of some Wisconsin lakes. *Ecol. Mon.* 10(4): 538-615.

Pepin, D.M. & F.R. Hauer. 2002. Benthic responses to groundwater-surface water exchange in two alluvial rivers in northwestern Montana. *J. N. Am. Benthol. Soc.* 21: 370-383.

Plante, C. and J.A. Downing. 1989. Production of freshwater invertebrate populations in lakes. *Can J. Fish. Aquat. Sci.* 46: 1489-1498.

Polis, G.A., W.B. Anderson and R.D. Holt. 1997. Towards an integration of landscape and food web ecology: the dynamics of spatially subsidized food webs. *Ann. Rev. Ecol. Syst.* 28: 289-316.

Pospisil, P. 1994. The Groundwater Fauna of a Danube Aquifer in the "Lobau" Wetland in Vienna, Austria. *IN*: Gibert, J., D. L. Danielopol and J. A. Stanford (eds.), *Groundwater Ecology*. Academic Press, San Diego, California, USA. 571 pp.

Poulson, T.L. 1964. Animals in aquatic environments: animals in caves. In: Dill, D.B ed. *Handbook of Physiology. Section 4: Adaptation to the Environment*. American Physiological Society, Washington DC.

Pusch, M., D. Fiebig, I. Brettar, H. Eisenmann, B.K. Ellis, L.A. Kaplan, M.A. Lock, M. W. Naegli, W. Traunspurger. 1998. The role of micro-organisms in the ecological connectivity of running waters. *Fresh. Biol.* 40: 453-495.

Reid et al. in prep A. Large scale invertebrate community dynamics in response to oxygen gradients in a floodplain aquifer. For submission to Freshwater Biology.

Reid et al. in prep B. Distribution and isotopic composition of organic matter in floodplain aquifer sediments. For submission to Biogeochemistry.

Reid et al. in prep C. Oxygen Dynamics and community respiration in a montane floodplain aquifer. For submission to Limnology and Oceanography.

Reid et al. in prep D. Effects of substrate, organic matter, and oxygen on invertebrate density, biomass and production in the hyporheic zone: a mesocosm experiment. For submission to JNABS

Revsbech, N. P. 1989. An oxygen microsensor with a guard cathode. *Limn. & Oceanogr.* 34(2): 474-478.

Riisgard, H.U. 1998. No foundation for a "3/4 powerscaling law" for respiration in biology. *Ecol. Lett.* 1(2): 71-73.

Ruby, E.G., H.W. Jannasch, W.G. Deuser. 1997. Fractionation of stable carbon isotopes during chemoautotrophic growth of sulfur-oxidizing bactera. *Appl. Env. Microbiol.* 53(8): 1940-1943.

Rudd, J.W.M., A. Furutani, R.J. Flett, R.D. Hamilton. 1976. Factors controlling methane oxidation in shield lakes: the role of nitrogen fixation and oxygen concentration. *Limn. & Oceanogr.* 21(3): 357-364.

Salonen, K., J. Sarvala, I. Hakala, M-L. Vitjanen. 1976. The relation of energy and organic carbon in aquatic invertebrates. *Limnol. & Oceanogr.* 21(5): 724-736.

Sarbu, S.M. 2000. Movile Cave: a chemoautotrophically based groundwater ecosystem. In: Wilkens, H., D.C. Culver and W.F. Humphreys, Eds. *Ecosystems of the World 30: Subterranean Ecosystems.* Elsevier.

Savage, V.M. 2004. Improved approximations to scaling relationships for species, populations, and ecosystems across latitudinal and elevational gradients. *J. Theor. Biol.* 227: 525-534.

Savage, V.M., J.F. Gillooly, W.H. Woodruff, G.B. West, A.P. Allen, B.J. Enquist, J.H. Brown. 2004. The predominance of quarter-power scaling in biology. *Func. Ecol.* 18: 257-282.

Simon, K.S., E.F. Benfield, S.A. Macko. 2003. Food web structure and the role of epilithic biofilms in cave streams. *Ecology* 84(9): 2395-2406.

Smock, L.A. 1980. Relationships between body size and biomass of aquatic insects. *Fresh. Biol.* 10: 375-383.

Smock, L.A., J.E. Gladden, J.L. Riekenberg, L.C. Smith, C.R. Black. 1992. Lotic production in three dimensions: channel surface, floodplain and hyporheic dimensions. *Ecology* 73 (3): 876-886.

Stanford, J.A. 1973. A centrifuge method for determining live weights of aquatic insect larvae, with a note on weight loss in preservative. *Ecology* 54(2): 459-451.

Stanford, J.A. and A.R. Gaufin. 1974. Hyporheic communities of two Montana rivers. *Science* 185: 700-702.

Stanford J.A., M.S. Lorang and F.R. Hauer. 2005. The shifting habitat mosaic of river ecosystems. *Verh. Internat. Verein. Limnol.* 29(1): 123-136.

Stanford, J.A. and J.V. Ward. 1988. The hyporheic habitat of river ecosystems. *Nature* 335: 64-66.

Stanford, J. A. and J. V. Ward. 1993. An ecosystem perspective of alluvial rivers: connectivity and the hyporheic corridor. *J. N. Am. Benthol. Soc.* 12(1):48-60.

Stanford, J. A., J. V. Ward and B. K. Ellis. 1994. Ecology of the alluvial aquifers of the Flathead River, Montana (USA), pp. 367-390. *IN*: Gibert, J., D. L. Danielopol and J. A. Stanford (eds.), *Groundwater Ecology*. Academic Press, San Diego, California, USA. 571 pp.

Stewart, K.W. and B.P. Stark. 2002. *Nymphs of North American Stonefly Genera (Plecoptera)* 2nd ed. The Caddis Press, Columbus OH.

Strayer, D.L. 1985. The benthic micrometazoans of Mirror Lake, New Hampshire. *Arch. fur Hydrobiol.* Suppl 72: 287-426.

Strayer, D.A., G.E. Likens. 1986. An energy budget for the zoobenthos of Mirror Lake, New Hampshire. *Ecology* 67(2): 303-313.

Strayer, D., S. May, P. Nielsen, W. Wollheim and S Hausam. 1997. Oxygen, organic matter, and sediment granulometry as controls on hyporheic animal communities. *Arch. Hydrobiol.* 140(1): 131-144.

Swanson, L. 2003. Gateway to Glacier. Unpublished report for the National Parks Conservation Association.

Teal, J.M. 1957. Community metabolism in a temperate cold spring. *Ecol. Mon.* 27(3): 283-302.

Teal. J.M. 1962. Energy flow in the salt marsh ecosystem of Georgia. *Ecol. Mon.* 43(4): 614-624.

Thienemann, A. 1926. Der nahrungskreislauf imWasser. *Verh. Deutsch Zool. Ges.* 31: 29-79.

Tillman, D.C., A. Moerke, C. Ziehl and G. Lamberti. 2003. Subsurface hydrology and degree of burial affect mass loss and invertebrate colonization of leaves in a woodland stream. *Fresh. Biol.* 48: 98-107.

Tremoliers, M. 2002. Functioning of Interfaces Surface Water/Groundwater/Forest in a Fluvial Hydrosystem: the Case of the Rhine Floodplain. IN: Griebler et al. eds., *Groundwater Ecology*. Austrian Academy of Sciences, Vienna.

Valett, H.M., S.G. Fisher, N.B. Grimm, P. Camill. 1994. Vertical hydrologic exchange and ecological stability of a desert stream ecosystem. *Ecology* 75(2): 548-560.

Vlasceanu, L. R. Popa, B.K. Kinkle. 1997. Characterization of *Thiobacillus thioparus* LV43 and its distribution in a chemoautotrophically based groundwater ecosystem. *Appl. Env. Microbiol.* 63(8): 3123-3127.

Ward, J.V. and M.A. Palmer. 1984. Distribution patterns of interstitial freshwater meiofauna over a range of spatial scales, with emphasis on alluvial river-aquifer systems. *Hydrobiologia* 287: 147-156.

Ward, J.V. and N.J. Voelz. 1994. Groundwater fauna of the South Platte River system, Colorado. pp. 391-423. *IN*: Gibert, J., D. L. Danielopol and J. A. Stanford (eds.), *Groundwater Ecology*. Academic Press, San Diego, California, USA. 571 pp.

West, G.B., J.H. Brown, B.J. Enquist. 2004. A general model for the origin of allometric scaling laws in biology. *Science* 276:122-126.

Wetzel, R.G. 1995. Death, detritus, and energy flow in aquatic ecosystems. *Fresh. Biol.* 33: 83-89.

Whited, D.C., M.S. Lorang, M.J. Harner, F.R. Hauer, J.S. Kimball, J.A. Stanford. In press. Hydrologic disturbance and succession: Driver of floodplain pattern. *Ecology*.

Whitticar, M.J. 1999. Carbon and hydrogen isotope systematics of bacterial formation and oxidation of methane. *Chem. Geol.* 161: 291-314.

Appendix A: How to distinguish hyporheic stonefly nymphs.

This list of attributes was developed from mature nymphs that were matched with adult Isocapnia emerging from wells in 2003.

Character	*Isocapnia integra (= I. missouri)*	*Isocapnia crinita*	*Isocapnia grandis*
Intercalcary Cercal Setae*	5-7 long hairs dorsal and ventral	13-15 long hairs dorsal and ventral	30+ dorsal hairs, 15+ ventral hairs
Cercal Basal Segments	Few long apical spines >3/4 length of segments	Short spines < ¾ length of cercal segments	Abundant long apical spines >3/4 length of segments
Abdomen **	Larger spines/setae covering terga	Short spines only, limited to edge of terga	Larger spines/setae covering terga
Femur***	Long, Dense setae on dorsal margin	Short sparse spines	Short sparse spines, few longer setae
Abdominal Terga	Long spines	Short spines	Long hairs
Pronotum	Long spines along fringe	Short spines along fringe	Short spines along fringe
Pre-Emergence Length **** (M)	9.7mm	14.3 mm	15.4 mm
(F)	12.2 mm	17.5 mm	18.5 mm
Life Cycle	1 year?	2 year?	2 year?

* Number of setae reduced in immature specimens
** This character can be used to separate *I. crinita*, even for very small nymphs (2.5 mm)
*** Not sure if this holds for smaller nymphs
**** Main character for distinguishing II and IG was size at maturity, and cercal setae

Note: very small Isocapnia spp can be distinguished from other genera by the mandibles (slide mounting the head capsule, see illustration in Stewart and Stark 2002). I did this when Capniidae were abundant at aquifer recharge sites, where other Capniids might also be present.

Other stonefly taxa:

1. *I. vedderensis*: 3-5 intercalcary setae; long hairs only on basal segments, abdomen, wingpads, femurs, pronotum (no spines or short hairs). Very long hairs on femurs. <1 year life cycle? Mature nymphs rarely collected during from well pumping.
2. *Paraperla frontalis*: no pleural fold, cerci much shorter than abdomen, abdomen dorso-ventrally compressed. (holds even for small <5mm nymphs). Smaller nymphs (<2mm) may be confirmed from mouthparts by slide-mounting the head capsule. From samples near the river, I assumed small nymphs were Chloroperlidae.
3. *Perlomyia utahensis*: distinguish from *Isocapnia* based on lack of pleural fold on last two segments. *Despaxia* with AB 1-5 (this taxa

is rare. No pleural fold on other leuctrids (not encountered at this site). Pleural fold is visible even on small nymphs by observing nymphs in a watch glass using low angle light. Submentum is not visible on leuctrids (*fide* P. Zwick – this character is very reliable for small nymphs). *Perlomyia* also tends to have missing legs post-sampling, which is a superficial trait useful for quick identification, and corresponds well with the submentum trait.

4. *Kathroperla perdita*: head longer than wide. Confirm by looking at mandible (squarish – see illustration in Stewart and Stark 2002).

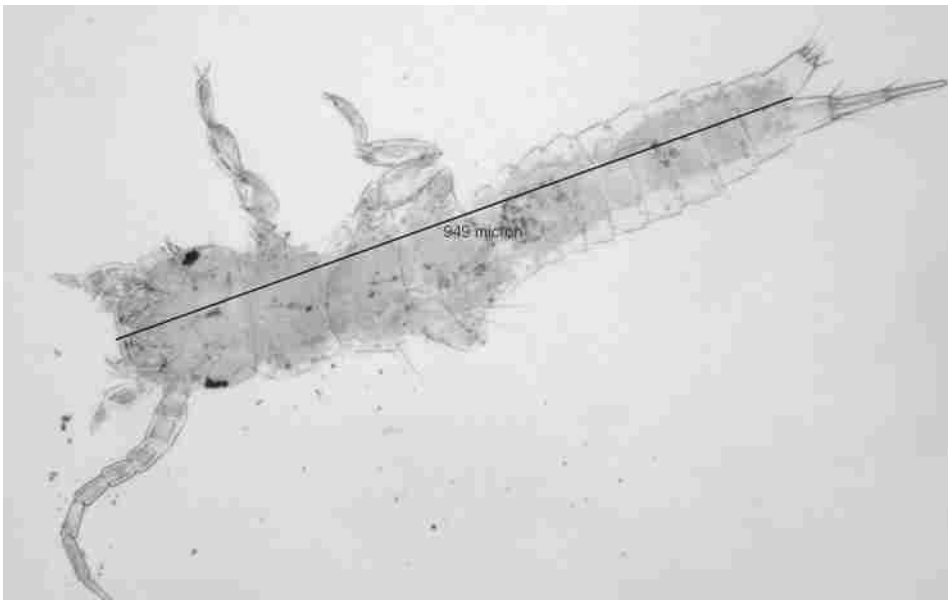

Paraperla frontalis (nymph < 1mm)

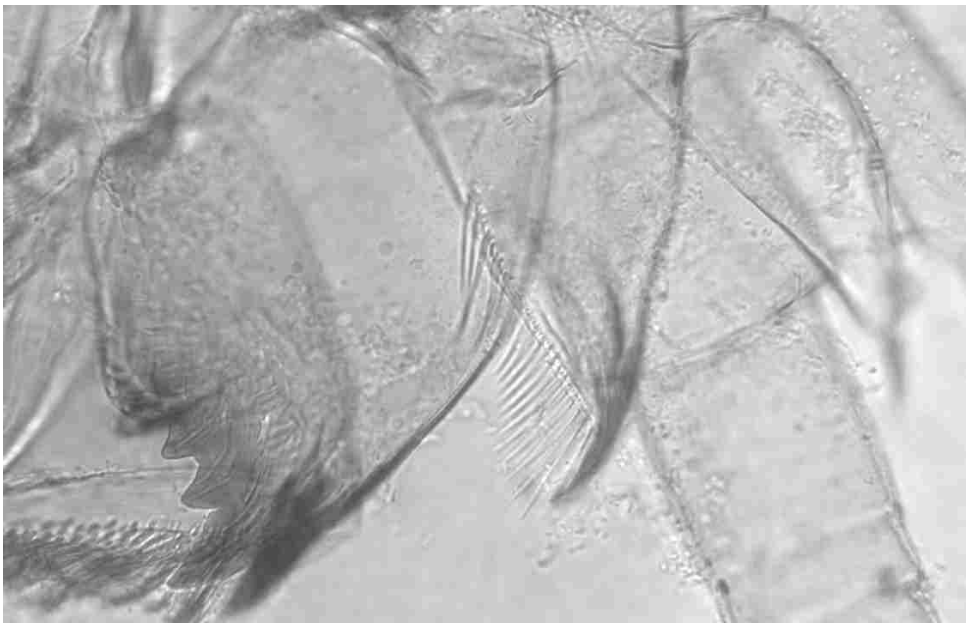

Isocapnia sp: mandible of early instar (<2mm) nymph

Appendix B: Hyporheic Species Composition and General Distribution

Habitat Description:

- Age of Site: Vegetation development as a surrogate for the age of corresponding gravel formation; **O** = Orthofluvial sites; **P** = Parafluvial sites

- Zone (Hyporheic Position): **R** = Aquifer Recharge; **M** = Flowpath Midgradient; **D** = Aquifer Discharge; **H** = Hypoxic Zone (DO<3 mg/l); **T** = Tributary (Hillslope Drainage)

Abundance:

- Frequency: **C** = Common; **U** = Uncommon (<10 occurrences); **R** = Rare (1-2 occurences)

DET: Taxonmonic Determination/Validation - all other determinations are by the author.

- **Abebe** = Euyalem Abebe, Elizabeth City State University, South Carolina;
- **Eisende** = Ursula Eisende, Univeristy of Vienna, Austria
- **Newell** = Bob Newell, Flathead Lake Biological Station;
- **Rhithron** = Rhithron Inc., Missoula MT;
- **Reid** = Janet Reid, JWR Associates, Virginia;
- **Taylor** = Howard Taylor, Florida.

REFERENCES

Matsumoto, K. 1976. An introduction to the Japanese groundwater animals, with reference to their ecology and hygienic significance. *Int. J. Speleol.* 8: 141-155.

Zloty, J., B.J. Sinclair, G. Pritchard. 2005. Discovered in our back yard: a new genus and species of a new family from the Rocky Mountains of North America (Diptera: Tabanomorpha). *System. Entom.* 30: 248-266.

	Habitat				
	Frequency	Age	Zone	DET	Notes
EPHEMEROPTERA					
Ameletus sp	C	OP	RD		
Cinygmula sp	U	OP	R		
Ephemerella sp	R	P	R		
Leptoplebia sp	R	P	R		
Paraleptophlebia sp	R	P	R		
PLECOPTERA					
Despaxia sp	U	P	R		
Diura sp	R	P	R		
Eucapnosis brevicaudata	R	O	RM		
Isocapnia crinita	C	OP	RDMH		
Isocapnia grandis	C	OP	RDMH		
Isocapnia integra	C	OP	RDM		
Isocapnia vedderensis	U?	P	RDM		
Isoperla sp	R	OP	RM		
Kathroperla perdita	U	OP	RDM		
Nemoura sp	R	P	R		
Paraperla frontalis	C	OP	RDMH		
Paraperla wilsoni	U	T	T		
Perlomyia utahensis	C	OP	RDMH		
Podmosta sp?	R	P	R		
Pteronarcella sp	R	P	R		
Sweltsa coloradensis	R	P	R		
Zapata sp	R	P	R		
DIPTERA					
Oreoleptis torrenticola	R	P	RM	Newell	Recently described family (Zloty et al 2005)
Ceratopogonidae	C	P	R		
Simulidae sp1	R	P	R		
Simulidae sp2	R	P	R		
Tipulidae sp	U	P	RM		
Corynoneura sp.	R	P	M	Rhithron	
Cricotopus sp.	U	OP	RM	Rhithron	
Heleniella sp. undescr.	R	P	R	Rhithron	Orthocladiinae nr Heleniella (undescribed)
Krenosmittia sp.	U	P	RM	Rhithron	
Micropsectra sp.	R	P	M	Rhithron	
Orthocladiinae sp1	C	OP	RMDH	Rhithron	Undescribed larvae (RAI taxon #0011)
Orthocladiinae sp 2	C	OP	RMH	Rhithron	Undescribed larvae (RAI taxon #0012)
Orthocladius sp	R	OP	RM	Rhithron	
Parametriocnemus sp.	R	O	RM	Rhithron	
Paratanytarsus sp.	R	P	M	Rhithron	
Polypeditum sp.	U	OP	RM	Rhithron	
Rheocricotopus sp.	U	P	R	Rhithron	
Rheosmittia	R	P	M	Rhithron	
Stempinella sp.	R	P	M	Rhithron	
Tanytarsus sp.	R	P	R	Rhithron	
Tvetinia sp	R	P	M	Rhithron	
Zavrelimyia sp.	U	P	M	Rhithron	
COLEOPTERA					
Dytiscidae	R	P	R		
Narpus sp	R	O	M		
Coleopter sp	C	OP	RMDH		Interstitial spp. (see Matsumoto 1976)
COLLEMBOLA					
Collembola spp.	C	OP	RMD		

	Habitat				
	Frequency	**Age**	**Zone**	**DET**	**Notes**
AMPHIPODA					
Stygobromus tritus	C	OP	RMDH		
Stygobromus sp nov	U	O	MDT		
COPEPODA					
Acanthocyclops montana	C	OP	RMD		
Acanthocyclops pennaki	C	OP	RMDT		
Acanthocyclops vernalis	C	OP	RD		
Bryocamptus hiemalis	C	OPH	RMDH		
Diacyclops languidoides	C	OPH	RMDH		
Diacyclops crassicaudis	C	OPH	RMDH		
Epactophanes richardii	U	O	M		
Eucyclops sp aspersus?	R	O	R		
Ameiridae gen nov	U	P	M	Reid	Undescribed genus
Harpacticoid sp 1	U	P	M		
Orthocyclops modestus	R	O	M		
Paracyclops poppei	C	OP	RD		
Parastenocaris sp 1	C	OPH	RMDH		nr P. italica
OSTRACODA					
Cavernocypris wardii	C	OP	RMD		
Ostracod sp 2	R	P	D		
CLADOCERA					
Alona sp	R	OP	R		
Eubosmina sp	R	OP	R		
Daphnia sp	R	OP	R		
BATHYNELLACEAE					
Bathynella sp riparia	C	OP	RMD		
Bathynella sp2	C	OP	RMD		
Bathynella sp3	U	OP	RMD		

	Frequency	Habitat Age	Habitat Zone	DET	Notes
ROTIFERA					
Abrochtha sp	U	O	RM		
Cephalodella forficula	U	P	R	Taylor	
Cephalodella sp1	C	OP	RM		
Cephalodella sp2	U	OP	RM		
Dissotrocha sp	C	OP	RMDH		
Rotaria sp.	C	OP	RMD		
Henocerus sp?	R	P	M		
Lepadella sp.	C	OP	RMH	Taylor	
Lepadella sp 2	R	P	R	Taylor	
Notholca sp squammula	U	OP	MH		
Notholca sp 2	R	P	R	Taylor	
HYDRACHNID					
Hydrovolzia sp	C	OP	RMD		
Stygothrombium sp	C	OP	RMDH		
Uchidistygocaris sp	U	P	RM		
Hydroma sp	U	P	RM		
TARDIGRADA					
Doryphoribius sp	C	OP	RMDH		
Isohypsibius sp?	R	O	M		
NEMATODA					
Achromadora sp.	C	OP	RMH	Eisende	misID Paracyathylaimus
Ethmolaimus sp.	R			Eisende	
Eudorylaimus sp.	C	OP	RMDH		
Hemicycliophora sp	C	OP	RM		
Labronema sp	U	OP	RMH		
Monhystera sp	C	OP	RMDH		
Mononchus sp	C	OP	RMD	Eisende	
Nygolaimus sp	C	O	RM		
Prismatolaimus sp	C	OP	RMDH	Eisende	
Rhabditidae	U	OP	RMH		
Theristus sp.	R			Eisende	
Tobrilidae	U	P	R	Eisende	reID Anonchus; need males
Triplya sp.	U	OP	RMH		
GASTROTRICH					
Chaetonotus sp.	R	O	R		
ANNELIDA					
Annelid spp.	C	OP	RMDH		
Troglochaetus sp.	C	OP	RMDH		